Preparation, characterisation and application of printed medical diagnostic biosensors

Wajiha Abbasi

Submitted in accordance with the requirements for the degree of

Doctor of Philosophy

The University of Leeds

Department of Colour Science

Faculty of Maths and Applied Science

August, 2014

The candidate confirms that the work submitted is his/her own and that appropriate credit has been given where reference has been made to the work of others.

This copy has been supplied on the understanding that it is copyright material and that no quotation from the thesis may be published without proper acknowledgement.

The right of Wajiha Abbasi to be identified as Author of this work has been asserted by her in accordance with the Copyright, Designs and Patents Act 1988.

DEDICATED TO MY

FATHER SAEED AHMAD ABBASI

&

MOTHER RABIA SAEED ABBASI

ACKNOWLEDGEMENTS

The work presented in this thesis would not have been possible without my close association with many people. I take this opportunity to extend my sincere gratitude and appreciation to all those who made this PhD thesis possible.

First and foremost, I would like to express my gratitude to my supervisor, **Prof. Long Lin**, who truly made a difference in my life. Thank you **Dr. Long** for provided me with direction, technical support and became more of a mentor and friend, than a professor. It was though your persistence, understanding and kindness that I completed my graduate degree. I doubt that I will ever be able to convey my appreciation fully, but I owe you my eternal gratitude.

I am grateful to **Prof. Dr. Paul Milner** from School of Biomedical Sciences, who gave me permission to work in his laboratory and use the facilities available there for bio-sensing experiments.

This research work would have never been completed without help of **Dr. Tim Gibson**. Thank you so much **Tim**, for introducing me to this exciting field of science. You have been a wonderful teacher who gradually became my biggest mentor. I highly appreciate your dedicated help, advice, inspiration, encouragement and continuous support, throughout my PhD. Your enthusiasm, integral view on research and mission for providing high-quality work, has made a deep impression on me.

I would like to thank **Dr. Kelvin Tapley** for being internal assessor of my thesis. Your comments and questions were very beneficial for my reports and thesis. I have learned a lot from your insight.

My special thanks go to **Mr. Algy Kazlauciunas** for his patience through out my research work. There were certain times when I needed to run my samples at short notice and you always extended your hand to help me out. Your heartiest and kind smile meant a lot to me.

I will always cherish the generous and enlightened talks of **Mr. Trevor Lambourne** at CIC office which helped eased my nerves before monthly meetings.

I want to thank all of my group fellows, **Qi**, **Saminu**, **Sam** and **Andy** for giving me a good company over three years. Their never-ending jokes and humour kept our room filled with laughter's and joys.

I can't thank my brilliant **mother** and **father** enough for giving me the greatest gifts of unconditional love, enthusiasm and constant support throughout my life. It is impossible to put into words how much you have done for me. This journey would not have been possible without the support of my father. We shared the same dream and strive for it together but he departed just before achieving it. He has been greatly missed and will always be part of this accomplishment. Thank you so much "**Abbu**" for encouraging me in all of my pursuits and inspiring me to follow my dreams. I am fortunate to have wonderful siblings, ever supporting brothers **Muazzam** and **Irqam** and their wives **Ashi** & **Huda**, the most loving sister **Saima** & her late husband **Imran**. You all have always been there for me. Thank you so much for being such a wonderful family.

My heart felt regard goes to my father in law, mother in law and brother in law **Kashif** & his wife **Bisma** for their love and moral support. Thank you so much for believing in me.

I owe my deepest gratitude towards my husband **Atif** for his eternal support and understanding of my goals and aspirations. His infallible love and support has always been my strength. Without his help, I would not have been able to complete much of what I have done and become who I am. Thank you **Atif** for everything you have done and standing besides me all the way long. I cannot forget how brilliantly and selflessly you have managed kids and home while I was busy at university. I would never be able to get this degree without your dedication and never ending love.

I do not have enough words to express my gratitude to my little angels **Inaya** & **Rayan.** There were times when mummy was preoccupied, tired and restless and they extended their little help either by going into bed early or just turning TV off. Thank you so much my beautiful gems for all little things you did for me, your smiles have brighten my world.

ABSTRACT

Over the past two decades, more accurate, convenient and earlier diagnoses have become a key strategy to reduce health care costs. The application of electronics to biology and medicine has enabled advanced technology of lab-on-a-chip biomedical diagnoses. The aim of this study was to explore possible interface or surfaces which could be printed and utilised to fabricate biosensor for the detection of potential diseases. Overall, the research work was carried out into two dimensions, and therefore, this thesis has been divided into two major sections. The first section (Chapters 1-3) comprises studies carried out on Quantum Tunnelling Composite (QTC) vapour sensors for the detection of potential biomarkers acetone and ammonia in breath. Recent developments in gas-sensing technology and pattern recognition methods made electronic nose technology an interesting alternative for health care devices. Therefore, initial experiments were carried out to evaluate QTC potential as vapour sensing material for an electronic nose. The second section (Chapters 4-10) comprises design, preparation and characterisation of labelless immunosensors for *Neisseria gonorrhoea* and *Chlamydia trachomatis.* Electrochemical impedance spectroscopy (EIS) was employed to investigate detection of analytes via impedimetric transduction. The successful construction of an immunosensor depends on effective immobilising of bio-recognition element onto the transducer surface. Thus, conducting polymers having amine functional groups were developed, utilised and evaluated as a suitable matrix for the covalent entrapment of antibodies. Fragments of antibodies were immobilised onto four different functionalised conducting surfaces which included polyaniline, poly (4-amino methyl) pyridine, polytyramine and 3-amino propyl pyrrole, respectively. Fully fabricated sensors were interrogated against various concentrations of *Neisseria gonorrhoea* and *Chlamydia trachomatis*. EIS was used to measure the charge transfer resistance of the sensors across a range of frequencies. These sensors were found to specifically detect the intended analytes with a limit of detection of 10^2 bacterial particles per ml in general. In addition, scanning electron microscopy was employed to study the surface morphologies of a sensor whereas FTIR spectroscopy was employed for the characterisation of all polymers.

LIST OF ABBREVIATIONS

3 & 4-AMP	3 & 4-amino methyl pyridine
ANN	Artificial neural network
ANI	Aniline
3APPy	3-aminopropyl pyrrole
APS	Ammonium per sulphate
ATR	Attenuated total reflectance
BQ	p-benzoquinone
BWA	Bulk acoustic wave
CPU	Central processing unit
CHL	Chlamydia trachomatis
CP	Conductive polymer
CV	Cyclic voltammetry
DFA	Direct fluorescent antibody
DMSO	Dimethyl sulphoxide
DMF	Dimethylformamide
DNA	Deoxyribonucleic acid
DBSA	Dodecylbenzene sulphonic acid
EAD	Electronic aroma detection

EASP	Electronic aroma signature pattern
ECL	Chemiluminescence substrate
EDTA	Ethylenediaminetetraacetic acid
ELISA	Enzyme-linked immunosorbent assay
EDC	1-Ethyl-3-[3-dimethylaminopropyl]carbodiimide hydrochloride
EN	Electronic nose
EIS	Electrochemical impedance spectroscopy
ES	Emeraldine salt
FRA	Frequency response analysis
FTIR	Fourier transform infrared spectroscopy
GC-MS	Gas chromatography mass spectrometry (GC-MS)
GPES	General purpose electrochemical system
HOMO	Highest occupied molecular orbital
HRP	Horseradish peroxidase
HQ	Hydroquinone
LB	Leucomeraldine base
LUMO	Lowest unoccupied molecular orbital
MS	Mass spectrometry
Na-pTSA	Sodium salt of p-toluene sulphonic acid
NG	Neisseria gonorrhoea

NHS	N-Hydroxysulfosuccinimide
NHS-LC-LC-Biotin	Succinimidyl-6-(biotinamido)-6-hexanamido hexanoate
NHS-ESTER	Sulphonated ester derivative of N-hydroxysulphosuccinimide
ODN	Oligonucleotide
PANI	Polyanilines
PBS	Phosphate buffered saline
PEG	Polyethylene glycol
PID	Pelvic inflammatory disease
PPY	Polypyrrole poly[1,3-diaminobenzene (DAB)
POLY-TYR	4-(2-aminoethyl) phenol
PPM	Parts per million
PS	Pernigraniline salt
PTCR	Temperature coefficient of resistance
PVC	Polyvinyl chloride
QTC	Quantum tunnelling composite
RNA	Ribonucleic acid
RI	Refractive index
SAM	Self-assembled monolayer
SAW	Surface acoustic wave
SEM	Scanning electron microscopy

SDBS	Sodium dodecyl benzene sulphonate
SDS	Sodium dodecyl sulphate
SMCC	Succinimidyl-4-(N-maleimidomethyl)cyclohexane carboxylate
SMPB	Succinimidyl-4-(N-maleimidophenyl) butyrate
STI's	Sexually transmitted infections
TCEP	Tris(2-carboxyethyl) phosphine
TWEEN 20	Polyoxyethylene (20) sorbitan monolaurate
VOCs	Volatile organic compounds

LIST OF SYMBOLS

A	Area of the electrode
C_{dl}	Double-layer capacitance
cm	Centimetres
C_{ox}	Oxidative concentration
C_{red}	Reductive concentration
CPE	Constant phase element
°C	Centigrade
F	Faraday's constant
Ihp	Inner helmholtz plane
Ohp	Outer helmholtz plane
τ	Time constant
φ	Phase shift
ΔH	Heat of vaporisation
δ	Solubility parameter
δ_s	Solution solubility parameter
δ_p	Polymer solubility parameter
Hz	Hertz
Δ	Hildebrand solubility parameter

kHz	Kilo hertz
kΩ	Kilo-Ohms
I	Current
J	Flux coefficient
kDa	Kilo dalton
i_{pc}	Peak current intensity
R	Gas constant
R_{ct}	Charge-transfer resistance
R_S	Resistance of the solution
R_i	Initial resistance
R_f	Final resistance
Z”	Imaginary impedance component
Z’	Real impedance component
|Z|	Absolute impedance
Z_w	Warburg impedance

LIST OF FIGURES

LIST OF TABLES

TABLE OF CONTENTS

SECTION I

QTC Vapour Sensor

Section I of this thesis reports research on Quantum Tunnelling Composite (QTC) based sensors for use in a diagnostic application, specifically its potential as a chemical vapour sensor. By utilising the interaction between metal/polymer composite and solvent vapours, it was hoped that a sensor could be developed which could detect volatile organic solvent vapours.

CHAPTER 1 DIAGNOSTIC POWER OF ODOUR

1.1 Introduction

In recent years, the demand has grown in the field of medical diagnostics for simple and disposable devices that also demonstrate fast response times, are user-friendly, cost-efficient, and are suitable for mass production. There exist certain materials that exhibit changes in their physical properties once exposed to liquids of chemical vapours. A vapour sensor is based on the principle of detecting changes and converting them into electrical signals via a suitable transduction mechanism. Polymers readily exhibit swelling in the presence of solvent vapours, which can be detected in many different ways. Thin film layers of gas-sensitive polymers are therefore at the centre of many gases and vapour sensor systems (Hands, 2003).

Recent developments in gas-sensing technology and pattern recognition methods make electronic nose technology an interesting alternative for health care devices (Chen and Choi, 2013).

The overall aim of this research work is to evaluate the potential of QTC composite as a vapour sensor which could be used in electronic nose as a point-of-care device for diabetes mellitus and pulmonary tuberculosis.

1.2 Breath analysis

Human breath is largely composed of oxygen, carbon dioxide, water vapour, nitric oxide, and numerous volatile organic compounds (VOCs) (Guo *et al*., 2010). The selective detection of various volatile compounds in human body odours is of great significance to early clinical diagnosis (Chen and Choi, 2013). The history of studying breath as a medical test is as old as medicine itself. Changes in the concentration of the molecules in VOCs could suggest various diseases. Similar to a fingerprint, every individual has a "breath print" that can provide useful information about his or her state of health. Such a print comprises thousands of molecules that are expelled with each breath we exhale.

During the last decade, a great number of clinical studies have been undertaken exploring the relationships between the chemical composition of exhaled air and patient's clinical status. Main targets of these investigations were different lung diseases, inflammatory and malignant processes in the body, and special diseased states such as allograft rejection and renal failure (Miekisch *et al*., 2004). As new biomarkers of disease are discovered, use of the electronic nose for detection of such biomarker VOCs should become increasingly useful for breath analysis and clinical diagnoses (Wang, 2009).

Table 1 lists some of the breath compounds and the conditions associated with them.

Table 1 Some breath compounds and associated conditions

Breath Compounds	**Associated Conditions**
Acetone	Diabetes (Minh, 2012)
Benzene,1,1-oxybis-, 1,1-biphenyl,2,2-diethyl, Furan,2,5-dimethyl-, etc.	Lung cancer (Phillips, 2007)
Pentane and carbon disulphide	Cystic fibrosis (McGrath, 2000)
Pentane, Carbon disulphide	Schizophrenia (Phillips, 1993)
Nitric oxide (NO), Carbonyl sulphide, Carbon disulphide, Isoprene	Lung diseases (Kharitonov, 2004)
Ammonia	Renal disease (Fend, 2004)
Nonane, 5-methyl tridecane, 3-methyl decane, etc.	Breast cancer (Phillips, 2003)

Research in the past few years has uncovered the scientific and chemical basis for such clinical observations and with the help of modern gas chromatography mass spectrometry (GC-MS) instruments, it is possible to identify thousands of unique substances in exhaled breath. Such substances include elemental gases, such as hydrogen, mono nitric oxide (NO), and carbon monoxide, and a vast array of volatile organic compounds (VOCs). Exhaled breath also carries aerosolised droplets that can be

collected as *exhaled breath condensate* that contains endogenously produced non-volatile compounds, such as dissolved proteins.

1.3 Techniques for breath analysis

Several techniques have been developed for the detection and measurement of breath compounds, they can be categorised into three major groups:

a) Methods based on gas chromatography coupled to mass spectrometry (GC-MS);
b) Chemical sensors; and
c) Laser-absorption spectroscopic techniques.

Some analytical methods based on these techniques are listed into Table 2.

Table 2 Analytical methods for human-breath analysis

Analytical methods	Marker	Detection range
GC/MS	Hydrocarbons, Aldehydes, Sulphides	pptv–ppbv
SIFT-MS	Ammonia, Ethanol	ppbv
Ion mobility	Ammonia, Acetone, Isoprene	ppbv
Laser Direct analysis	Ethane, CO	pptv
PTR-MS	Isoprene, CO, Aromatic compounds	pptv
Sensor	Nitric oxide	ppt–ppbv
Sensor arrays	Different VOCs	ppbv

The sensitivity of these techniques in terms of limits of detection of volatile compounds in breath, tends to fall in a relatively wide range e.g. from parts per trillion (ppt) to parts per million (ppm) (Kim *et al*., 2012).

1.4 Electronic nose

Electronic nose (EN) is the informal name for an instrument made up of chemical sensors combined with some sort of pattern recognition system, enabling discrimination and recognition of simple or complex odours (Gibson, 2000). The function of an EN is to mimic the mammalian olfactory system and produce a unique classification based on the volatile organic compounds (VOCs) present in the headspace gas being analysed (Kolk *et al*., 2010).

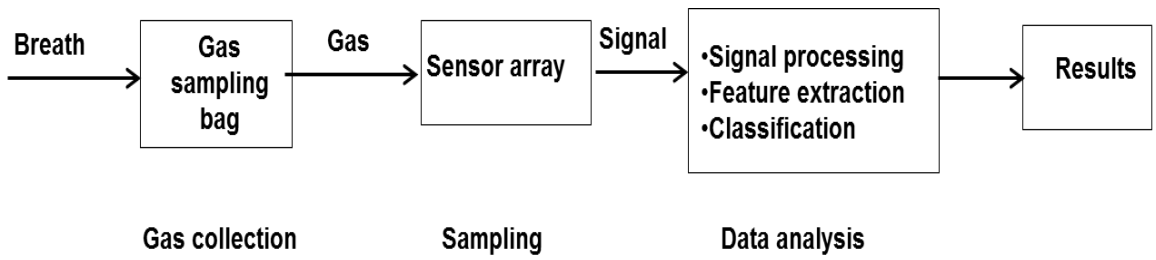

Figure 1 Working flow of electronic nose

A typical system shown in Figure 1 operates in three phases; gas collection, sampling, and data analysis with a subject first breathing into a gas-sampling bag. The collected gas is then injected into a chamber containing a sensor array where a measurement circuit measures the interaction between the breath and the array. Once signals are received they are filtered, amplified and sent to computer for further analysis.

1.4.1 Electronic aroma detection sensor types

The sensor array in an electronic nose performs very similar functions to the olfactory nerves in the human olfactory system. Therefore, the sensor array may be considered the heart and most important component of the electronic nose. The instrument is completed by interfacing with the computer central processing unit (CPU), recognition library and recognition software that serve as the brain to process input data from the sensor array for subsequent data analysis. A good sensor should fulfil a number of criteria. Such as sensor should have a highest sensitivity to the target group of chemical compound(s) intended for detection and with a threshold of detection similar to that of the human nose, down to about 10^{-12} g ml^{-1} (Baietto, 2009). There are different types of sensing materials utilised in electronic nose, including metal-oxides, semiconductive

polymers and conductive electroactive polymers, which are capable of direct electronic detection and identification of complex mixtures in sampled air (Wilson, 2004).

There exist a variety of advantages and disadvantages of using various EN sensors based on their response and recovery times, sensitivities, detection range, operating limitations, physical size, inactivation by certain poisoning agents and other limitations which are specific to individual sensor types (Baietto, 2009).

1.5 Vapour sensing materials

Recently, gas sensing is receiving increasing attention in both industry and academia. Gas sensing technology has become more significant because of its widespread and common applications in the following areas: (1) industrial (methane detection in mines); (2) automotive industry (e.g. detection of polluting gases from vehicles); (3) medical applications (e.g. electronic noses simulating the human olfactory system); (4) indoor air quality supervision (e.g. detection of carbon monoxide); (5) environmental studies (e.g. greenhouse gas monitoring) (Liu, 2012).

When exposed to liquids or chemical vapours, many materials may display a change in some of their physical properties. Such materials are being used for developing a gas or vapour sensor which detect any changes and convert them to electrical signals via a suitable transduction mechanism.

1.5.1 Metal oxide semiconductor

The most common sensing materials are metal oxide semiconductors, which provide sensors with several advantages such as low cost and high sensitivity. Sensors based on metal oxide semiconductors are mainly employed to detect target gases through redox reactions between the target gases and the oxide surface. This process includes two steps: (1) redox reactions during which O^- distributed on the surface of the materials reacts with molecules of target gases, leading to an electronic variation of the oxide surface; and then (2) this variation is transduced into an electrical resistance variation of the sensors. The resistance variation could be detected by measuring the change of capacitance, work function, mass, optical characteristics or reaction energy.

Metal oxides, such as SnO_2, CuO, Cr_2O_3, V_2O_5, WO_3 and TiO_2, can be utilised to detect combustible, reducing, or oxidising gases with sensors which are mainly based on the resistance change responding to the target gases.

1.5.2 Polymers

Generally, sensors based on metal oxide semiconductors exhibit significantly greater sensitivity to inorganic gases such as ammonia and a few VOCs such as alcohol (C_2H_5OH) and formaldehyde. However, there are certain VOCs which could cause adverse health effects when their concentration over a certain threshold cannot be detected by metal oxide semiconductor-based sensors. According to the different changes in physical properties, polymers used for gas sensing can be further classified into two groups: (1) conducting polymers, and (2) non-conducting polymers.

1.5.2.1 Conducting polymers

Conducting polymers (CPs) that can be used as gas-sensing materials include polypyrrole (PPy), polyaniline (PAni), polythiophene (PTh) and their derivatives. The conductivity of polymers can be improved through different processes of doping by redox reactions or protonation. After the doping process, polymers become conductors or semiconductors. The most important feature is that the doping level can be changed by chemical reactions between the polymers and target gases which make the detection of analytes based on these conducting polymers practical. The polymers suitable for detecting different analytes are doped through redox reactions.

1.5.2.2 Non-conducting polymer

Polymers with different properties can be coated onto respective transducers. Non-conducting polymers such as polyimide have been widely utilised as absorptive coatings on different sensor devices. Once coated, polymer layers can change resonance frequency, dielectric constant and enthalpy upon absorption/desorption of analytes which can be converted into an electrical signal output.

Polymer-based gas sensors have advantages such as high sensitivities and short response times. Furthermore, while operation temperatures of metal oxide

semiconductor-based sensors are usually more demanding whereas polymer-based sensors operate at room temperature. Polymer-based gas sensors also have some disadvantages such as long-time instability, irreversibility and poor selectivity (Liu *et al*., 2012).

1.5.3 Carbon nanotubes

Conventional sensing materials such as metal oxide semiconductors are often associated with the problem of poor sensitivity at room temperature, while carbon nanotubes (CNTs) attract more attention because of their unique properties and have become the most promising materials for high-sensitive gas sensors. As a promising sensing material, CNTs possess electrical properties and are highly sensitive to extremely small quantities of gases such as alcohol, ammonia (NH_3), carbon dioxide (CO_2) and nitrogen oxide (NO_x) at room temperature, while other materials such as metal oxides have to be heated in order to operate normally. The high sensitivity of CNTs eliminates the need of assisting technologies such as pre-concentration, and contributes to the advantages of low cost, low weight and simple configuration (Liu *et al*., 2012).

1.5.4 Metal-polymer composites

Typically, metal-polymer composites consist of a conductive powder mixed into a non-conductive polymeric matrix. Filler powders vary greatly in their shape, size and composition. Metallic filler powders are often chosen, offering a wide variety of electrical and magnetic properties. Examples include silver, gold, copper, nickel and zinc. However, carbon black and other furnace-blacks are usually favoured due to their low cost, wide availability and good conductive properties. More recently, carbon nano-tubes have also been incorporated into such composite systems. Filler particle sizes range from nano-scale to hundreds of microns, and have wide morphological variety. The insulating matrix may be formed from any non-conducting material, but is usually a polymer. Examples include poly (ethylene), poly(urethane) and natural rubber. The polymer is normally non-conducting, but conducting polymers have also been used. Polymers are primarily chosen according to their wetting ability and mechanical properties. Polymer blends are also often used to help obtain a composite with the desired physical and electrical characteristics. The presence of conducting particles within a metal-polymer composite imparts improved electrical properties upon the

material. These properties can be adjusted either by simple alteration of the respective component materials, or by changing the loading ratio of filler in the polymer. The most important property of such composites is their change in resistivity when subjected to mechanical distortions. Compressing the composite causes the conductivity to increase, whilst conversely, stretching causes a decrease in conductivity. In addition, such materials display sensitivity to changes in temperature, often displaying a positive temperature coefficient of resistance (PTCR) effect.

A summary of the types and mechanisms involved with some common gas sensor technologies are listed in Table 3.

Table 3 Types and mechanisms of common electronic nose gas sensors

Sensor Type	**Sensitive material**	**Detection principle**
Acoustic sensors: Quartz crystal microbalance (QMB); surface & bulk acoustic wave (SAW , BAW)	Organic or inorganic film layers	Mass change (frequency shift)
Calorimetric; catalytic bead (CB)	Pellistor	Temperature or heat change (from chemical reactions)
Colorimetric sensors	Organic dyes	Colour changes, absorbance
Conducting polymer sensors	Modified conducting polymers	Resistance change
Electrochemical sensors	Solid or liquid electrolytes	Current or voltage change
Fluorescence sensors	Fluorescence sensitive layer	Fluorescence light emission
Infrared sensors	IR sensitive detector	Infrared radiation absorption
Metal oxides semi conducting	Semi-conducting metal oxides (SnO_2, GaO)	Resistance change
Optical sensors	Photodiode, light sensitive	Light modulation, optical changes

CHAPTER 2 QUANTUM TUNNELLING COMPOSITE (QTC)

2.1 Introduction

Peratech, the company is a high-tech materials development company, based in Darlington, UK. In 1997 they invented a new form of metal-polymer composite, which has named Quantum Tunnelling Composite (QTC) (Hands, 2003). The material made by patented manufacturing process gives rise to a composite with unique electrical properties. The composite is intrinsically electrically insulating, but drastically increases its conductivity over many orders of magnitude, when subjected to mechanical deformation, such as compression, tension, bending or torsion. This is contrary to most standard composites whose conductivity increases only under compression, whilst tension results in a decrease in conductivity. At very large strains however, an irreversible conductivity increase is sometimes observed in standard composites. Under such extreme conditions, severe and irreversible narrowing of the polymer occurs, as the material's behaviour changes from elastic to plastic. The result of this narrowing may then give rise to a permanent conductivity increase, as metallic particles are pushed closer together.

The properties of various composites comprising electrically conductive particles dispersed in an insulating polymer matrix have been studied for over 50 years. Carbon and metal powders, e.g. Ni, Cu, Ag, Al and Fe, have all been used as fillers. Carbons utilised include carbon nanotubes, carbon fibre, graphite, pyrolytic carbons and carbon blacks, the latter having large variations in purity and morphology. The metal powders offer well-defined morphology and a higher intrinsic conductivity than carbon black. In general, at low filler content the conductive particles are well separated and the composite is insulating, with an electrical conductivity only slightly higher than that of the polymer. Initially, the conductivity increases slowly with filler concentration, but then rises rapidly over a narrow concentration range to give a high conductivity with only a weak dependence on further increase in filler concentration (Bloor, 2006).

QTC however, is unique in that it displays a fully reversible conductivity increase with increasing tension at low strains as well as the extreme high strain case described above. In addition, QTC displays extreme sensitivity to such deformations, changing its

resistivity over many orders of magnitude. This is far in excess of the ranges displayed by standard, conventional metal-polymer composites. Peratech has developed a variety of QTC materials by using different fillers consisting of nickel powder and copper. Along with various fillers the polymer type has also been varied. The standard composite uses silicones, but in QTC material other polymers including poly(urethane), poly(butadiene), poly(iso-butyl acrylate) poly(vinyl alcohol) and poly(acrylic acid) have been used.

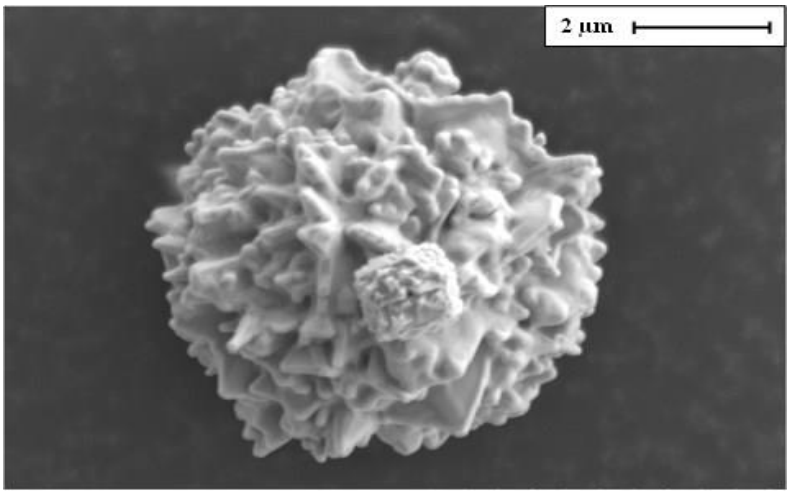

Figure 2 A typical nickel particle used in QTC™ materials

QTC composite contains nickel particles of diameter 1 – 10 µm with sharp nano-scale projections, as shown in Figure 2 (Graham, 2008). The nickel particle has a spiky surface morphology, with clearly visible surface protrusions. These nanoscale features give the material unusual electrical properties. This is in contrast to most other metal polymer composites made from a variety of materials including copper, silver, zinc and more commonly carbon black particles. These more typical composites generally have smoother surface profiles and conduct through a mechanism described by percolation theory, where charge is transferred between particles in close proximity, standard QTC does not. Due to the spiky nature of the Nickel particles, high electric fields are produced at the tips of the spikes which allow conduction described by the Fowler-Nordheim tunnelling mechanism. Furthermore, the particles are fully wetted in the polymer matrix so at high filler concentrations there is no direct contact of the particles and conduction is primarily through field assisted quantum tunnelling across relatively thick barriers (Bloor, 2006). The structure provides unique electronic behaviour including high resistivity above the expected percolation threshold and an exponential increase in

conductivity over several orders of magnitude under all types of mechanical deformation (Hands, 2003).

2.2 Applications of QTC

QTC is currently employed in a number of different applications in commercial, industrial and scientific areas. The first and probably most widespread use of QTC is as a switch in wearable electronic systems, utilising transition from high to low resistance under applied pressure. It is also employed as a pressure sensor in electrical devices. The exponential response of QTC to deformation allows for very sensitive touch response in the material. Variation of nickel loading and blending of additional materials can be used to tune the QTC into a specific sensitivity range. A further property of the QTC that lends itself to application is that the field assisted tunnelling conduction mechanism is noncontact (Graham, 2008).

One of the potential applications for the QTC presented in the later parts of this study is as a chemical vapour sensor. The intrinsically conductive sensors presented later showed a significant electrical response in the presence of chemical vapours. The use of a number of different sensors all tuned slightly differently can be employed to give a fingerprint that can characterise a certain combination of gasses. With some careful calibration and a data bank of known vapour responses, this setup could be used as an artificial olfactory system known as electronic nose.

Polymers are particularly useful as vapour sensing elements due to their ease of manufacture and broad chemical variety. Polymers readily exhibit swelling in the presence of solvent vapours, which can be detected in many different ways. Conducting polymer shows a change in resistivity in the presence of solvent vapours. This is sometimes due to a polymer swelling effect. However, analytes may also cause oxidation or reduction of the polymer chain, giving rise to a change in charge carrier mobility, and therefore a change in conductivity. The most common polymers employed for such sensors are poly (pyrrole), poly (aniline) and poly (thiophene). Conducting polymer sensors have the advantage that they are easy to produce and have a rapid response and recovery. However, problems with drift of the electrical baseline and of sensitivity to humidity still need to be addressed (Hands, 2003).

This chapter will outline a number of relevant theories concerned with vapour absorption and diffusion through polymer material.

2.3 Theory of vapour absorption and diffusion

Solvent penetration into a metal-polymer composite may cause an electrical conductivity change via number of different mechanisms. Electrochemical interactions may occur between solvent and polymer, and also between solvent and metallic filler particles. Charge may be donated or accepted by solvent molecules, resulting in a change in the quantity of charge available for conduction. Alternatively, the work function of the polymer may be modified, thus affecting tunnelling probabilities. In addition, the capacitive and dielectric properties of the material are likely to be modified. Changes in ionic conductivity may also result, especially where polar solvents are concerned. However, all of the above effects are usually negligible compared to polymer swelling, which dominates wherever solvents and elastomers are present within the same system.

Whatever the transduction mechanism is utilised in an effective sensor, the electrical response to the test vapour should be fast acting and fully reversible. Stable baselines and repeatable responses are required, with large signal to noise ratios. The signal should also be proportional in some way (preferably linearly) to the concentration of the test vapour, if effective quantitative analysis is to be performed. In addition, for qualitative analysis, a wide variety of responses should be obtainable from many different polymer solvent combinations.

2.3.1 Vapour absorption in polymers

The response of a polymer after exposure to a solvent vapour is governed by absorption thermodynamics and diffusion of the solvent into the polymer. Diffusion of the vapour into the polymer results in mixing between the polymer and vapour molecules which increases the entropy of the system. However, the absorbed vapour molecule also cause dilation of the polymer and reduces the number of possible orientations of the polymer chains. As the chains orientate to decrease their entanglement, the order of the system increases and thus the entropy decreases. In order for the vapour-polymer reaction to occur, the entropy decrease caused by polymer swelling must be overcome by the

entropy increase caused by the vapour-polymer mixing process. Only then more solvent can be absorbed. If the polymer swelling contribution outweighs that of the mixing process, no more vapour is absorbed (Hands *et al.*, 2013).

In 1936 Joel H. Hildebrand proposed the square root of the cohesive energy density as a numerical value indicating the solvency behavior of a specific solvent as shown in equation 1.

$$\delta = [(\Delta H_v - RT) / V_m]^{½} \quad (1)$$

Where δ is solubility parameter, ΔH is heat of vaporisation, R is gas constant, T is temperature and V_m is molar volume.

Solubility parameters can be used to determine the solubility of polymers and solvent pairs. The following relationship can be used to estimate how compatible a polymer-solvent pair is. If the square root of the value of the solubility parameter of the solvent, δ_s, minus the solubility parameter of the polymer, δ_p, is less than 1, then the solvent will most likely dissolve the polymer. This is summarised in equation 2.

$$((\delta_s - \delta_p))^{1/2} \leqslant 1, \quad (2)$$

Where δ is the Hildebrand solubility parameter, and the subscripts s and p refer to the solvent and polymer respectively. For a value less than 1, the solvent will dissolve the polymer (Dempsey *et al.*, 2013).

2.3.2 Vapour sensing in conductive polymer composites

Composites consisting of electrically conductive filler particles dispersed in an insulating matrix have been studied for over 60 years, where typical fillers include carbon black, expanded graphite and carbon nanotubes. The filler loading affects the intrinsic conductivity of the composite; for a loading at or above the percolation threshold the conductivity is seen to increase dramatically. This is primarily explained by percolation theory or effective medium models. Under exposure to a vapour, the polymer matrix may swell, increasing the distance between neighbouring filler particles so that the electrical conductivity of the composite decreases. Swelling of the polymer is greatest when there is a match between the solubility parameter of the polymer and that of the

vapour. Each element in an array of sensors can be designed to give an optimum response to collection of chemical vapours, thus producing an electronic nose. The typical response time is usually of the order of a few minutes. The largest responses are produced by operating the system close to the percolative conduction threshold. However, near the percolation threshold, small changes in filler content result in large changes in electrical response so that it becomes difficult to produce reliable sensors capable of giving repeatable results. Here, the material consists of nickel particles fully wetted by a silicone elastomeric binder. Because the nickel particles are completely wetted by the polymer, even at loadings above the percolation threshold there is no direct contact between adjacent particles and the material has a very high resistance.

However, upon any mechanical deformation, the material has been shown to exhibit a very large decrease in resistance. For example, during compression the sample's resistance can fall by a factor of $> 10^{14}$. It has also been shown that charge concentration at the tips of the spiky filler particles results in large electric fields, so that charge transport occurs through field-assisted quantum tunnelling rather than by direct contact between the particles.

The granular form of QTC material can be used to produce a vapour sensor. The granules are further mixed into an additional polymer matrix, which binds and compresses the granules so that, as-made, the sensor has a low start resistance. Under exposure to a vapour, the polymer swells and releases the pressure on the granules, causing an increase in resistivity. The field-assisted quantum tunnelling mechanism means that the observed response is typically large (Graham, 2008).

2.4 QTC –vapour sensing material

Previous work on QTC material in a granular form has shown that the electrical resistance of the granules can change over several orders of magnitude upon exposure to a range of VOCs, where the response time is typically of the order of few seconds. Additionally, work by Graham *et al* investigated the dispersion of QTC granules in a host polymer, producing an ink material that can be printed onto electrodes, in order to create a basic electronic nose (Hands *et al*., 2012). Peratech Ltd. already holds a patent regarding the vapour sensing properties of this material. Further development of this

material may make it suitable for screen printing, allowing an electronic nose to be printed onto a wide range of base materials quickly and cheaply. Inkjet printing has shown to be a viable option for other vapour sensors, for example polythiophene conductive polymers (Dempsey *et al,* 2013).

CHAPTER 3 ANALYSIS OF QTC VAPOUR SENSOR

A series of experiments were performed to investigate the response of QTC sensor, to acetone and ammonia vapours. The QTC sensor response was recorded and the obtained data was used to determine the practical applicability of QTC in a vapour sensing device.

3.1 Chemicals

Acetone (96%) was obtained from Sigma Aldrich whereas ammonium hydroxide (37%) was supplied by Acros organics. Both reagents were used without further purification.

3.2 QTC Sensors

Peratech, The company provided two types of fully fabricated QTC sensors based on size. The smaller sensor was of 5mm and the larger sensor ranges 15mm. Both sensors were printed on polyester film and had interdigitated electrodes with silver connectors as shown in Figure 3.

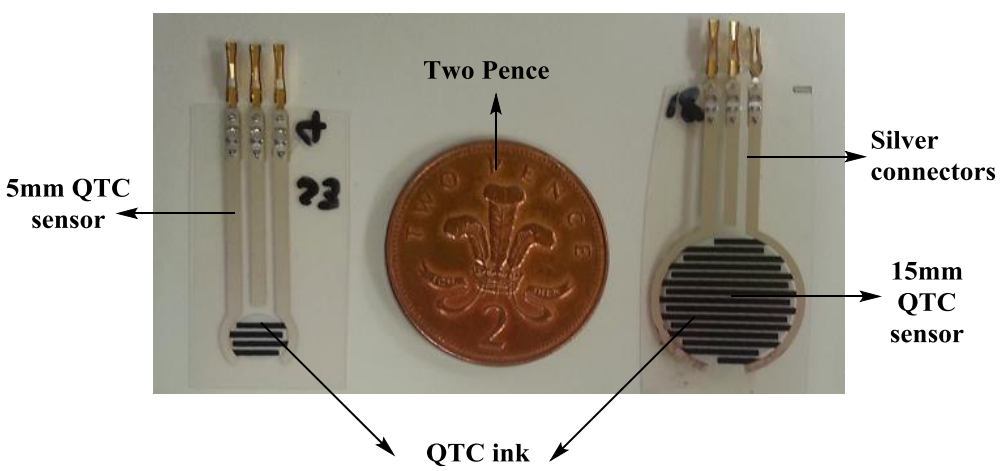

Figure 3 QTC vapour sensors

The vapour sensing unit used to expose QTC sensors to solvent vapours was designed and built in laboratory as schematically shown in Figure 4.

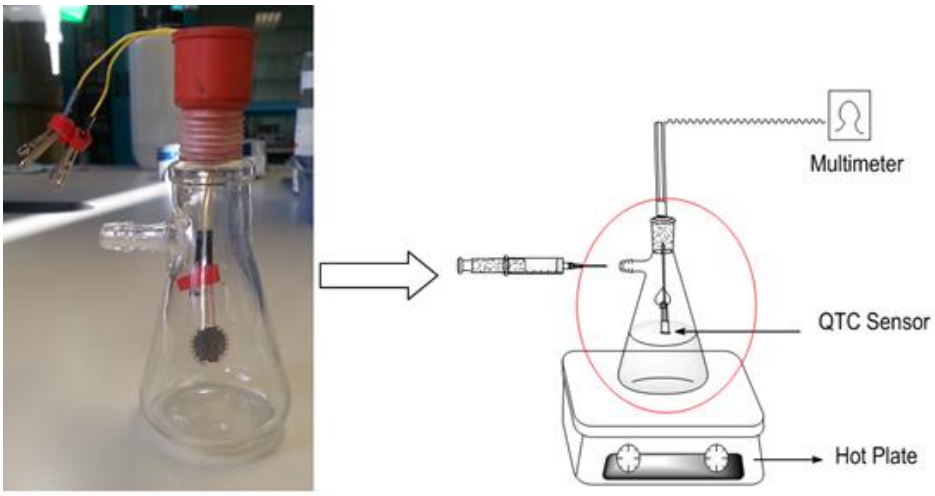

Figure 4 Laboratory setup for vapour sensing experiments

The experimental setup comprised of Büchner flask sealed with parafilm and a rubber stopper to prevent escape of volatile vapours. QTC sensor was connected to digital multimeter and inserted into the flask through wires to record any change in resistivity while sensor exposed to volatile compound (VC). To recorde any change in resistivity small volume of known concentration of particular VC was added into the flask through syringe and the flask was placed onto the hot plate for rapid evaporation of solvent. Once initial and final readings were obtained the experiment was repeated with higher concentration until a set of concentrations are tested against QTC sensors.

3.3 Vapour sensing experiments

It is important to identify solvent vapours which readily create significant response in order to investigate the effects of the variables of sample composition. Initially two volatile compounds (VC's) acetone and ammonia were considered for exposure. A series of experiments were performed to investigate the response of QTC sensor against selected VC's in liquid and gaseous forms. The results obtained after exposure are discussed in detail in the later part of this chapter.

3.3.1 QTC sensor exposed to liquid VOCs

The first set of experiment was based on various concentrations of aceone exposed to both 5mm and 15mm QTC sensors. Initially a set of solutions were prepared in distilled

water with concentration ranging from 0.1 ppm to 100,000 ppm for acetone and ammonia, respectively.

The initial resistance of the QTC sensor was recorded before exposure to any solution. After recording the initial resistance, the lowest concentration (0.1ppm) acetone solution was exposed to the sensor and change in resistivity was recorded. After the exposure, the sensor was purged with nitrogen (inert) gas to regain the initial resistance. Once the sensor regain steady reading it was exposed to second concentration of acetone comprising 0.5ppm. The whole procedure was repeated with each of the acetone concentrations and data was recorded for further interpretation and analysis. In addition, QTC sensor was also tested against various concentrations of ammonia and change in resistance was recorded.

3.3.2 QTC sensor exposed to gaseous VOCs

After the study involving QTC sensor exposed to liquid solutions, it was found that water vapours had remarkable effect. It was found that the resistivity kept increasing because of the vapour pressure. A repeat set of experiments were performed under the same reaction conditions but results varied significantly. It was obvious that water vapours had a significant effect on the resistance of sensors. Therefore, the next task was to eliminate the effect of water vapours by studying the sensors in gaseous form.

As the second series of experiments were aimed to eliminate water vapour, therefore volume of air in the flask (250ml) was employed to dilute the VOC to desired concentration instead of water. The flask was placed on the hot plate for rapid evaporation as shown in Figure 4. The initial resistivity of QTC sensor was recorded before exposing to vapours. The same procedure was followed as mentioned previously. Approximately 0.1 ml of selected VC was added into the flask and any change in resistivity was noted after complete evaporation of liquid acetone. Once steady resistance was obtained another volume of 0.1 ml of acetone was added into the flask and change of resistivity was recorded. The data obtained through exposing gaseous forms of acetone and ammonia concentrations ranging from 1ppm to 100,000ppm for both types of sensor was interpreted through graph discussed in detail under results and discussion.

3.4 Results and discussion

The exposure of QTC sensor to volatile solvent showed a different response magnitude for each vapour type, which is promising as a potential future application. However, time constraints lead to only acetone and ammonia vapours being used as the test vapours for initial experiments. Both acetone and ammonia generated the largest response magnitude upon exposure to the QTC sensor, and as such, they were selected as volatile compounds. The vapour sensors developed using compressed granules showed large, fast response to a range of organic vapours over a wide range of vapour concentrations. However the design of the experimental setup meant that repeatability of sample conditions was poor. It was difficult to obtaining the same starting resistance with both 5mm and 15mm QTC sensor.

QTC sensors exposed to various concentrations of ammonia and acetone exhibited that there is considerable effect of water vapours on the resistivity therefore to obtain a baseline and minimise the effect of water on the volatile vapours QTC sensors were exposed to deionised water. The change in resistance was recorded and all of the values were taken in kΩ. Once exposed to water, the QTC sensor exhibited a remarkable change in resistivity which kept increasing with the passage of time.

The magnitude of peak response was measured for each set of experiments. The magnitude was calculated as the difference between resistance values immediately before exposure (initial resistance R_i) and immediately before purging is initiated (final resistance R_f). Thus the difference $\Delta R = R_f - R_i$ can be calculated for each response of the sensor to each exposure. In order to interpret the data from different concentrations with different start resistances, the response was normalised by dividing difference by R_i resistance values, a $\Delta R/R_i$ value for each response was therefore used in data analysis.

The normalised resistivity values of both 5mm and 15mm QTC sensors were plotted against various concentrations. Figure 5 shows the change in resistivity of both types of QTC sensors against various liquid concentrations of acetone. It is apparent that the resistivity of 5mm QTC sensors increased as the concentration increased but started to decrease at the highest concentration. Compared to that, the resistivity pattern of the 15mm QTC sensor remained almost the same. There was a consistent increase in

resistivity along with increase in acetone concentration which increased sharply at highest concentration. To investigate the change in resistivity at lower concentration, the data was plotted on an expanded scale as shown in Figure 5(b).

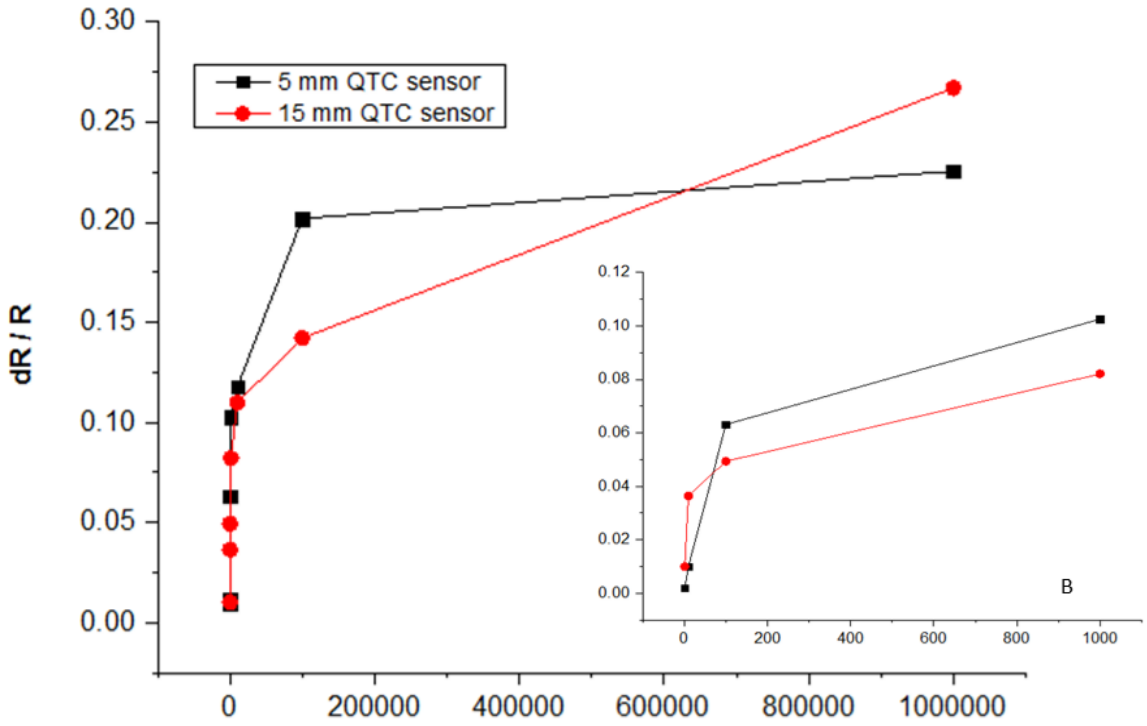

Figure 5 Change in resistance of QTC Sensors (5mm &15mm) exposed to various acetone concentrations in water

Similarly, the normalised resistivity values of 5mm and 15mm QTC sensors were plotted against various liquid concentration of ammonia. There was steady increase in resistivity along with concentration for both types of sensor as shown in Figure 6. Similarly the changes in resistivity at lower concentration were plotted to highlight the smaller changes seen in Figure 6(b).

A possible explanation for such a change in resistance could be explained on the basis of interactions between gas molecules and QTC sensors. Previous studies have shown that polymers swells once exposed to VOCs vapours. The swelling of polymer after vapour absorption could be detected through change in resistivity. In the case of QTC sensors the extent of swelling is based on filler loading density. Any swelling in the QTC material causes the filler density fall below the percolation threshold, producing the large response. The electrical response obtained through swelling of material is directly proportional to vapour concentration.

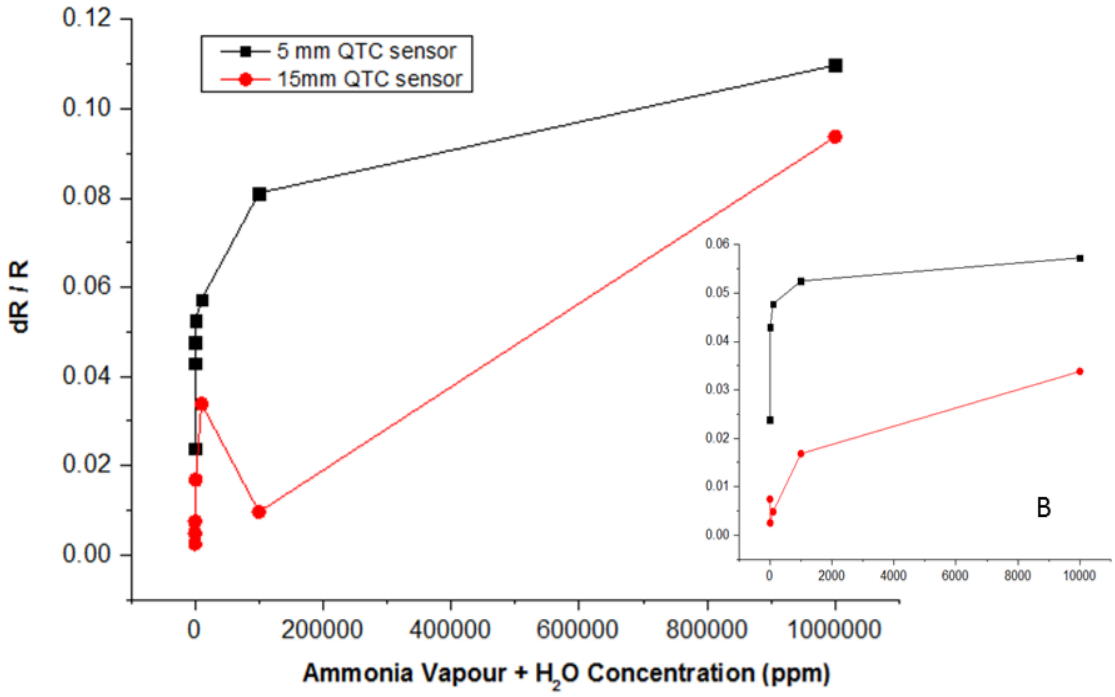

Figure 6 **Change in resistance of QTC Sensors (5mm &15mm) exposed to various ammonia concentrations in water**

It was also found that QTC vapour sensors had high sensitivity towards water vapours. Water vapours had remarkable effect and because of the vapour pressure the resistivity increased which indicates the saturation of the polymer matrix. Furthermore, it is also found that different vapour types can generate varying degree of swelling within the same material which explains the change in resistivity pattern of acetone and ammonia concentrations. Once a polymer is exposed to any volatile compound, the weight of the polymer could increases gradually along with the time. The full dynamics behind the response to vapour absorption could be discussed by referring to Case-II diffusion (Graham, 2008).

Case-II diffusion can be divided into two stages, the initiation stage where solvent concentration builds closer to the polymeric surface and front formation occurs and later stage where the concentration at front propagates linearly. The rate of solvent absorption is comparable to the swelling rate controlled by the steady deformation of the surrounding polymer. The deformation is subsequently dependant on the vapour pressure of the solvent which drives the swelling and viscoelasticity of the polymer.

It has been shown that there could be large decrease in viscoelasticity and increases in diffusivity over just a small change of solvent concentration. These changes are caused by plasticisation of the polymer upon absorption of the solvent. The solvent absorption causes a decrease in polymer relaxation times, ranging from long times associated with glassy behaviour, to short times associated to rubbery behaviour.

The solvent vapours occupy regions of space between polymer chains. If we consider the polymer in the glassy state, the polymer chains are in a random close-packed arrangement therefore it has less free volume. Thus, if the concentration, or volume fraction, of solvent is greater than the volume fraction of free volume then there is a resistance of the polymer to absorption and relaxation times are longer and the polymer chains will have limited space to move apart. If the polymer is at a temperature above its glass transition temperature and rubbery in nature, its molecular chains can readily move apart by processes involving rotation of the main chains and so concentration equilibrium is obtained very quickly.

Once the QTC sensor was exposed and change of resistance was recorded, the sensors were purged with nitrogen and resistance started to drop again. The rate of recovery was much slower than the rate of response. This could be attributed to different vapour concentration differentials between the two regimes which describe a wave-front propagating through a material with a concentration gradient driving it into the polymer. However, upon leaving the polymer there was no wave front and so solvent molecules are drawn out because of a concentration gradient caused by the differences of vapour pressure inside and outside of the polymer material of the analyte.

After QTC sensor was purged for 10 minutes, it was exposed to sample again. This time the sample did not return to its original start resistance upon recovery. The subsequent responses recovered to a consistent baseline after the second exposure. The step up from the start to the baseline through the rest of the responses was attributed to stress relaxation in the polymer upon first exposure.

Upon first exposure, the molecular chains in the polymer expanded due to swelling which reduces the entropy of the system. After the first purge the polymer chains are relaxed and reformed to a more energetically favourable formation that was different to the initial conditions. This was a one off occurrence and was only seen in the first

response as subsequent expansions then returned to the new configuration during purging.

After being exposed to VC concentrations in water both QTC sensors were exposed to gaseous vapours of acetone and ammonia changes in resistance were recorded as shown in Figures 7 and 8 respectively. Once water vapour effect was eliminated a linear change in resistance was obtained against each VC. It shows that the QTC vapour sensors are concentrations dependent as there is larger response for higher concentrations.

The graph shown in Figures 7 and 8 shows two distinct trends in the data, a "low concentration" region, 100 ppm and a "high concentration" region 100,000 ppm. This suggests that the trends relate to the fundamental absorption physics rather than any polymer specific attributes. In order to further justify the relation to Case-II diffusion, study shown by Hui (1987) was taken into consideration.

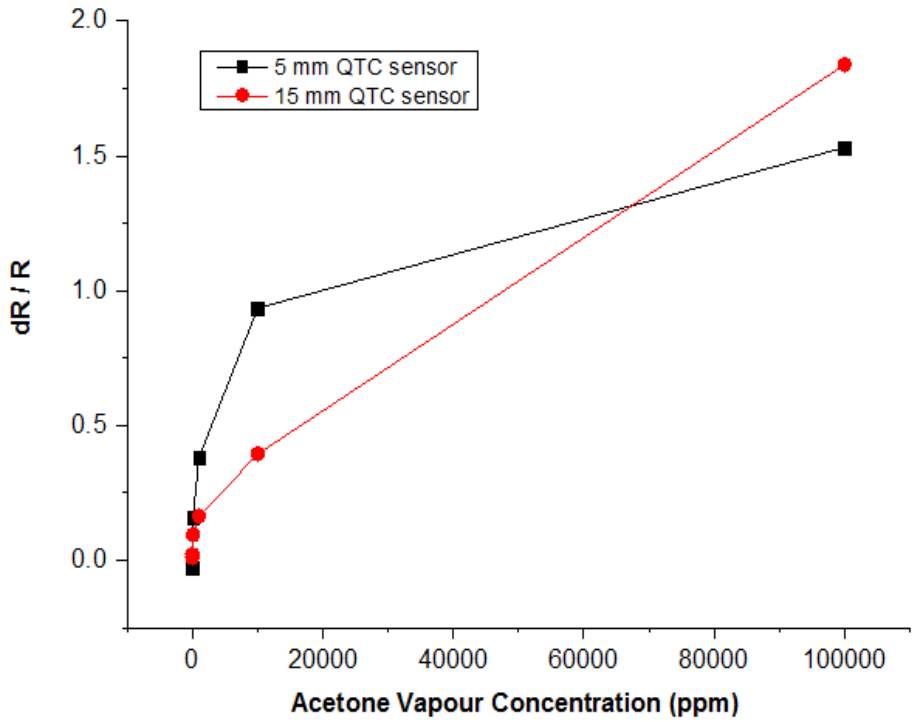

Figure 7 Change in resistance of QTC Sensors (5mm & 15mm) exposed to acetone vapours

The repeated experiments of both types of QTC sensors 15mm and 5mm exposed to various concentrations of selected volatile compounds showed considerable variation over each experiment therefore a calibration bar graph was constructed to calculate standard mean deviation.

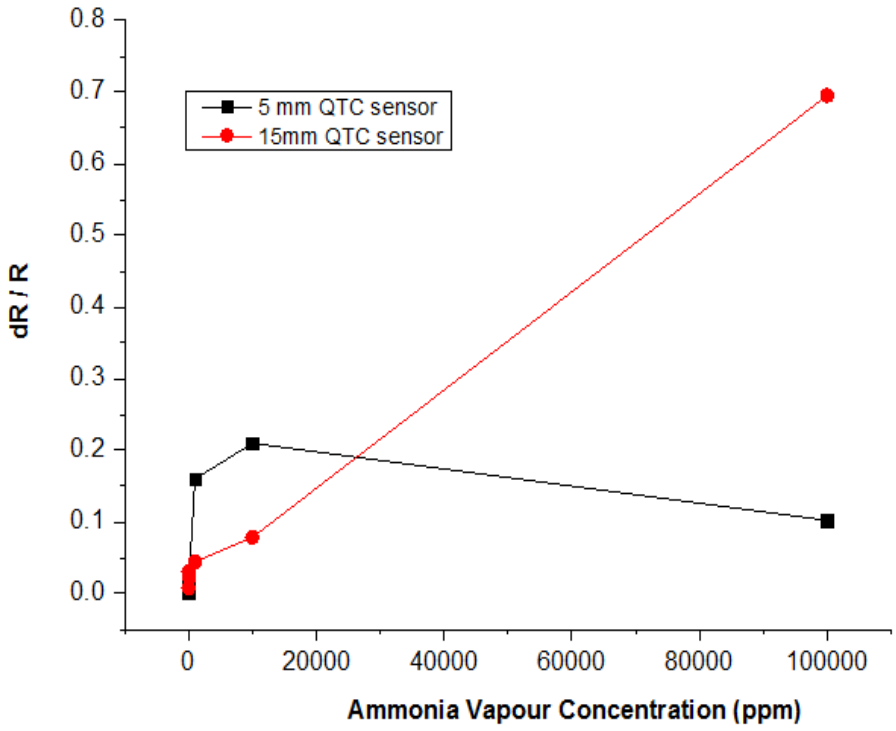

Figure 8 Change in resistance of QTC Sensors (5mm & 15mm) exposed to ammonia vapours

It is proposed that in the low concentration regime the conduction is not in fact a direct result of swelling in the polymer, but a result of changing dielectric permittivity, acting against the swelling induced resistance increase. The dielectric constant of the vapour analyte acetone is 20.7 and of ammonia 16.5. The dielectric constants for both analytes are higher than that of the silicone rubber in the QTC sensor which is 2.81. Therefore, upon absorption the polymer matrix experiences an induced permittivity increase. This decreases the energy barriers for charge transport and therefore acts as a counter to the resistance decrease caused by swelling. In order for this effect to occur, there can only be a very small amount of swelling, with the absorbed analyte molecules filling voids within the polymer matrix to provide an effective increase in overall dielectric constant. As the concentration increases so does the swelling, countering the effects of the dielectric change. The void filling mechanism will remain dominant until the degree of swelling outweighs it. This hypothesis is supported by similar work conducted on vapour absorbing conductive polymers by Krasteva, Hands and Graham (Hands, 2003; Graham, 2008; Krasteva, 2007).

Figure 9 shows the standard deviation of QTC sensors against selected concentrations of acetone. There was very high deviation of results among experiments repeated for

multiple times. Figure 9 (a) represents standard deviation of 5mm QTC sensor whereas Figure 9 (b) represents standard deviation of 15 mm QTC sensor against various concentration of acetone.

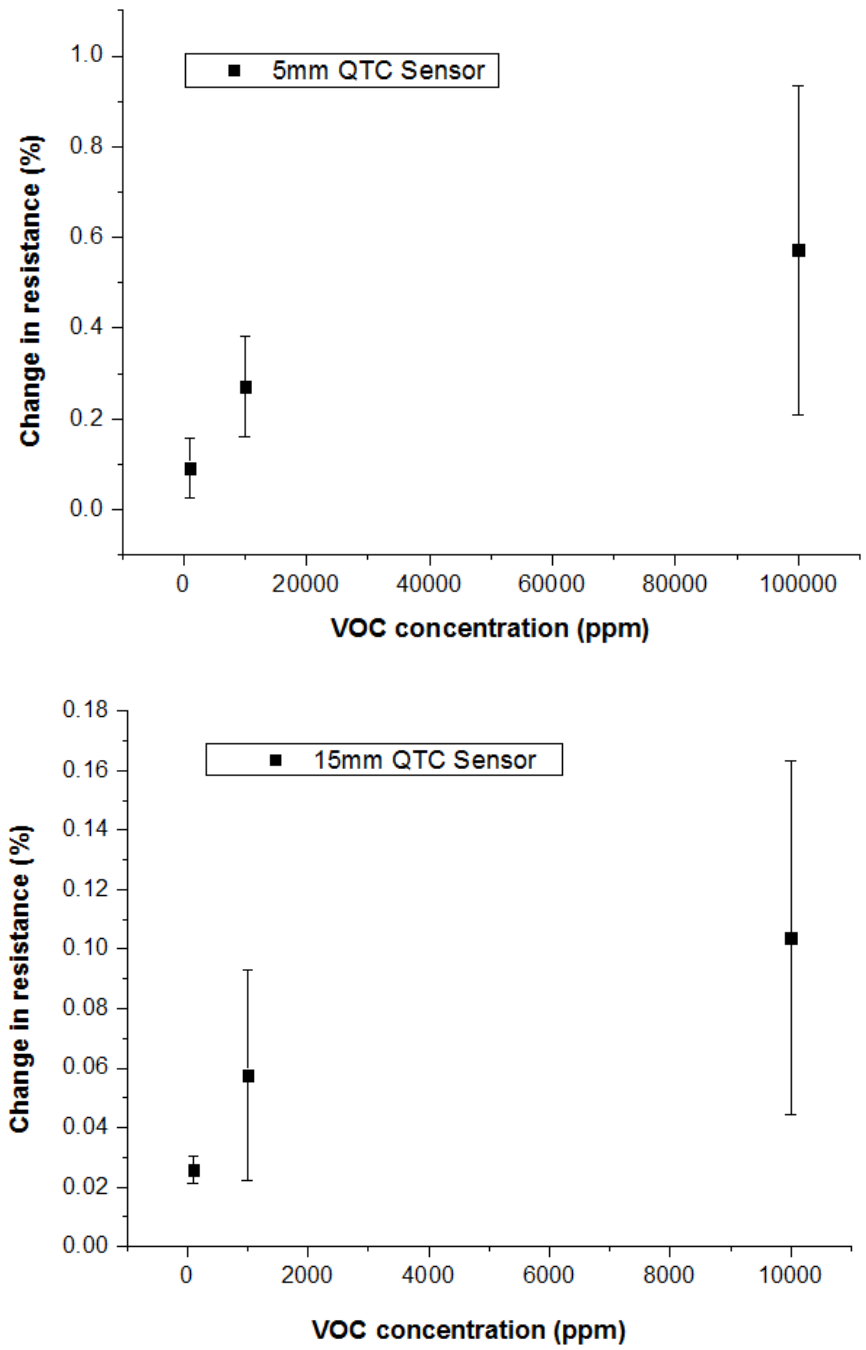

Figure 9 Standard deviation of QTC sensors (a) 5mm QTC sensor (b) 15 mm QTC sensor

3.5 Conclusions

The aim of this research work was to investigate and develop the use of intrinsically conductive QTC vapour sensors, in order to assess their potential for use in the electronic nose. Similar to other conductive polymer composites, comprising an electrically conductive filler particle embedded in a polymer matrix, QTC granules exhibit an increase in resistance upon the exposure to volatile vapours. However, the resistance of these granules may increase by over 8 orders of magnitude in a time of typically a few seconds, which offers a vast improvement over other polymer composites where the response is smaller and over a longer period of time. QTC materials have been shown to undergo field-assisted quantum tunnelling, rather than direct percolative conduction, aided by the nano scale surface morphology which allows charge build-up at the spiky tips on the nickel particles. This gives them an increased sensitivity. Sensors made from QTC granules bound in a PVC polymer had been tested with high concentrations of ammonia and acetone vapours.

In summary, QTC sensor exhibit great potential for application in a number of different sensing areas. The conduction mechanisms within the material provide extreme sensitivity in the QTC vapour sensors, making it unique to other materials used in similar applications.

3.6 Future research potential

Future work could aim to expand on the preliminary results reported here in order to fully assess the repeatability of the sensor response to ammonia and acetone vapours. As sensor aging might cause an effect, which cannot be explained by the difference in the test vapour concentration alone, a range of experiments should be designed in order to fully characterise the effect of aging on the QTC granular sensors. Heat treatment may be used to give an accelerated aging process.Furthermore, a wider range of VOCs may be tested, to further investigate the role of solubility parameters in characterising the magnitude of the observed response.

Despite the interesting results seen, the study on QTC vapour sensor was discontinued due to a confidentiality issue between Peratech and Ministry of Defence.

SECTION II

Immunosensors for the Detection of *Neisseria gonorrhoea* and *Chlamydia trachomatis*

CHAPTER 4 INTRODUCTION TO IMPEDOMETRIC IMMUNOSENSORS

4.1 Biosensors - general review

Control of diseases is essential to improve in the quality of our lives, which is greatly dependent on diagnosis by monitoring various biochemical compounds in the body fluid. The diagnosis of a disease by measuring the constituents in the body fluids first took place in the middle ages. For example, diabetes mellitus was first diagnosed by tasting the sweetness of urine. The monitoring of the biochemical compounds in the body fluid require typical analytical methods for biochemical test, experts to run the tests, and time for performing clinical tests. Since the levels of various compounds in a body system are directly related to some diseases, it is possible to monitor the progress of diseases by monitoring the concentration of these compounds. Therefore, continuous, fast, and sensitive monitoring is required to measure concentration of the body fluid efficiently.

Diagnostics methods must be simple, sensitive and able to detect multiple biomarkers that exist at low concentrations in biological fluids or samples. In recent years, the demand has grown in the field of health care for simple and disposable devices that also demonstrate fast response times, are user-friendly, cost-efficient, and suitable for mass production. Biosensor technologies offer the potential to fulfil these criteria through an interdisciplinary combination of approaches from nanotechnology, chemistry and medical science. However, biosensor devices need to be further developed and improved to face these new challenges to allow, for example, multiplex analysis of several biomarkers where arrays of sensors need to be developed on the same chip. In this context, electrochemical biosensor is a promising analytical method for sensitive and selective detection of biomolecules (Shruti *et al.*, 2011).

A biosensor is generally defined as an analytical device which converts a biological response into a quantifiable and processable signal. Figure 10 adapted from Grieshaber *et al.*,2008 shows schematically the parts comprising a typical biosensor: a) bioreceptors that specifically bind to the analyte; b) an interface architecture where a specific biological event takes place and gives rise to a signal picked up by c) the transducer

element; the transducer signal is converted to an electronic signal and amplified by a detector circuit using the appropriate reference and sent for processing by d) computer software to be converted to a meaningful physical parameter describing the process being investigated; finally, the resulting quantity has to be presented through e) an interface to the human operator. Biosensors can be applied to a large variety of samples including body fluids, food samples, cell cultures and be used to analyse environmental samples (Grieshaber *et al.,* 2008).

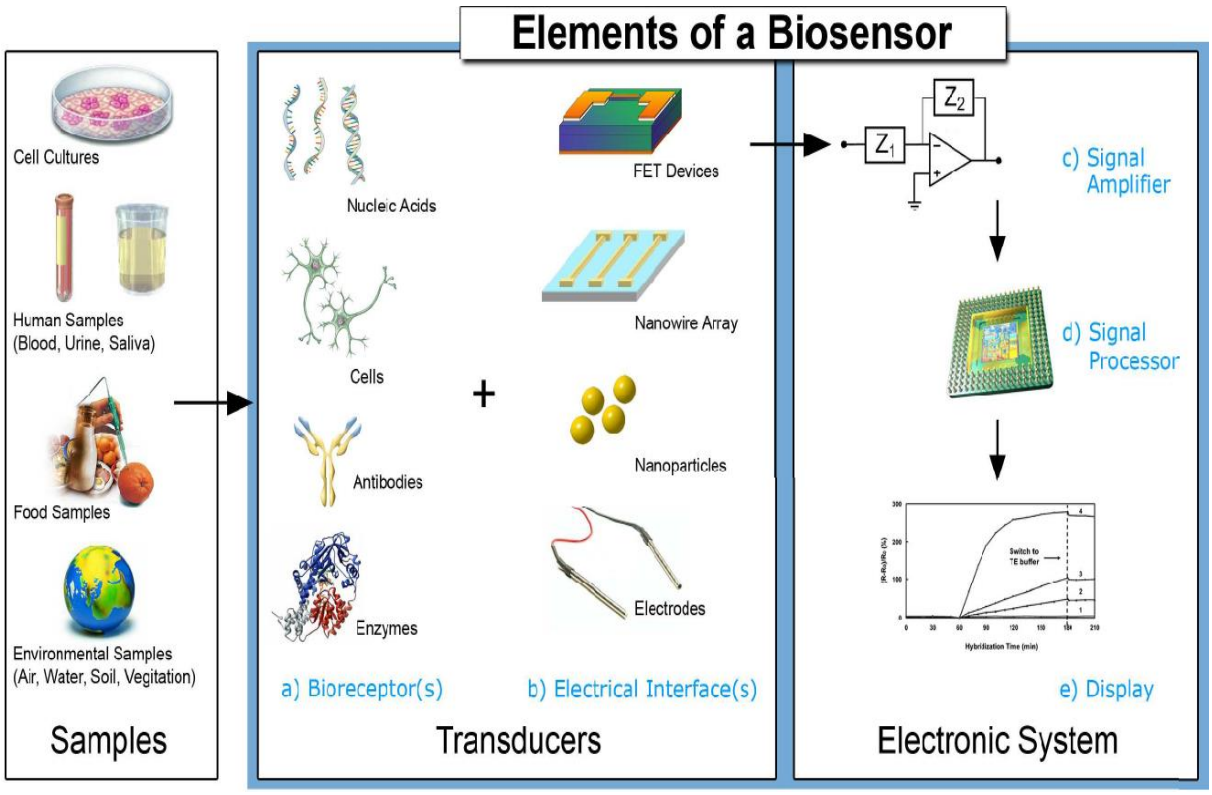

Figure 10 Elements and selected compounds of a typical biosensor

4.2 Bio-receptors and immobilisation methods

Biosensors may be classified according to the biological specificity conferring mechanism, or to the mode of signal transduction or, alternatively, a combination of the two. Figure 11 shows typical biosensor transduction techniques and some bio-receptors in a hierarchical format. Biological elements include enzymes, antibodies, micro-organisms, biological tissue, and organelles. The method of transduction depends on the

type of physicochemical change resulting from the sensing event (Lu *et al.,* 2011). The most commonly used sensing elements and transducers are described as follows.

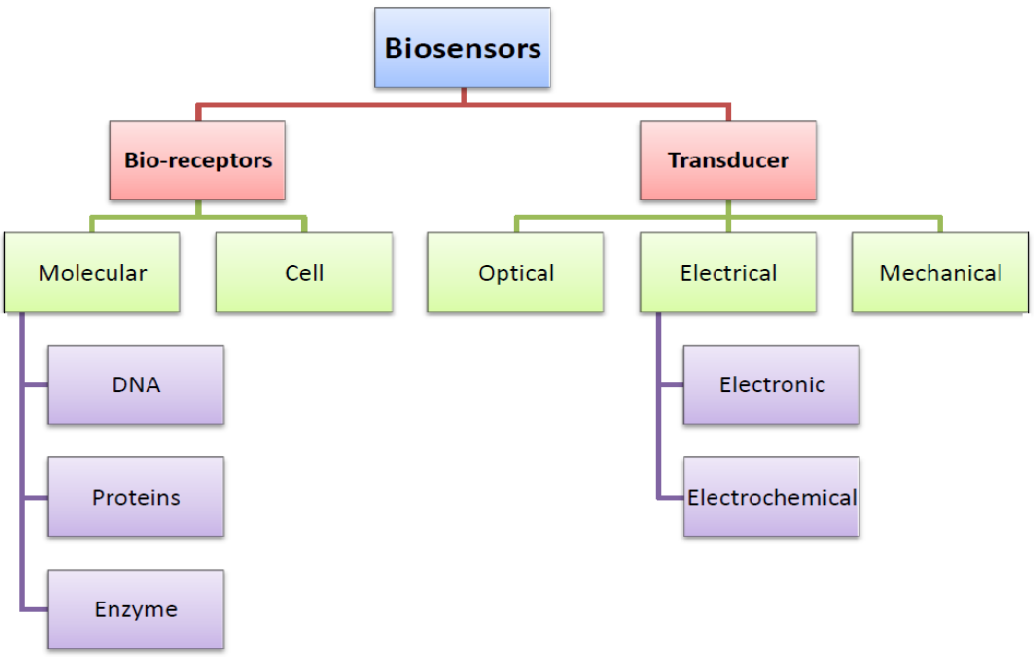

Figure 11 Biosensor transduction techniques coupled with bio-receptors

4.2.1 Sensing elements

4.2.1.1 Enzymes

Enzymes are proteins having high catalytic activity and selectivity towards substrates (Cheng *et al.,* 2007). Their commercial availability at high purity levels makes them very attractive for mass production of enzyme sensors. Their main limitations are that pH, ionic strength, chemical inhibitors, and temperature affect their activity. Enzymes have been immobilised at the surface of the transducer by adsorption, covalent attachment, entrapment in a gel or an electrochemically generated polymer, in bilipid membranes or in solution behind a selective membrane and are commonly coupled to electrochemical and fibre optic transducers.

4.2.1.2 Antibodies

Antibodies are proteins that show outstanding selectivity. They are produced by b-lymphocytes in response to antigenic structures, that is, substances foreign to the organism. Molecules larger than about 10 kDa can stimulate an immune response. Smaller molecules for example vitamins or steroids can be antigenic but they do not cause an immune response unless they are conjugated to larger ones like bovine serum albumin. Many antibodies are commercially available and commonly used in immunoassays. Antibodies are usually immobilised on the surface of the transducer by covalent attachment through conjugation of amino, carboxyl, aldehyde, or sulphydryl groups. The surface of the transducer must be previously functionalised with an amino, carboxyl, hydroxyl, or other group. Antibodies share similar limitations with enzymes. Furthermore, binding may not be reversible and regeneration of the surface may require drastic changes in conditions such as low pH, high ionic strength, detergents, etc. Therefore, efforts are being made to produce low cost, single use sensors. Probably the main potential advantage of immunosensors over traditional immunoassays is that they could allow faster and in-field measurements.

4.2.1.3 Micro-organisms

The use of micro-organisms as biological elements in biosensors is based on the measurement of their metabolism, in many cases accompanied by the consumption of oxygen or carbon dioxide, and is, in most cases, measured electrochemically (Pie and Prasad, 2006). Microbial cells have the advantage of being cheaper than enzymes or antibodies, can be more stable, and can carry out several complex reactions involving enzymes and cofactors. Conversely, they are less selective than enzymes; and have longer response and recovery times, and may require more frequent calibration.

4.2.2 Transducer surfaces for electrochemical biosensors

Once a suitable bioreceptor has been selected, it must be immobilised onto solid phase transducers to form a functional sensing platform. The type of transducer surface depends on the properties of the bioreceptor and the interrogation method to be used.

Impedance immunosensors are typically constructed either using a self assembled monolayer (SAM) as a base layer (Billah *et al.,* 2008; Chaki and Vijayamohanan 2002; Hays *et al.,* 2006; Milner *et al.,* 2009b) or a conducting polymer base layer (Barton *et al.,* 2009; 2008). Bioreceptors are often immobilised by physioabsorption onto a conducting polymer surface (e.g. polypyrrole or polyaniline) or an SAM (e.g. phospholipids) by covalent coupling to a linker molecule via carboxyl, maleimido, amino or thiol groups (Billah *et al.,* 2008; Gooding *et al.,* 2003; Hays *et al.,* 2006; Karyakin *et al.,* 2000; Munoz-Berbel *et al.,* 2008; Wark *et al.,* 2010; Weiss *et al.,* 2005). The linker molecule is attached to the transducer surface using streptavidin/biotin affinity, silanisation, protein A or direct attachment (Brynda *et al.,* 1998; Liebes *et al.,* 2009; Prieto-Simon *et al.,* 2008; Zheng *et al.,* 2010).

Which ever transducer material is chosen for use in the biosensor construction, the immobilisation of the bioreceptor to the surface is fundamental for functionality and integrity of the sensor i.e. the antibody epitope binding site must be orientated to facilitate binding to the target analyte. Often steric hindrance and denaturation of the bioreceptor is an issue for reproducibility and sensitivity (Bonroy *et al.,* 2006; Chaki and Vijayamohanan 2002; Chen *et al.,* 2003; Milner *et al.,* 2009a; Prieto-Simon *et al.,* 2008). Another problem can be non specific binding between bioreceptors and non-target molecules. This can be addressed by selecting appropriate and highly specific bioreceptors for the bacterial antigens and by blocking the non-specific binding sites of the sensor surface with a protein or chemical agent (e.g. BSA) before use.

Organic conjugated polymers (conducting polymers) have emerged as potential candidates for electrochemical sensors. Due to their straightforward preparation methods, unique properties, and stability in air, conducting polymers have been applied to energy storage, electrochemical devices, memory devices, chemical sensors, and electrocatalysts (Bhadra *et al.,* 2009).

Conducting polymers (CPs) are polyconjugated polymers with electronic properties resembling those of metals, while retaining properties of conventional organic polymers. Since the observation of the remarkably high electrical conductivity of polyacetylene, a number of other conjugated polymers have been transformed from an insulating into a highly conductive state (Hui *et al*., 2009). The most widely investigated conducting

polymers include polyacetylene, polyaniline, polypyrrole and polythiophene are shown in the Figure 12.

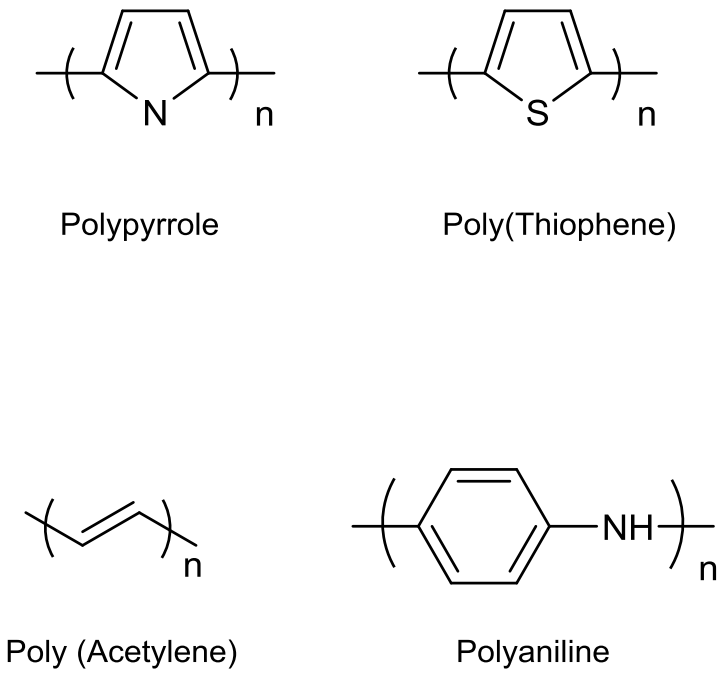

Figure 12 Structures of some common CP's

Conducting polymers are also known for their ability to be compatible with biological molecules in neutral aqueous solutions. Moreover, the polymer itself can be modified to bind biomolecules to a biosensor. Another advantage of conducting polymers is that the electrochemical synthesis allows direct deposition of a polymer film on the electrode substrate followed by biomolecules immobilisation. It is thus possible to control the spatial distribution of the immobilised enzymes, the film thickness, and modulation of enzyme activity. Conducting polymers can act as an electron promoter.

Mechanism of electro polymerisation of CP can be best explained by using PPy as an example presented in Figure 13 (Ahuja *et al*., 2007). The first step involves the formation of pyrrole radical cation by electrode surface. It is followed by dimerisation by deprotonation. The dimer oxidises slightly more easily than the monomer and thus gets reoxidised to allow further coupling reaction to proceed. The oxidation potential of the polymer is always lower than that of monomer. The polymer is electrochemically ionised to a conducting state and the overall electrical neutrality is maintained by incorporation of the counter ion from the supporting electrolyte. This is essential because precipitation of the unoxidised, insulating polymer would stop the reaction.

During the process of electrochemical polymerisation negatively charged molecules are present in the electrolytic solution such as anions.

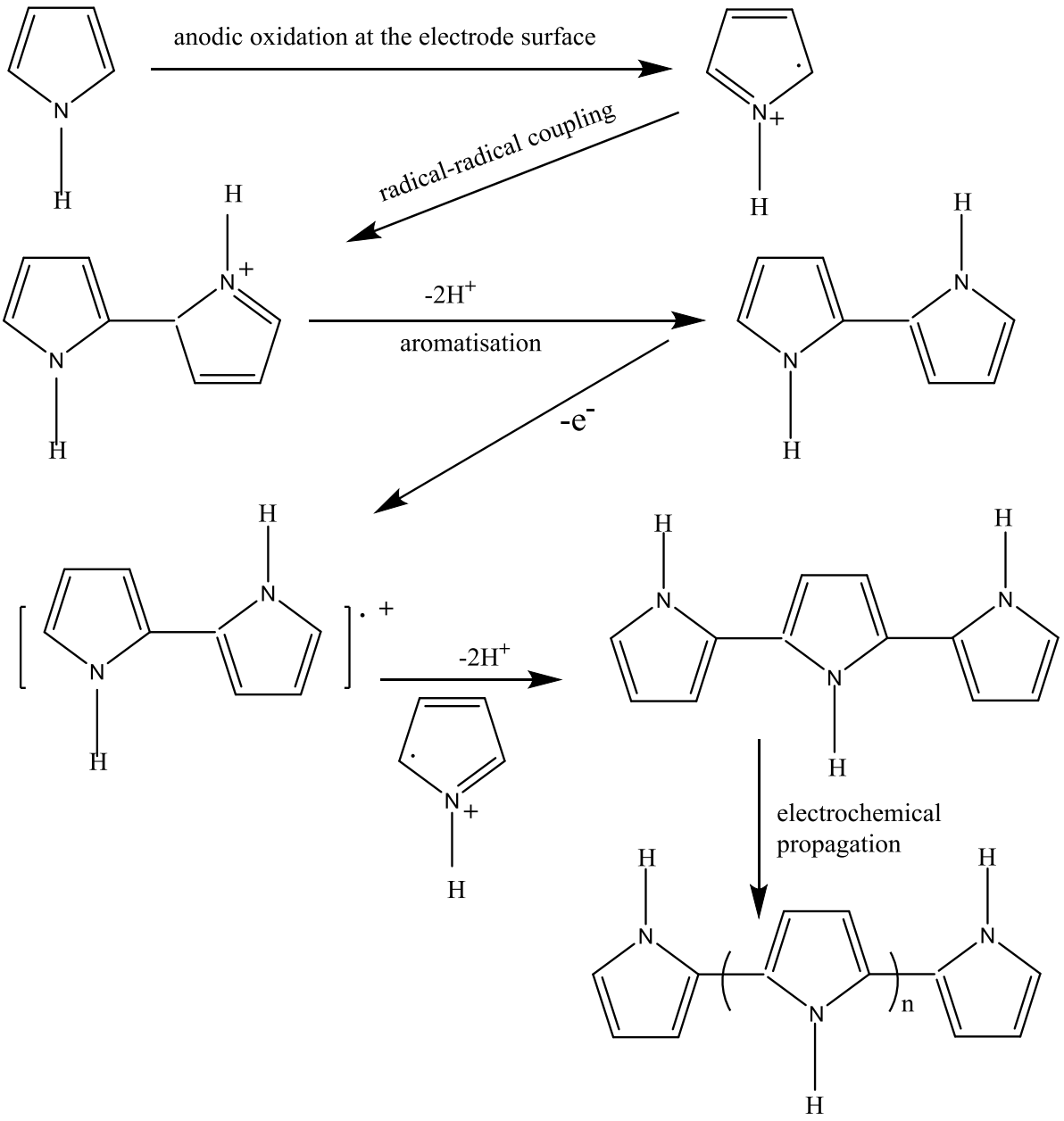

Figure 13 Electropolymerisation mechanism of polypyrrole

Polymers and enzymes can be embedded into the positively charged backbone as dopants (Cassagneau *et al.*, 2002). This promotes an attractive route to trap functional molecules within organic polymers during their electro generation of electrode, and offers a new means to fabricate a range of novel composite material with novel properties (Ahuja *et al.*, 2007).

Moreover, conducting polymers can be deposited over defined areas of electrodes. The unique properties of conducting polymers have been exploited for the fabrication of electrochemical sensors and biosensors (Rahman, 2008). For example, an amperometric biosensor can be easily fabricated by entrapping the enzyme during electrochemical polymerisation (Musameh, 2003).

4.3 Electrochemistry as a signal transduction for biosensor

There are a range of sensors which use electrochemical interrogation including current, potential and impedance changes to transduce the biological recognition event (Katz and Willner, 2003; Wang, 2006). Electrochemical biosensors were first developed in 1962 with the glucose electrode (Clark and Lyons, 1962) and combine the analytical power of electrochemical techniques with the specificity of biological recognition (Bard and Faulkner, 2001; Wang, 2006).

Early efforts concentrated on sensing small analytes e.g. metabolites such as urea or lactate and glucose (Albers *et al.,* 2003) amperometrically, but in recent years the detection of larger macromolecules has emerged. In this case, the binding event of the antigen to the bioreceptors is detected using electrochemical transduction across the sensor surface (Barton *et al.,* 2009; Billah *et al.,* 2008; Hays *et al.,* 2006; Hianik *et al.,* 2001). The complex formed from the bioreceptor and the antigen binding at the sensor surface results in a detectable change, converted into a quantitative amperometric, potentiometric or impedimetric signal. Compared with nearly all other analytical techniques, electrochemical detection assays have the advantage of being inexpensive, robust and relatively simple to operate (Brossier *et al.,* 2001; Ding *et al.,* 2008; Hahn *et al.,* 2005; Kerman *et al.,* 2004; Milner *et al.,* 2009a; Pumera *et al.,* 2007).

The use of biosensors for medical, industrial and environmental analysis (Kuila *et al.,* 2011) is very important. The popularity of analytical biosensors is due to their specific detection, simple use and low cost. For example an electrochemical biosensor can be used to detect Salmonella and E. coli in less than 90 min (Arora *et al.,* 2011). The iconic example being the modern glucose biosensor which requires nl to a few µl of whole blood to report the glucose concentration under one minute.

4.3.1 Amperometry

In amperometric biosensors, the potential between the two electrodes is set and the current produced by the oxidation or reduction of electroactive species is measured and correlated to the concentration of the analyte of interest. In amperometry, the immobilised redox active species is usually an enzyme and contains a prosthetic group or a co-substrate that is reduced and facilitates the catalysed oxidation of a substrate, such as lactate or glucose for example. The ability of the enzyme's groups or co-substrate to re-oxidise is related to the measurable current across the electrode. This allows the enzyme to be regenerated for further chemical reactions. Electrons are only transferred, causing a signal to be generated, when the enzyme is re-reduced.

Amperometry relies on the system under investigation to drive a redox reaction after a current has been applied, usually through a redox active species immobilised on the surface of the electrode, whereas in voltammetry, the voltage is measured when no current is passed (Wijayawardhana, 2002; Yu *et al*., 2005).

In amperometry, the immobilised redox active species is usually an enzyme and contains a prosthetic group or a co-substrate that is reduced and facilitates the catalysed oxidation of a substrate, such as lactate or glucose for example. The ability of the enzyme's groups or co-substrate to re-oxidise is related to the measurable current across the electrode. This allows the enzyme to be regenerated for further chemical reactions. Electrons are only transferred, causing a signal to be generated, when the enzyme is re-reduced.

How much current is produced can be determined using Faraday's law shown in equation 3,

$$I = nFAJ \qquad (3)$$

Where I = current produced, typically nA – mA, n = the number of electrons transferred, F = Faraday's constant, A = area of the electrode, J = flux coefficient, which is the transfer of substrate to the electrode.

The current produced is also dependent on the voltage between the electrodes, so a potentiostat is used to fix the potential, against which the current can be measured.

The first glucose biosensor developed by Clark and Lyons (1962) was based on an oxygen electrode that had a selective permeable membrane to which an enzyme was attached. Although it was successful to detect oxygen yet it was not possible to determine between the oxygen already in the sample and quantity generated through the redox process catalysed by glucose oxidase. After first generation amperometric sensor several generations have since evolved (Habermüller *et al.,* 2000). The main issues with amperometric sensors are- a) differentiation between generated molecules and those present already; b) ensuring adequate diffusion of the analyte from solution to the electrode to measure the signal response and c) fluids in which sensors aim to detect such as blood also contain many compounds that will undergo oxidation or reduction at the same potential as the molecule the sensor aims to detect.

Subsequent generations overcame some of these issues by using electroactive mediators that replaced the natural oxygen co-substrate of the enzyme (Cass *et al.,* 1984; Kulys *et al.,* 1980). These usually contained soluble metal complexes, such as $Fe(CN_6)^{3-/4-}$ to transport the electrons between the enzyme and the electrode, resulting in the use of lower positive potentials. This limited the interference from other redox species within the sample solution. The mediators were located in the solution surrounding the electrode, or incorporated into the electrode surface, resulting in 'reagentless' biosensors. However, typically concentrations of mediator had to be high within the surface due to leaching during measurement. Eventually, amperometric sensors were later developed to include immobilisation to the electrode using electroactive materials such as copolymers including polypyrrole and polyaniline (Habermüller *et al.,* 2000; Reiter *et al.,* 2001; Warriner *et al.,* 1997; Warrington, 2001). This negated the need for external electroactive mediators and allowed rapid electron transfer through the polymer matrix that could also be used to immobilise the enzyme.

4.3.2 Potentiometry

In potentiometry, the voltage is measured when no current is passed whereas in amperometry, a potential is applied and the resulting current is measured (Wijayawardhana 2002; Yu *et al.,* 2005). This electrochemical technique measures specific ion concentration and is the basis of modern pH meters. Potentiometric devices measure the accumulation of a charge potential at the working electrode compared to

the reference electrode in an electrochemical cell when zero or no significant current flows between them (D' Orazio, 2003).

Potential on an electrode depends on the ions present in the solution and their concentration. The electrochemical cells can be used to determine ions and their concentration in solution. The dependence of potential between electrodes from concentration of ions is expressed by Nernst equation shown in equation 4.

$$E = E^0 - 0.0591\ V/n \ln Q \qquad (4)$$

Where F = Faraday's constant, R = gas constant and n = charge of the ion or number of electrons participating in the reaction, E = electrode potential, E^0= standard potential of the electrode, T = temperature in kelvins, and Q= reaction quotient.

When the reaction quotient is equal to the equilibrium constant of the reaction for a given temperature, i.e. when the concentration of species are at their equilibrium values, the Nernst equation gives the equilibrium voltage of the half-cell (or the full cell), which is zero at equilibrium (Wahl, 2005).

It is very important to explain the Nernst Equation here because it is an equation that can be used to determine the equilibrium reduction potential of a half-cell in an electrochemical cell. In the electrochemical cell, if a high impedance device like a voltmeter is placed between the indicator and reference electrodes, no current will flow between the two compartments. Under these conditions it is possible to measure the potential difference between the two electrodes. The standard cell potential, E^0 will be the measured cell potential where all reactants are present at unit activity. The unit activity can be defined as an effective concentration of a particular species along with all the interionic interactions of the ions present in the solution.

The redox system under equilibrium conditions can be characterised through Nernst equation. It allows the calculation of relative activities of the species in a redox reaction as a function of the measured electrode potential (E) and the standard reduction potential (E^0) for the half reaction. For the general redox reaction given in equation 5,

$$aOx + ne^- \leftrightarrows bRed \qquad (5)$$

The Nernst equation takes the form as shown in equation 6.

$$E = E^0 - RT/nF \ln (Red)^b/(Ox)^a \quad (6)$$

Where R is the gas constant (8.314 J K^{-1} mol^{-1}), T is temperature in K, n is the stoichiometric number of electrons involved in the process, F is the Faraday constant (96,485 C mol^{-1}) and $(Red)^b$ and $(Ox)^a$ are the activities of the reduced and oxidised members of the redox pair, respectively. At 25°C, the value of (RT/F) is equal to 0.0591, and the Nernst equation becomes as given in equation 7,

$$E = E^0 - 0.0591\ V/n \log_{10} (Red)^b/(Ox)^a \quad (7)$$

Potentiometry relies on a change in the ionic concentration of a solution due to enzyme action in a sensing device which creates a measurable potential. The potential generated is related to the concentration of the substrate and the range for ion detection is often broad, usually 10^{-4} – 10^{-2} M, but accuracy can be low. This is because potentiometric devices can be poorly selective, leading to false positive detection.

The potentiometric biosensor is recommended for the determination of simple ions, especially for pH and physiological electrolytes. Bioaffinity-based biosensor systems are strongly desired for the needs of clinical immuno- and genoanalysis (Koncki, 2007). However, at present potentiometry seems rather to be not promising for such applications. Label-based methods with various radiochemical, enzymatic, fluorescent and nanoparticle markers exhibit significantly better analytical characteristics when amperometric and optical detection systems are applied. Potentiometric label free sensing schemes are based on the unclear principles of signal generation and are strongly influenced by non-specific effects from several components of analysed samples.

4.3.3 Impedance

EIS provide electrochemical examination of electrical properties of electrode surface; on the other hand it can be called as electrochemical surface characterisation. Therefore, it is possible to study the electrode surface after any modification. In biosensor technology EIS is used for monitoring biosensor modifications, layer formation on electrode surface and binding kinetics between molecules such as DNAs, receptors, antibodies, antigens,

proteins, ions etc. The binding kinetics of molecules can be calculated by recording impedance spectrum for subjected molecules which leads to label-free detection (Uygun *et al.,* 2013).

Impedance is a measure of the ability of a circuit to resist the flow of electrical current, but electrochemical impedance is usually used by applying an AC potential to an electrochemical cell and then measuring the current through the cell. When sinusoidal potential is applied the AC current signal is received as a response. This current signal can be considered as a sum of sinusoidal functions (a Fourier series). For AC conditions the Ohm's law work for changing currents, and can be redefine as shown in equation 8, where Z is the impedance of the system.

$$E = I \times Z \qquad (8)$$

The impedance can be calculated by setting the input potential and measuring the induced current.

Electrochemical impedance spectroscopy (EIS) has become an attractive method for biosensor development because of simple detection system. Since every part of human body, such as cells, proteins, and deoxyribonucleic acid (DNA) have their unique impedance value, EIS appears as a well suited and powerful technique for biological sensing. Furthermore, the availability of quantitative data (resistance, capacitance, dielectric permittivity, etc.) offered by EIS may provide in-depth information of biochemical phenomena occurring at electrode-electrolyte surface (Yusof *et al*., 2011).

4.3.4 Voltammetry

Cyclic voltammetry (CV) is a type of potentiodynamic electrochemical measurement. It is widely used technique to acquire qualitative information about electrochemical reaction. Cyclic voltammetry can measure various types of reactions such as thermodynamics of redox processes, the kinetics of heterogeneous electron-transfer reactions and coupled chemical reactions or adsorption process. In a cyclic voltammetry experiment, the potential of the working electrode is measured against a reference electrode which maintains a constant potential, and the resulting applied potential produces an excitation signal. Figure 14 shows a typical reduction occurring from (a) to (d) and an oxidation occurring from (d) to (g). In the forward scan, the

potential first scans negatively, starting from a greater potential (a) and ending at a lower potential (d). The potential extreme (d) is called the switching potential, and is the point where the voltage is sufficient enough to have caused an oxidation or reduction of an analyte. The reverse scan occurs from (d) to (g), and is where the potential scans positively.

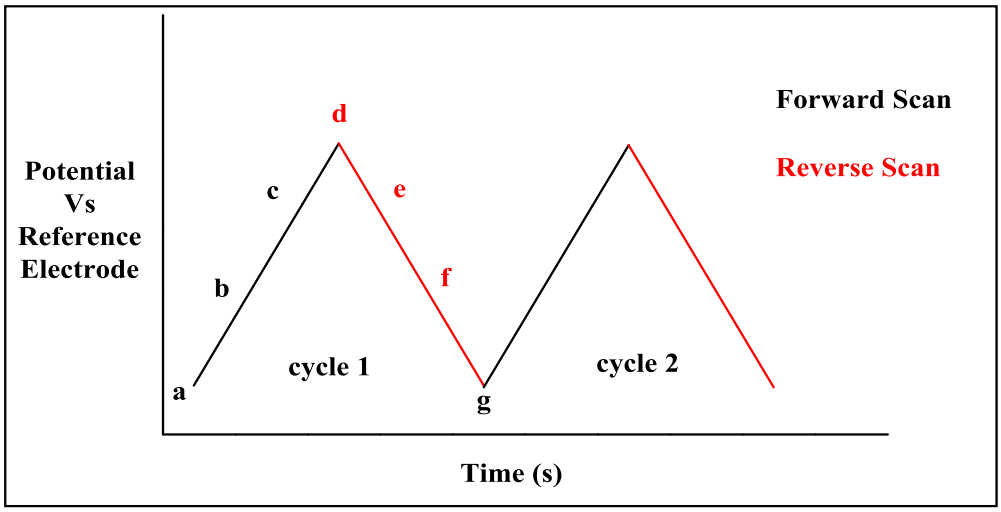

Figure 14 A cyclic voltammetric excitation signal

It is important to note that some analytes undergo oxidation first, in which case the potential would first scan positively. This cycle can be repeated, and the scan rate can be varied. The slope of the excitation signal gives the scan rate used.

Depending on the information required, single or multiple cycles can be used. During the potential sweep, a potentiostat measure the current resulting from the applied potential. The resulting plot of the current at the working electrode vs. the applied voltage gives the cyclic voltammogram of the reaction (Bard *et al.,* 2000).

A cyclic voltammogram is obtained by measuring the current at the working electrode during the potential scans. Figure 15 shows a cyclic voltammogram resulting from a single electron reduction and oxidation.

Consider the following reversible reaction shown in equation 9:

$$M^{+} + e^{-} \leftrightarrows M \qquad (9)$$

The reduction process occurs from (a) the initial potential to (d) the switching potential. In this region the potential is scanned negatively to cause a reduction. The resulting current is called cathodic current (i_{pc}). The corresponding peak potential occurs at (c), and is called the cathodic peak potential (E_{pc}). The E_{pc} is reached when all of the substrate at the surface of the electrode has been reduced. After reaching the switching potential (d), the potential scans positively from (d) to (g). This results in anodic current (I_{pa}) and oxidation to occur. The peak potential at (f) called as anodic peak potential (E_{pa}) is reached when all of the substrate at the surface of the electrode has been oxidised. The important parameters for a cyclic voltammogram are the peak potentials E_p and peak currents i_p shown in Figure 15.

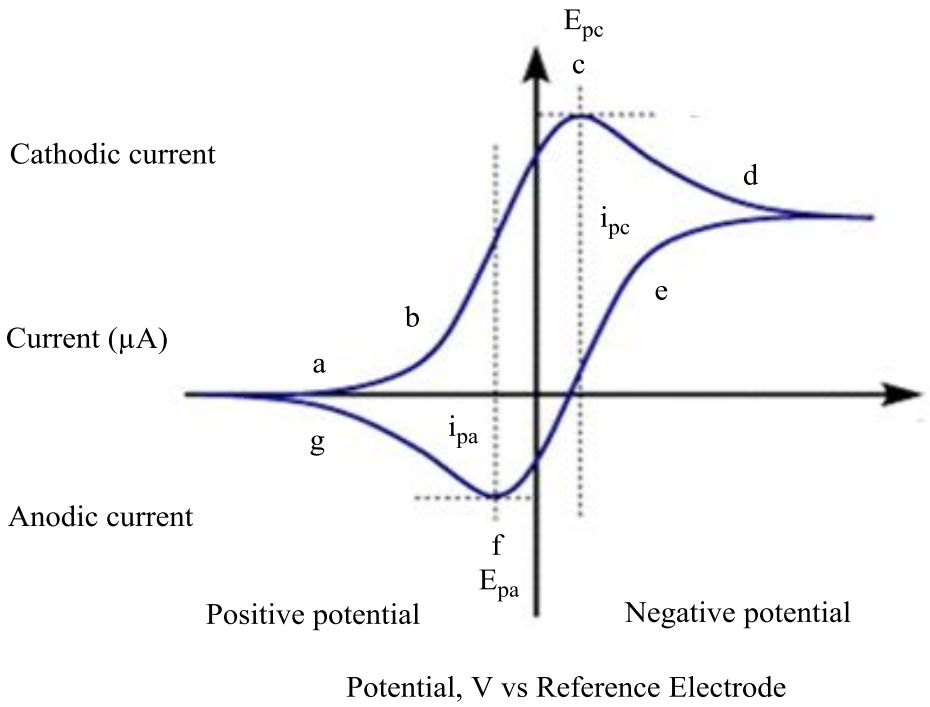

Figure 15 Typical voltammogram of a reversible redox couple (Research, 2014)

4.4 Other methods of signal transduction for biosensors

4.4.1 Optical transduction

Optical biosensors are generally based on two types of detection methods. The first detection method is fluorescence-based whereas second detection method is label-free.

In fluorescence-based detection, either target molecules or biorecognition molecules are labelled with fluorescent tags, such as dyes; the intensity of the fluorescence indicates the presence of the target molecules and the interaction strength between target and biorecognition molecules.

In the label-free detection, target molecules are not labelled or altered, and are detected in their natural forms. This type of detection is relatively easy and cheaper to perform. Label-free detection also allows quantitative as well as kinetic measurement of molecular interaction. Some label-free detection mechanisms measure refractive index (RI) change induced by molecular interactions. The change in refractive index is related to the sample concentration or surface density, instead of total sample mass (Fan and Suter, 2009).

4.4.2 Electromechanical transduction

Electromechanical biosensors include piezoelectric techniques such as quartz crystal microbalance (QCM) surface acoustic wave devices and atomic force microscopy (AFM).

4.4.2.1 Surface acoustic wave devices (SAW)

SAW devices used in biosensors are based on acoustic waves. The working principle of SAW device is based on change in resonant frequency of the wave which propagates through or across the sensor. For such type of sensors thick quartz crystals are used along with interdigitated metal electrode arrays. The acoustic Rayleigh waves are propagated between the electrode array and across the crystal surface. The waves have both longitudinal and vertical components which are sensitive to changes in the mass and mechanical properties of substance bound to the surface. It is possible to detect molecule through change in frequency of the wave however it is not suitable for biological samples because of attenuation of waves in liquid medium. SAW devices are often used in gaseous environment. (Lee *et al*., 2009)

4.4.2.2 Atomic force microscopy (AFM)

Atomic force microscopy (AFM) utilises a sharp tipped oscillating cantilever to characterise the surface of an electrode. The cantilever it is deflected because of the

interaction of the tip with the functionalised surface, e.g. the smooth electrode surface gets modified after immobilisation of biological components. Atomic Force Microscopy (AFM) can provide sensitive resources to measure and to map the surface chemistry information and to quantify the adhesive or repulsive forces associated to inorganic materials and biological samples, through the control of chemical interactions between the AFM tip and the sample. Among AFM techniques, there is a very useful tool known as Chemical Force Microscopy (CFM), which is based on AFM tips chemically modified with specific exposed functional groups, carefully architected to carry out a specific function in a system. There are several ways to functionalise the AFM tip. Two of the commonest methods are known as mixing self-assembled monolayers (SAMs) and vacuum, thermal evaporation thermal vapor deposition and even, sputtering. The method of self-assembled monolayers (SAMs) is widely used to functionalise tips and surfaces. Terminal functional groups (-COOH, $-CH_3$) are grafted onto alkane thiols that spontaneously form monolayers, under controlled conditions, on gold surfaces (Steffens *et al*., 2012). The electrode surface can be characterised by observing the amplitude, phase and resonance frequency of the cantilever (Ferreira *et al*., 2008). The signal is extrapolated to give a pseudo-3D image of the surface, whereby individual molecules can be visible if the substrate surface is flat enough. The best AFM images can be obtained by scanning surfaces that are atomically flat, such as silicon wafers coated in gold.

4.4.2.3 Quartz crystal microbalance (QCM)

QCM is based on a quartz crystal which oscillates at a certain frequency when an alternating voltage is applied. The quartz surface is often coated in a thin gold, or other metal, layer which doubles as a conductor for the AC current flowing and also provides an attachment surface for a bio-receptor. QCM crystal transducers are known to be highly precise, stable oscillators and are capable of detecting subnanogram mass changes (Yao *et al*., 2010). The deposition of the bio-receptor can be monitored by the frequency down-shift caused by the additional mass on the crystal. Once the bio-receptor has bound to the surface then the crystal can be rinsed before addition of the biological target in suspension which again, adds to the mass and reduces the frequency further.

4.5 Electrochemical impedance spectroscopy (EIS)

Impedimetric immunosensors have recently received particular attention due to number of attractive characteristics such as mass production of low cost electrode, cost effective instrumentation, the ability to be miniaturised and to be integrated into multi-array or microprocessor-controlled diagnostic tools, remote control of implanted sensors, etc. Due to these characteristics, electrochemical impedance spectroscopy (EIS) based sensors are considered as promising candidates for use at on-site applications.

4.5.1 Theory of electrochemical impedance spectroscopy for biosensors

In an enzyme based biosensor, a molecule needs to be transformed into another molecule by enzyme to obtain electroactive signal. Electroactive signal can be disturbed by the presence of other molecules, which has same oxidation reduction potentials as analyte molecule. Electrochemical impedance spectroscopy overcomes this problem and provides non-electroactive detection of molecules.

Electrochemical impedance immunosensor is based upon change in conductivity across the immunosensor surface after the hybridisation between the bio-receptor and the bacterial antigen. The response is analysed in terms of change in the resistance and/or double-layer capacitance following analyte capture (Wijayawardhana, 2002). Detection of the change in capacitance is easier to measure as no reference electrode is required and therefore it is more durable 'in-field'. However, this technique can be less sensitive and non-specific binding can lead to false positive results (Katz and Willner 2003; Wijayawardhana 2002). This can be overcome by 'blocking' the non-specific binding sites of the surface with a protein, such as Bovine serum albumin (BSA).

Impedance spectroscopy is a very powerful tool for the analysis of interfacial properties such as changes of modified electrodes upon bio-recognition events occurring at the modified surfaces. Formation of the complex on a conductive or semi-conductive surface alters the capacitance and the resistance at the surface electrolyte interface. Furthermore, the build-up of the sensing biomaterial film on the conductive or semi-conductive support alters the capacitance and resistance properties of the solid support-electrolyte interface. Impedance measurements provide detailed information on capacitance/resistance changes occurring at conductive or semi-conductive surfaces.

Impedance spectroscopy for biosensor technology has the same working principle as other electrochemical measuring techniques. EIS is composed of electrical circuits based on AC current, which is generally used for impedimetric experiments.

Impedance is calculated as the ratio between the change in the applied voltage and the change in the current of an electrochemical cell which is measured as a phase angle shift between the sine wave of amplitude *vs.* time. This is determined using the equations 10,

$$V = V_m \sin \omega t \qquad (10)$$

Where t = time in seconds; ω = the angular frequency in radians sec^{-1} and is equal to 2πf, where f is the frequency in Hz; V_m = amplitude and V = the voltage at any given instant.

The resulting current, I, is then given by equation 11,

$$I = I_m \sin (\omega t + \theta) \qquad (11)$$

Where t = time in seconds; ω = the angular frequency in radians sec^{-1} and is equal to 2πf, where f is the frequency in Hz; I_m = the maximum current; θ = the phase angle and I = the current at any given instant.

The complex impedance can be presented as the sum of the real, Z', and imaginary, Z" components that originate mainly from the resistance and capacitance of the cell, respectively. The most popular formats for evaluating electrochemical impedance data are the Nyquist and Bode plots. In the Nyquist format, the imaginary impedance component (Z") is plotted against the real impedance component (Z') at each excitation frequency giving information about the electrified interface and the electron transfer reaction. Whereas in the Bode format, both the logarithm of the absolute impedance, |Z| and the phase shift, φ, are plotted against the logarithm of the excitation frequency (Pie and Parsad, 2012).

In order to express the characterisation of surfaces, layers or membranes after the immobilisation of biomolecules and bacteria binding, EIS is often analysed using an equivalent circuit which is used to curve fit the experimental data and extracts the necessary information about the electrical parameters responsible for the impedance change. Since the electrochemical cell is a complex system, more than one circuit model

can fit the experimental data. The simplest, and in fact the most frequently used equivalent circuit for modelling the EIS experimental data is the so-called Randles circuit shown in Figure 16(A), which comprises the uncompensated resistance of the electrolyte (R_s), in series with the capacitance of the dielectric layer (C_{dl}), the charge-transfer resistance (R_{ct}) and the Warburg impedance (Z_w). In the Nyquist plot shown in Figure 16(B), a typical shape of a Nyquist plot includes a semicircle region lying on the real axis followed by a straight line.

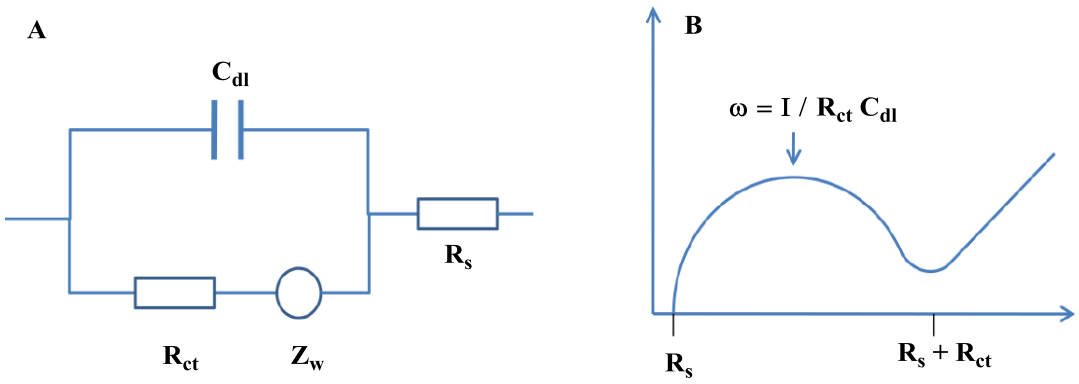

Figure 16 (A) the typical Nyquist diagram for the AC impedance measurements; (B) the Randle equivalent circuit

The linear part ($\psi = \pi/4$), observed at the low frequency range, implies a mass-transfer limited process, whereas the semicircle portion, observed at high frequency range, implies a charge-transfer limited process. From the Nyquist plot, the values for R_s and R_{ct} can be easily determined. The double layer capacitance can be calculated from the frequency at the maximum of the semicircle ($\omega = 2\ f = 1/R_{ct}\ C_{dl}$). The charge-transfer resistance R_{ct} and the double layer capacitance C_{dl} are the most important electrical parameters in analysing the impedance signal change for detection of bacteria.

This technique is useful for transduction of bioaffinity events in connection to modern electrochemical immunosensors and DNA sensors. Such transduction of bioaffinity relies on the increased insulation of the electrode surface on binding large biomolecules in respect to redox probes, e.g. $Fe(CN_6)^{3-/4-}$, present in the solution. Therefore, in essence, the antigen binding retards the electron transfer, which is measurable by electrochemical impedance spectroscopy (EIS).

4.5.1.1 Equivalent circuit

Useful data can be extrapolated from EIS experimental impedance spectra by modelling the electrochemical transformations occurring at the electrode-solution interface using corresponding components of the electronic equivalent circuitry.

The common model for fitting impedance spectra is Randles equivalent circuit shown in Figure. 15 (Randles, 1947) which shows the corresponding components of a circuit to impedance spectra, where R_s is the solution resistance, R_{ct} is the charge transfer resistance, C_{dl} is the charged double layer and Z_w is Warburg impedance.

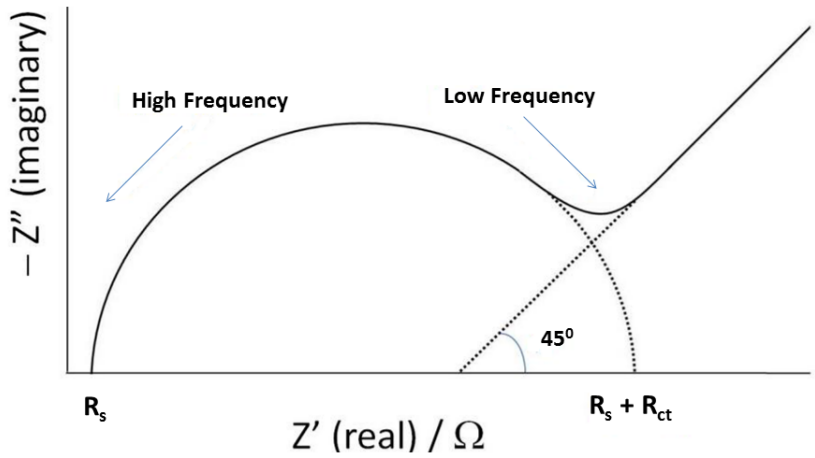

Figure 17 Typical Nyquist plot showing the real and imaginary component of impedance

A typical Nyquist plot shown in Figure 17 depicts that the resistance of the solution (R_s) and the charge transfer resistance (R_{ct}) can be calculated from the interception of the (Z') x axis. Warburg impedance is characteristically shown by a 45° angle of data at low frequencies. This model arises from processes where either charge or electrons are transferred across the interface (faradaic) or when current flows without charge transfer (non-faradaic) resulting charge accumulation on a capacitor.

The surface resistance can be divided into two parts - charge transfer resistance (R_{ct}) and Warburg impedance (Z_w). R_{ct} results from resistance of the surface to electron movement across the insulating layer (from bioreceptor, or bioreceptor binding analyte), whereas Warburg impedance correlates to diffusion of ions through the bulk solution or

mass transfer resistance, which is frequency dependent. Warburg impedance can be reduced or eliminated completely by using an electroactive mediator such as $Fe(CN_6)^{3-/4-}$. R_s is the resistance of the solution between the electrodes in an electrochemical cell and arises from a finite conductance of ions in the bulk solution. This is often constant before and after analyte capture due to the use of a buffered mediator, which makes R_{ct} the main resistive component of impedance.

4.5.1.2 Double- layer capacitance

When an electrolyte comes in contact with a metallic electrode, there is an ion electron exchange. The term "double layer" refers to the displacement of electrical charges associated with the electrode surface exposed to aqueous solution. There is a tendency for ions in the solution to combine with the metallic electrode and also for the metallic ions to enter the solution (Barsoukov, 2005).

The basic type of charge distribution proposed by Helmholtz (1879) postulated that there exists a layer of charge of one sign tightly bound to the electrode and a layer of charge of the opposite sign in the electrolyte. This separation is called the electrical double layer and is measured in ionic dimensions.

A schematic representation of an electrical double layer is presented in Figure 18. A plane (m) is associated with an excess concentration of electrons near the physical surface of the electrode, represented by a solid line. The inner Helmholtz plane (ihp) is associated with ions that are specifically adsorbed onto the metal surface. The outer Helmholtz plane (ohp) is the plane of closest approach for solvated ions that are free to move within the electrolyte. The ions within the electrolyte near the electrode surface contribute to a diffuse region of charge.

The Helmholtz-Gouy-Chapman model with Sterns correction is an acceptable model for representing the charge distribution dynamics at the metal solution interface, where Gouy-Chapman theory defines the electrical double layer binding and the surface charge densities. Based on this theory, as the concentration of the solution increases, a high polarisation is created between the electrode and the solution which then attracts ions to the metal surface until the separation between them continuously decreases to zero.

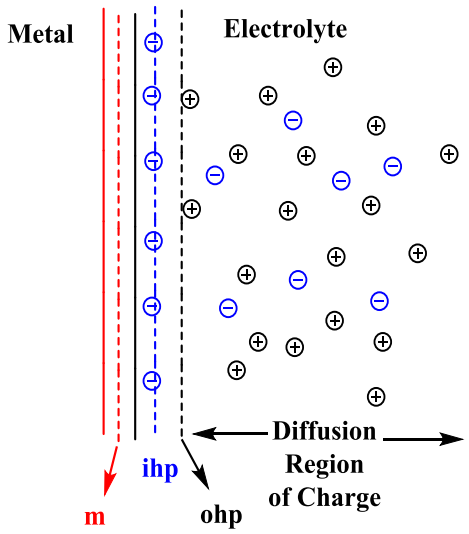

Figure 18 The structure of the electrical double layer

Electrical double layer capacitance in an immunosensor is associated with biomolecule binding after immobilisation onto electrode. As the immobilisation takes place, an electrical double layer is formed. Once solid (electrode) is immersed in the electrolyte, a major reaction with the solid-liquid interface occurs and eventually leads to an equilibrium condition. The two-way transfer resulting on the surface creates an electrical double layer, which leads to a variation of the capacitance as the biomolecule bind together.

The C_{dl} component of the Randles circuit represents the capacitance of the surface dielectric that forms between the electrode and the electrolyte, separated by the coating on the electrode surface. When the coating on an electrode is uniform, it becomes a pure resistor and can be modelled in series with the resistive components of the system. This is often not the case with biosensors as coatings are usually imperfect, which gives the Nyquist plot its distinctive semi-circular shape and results in the C_{dl} modelled in parallel to the resistive components. The behaviour of C_{dl} has been extensively studied and can be modelled on either the Helmholtz model, Gouy-Chapman model or Stern model (Bedzyk *et al.,* 1990).

C_{dl} occurs when an electrode is immersed in an ionic solution, as an unequal distribution of charge forms generating a potential which attracts oppositely charged ions from the solution across the surface. This specifically adsorbed layer is called the Helmholtz layer.

Thermal motion of the ions results in a localised charge of the electrode and because of this a diffuse layer called 'Debye length' forms. The Debye length or thickness describes a gradient of ionic concentration formed moving away from the electrode.

Depending on the design of a biosensor, it will show a greater change in either capacitance or resistance values of impedance. For a capacitive biosensor, the bioreceptor must cover the entire electrode surface in order to produce a measurable phase shift in the current relative to the applied voltage, whilst providing sufficient attachment sites for analyte capture (Gebbert *et al.,* 1992). Any gaps in the sensing layer will allow electrons to flow through, reducing the sensitivity of capacitive changes. Although, upon analyte binding, this can be a parameter through which structural changes in the sensing layer can be measured.

When a bioreceptor does not uniformly cover the electrode surface, or causes a thick insulating layer (as often antibodies do) then the biosensor can be interrogated for changes in R_{ct} which is more dependent on thickness and polarity of the electrode surface. Immunosensors are therefore commonly based on Faradaic impedance spectroscopy as large analytes binding to and changing the thickness of the sensing layer give measurable responses for the resistive component of impedance. These sensors require a suitable sized electron mediator to enable current and potential to freely flow through the electrochemical cell, reducing the frequency dependency of the response. As such, the defects to the sensing platform caused by binding of an analyte to the bio-receptor can be measured as shifts in resistance across the electrode.

In conclusion, measurement of the resistive component of impedance is commonly used in biosensing in preference to the detection of capacitive changes. This is advantageous because it is not frequency dependent and does not require the surface of the electrode to be uniform and completely coated.

4.6 Immunosensors for rapid detection of diseases

In the 1950s, scientists began to develop tests known as immunoassays that use antibodies (physical binding, or recognition, proteins that are made by B cells, a type of

white blood cell, in the bodies of vertebrates) to bind to pathogens, as shown in Figure 19.

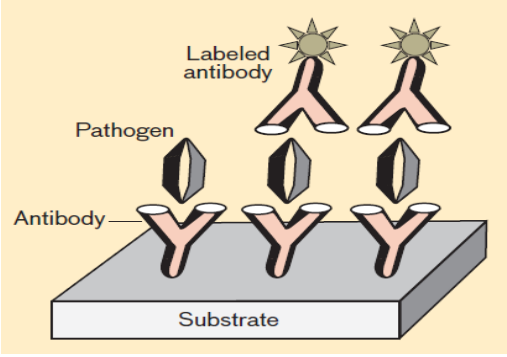

Figure 19 Schematic presentation of antibodies binding with pathogens

While ELISA can be reasonably sensitive (detection of a few thousand particles), it is generally too slow. It requires about 15 minutes for the binding events and detection to occur. A home pregnancy test is one example of this technology.

Antibody assays typically examine the surface features of pathogens; other assays test for the presence of genetic material. The immunoassay technique employs antibodies on a substrate that bind to pathogens. If the binding sites on the antibodies match the corresponding surface features on the pathogens, the pathogens will adhere to the antibodies. Corresponding labelled antibodies wash over the surface, interact with the bound pathogens, and signal the detection typically by changing colour.

Immunosensors based on the direct detection of antigen–antibody binding events are of interest since no labelled reagent is needed and the analysis is hence less complicated (Daniels, 2007) (Ivarez *et al*., 2008). For the development of such immunosensors, electrochemical transducers have been extensively assessed due to their beneficial features such as low cost, highly sensitive and easy to operate (Ricci *et al*., 2007; Liu, 2007). One of the highly sensitive electrochemical detection principles that have been applied for label-free detection is potentiostatic capacitance measurement. This technique is based on the electrical double-layer theory to measure changes in dielectric properties when an antibody–antigen complex is formed on the transducer surface (Berggren, 2001). Capacitive transducers with immobilised antibodies have proved capable to detect certain analytes with detection limits down to 10–15 pmoles per litre (Pingarro *et al*., 2008). Hence, the capacitive biosensor would be well suited for the

detection of exceedingly low levels of bacterial contaminants present in the environment. One way to obtain higher sensitivities is to enhance the association capacity of the surface by increasing the ligand density of the sensing surface. Nanoparticles have been exploited for this purpose because of their high surface- to-volume ratio and biocompatibility (Luo *et al*., 2006; Niemeyer *et al*., 2001; (Willner, 2004).

Immobilisation of antibodies on a gold surface is usually done via a self-assembled monolayer (SAM) (Chaki *et al*., 2002; Gooding *et al*., 2003). Although it is easy to prepare with strong interactions of SAM with gold, the roughness of the gold substrate can affect the formation and packing density of monolayers. One alternative is then to utilise polymer films. Electropolymerisation of polymer films has been employed as a simple and efficient method for the immobilisation of biomolecules and is widely utilised in biosensing (Gerard *et al*., 2002).

4.6.1 Detection of sexually transmitted infections (STIs)

There is also a need for rapid point-of-care diagnostic tests to ensure treatment and control of diseases, such as sexually transmitted infections have a high rate of medication complications.

4.6.1.1 Chlamydia trachomatis

Chlamydia is one of the common sexually transmitted infections (STIs) in the UK. In 2012, 206,912 people tested positive for chlamydia (NHS, 2013) out of which 64% of people diagnosed with chlamydia were under 25 years old. The majority of persons with *Chlamydia trachomatis* infection are not aware of their infection because they do not have symptoms that would prompt them to seek medical care. Consequently, screening is necessary to identify and treat this infection. Untreated, *chlamydia* infections can lead to serious complications.

On an average, ≤40% of women with untreated *chlamydia* infections experience pelvic inflammatory disease (PID) (Stamm, 1984). Of these, the majority have symptoms that are too mild or nonspecific for them to seek medical treatment. Regardless of symptom severity, the consequences of PID are severe. Of those with PID, 20% will become

infertile; 18% will experience debilitating, chronic pelvic pain; and 9% will have a life-threatening tubal pregnancy. *Chlamydia* infection during pregnancy leads to infant conjunctivitis and pneumonia and maternal postpartum endometritis. Estimated tangible costs of *chlamydia* illness in the United Kingdom exceed £1.4 billion annually. Also critical are the intangible costs, including the psychological and emotional injury caused by infertility and ectopic pregnancy.

4.6.1.2 Neisseria gonorrhoea

Neisseria gonorrhoea infections are the second most common notifiable communicable disease. The WHO estimates that 62 million cases of gonorrhoea occur each year. Gonococcal infections tend to cause a stronger inflammatory response than *chlamydia* but are typically asymptomatic in women until complications such as PID develop. *Gonorrhoea* can be acquired at birth and it can cause severe conjunctivitis, which can result in blindness if untreated and, rarely, sepsis with associated meningitis, endocarditis, or arthritis (Johnson *et al*., 2002).

4.6.1.3 Techniques to detect STIs

The standard test for detecting *Chlamydia trachomatis* and *Neisseria gonorrhoea* is culture test. However culture methods are difficult to standardise therefore other tests methods are needed which are less demanding and expensive. It is difficult to maintain the viability of bacterial organisms during transport and storage in the diverse settings in which testing is indicated. Keeping in view of growing demands for accurate and reliable diagnostic test some non-culture tests are developed which does not require viable organisms and can be automated. The first non-culture screening test for *Chlamydia trachomatis* and *Neisseria gonorrhoea* included enzyme immunoassays (EIAs), which detect specific chlamydial gonococcal antigens. Another screening test is direct fluorescent antibody (DFA) test for *chlamydia*, which uses fluorescein-conjugated monoclonal antibodies that bind specifically to bacterial antigen in smears. These antigen-detection tests were followed by nucleic acid hybridisation tests, which detect *Chlamydia* specific or *gonorrhoea*-specific deoxyribonucleic acid (DNA) or ribonucleic acid (RNA) sequences. The primary drawback of these tests, chiefly for *chlamydia*, is that they fail to detect a substantial proportion of infections.

4.7 Aim of research study

Conventional STIs detection methods are time consuming and expensive, and consequently, demand for accurate detection by rapid detection systems is increasing. The overall aim of the research work presented in this section of the thesis was to develop an impedimetric immunosensor for the rapid detection of *chlamydia* and *gonorrhoea* to aid point of care diagnosis that had a potential for mass production.

EIS methods can be employed to investigate 'labelless' detection of analytes via impedimetric transduction. EIS can be used to study electrical characteristics of electrode surface for every layer formation and every interaction between molecules along with the obtained signal variations. Once polymer is deposited onto the electrode surface, it changes the electrical characteristic of the electrode surface which subsequently changes the capacitive current which results in increase or decreases of the impedance of the system.

A number of different surface chemistries were used during fabrication of sensors but all sensors were based on gold transducer surface. Generally, sulfo-SMCC protocol was followed for the immobilisation of half generated antibodies onto conducting polymer surfaces. EIS studies were carried out on four different types of conductive polymeric surfaces. Once antibodies were successfully immobilised, all sensors were interrogated against various concentrations of respective analytes and any change in impedance was recorded and plotted in the form of Nyquist plot.

CHAPTER 5 IMMOBILISATION OF BIOMOLECULES

5.1 Introduction

The common feature of detection techniques is the biosensitive layer that confines the biological event in the very close vicinity of the transducer. A target biomolecule is detected when a specific interaction/recognition takes place in the sensitive layer where a bioreceptor has been attached. Any specific interaction gives rise to a "chemical signal" at the surface that is detected by transducer. A chemical signal can be generated by variation of local concentration of ionic species or pH in the sensitive layer, formation of absorbing or fluorescent complex species, electron transfer to a conducting surface, variation of refractive index of the sensitive layer etc.

5.2 Surface functionalisation

Biosensors are based on a large range of detection techniques ranging from electrochemistry to optics. The properties of solid support may contribute to the sensitivity of the transduction of the chemical signal. The active supports or surface layers are absolutely required for transduction of the signal. For example, electronic detection requires conductive materials (carbon, gold surface etc.). In addition, analytical properties such as senstivity, detection limit, specificity and lifetime depend on the bulk and surface properties of the solid support and the sensitising layer (functionalised surface). Senstivity and detection limit can be improved by

(1) an appropriate design of the biomolecular coupling (i.e., uniform and oriented covalent coupling);
(2) increasing the loading capacity of active molecule (surface coverage) while avoiding steric or electronic hindrance; and
(3) limiting the adsorption of biomolecules that leads to denaturation of active species and/or to background signal in case of nonspecific adsorption.

The aim of the surface functionalisation is to place detection biomolecules close to the transducer and in an environment similar to that of their natural medium where

biological interactions take place. Thus, the functional solid support can be viewed as a mixed interface.

Improved accessibility of biomolecules is achieved by attaching them to the surface through a linker that moves them away from the solid interface. The linker must be sufficiently long to eliminate unwanted steric interference from the support and preferably hydrophilic enough to be swollen in aqueous solution (Guo *et al*., 1994; Hodneland *et al*., 2002).

The interface underneath the immobilised receptors is either the bare solid support or a layer of organic molecules that confers specific properties in relation to the biomolecular assay. This sub-layer or surrounding matrix plays an important role in the functionalisation and on the analytical properties of biosensors. It may also be designed to protect the solid surface or the grafted surface from degradation.

5.3 Methods of immobilisation

Several problems surfaced relating to functioning of enzyme system like loss of enzyme (especially expensive enzymes), maintenance of enzyme stability and shelf life of the biosensors during the development of biosensors. In addition to this there is a need to reduce the time of enzymatic response and offer disposable devices, which can easily be used (Amine *et al*., 2006) in stationary or in, flow systems. In order to overcome these problems, several immobilisation procedures have been developed. The procedure of biomolecule immobilisation on conductive surfaces remains a key step for the performance of the resulting electrochemical devices. For efficient deposition of a biomolecule, it must satisfy a few pre-requisites, thus

a) there must be an efficient and stable immobilisation of the biological macromolecules on transducer surfaces;
b) it must retain its biological properties completely;
c) it should be compatible and chemically inert towards host structure; and
d) it should be accessible when immobilised (Cosnier, 2003).

Immobilised enzyme has many operational advantages over free enzyme such as reusability, enhanced stability, continuous operational mode, rapid termination of

reaction, easy separation of biocatalyst from product, and reduced cost of operation. Immobilisation of biomolecules can be carried out using many different procedures, like physical adsorption, covalent linking and electro immobilisation, while retaining the biological recognition properties of the biomolecules (Ahuja, 2007).

5.3.1 Physical adsorption

In a physical adsorption process, the biomolecule gets adsorbed in the polymer/solution interface due to static interactions between the poly-cationic matrix of the oxidised polymer and the total negative enzyme charge at a pH higher than the isoelectric point (pI) of the enzyme. But this process has some known disadvantages such as binding forces can change with pH, adsorption is limited to one monolayer on the polymer surface hence amount of enzyme incorporated is very small. Also, the biomaterial gets leached out into sample solution during measurements since it is immobilised on the outer layer of conducting polymer. This decreases the lifetime stability of enzyme electrode (Rajesh *et al*., 2005).

Immobilisation by physical adsorption also involves cross-linking. Cross-linking gives sensors with short response times but poor stability because enzyme is directly exposed to the bulk solution and partly denaturised by the cross-linking (Ahuja, 2007).

5.3.2 Covalent immobilisation

In order to achieve an increased lifetime stability of enzyme electrode, it is necessary that there should be a strong and an efficient bonding between the enzyme and the immobilising material. Hence, covalent linking of biomolecules on transducer is an efficient method of immobilisation. It has an advantage of low diffusional resistance and such a sensor shows good stability under adverse conditions. Covalent linking of a biomolecule to polymer matrix is accomplished in a two step process i.e. synthesis of functionalised polymer followed by covalent immobilisation. Since immobilisation takes place only on the outer surface of the polymer, it permits selection of optimum reaction conditions for each step (Vida and Castillo, 2003).

5.3.3 Electrochemical immobilisation

Although, the conventional procedures for deposition of biomolecules on to the transducers like, physical adsorption, covalent linkage, entrapment and cross-linking have been used extensively yet they suffer from a low reproducibility and have a poor spatially controlled deposition. In recent years, the focus of immobilisation has been shifted towards the entrapment of biomolecules in the layers of electrochemically synthesised polymers. The electrochemical formation of polymer layers of controlled thickness and enzyme activity in galvanostatic or potentiostatic conditions offers numerous advantages over conventional procedures for the design of biosensors, such as complete coverage of the active surface, greater control over film thickness and greater reproducibility. The major advantages of the electrochemical immobilisation techniques is: it is a one-step procedure, faster than all immobilisation procedures (Bidan, 1992). However, it should be noted that electropolymerisation process requires high concentrations of monomer and biomolecules (Cosnier, 2003).

5.4 Immobilisation through amino groups of biomolecules

The most widely used route to conjugate biomolecules to solid supports is through reactions involving primary amino groups (-NH_2). The utility of amines stems from their high nucleophilic character and the existence of a wide variety of amine base coupling chemistry suitable for use under aqueous conditions. The amino group is the nucleophilic is a reactive form of amines that exists in basic medium. The reactivity of amines in water depends on the pH according to the equilibrium between the protonated (acidic) and unprotonated (basic) forms given by the pKa value. Increasing pH shifts equilibrium toward the unprotonated form and makes the reaction kinetics faster. The competition between the acylation of amines and hydrolysis depends on the relative concentrations of amine and water. Hence, high concentration of amine is preferred.

5.4.1 Functionalisation using activated ester

NHS-ester as other activated esters (e.g. the sulphonated ester derivative of N-hydroxysulphosuccinimide that has higher water solubility), N-hydroxybenzotriazole, p-nitrophenol, tetrafluorophenol allow acylation of primary amines in high yield.

Aminolysis of these activated esters is notably much faster than hydrolysis, enabling reaction to be achieved in aqueous medium (Lee *et al*., 2003; Salmain and Jaouen, 2003). Unlike other nucleophilic reactive groups, NHS-ester has low activity with secondary amines, alcohols, phenols and histidine. NHS-esters can be stored for long periods in cold and dry conditions. NHS-ester functional groups are thus versatile; they are widely used in peptide synthesis, preparation of biomolecules conjugates, and in surface immobilisation.

NHS and Sulfo-NHS are used to prepare amine-reactive esters of carboxylate groups for chemical labeling, crosslinking and solid-phase immobilisation applications. Carboxylates (-COOH) may be reacted to NHS or Sulfo-NHS in the presence of a carbodiimide such as EDC (1-Ethyl-3-[3-dimethylaminopropyl]carbodiimide hydrochloride), resulting in a semi-stable NHS or Sulfo-NHS ester, which may then be reacted with primary amines ($-NH_2$) to form amide crosslinks as shown in Figure 20. Although NHS or Sulfo-NHS is not required for carbodiimide reactions, their use greatly enhances coupling efficiency. Furthermore, using NHS or Sulfo-NHS makes it possible to perform a two-step reaction.

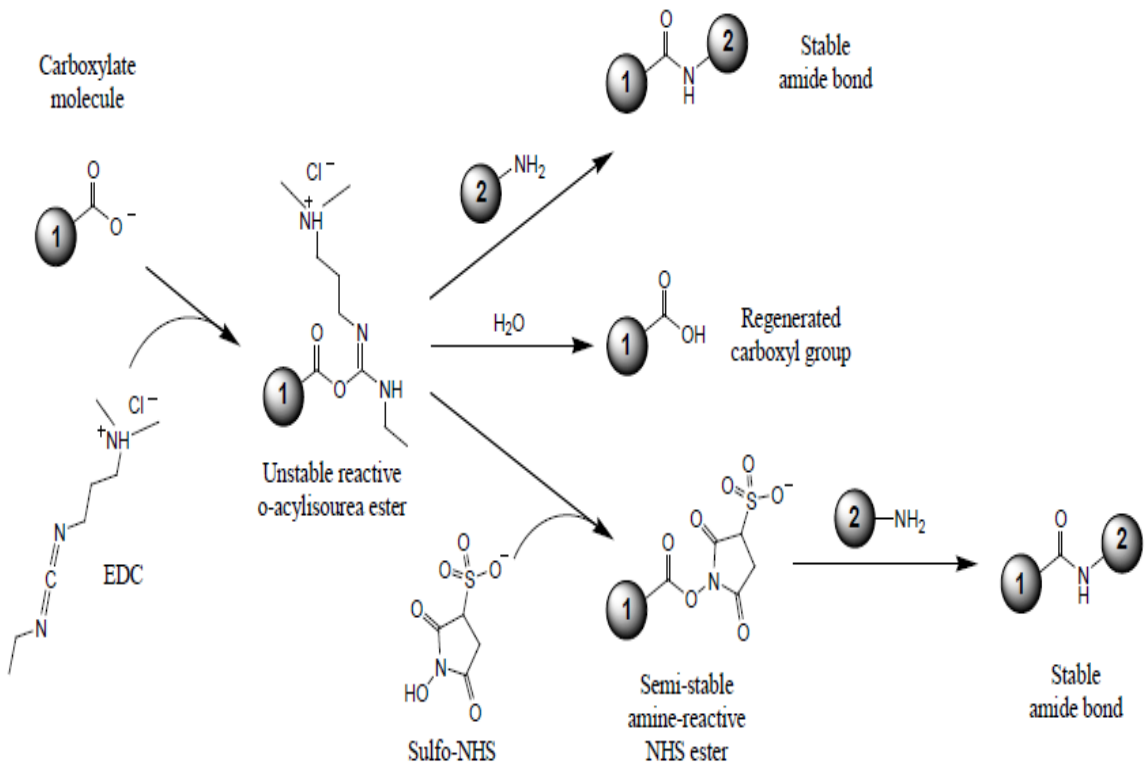

Figure 20 NHS ester activation reactions involving EDC (Thermo, 2014)

Both NHS and Sulfo-NHS are soluble in aqueous and organic solvents. Activation with NHS, however, decreases water-solubility of the modified carboxylate molecule, while activation with Sulfo-NHS preserves or increases water-solubility of the modified molecule, by virtue of the charged sulfonate group. Although prepared NHS or Sulfo-NHS esters are sufficiently stable to process in a two-step reaction scheme, both groups will hydrolyse within hours or minutes, depending on water-content and pH of the reaction solution. NHS esters have a half-life of 4-5 hours at pH 7, 1 hour at pH 8 and only 10 minutes at pH 8.6 (Thermo, 2014).

5.5 Immobilisation through sulphydryl groups of biomolecules

The chemical immobilisation of complex recognition molecules like proteins onto the active layer of a biosensor is quite challenging. Specific concerns are:

(1) To attach these molecules by one anchoring point in order to obtain a repeatable, uniform and oriented layer; and

(2) To avoid alteration of the active sites or denaturation that leads to loss of activity.

The regio-specificity of immobilisation using either amine or carboxylic acid moieties is difficult to control because there is large number of these hydrophilic residues Lysine, Glutamic acid, acylation-stimulating-protein (Lys, Glu, Asp) on the periphery of proteins where binding takes place. This leads to heterogeneity of the attachment and random orientation of the protein on the surface. Unlike amine or carboxylic groups, proteins possess a limited number of cysteine residues at their periphery. Covalent coupling strategies using thiol groups allow site-specific reactions. The sulphur atom of cysteine belongs to form a sulphydryl (or thiol) group. The low accessibility of cysteine in protein restricts the use of thiol groups for the immobilisation of biological molecules. This turns out advantageous in order to introduce solvent accessible reactive groups on protein surface. Cysteine residues involved in disulphide bonds can be chemically or enzymatically cleaved (Brogan *et al.*, 2003) before a subsequent reaction with activated surfaces. Thiol groups allow very specific reactions because they are very reactive toward various chemical functions that are quite stable in water. The simplest approach

is the reaction of thiol group onto supported thiol groups by formation of disulphide linkage.

But disulphide bonds are unstable under reducing conditions. The reactions of oxygen with thiols in aqueous solution give disulphides quite easily (pH 7–9) (Bagiyan *et al*., 2003). In order to regenerate the free reactive form, disulphide dimers are cleaved immediately before the coupling reaction (Chassignol and Thuong, 1998). Some common disulphide-reducing agents are dithiothreitol (DTT), b-mercaptoethanol or tris (2-carboxyethyl) phosphine (TCEP).

5.5.1 Maleimide Functionalisation

The double bond of maleimide undergoes a Michael addition reaction with sulphydryl groups to form stable thioether bonds. It is also reactive toward unprotonated primary amines and hydroxide anions (Shen *et al*., 2004). Interestingly, reaction of maleimide and sulphydryl groups is specific in the pH range 6.5–7.5. The reaction of maleimide with sulphydryl at pH 7 proceeds at a rate 1,000 times faster than the reaction with amines.

The surface functionalisation with maleimide is achieved by coupling hetero-difunctional cross-linkers to surface terminal amino groups. During and after derivatisation of surface amine groups by difunctional cross-linkers, maleimide groups are exposed to reaction with amino groups. Once grafted, the close proximity of the maleimide groups and residual amino groups remaining on the solid support may lead to a fast decrease of surface activity. A capping reaction of the amine groups with a large excess of highly reactive reagents such as isothiocyanate or succinimidyl ester groups is to be made in order to avoid the deactivation by residual amines. The main maleimide heterodifunctional crosslinkers used for the immobilisation of biomolecules are the succinimidyl-4-(N-maleimidomethyl) cyclohexane-1-carboxylate (SMCC) and succinimidyl-4-(N-maleimidophenyl) butyrate (SMPB) or its sulphonated analogue sulpho-SMPB (Strother *et al*., 2000; Shen *et al*. 2004). Maleimide-activated solid supports cannot be stored for long time because of base-catalysed addition of water to the imide bond and ring-opening the maleimide by hydrolysis (Shen *et al*., 2004).

A schematic presentation adapted from (Zimmermann *et al*., 2010) is presented in Figure 19. The immobilisation of an antibody through sulphydryl group has been

schematically shown in step by step process. In the first step a conductive polymer with amino functionality is deposited onto the electrode surface. Once a polymeric layer is formed the modified electrode surface is activated with NHS–maleimide. In the second step, the antibodies are reduced through TCEP which generates fregments of antibodies through disulphide bond cleavage. Finally, the reduced biomolecules are coupled to the activated surface displaying thiol reactive maleimide groups. The schematic presentation of immobilisation of antibodies through sulphydryl group on to maleimide active electrode surfaceis presented in Figure 21 .

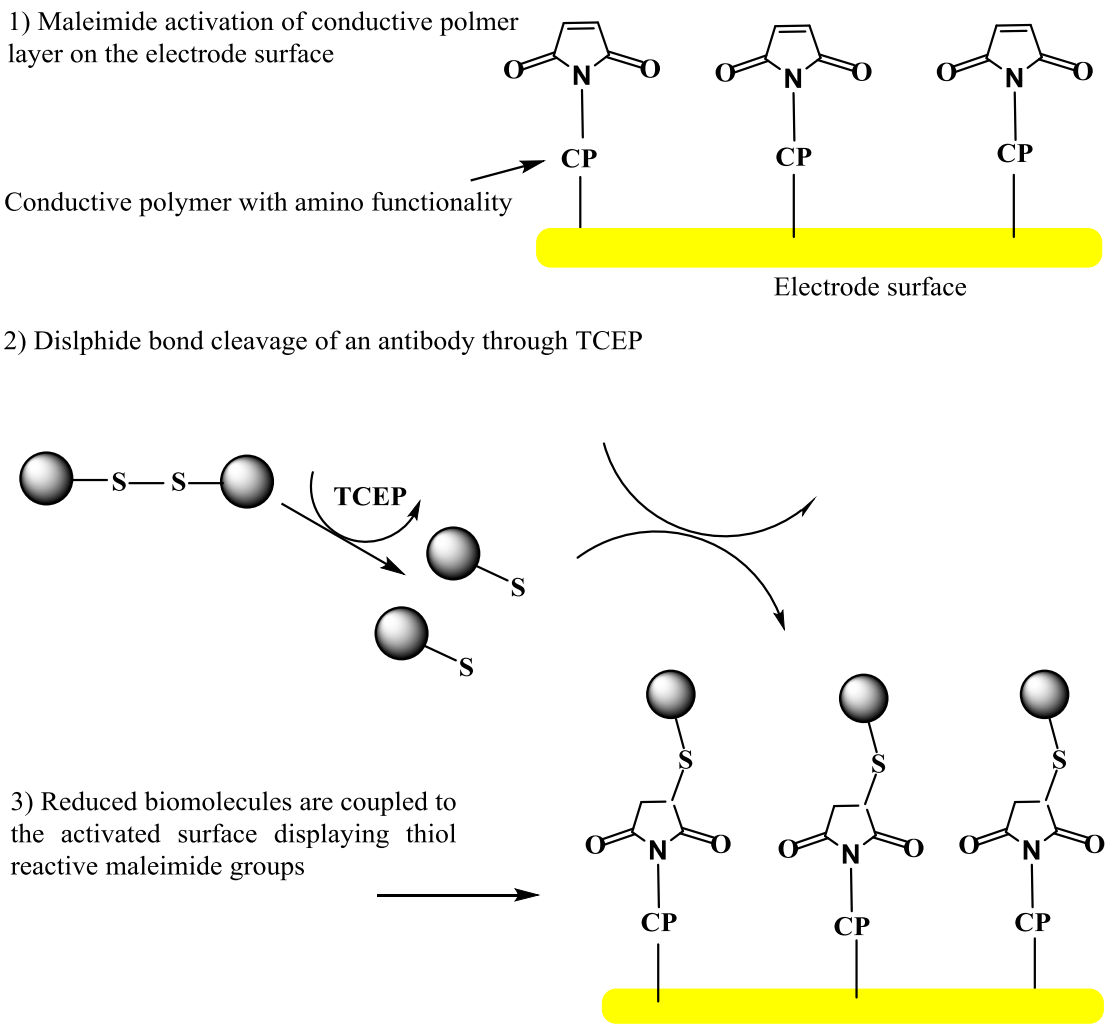

Figure 21 **Schematic presentation of immobilisation of antibody through sulphydryl group on to maleimide active electrode surface**

5.6 Covalent and selective immobilisation of biomolecules

The sensitivity and selectivity of biosensors depend on the quality of the interface and the activity of the biomolecules. This activity is closely correlated to the surface configuration of the immobilisation, that is, the active site must remain accessible. Direct immobilisation techniques rely on either adsorption, or direct covalent attachment of biomolecules to chemically activated surfaces (MacBeath, 2000). The adsorption of proteins to interfaces causes possible denaturation and also limits the availability of active sites. Adsorption is often associated to losses of activity and poor selectivity. As adsorption is reversible, therefore reactive amino or thiol groups of large protein molecules are scattered throughout the biomolecules. Hence, grafted proteins are randomly immobilised under various orientations. Protein immobilisation after site-directed modification of proteins allows selective attachment of proteins to a solid support in a uniform orientation (Hodneland *et al.*, 2002). Figure 22 depicts schematic presentation of different types of bimolecular immobilisation. A probe can be adsorbed to the surface (1), immobilised by random reactions (2) and site specifically immobilised to the surface. The adsorption and random immobilisation results in loss of activity compared to the uniform orientation of site specifically immobilised bioprobes (MacBeath, 2000).

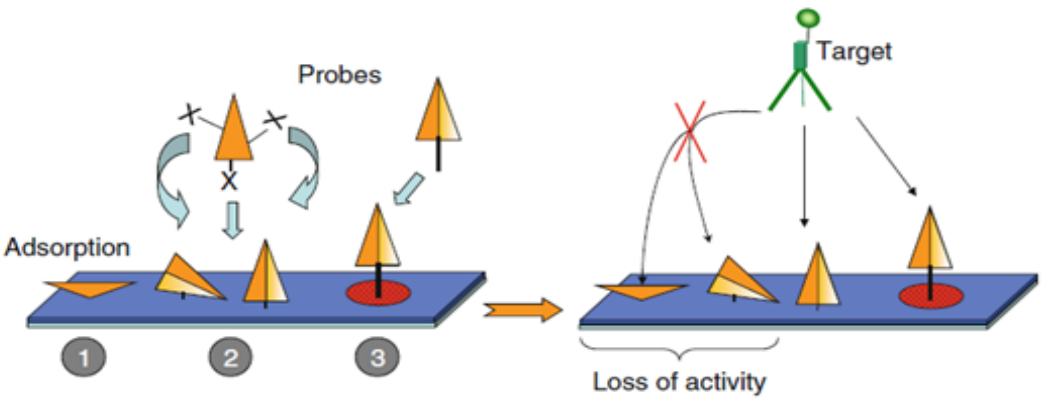

Figure 22 Schematic representation of three different ways of bioprobes immobilisation

Proper orientation of the immobilised proteins compared to random immobilisation improve the biological activity (homogeneous-binding activity, kinetics of reactions) and thus measured signals (Vijayendran and Leckband, 2001; Zhu *et al.*, 2001).

5.6.1 Antibodies

Due to high specificity, antibodies are widely used for purification/concentration of specific molecules in biological fluid by immunoaffinity chromatography or for diagnostic purposes in immunoassays. Whatever the nature of the attached molecular probe, uniform layers of well-oriented molecules are obtained by site-directed reaction which keeps the binding site accessible. Three specific reaction sites leading to three main strategies of oriented immobilisation are used for antibodies (Lu *et al*., 1996).

The first strategy is the "biochemical approach" which takes advantage of the selective binding of the Fc fragment of antibodies to specific receptors (protein A, protein G). This approach involves biofunctionalisation of the solid support by Fc receptors followed by binding of the antibody by its Fc fragment (Vijayendran and Leckband 2001; Grubor *et al*., 2004; Briand *et al*., 2006).

The two others approaches involve chemical immobilisation of antibodies to solid support:

- The reduction of the disulphide bonds linking the heavy and light chain of the fragment antigen-binding (Fab) fragment in the Hinge region is made by chemical, photochemical or enzymatic treatments. This creates site-specific thiol groups far from the binding sites (Brogan *et al*., 2003).
- Straight forward immobilisation of antibody fragments containing thiol site-specific group can be realised directly onto gold surface (Brogan *et al*., 2003). However, higher immobilisation efficiencies are obtained on thiol reactive surfaces.

Direct grafting of antibodies is obtained by reaction of the aldehyde groups onto amino or hydrazide functionalised solid supports (Arenkov *et al*., 2000). Indirect grafting is achieved by using heterodifunctional cross-linkers (4-(N-maleimidomethyl) cyclohexan-1-carboxylhydrazide, or Biotin-LC-hydrazide) which also gave excellent results (Vijayendran and Leckband, 2001).

5.7 Summary

Development of a solid-phase environment that provides optimum bioactivity without biomolecule loss, displacement, or surface migration is a common goal of research scientists, clinical laboratories, and diagnostic kit manufacturers. Antibody molecules and antibody fragments in particular, have enormous potential in the development of biosensors. Conventional immobilisation approaches used in immunoassays typically yield unstable and mostly incorrectly oriented antibodies resulting in reduced detection sensitivities for already low concentration analytes.

One likely approach is the facile and covalent immobilisation of protein molecules without the use of any special tag or chemical modification. This can be achieved conveniently via chemical reactive group, maleimide, towards the available sulphydryl (–SH) groups on the surface of protein molecules.

During the research work presented in this study, the maleimide activation of sensors surface was done through sulpho-SMCC reagent. The maleimide derivatised surface covalently binds sulphydryl groups that become available in biomolecules after the reduction of disulphide bonds.

Many reducing agents carry a free thiol group themselves such as dithiothreitol or 2-mercaptoethylamine. These free thiol groups interferes with the coupling reaction. Considering the difficulty, the most efficient reduction procedure was adapted and TCEP tris (2-carboxyethyl) phosphine was used as the reducing agent. The use of TCEP provides a convenient and fast way for disulphide bond reduction.

CHAPTER 6 MATERIALS AND METHODS

In this chapter, a brief description of the materials and solutions used for the sensors preparation along with experimental techniques are presented.

6.1 Materials

6.1.1 General chemicals

Aniline monomer (99.9%), toluene, methanol (99.9%), acetone (96%), formic acid (95%), HCl (35%) used as doping agent, TWEEN 20 (polyoxyethylene (20) sorbitan monolaurate) and acetonitrile (99%) supplied by Sigma Aldrich. Sodium dodecyl sulphate (SDS 99%, Sigma) was used to form micelles in solution. Ammonium per sulphate (APS 98%, Alfa Aesar Chemical Co.) was used to initiate the polymerisation. All reagents were used as received without further purification. 3-amino methyl pyridine (3-AMP)& 4-amino methyl pyridine (4-AMP) used in preparation of pyridine sensors along with dry diethyl ether, tyramine, ferric chloride, 1-cyanoethyl pyrrole and pyrrole used in sensor preparation were also supplied by Sigma. Dodecyl benzene sulphonic aicd (DBSA), Potassium phosphate dibasic (K_2HPO_4) and lithium aluminium hydride used for oxidation of 1-cyano ethyl pyrrole was supplied by Fisher Scientific (Acros Organics).

Potassium chloride, sodium chloride, potassium ferrocyanide, disodium phosphate (Na_2HPO_4) and monopotassium phosphate (KH_2PO_4) were supplied by Sigma. All of these chemicals were used to make PBS buffer solution of pH 7.2 which was used as redox mediator as well as solvent for making various antibodies concentrations.

Toluene sulphonic acid, dimethyl sulphoxide (DMSO), sodium dodecyl benzene sulphonate (SDBS) 80% and 4-aminothiophenol 97% were supplied by Sigma whereas HCl (2N) was supplied by Fluka. The reagents were of analytical grade and de-ionised water was used throughout the experiments.

6.1.1.1 NHS-Biotin

N-Hydroxysulphosuccinimide (NHS) esters of biotin (Figure 23) purchased from Calbiochem are the most popular type of biotinylation reagent. NHS-activated biotins react efficiently with primary amino groups (-NH_2) in alkaline buffers to form stable amide bonds. Proteins (e.g., antibodies) typically have several primary amines that are available as targets for labelling, including the side chain of lysine (K) residues and the N-terminus of each polypeptide. NHS-Biotin reagents are not directly water soluble and must be dissolved in organic solvents such as DMSO or DMF (dimethylformamide) before addition to aqueous solutions at the final concentration for the labelling reaction. 0.0004g NHS-Biotin was dissolved into 80µL PBS and 20µL DMSO.

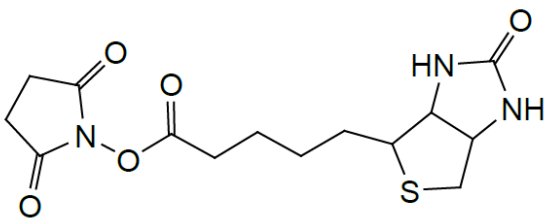

Figure 23 NHS-Biotin

6.1.1.2 NHS-LC-LC-Biotin

NHS-LC-LC-Biotin (succinimidyl-6-(biotinamido)-6-hexanamido hexanoate) shown in Figure 24 was purchased for Thermo Scientific enables simple and efficient biotin labelling of antibodies, proteins and any other primary amine-containing macromolecules. 10mM solution of NHS-Biotin was immediately used by dissolving 0.0004g into 80µL PBS and 20µL DMSO solution.

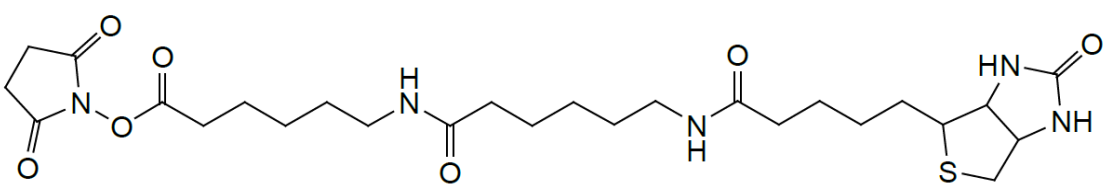

Figure 24 NHS-LC-LC-Biotin

6.1.1.3 Western blotting substrate

The Thermo Scientific Pierce enhanced luminol-based chemiluminescent (ECL) Western Blotting Substrate is a highly sensitive nonradioactive substrate for the detection of horseradish peroxidase (HRP) on immunoblots. Pierce ECL Western blotting substrate enables the detection of picogram amounts of antigen and allows for easy detection of HRP using photographic or other imaging methods. Equal amounts of both substrates were mixed for imaging free -NH_2 groups.

6.1.1.4 Amicon membranes

Amicon Ultra-0.5, Ultracel-100 Membrane, 100 kDa and Amicon Ultra-0.5, Ultracel-50 Membrane, 50 kDa supplied by Millipore were used for biotinylation and generating half antibodies. These membranes are used for the size exclusion and protein fractionation and also concentration of biological samples containing antigens, antibodies, enzymes or nucleic acids.

6.1.1.5 TCEP.HCl

TCEP.HCl supplied by Thermo Scientific selectively and completely reduces even the most stable water-soluble alkyl disulphides over a wide pH range. Reductions frequently require less than 5 minutes at room temperature. Schematic presentation of reduction of disulphide bond is shown in Figure 25.

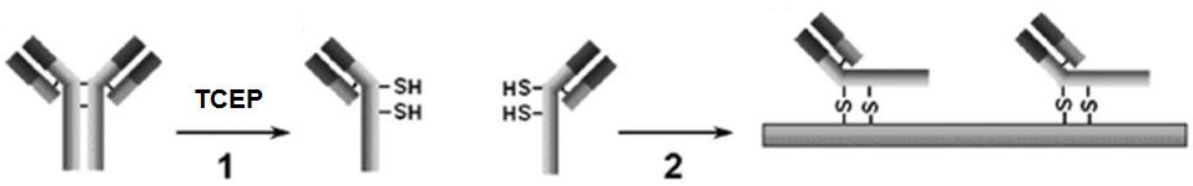

Figure 25 Reduction of organic disulphide bonds with TCEP

As TCEP does not contain thiols therefore it does not have to be removed from solutions before performing reactions involving maleimide labelling or cross-linking reagents. In most situations, TCEP concentrations < 10-20mM are compatible with maleimide reaction chemistry. Initially 10mM stock solution of TCEP was prepared in PBS and further diluted to 3mM for biosensor preparation and immobilisation of antibodies.

6.1.1.6 Sulfo-SMCC crossLinker

Sulfo-SMCC was supplied by Thermo Scientific. It is a heterobifunctional crosslinker which contain *N*-hydroxysuccinimide (NHS) ester and maleimide groups as shown in Figure 26 which allow covalent conjugation of amine- and sulphydryl-containing molecules. NHS esters react with primary amines at pH 7-9 to form amide bonds, while maleimides react with sulphydryl groups at pH 6.5-7.5 to form stable thioether bonds. 10mM solution of SMCC was prepared by dissolving 0.0003g into 20µL DMSO and 80µL PBS solution.

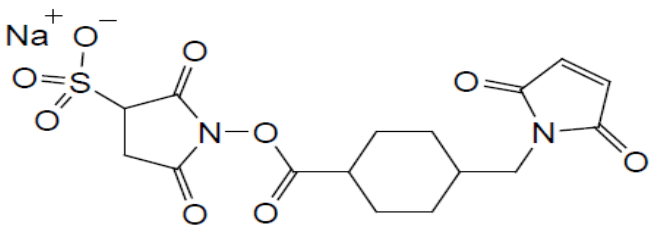

Figure 26 Sulfo-SMCC

6.1.1.7 Bovin serum albumin (BSA)

Bovin serum albumin (BSA) was selected as the blocking solution for the immunoassay. This blocking solution was specially selected to impede the nonspecific molecule binding during immobilisation. Commercially available BSA was supplied by Pierce.

6.1.2 Solutions

6.1.2.1 Potassium phosphate buffer, 0.1 M

Two different solutions referred as stock solution A and stock solution B were initially prepared and later mixed by following the Table 4 to get the desired pH.

Solution A: 27.2 g KH_2PO_4 per litre (0.2 M final) in water.

Solution B: 34.8 g K_2HPO_4 per litre (0.2 M final) in water.

Referring to Table 4 for desired pH, the indicated volumes of solutions A and B were mixed, then diluted with water to 200 ml. Filtered when necessary and then stored up to

3 months at room temperature. This buffer may also be made as a 5- or 10-fold concentrate simply by scaling up the amount of potassium phosphate in the same final volume.

Table 4 Preparation of 0.1 M sodium and potassium phosphate buffers

Desired pH	Solution A (mL)	Solution B (mL)	Desired pH	Solution A (mL)	Solution B (mL)
5.7	93.5	6.5	6.9	45	55
5.8	92	8	7	39	61
5.9	90	10	7.1	33	67
6	87.7	12.3	7.2	28	72
6.1	85	15	7.3	23	77
6.2	81.5	18.5	7.4	19	81
6.3	77.5	22.5	7.5	16	84
6.4	73.5	26.5	7.6	13	87
6.5	68.5	31.5	7.7	10.5	90.5
6.6	62.5	37.5	7.8	8.5	91.5
6.7	56.5	43.5	7.9	7	93
6.8	51	49	8	5.3	94.7

Phosphate buffers show concentration-dependent changes in pH, after checking the pH of the concentrate by diluting an aliquot to the final concentration. To prepare buffers with pH intermediate between the points, first concentration was prepared closest to higher pH, and then titrated with solution A.

6.1.2.2 Phosphate buffered saline (PBS)

PBS was consumed throughout the assay. Most of the molecules and proteins were diluted in this buffer. After incubation sensor surfaces were washed with PBS in order to extract the unbound particles or proteins. The phosphate buffered saline (PBS) of pH 7.2 was prepared by dissolving 8g (0.137 M) of NaCl, 0.2g (2.7 mM) KCl, 0.24 g (1.4mM) KH_2PO_4, and 1.44 g (0.01M) Na_2HPO_4 in one litre of distilled H_2O.

6.1.2.3 Triton X-100, 10% (w/v)

One mL of Triton X-100 was dissolved into 10 mL of distilled H_2O, stirred and stored while protected from light for up to 6 months at room temperature.

6.1.2.4 Tween 20

0.1% (w/v) polyoxyethylenesorbitan monolaurate (Tween 20) was dissolved in PBS. It can be stored up to several months at 4°C.

6.1.3 Electrodes

6.1.3.1 Screen printed gold electrodes

Gold was chosen as the working electrode material due to its availability, ease of preparation (electrodeposition, sputtering and physical vapour deposition) and patterning using screen printing. In addition to this, it is a relatively inert metal as it does not oxidise at temperatures lower than its melting point and does not show reactivity towards chemicals and atmospheric oxygen. This is advantageous as experiments do not require a clean room environment or a vacuum, making this material suitable for biological applications.

6.1.3.1.1 Electrode design and production

The electrode used in the project is screen printed with high temperature curing inks designed and produced by DropSens (Asturias, Spain) is shown in Figure 27.

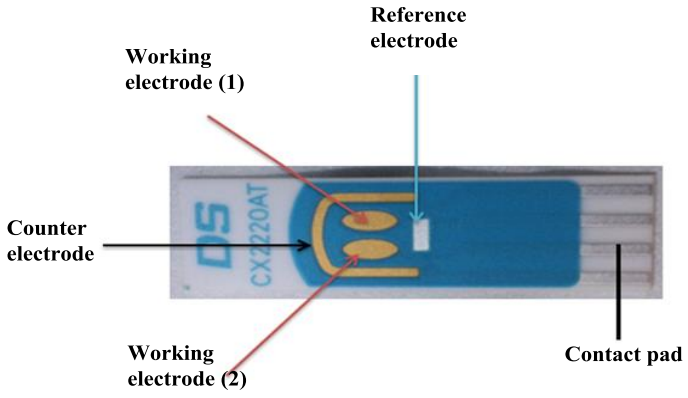

Figure 27 Drop sensor gold electrode design

Disposable gold electrodes are ideal for working with microvolumes, or by dipping them in solution and are suitable to develop specific biosensors.

The dimensions of a simple screen printed electrode are given in Table 5. These electrodes are specifically designed to work in solution by entirely immersing sensing area.

Table 5 Dimensions of screen printed gold electrodes

Ceramic substrate	L33 x W10 x H0.5 mm
Electric contacts	Silver
Working electrode	Gold
Counter electrode	Gold
Reference electrode	Silver

a) Working electrode

It is the electrode on which the reaction occurs in an electrochemical system (Zoski, 2007). In an electrochemical system with three electrodes, the working electrode (WE) can be referred as either cathodic or anodic depending on the reaction on the working electrode is a reduction or an oxidation. There are many kind of working electrodes such as glassy carbon electrode, screen printed electrode, Pt electrode, gold electrode, silver electrode, Indium tin oxide coated glass electrode, carbon paste electrode, carbon nanotube paste electrode etc.

Screen printed electrodes are prepared with depositing inks on the electrode substrate (glass, plastic or ceramic) in the form of thin films. Different inks can be used to get different dimensions and shapes of biosensors. Screen-printed electrochemical cells are widely used for developing amperometric biosensors because these biosensors are cheap and can be produced at large scales. This could be potentially used as disposable sensor that decreases the chances of contamination and prevents loss of sensitivity. Performance factors of an electrochemical biosensor are: Selectivity, response time, sensitivity range, accuracy, recovery time, solution conditions and the life time of the sensor.

Working electrodes used in this research work were screen printed gold electrodes. These comprised of two oval shaped gold working electrodes (WE1 and WE2), both fired onto a ceramic base along with U shaped counter and silver reference electrode which were also printed on the same transducer base.

a) Reference electrode

Reference electrodes (RE) are chosen due to their ability to maintain a stable double layer, and therefore potential, against which other potentials may be compared. Typically a reference will measure the potential difference between the working electrode and the counter electrode. This allows the system to maintain a controlled applied voltage to the working electrode throughout experiments.

Ag/AgCl electrodes are commonly used in electrochemistry due to their well-studied and highly efficient redox mechanism.

A typical redox reaction is shown in equation 12.

$$Ag^{+} + Cl^{-} \leftrightarrow AgCl \qquad (12)$$

The reference potential provided depends upon the number of Cl^{-} ions in solution, but typically an Ag/AgCl gives a potential of 0.199 V *vs*. normal hydrogen electrode in 1 M KCl. They are suitable for use in biological applications as they are non-toxic, can operate over a range of temperatures and do not alter pH.

Reference electrodes are also called non-polarisable electrodes as the potential of the electrode will not change from its equilibrium potential, irrespective of current flow in the electrochemical cell (Scott and Lukehart, 2007). The Ag/AgCl reference electrode used in this research work was integrated and printed onto the ceramic transducer base. The rig used for the DropSensor electrodes is shown in Figure 28 (A) and the electrode holder is shown in (B).

The counter or auxiliary electrode (CE) is the final electrode in the three electrode system. Its purpose is to complete the circuit by providing current to the working and reference electrodes and should be comprised of an inert conductor. The auxiliary electrode functions as a cathode whenever the working electrode is operating as an

anode and vice versa. The potential of the auxiliary electrode is not measured against the reference electrode but adjusted to balance the reaction occurring at the working electrode. This configuration allows the potential of the working electrode to be measured against a known reference electrode. The counter electrode must be at least ten times the surface area of the working electrode to allow efficient exchange of electrons such that the electrochemistry is not limited.

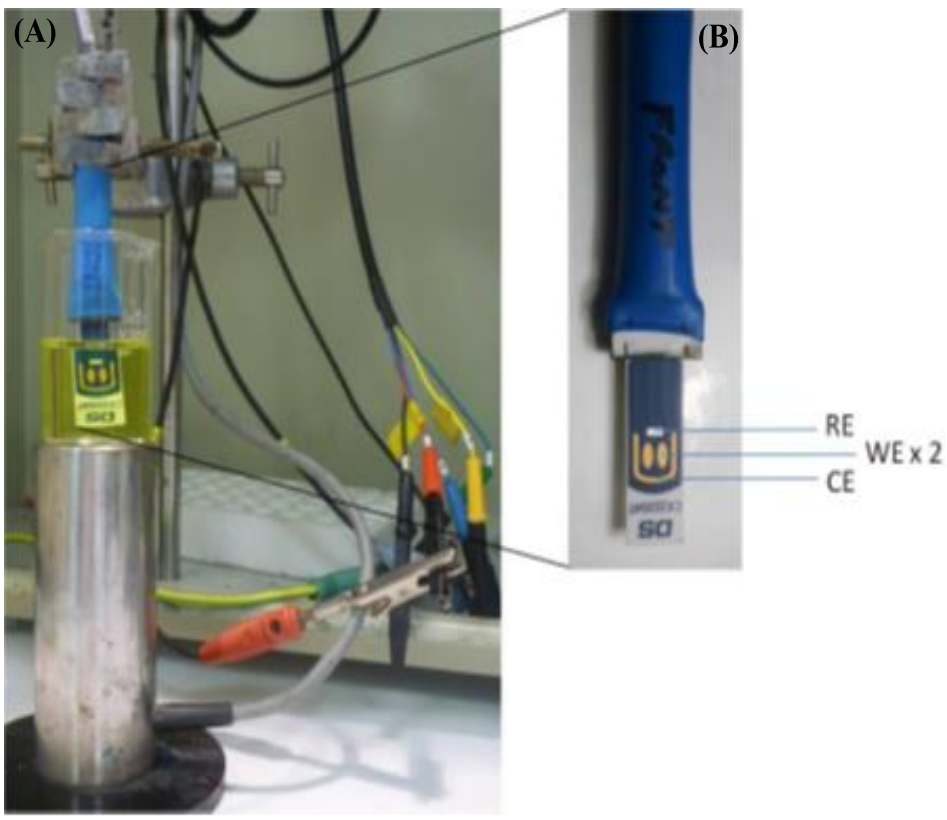

Figure 28 (A) The three electrode rig and (B) electrode holder used in impedance studies

b) Counter electrode

Auxiliary electrode is often fabricated from electrochemically inert materials such as gold, platinum or carbon. A gold counter, fired in the same way as the working electrodes located on the DropSensor chip was auxiliary electrode.

6.1.4 Conductive sensing layer

The most important component of the sensor is the sensing layer. Conductive polymers are excellent platforms for the immobilisation of biomolecules at electrode (Tully *et al*.,

2008). Various types of conductive polymers were considered as suitable conductive inks for the immobilisation of antibodies onto the sensor.

Polyaniline, polythiophene, and polypyrrole are biocompatible among conducting polymers. These polymers cause minimal and reversible disturbance to the working environment and protect electrodes from fouling. However, only polyaniline, polypyrrole are most extensively used in biosensors.

In a biosensor fabrication the microstructure orientation and the high surface area also facilitate high biomolecule loading and hence highly sensitive detection is possible. Moreover, the relative stability of a biosensor is increased due to efficient bonding of biomolecule on the transducer surface which improves reproducibility (Arshak *et al*., 2009).

Conductive nanoparticles with amino functionality could be used as electro conductive molecular glue's to act as immobilisation coatings for the antibodies. Keeping in account functionality and properties four different conductive polymers (CP's) have been synthesised and deposited onto the electrode surface for initial testing against *Neisseria gonorrhoea* and *Chlamydia trachomatis* antibodies. These CP's includes polyaniline, poly (4-amino methyl) pyridine, poly (3-amino propyl) pryrrole and polytyramine. Each of these polymers will be discussed in details individually in the following chapters.

6.1.5 Pathogens

Neisseria gonorrhoea β-lactamase (+) ve and (-) ve strains were cultured at biochemistry department, University of Leeds. Both types of pathogens were heat killed before testing against any sensors.

Chlamydia trachomatis inactivated pathogens strain 434 cultured in mouse L cell was purchased from AbdseroTec.

6.1.6 Antibodies

Various antibodies were used to make, characterise and test biosensors. A list of antibodies along with their origin and source are given in Table 6.

Table 6 List of antibodies

Antibody	Origin	Source
Anti-neisseria gonorrhoea β-lactamase (+)ve	Rabbit polyclonal IgG	GenScript (USA)
Anti-neisseria gonorrhoea β-lactamase (-)ve	Rabbit polyclonal IgG	GenScript (USA)
Anti-chlamydia	Goat polyclonal IgG	AbDseroTec
HRP-conjugated IgG	Goat monoclonal IgG	Sigma
HRP-streptavidin IgG	Goat monoclonal IgG	Sigma
Anti-digoxin	Sheep polyclonal IgG	Therapeutic Antibodies UK Ltd.

6.2 Methods and techniques

6.2.1 Electrochemistry experiments

All electrochemistry experiments were based on a three electrode system in an electrochemical cell. The experiments were carried out by using transducers that integrated all three onto one sensing chip. The working and counter electrode used were gold, where as the reference was Ag/AgCl. The three electrode system was controlled by an EcoChemie μAutolab Type III frequency response analyser (FRA-2) (Windsor Scientific Limited, Slough, Berkshire, UK) potentiostat. This was used to apply a current to the electrochemical cell through the counter electrode. The voltage difference between the working electrode and the reference electrode was then measured. The Autolab measured the difference between the cell voltage and the desired voltage completing a feedback loop, causing an amplifier to drive current into the cell to maintain the voltages. Autolab software was used to acquire electrochemical measurements and for further data analysis. All electrochemical interrogation was done at room temperature.

6.2.1.1 Cyclic Voltammetry Analysis

Cyclic voltammetry (CV) was used at different stages of construction to characterise the sensor surface using GPES software on μ AUTOLAB type III.

6.2.1.2 Electrochemical impedance spectroscopy analysis

Electrochemical impedance spectroscopy (EIS) was used to monitor analyte recognition using FRA software on FRA-2 μAUTOLAB type III. The impedance analysis was performed over a range of frequencies ranging from 0.1 Hz to 10,000Hz, using a modulation voltage of 10 mV at an applied voltage of 0.4 V. Both impedance and CV experiments were mainly performed in an electrolyte solution of 10 mM $K_3[Fe(CN)_6]/K_4[Fe(CN)_6]$ (1:1 ratio) in 100 mM PBS, pH 7.0. EIS reading was taken at each layer of sensor construction and also before and after bacterial incubation. All the experiments were replicated (n =>3) with independent sensor surfaces and change in

impedance after analyte addition was normalised against sensor level impedance (with no bacteria incubated).

6.2.2 Scanning electron microscopy (SEM)

Various polymers were prepared through chemical polymerisation and the morphologies and size of these particles were studied with field emission scanning electron microscopy (JOEL JSM-6610LV). All SEM pictures were taken after drop casting polymer suspension onto chip and coated with gold by sputtering for 10 s. Photographs were obtained at 5 or 15 kV and at a working distance 1μm-100μm.

6.2.3 FT-IR analysis

Polyaniline, poly (4-aminomethyl) pyridine, poly (3-aminopropyl) pyrrole and polytyramine were characterised by attenuated total reflectance (ATR) spectra recorded by Alpha FT-IR Spectrometer.

6.2.4 Preparation of antibody for immunosensor

6.2.4.1 Biotinylation of antibodies

Biotin modification of protein molecules is called biotinylation, resulting in covalent derivatives containing one or more bicyclic biotin rings extending from the parent structure. These biotinylation sites are still capable of binding avidin or streptavidin with the specificity of free biotin in solution. Since the biotin components are relatively small. Macromolecules can be modified with these reagents without significantly affecting their physical or chemical properties. Figure 29 shows a schematic presentation of biotinylation of protein through sulpho-NHS-biotin.

Biotinylation was performed by dissolving 0.8mg of NHS-biotin in 35μL of 20% DMSO and volume made up to 200μL with PBS buffer solution (P^H 7.2). Antibodies (5 mg ml^{-1}) were incubated with (+)-Biotin N-hydroxysuccinimide ester (NHS-biotin; 0.2 mg ml^{-1}) in PBS under gentle agitation for 1 hour. Unbound NHS-biotin was removed by three rounds of centrifugation through a 30 kDa molecular weight cut-off filter at 14, 000 rpm for 2.5 min each time.

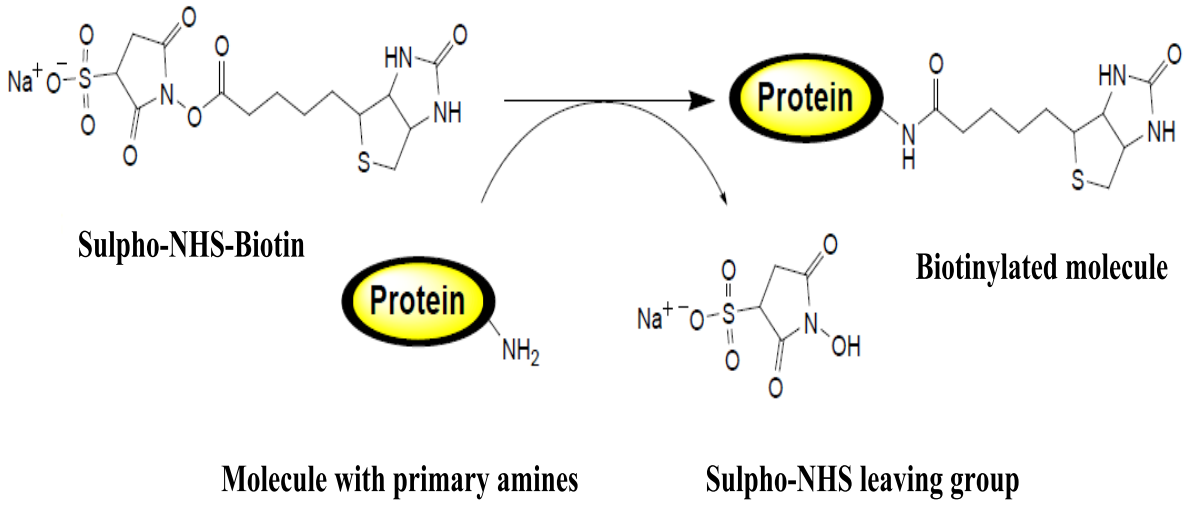

Figure 29 Reaction of sulpho-NHS-biotin with primary amine (Thermo, 2014)

6.2.4.2 Reductive cleavage of antibodies

Equal volume of Ab (~ 5-7 mg/ml) were added into 3mM TCEP.HCl solution in PBS-EDTA (pH 7.2), for example 50 µl of Ab plus 50 µl of TCEP.HCl to keep the ratio 1:1. After incubating the mixture for 30 minutes at room temperature, 50 µl of reaction mixture was taken into 100 kDa filter. To make the total volume upto 400 µl, 350 µl of PBS-EDTA was added into it. The filter was spun at 14,000 rpm for 2.5/3 min and repeated the procedure 2 more times with top up with PBS-EDTA each time. After the third run roughly ~50 µl in the filter was obtained. The filter was inverse spun at 1000 rpm for 30 s to get the product in an empty tube. The collected product was then transferred into 50 kDa filters and spun again at 14,000 rpm for 2.5/3 min. The desired concentrated half antibody population was collected into the filtrate and used straight away onto neutravidin or SMCC activated surfaces of a biosensor to avoid any recombining.

Neisseria gonorrhoea β-lactamase (+) ve, Neisseria gonorrhoea β-lactamase (-) ve and *Chlamydia* were used as specific antibodies where as *antidigoxin* was used as negative control for nonspecific binding.

6.2.5 Construction of immunosensor

6.2.5.1 Modification of electrode surface

Immunosensors based on conducting polymers were prepared by three different methods. All three types of electrodes based on different methods of polymer film deposition are given in Figure 30.

Figure 30 Sensors fabricated by (A) Electrodeposition (B) in-situ polymerisation (C) drop casting

The first set of sensors was prepared by electrodepositing aniline, 4AMP, 3APPy and tyramine onto clean gold electrodes via cyclic voltammetry. The electrode labelled as (A) is prepared through electropolymerisation of polyaniline. In the second set all polymers were deposited onto electrode surfaces through in-situ polymerisation. The elecyrode labelled as (B) is prepared through placing 2µl of aniline solution in HCl and KCl solution and 2µl of 1M APS solution onto the working electrodes surfaces. Once oxidant was added into the monomer, polymerisation started and after one minute the electrode was washed thoroughly with distilled water and dried. The final set of sensors was prepared through dropcasting the polymeric suspensios onto gold electrodes. The sensor labelled as (C) is prepared through casting a drop of chemically polymerised polyaniline onto the gold surface. The same procdure was employed for other polymers as well. Once all sensors were fabricated, they were washed several times with buffer and dried under an Ar_2 stream.

6.2.5.2 Immobilisation of antibodies

The immobilisation of antibodies was carried out on polymer coated gold electrode and modified through SMCC. A schematic presentation of immobilisation of antibodies onto the electrode surface is given in Figure 31. Depending on steric hindrance and type of IgG, the thiol groups may react with more than sulfo-SMCC linker and in reality would not be orientated as shown in Figure 31. The scale shown in the schematic presentation does not correspond to the real size of the species involoved.

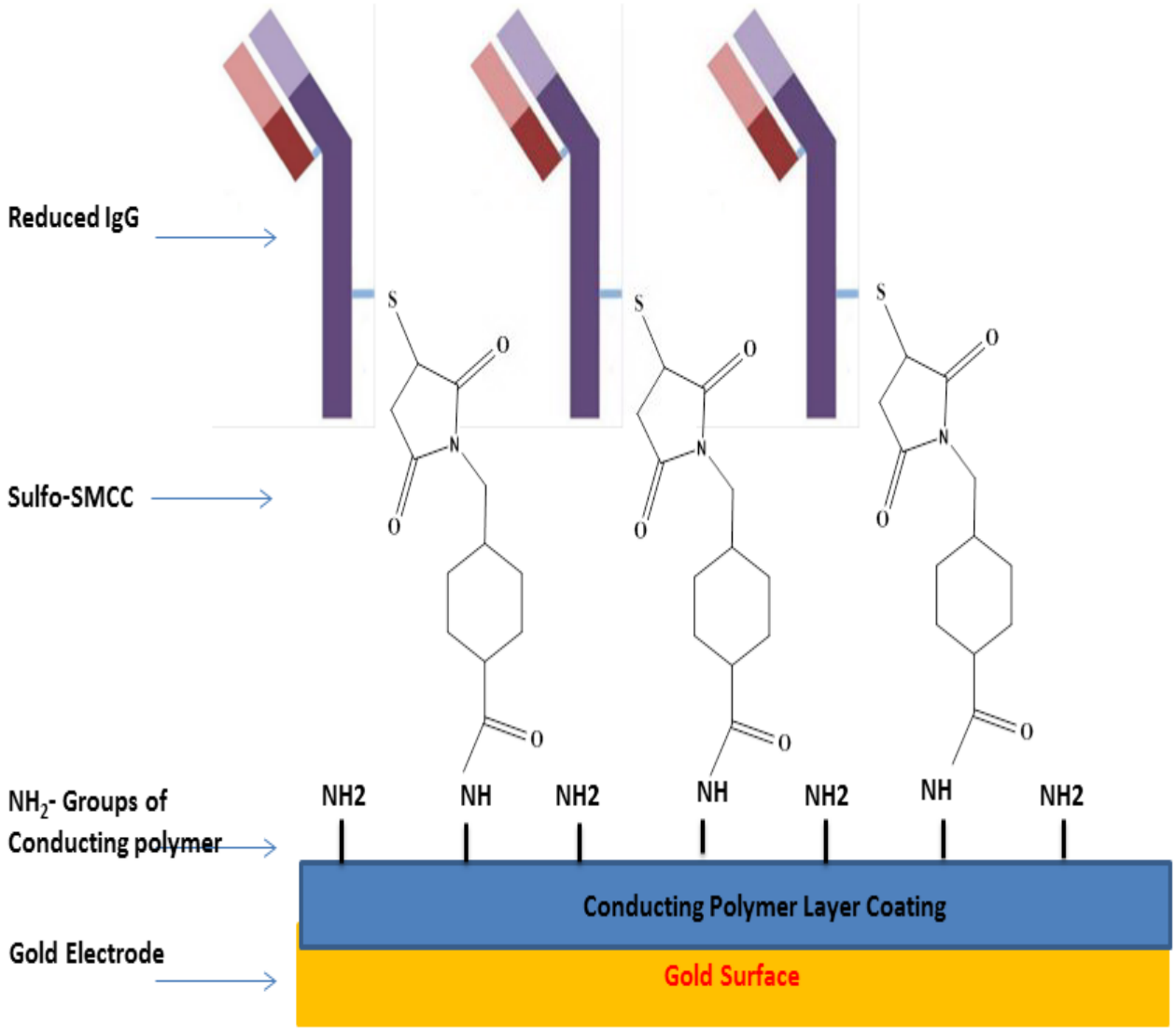

Figure 31 Schematic presentation of immobilisation of ½ antibody onto SMCC modified poly(4-aminomethyl)pyridine electrode

Once the polymer was coated onto the electrode, they were incubated with 5 mM sulphosuccinimidyl 4-[N-maleimidomethyl] cyclohexane- 1-carboxylate (sulpho-SMCC) solution in 10 mM PBS-EDTA (pH 7.2) for 1 hour at room temperature (Tully *et al*., 2008). The modified electrodes were then rinsed several times with buffer before drying under an Ar_2 stream. Previously reduced non specific antibody (*antidigoxin*) discussed under section 6.2.4.2 was applied onto sulpho-SMCC modified surface of WE1 where as specific antibodies (*Neisseria gonorrhoea* and *Chlamydia trachomatis*) were applied on WE2 and incubated for 1 hour. After incubation, the electrodes were washed with 3% sucrose solution. These electrodes were then interrogated electrochemically against various concentrations of *Neisseria gonorrhoea β-lactamase (+) ve*, *Neisseria gonorrhoea β-lactamase (-) ve* and *Chlamydia trachomatis* heat killed pathogens for analyte detection.

6.2.5.3 Construction of calibration curve

A calibration curve (or standard curve) establishes the relationship between the amount of material present and the signal intensity measured. In the case of immunoassays, this would represent the relationship between the antigen concentration and the signal intensity obtained. This relationship is often non-linear, and in many applications displays a dynamic range (or response range) of approximately two orders of magnitude in the concentration of targeted antibody. To perform a quantitative immunoassay, a set of "calibration standards" containing the antigen were prepared through serial dilutions ranging from 10^2 to 10^8 in PBS-EDTA pH 7.2.

A calibration curve was constructed against *Neisseria gonorrhoea β-lactamase (+) ve and (-) ve* along with *Chlamydia trachomatis*. Each type of sensor based on polymer was incubated with a respective concentration, starting from the lowest and incubated for atleast 10 minutes each. After incubation, the sensor was rinsed and washed thoroughly with PBS solution and impedance scan was recorded in $K_3[Fe(CN)_6]/K_4[Fe(CN)_6]$ solution. For the calibration purposes, each concentration was tested against multiple sets of electrodes and once impedance data was collected a Nyquist graph was plotted.

A general experimenta scheme of sensor preparation and testing against antibodies is presented in Figure 32.

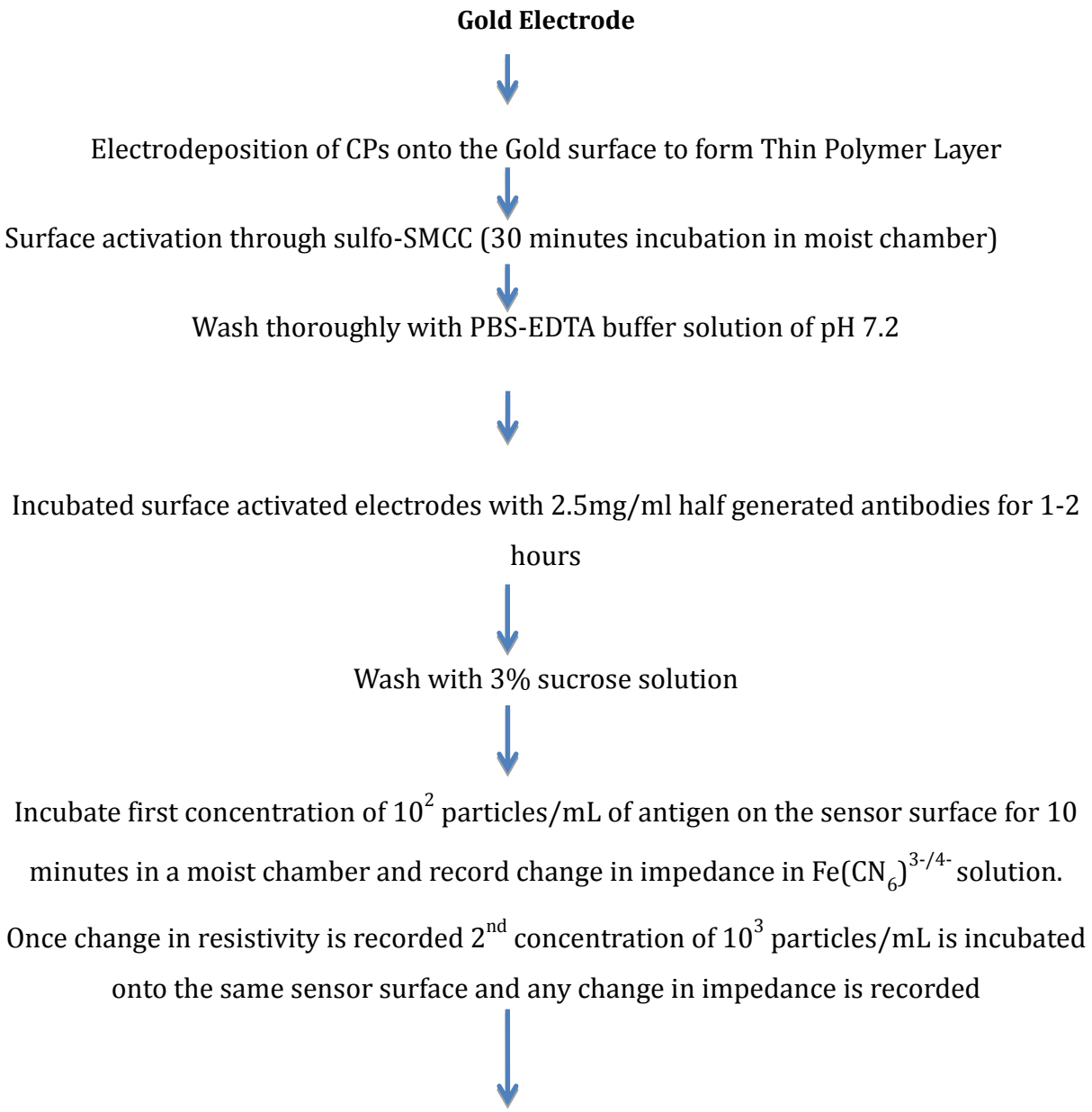

Figure 32 Schematic presentation of immunosensor preparation protocol

6.2.6 *Midland blotting*

Midland blotting, a chemiluminescence-based, semi-quantitative technique was used to rapidly interrogate a number of key features of sensor surfaces. The technique is based upon the commonly-used biochemical western blotting procedure which allows the visualisation and quantification of proteins based upon chemiluminescence from specifically-bound reagents. Figure 33 presents a schematic outline of the midland blotting technique.

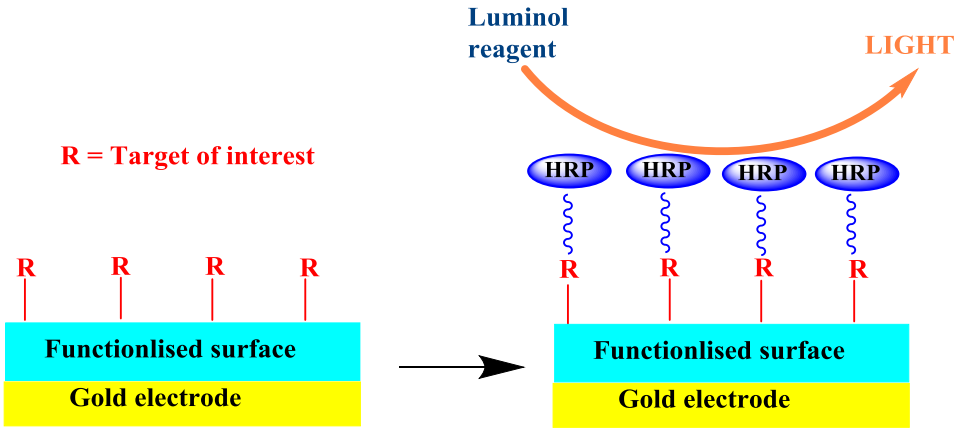

Figure 33 Overview of midland blotting

During biosensor construction, the electrode surface is typically functionalised with either a polymer or co-polymer, or a self-assembled monolayer (SAM). The transducer layer presents functional groups to which bioreceptors can be attached, which facilitate the specific detection of bound analyte. Midland blotting allows the detection of any component of the biosensor surface through the attachment of a horseradish peroxidase (HRP)-conjugated reagent to the target. Once enhanced chemiluminescence substrate (ECL) is added, HRP catalyses the oxidation of luminol into a reagent which emits light when it decays. The light signal is proportional to the bound HRP on the sensor surface. Two types of sensors were fabricated for chemiluminescence analysis, (A) through electrodeposition of polymer (B) by drop casting chemically polymerised polymer suspension. For the detection of free amine ($-NH_2$) groups, functionalised electrodes were incubated in the presence of NHS-biotin (4 mg ml^{-1} in PBS containing 20% (v/v) DMSO) for 30 min in order to attach biotin to the free amine groups. All incubations were conducted in a moist chamber comprising of a closed petri dish

containing moist tissue to avoid any evaporation as small volumes of reagents were pipetted on the electrode (Barton *et al.*, 2009). After incubation all sensors were washed at least three times with dH_2O followed by drying in argon. Later, all electrodes were incubated with HRP-streptavidin (1 µg ml^{-1} in PBS) for 30 min (Billah *et al.*, 2010) and were washed again three times with PBS and once with PBS containing 0.1% (v/v) Tween-20 to aid removal of non-specific binding, with a final wash with PBS. Electrodes were dried in argon in between incubations and after washing steps to allow precise pipetting of reagents onto the working electrodes. Finally, ECL reagent was pipetted carefully onto the working electrodes and chemiluminescence detected after few minutes using a G:BOX Gel Imaging System (Syngene Ltd., Cambridge, UK). Images presented are either chemiluminescence (white light on a black background).

Figure 34 shows intensity of signals for available free amino groups in all four polymers modified sensors. The high intensity of light is considered as a strong signal which shows maximum number of amino groups. Figure 34 (A) presents intensity of free $–NH_2$ on electrodeposited polymer layer onto the electrode and it shows very high intensity of $–NH_2$ groups with even distribution onto the surface. Whereas Figure 34 (B) presents intensity of free $–NH_2$ on drop casted sensors which are randomly distributed onto the gold surface.

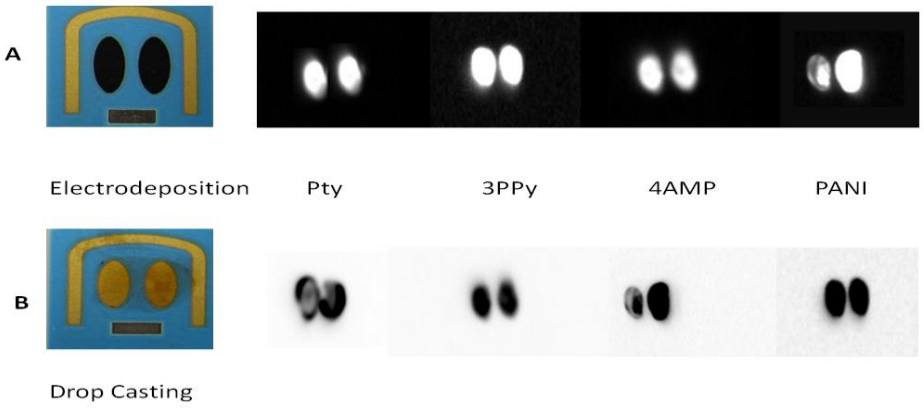

Figure 34 Chemiluminescence analysis of electrodeosited and drop casted sensors

As drop casted sensors have uneven polymeric layer therefore the signal strength is high at more dense and thick polymer layer and low at thin coated area.

CHAPTER 7 POLYPYRIDINE BASED BIOSENSORS

7.1 Introduction

Electronically conducting polymers have been receiving a great deal of attention due to their novel properties and their possible applications to many devices. Of various possible applications, modification of electrode surfaces with these polymers so that they selectively interact with biomolecules has been an important area of research in biochemistry. The novel example of conducting polymer used in fabrication of a biosensor is polyaniline which has amino groups and it interacts with heavy proteins such as antibodies by forming a complex with amine groups in the polymer matrix. A similar system may be found if aminopyridine is polymerised since it has a pyridine type of nitrogen that may act as an additional functional group.

Only a few studies have been reported on electrochemical oxidation of 2-aminopyridine (Kumar, 1988) and the electrochemical polymerisation of aminopyridines in the literature (Hayat, 1987; Park *et al*., 1996). In these studies, polymerisation reactions have been studied and their products are identified.

None of these studies has addressed its biological applications. In this study the electrochemical and chemical oxidative polymerisation 4-aminopyridines were carried out and the resulting polymer was characterised in terms of their biochemical properties. The resulting polymer was characterised through FTIR and SEM.

7.2 Polymerisation of 4AMP

7.2.1 Chemical polymerisation

There are currently conductive polymers can be synthesised by either chemically or electrochemically. During chemical synthesis the monomer solution is mixed with an oxidising agent (e.g. ferric chloride, ammonium persulphate). This process creates a powder or a thick film of the polymer, and allows its bulk production, which makes it

the method of choice for commercial applications (Balint *et al.*, 2014). 4-aminomethyl pyridine has never been reported to be used as biosensing material in literature before. In this research work experimental work was carried out to study the feasibility of 4AMP as potential platform for immobilisation of antibodies. As 4AMP has amino group available to facilitate protein immobilisation therefore various sets of sensors were prepared based on poly (4AMP) and tested against various concentrations of antigens.The electropolymerisation of 4AMP has been reported by Park *et al.*, 1996 but the chemical synthesis of poly (4-amino methyl pyridine) has never been reported before. Therefore efforts were made to synthesised poly (4-amino methyl pyridine) through oxidative polymerisation. Figure 35 depicts the polymerisation scheme of 4AMP. A set of experiments were carried out to optimise the concentration of monomer andoxidant ratio.

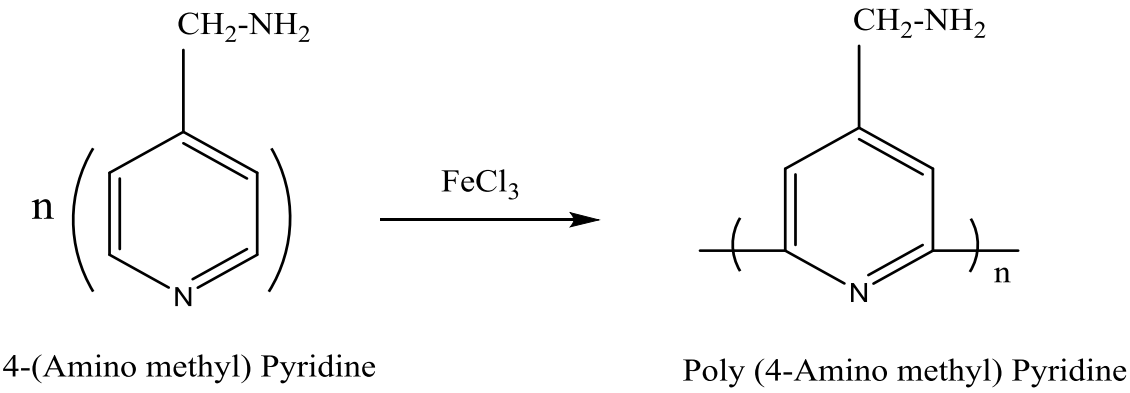

Figure 35 Proposed scheme of polymerisation of 4-(amino methyl) pyridine

Initially 200mM solution of 4-amino methyl pyridine (4AMP) was prepared in 1M HCl. The oxidant solution (1M ammonium per sulphate in HCl) was added into the solution dropwise with continuous stirring but no precipitation occurs. In a second set of experiment, 200mM solution of 4AMP was prepared in 50mL of 1M NaOH solution.10 ml of 0.5M $FeCl_3$ used as an oxidant was added dropwise into the solution mixture with a continuous stirring. As soon as the oxidant was added into the reaction mixture, thick deep brown precipitates were formed instantly. The polymerisation was allowed to continue under continuous stirring for one hour. After one hour, the precipitates were filtered and washed with water for several times to remove any traces of unreacted monomer.

The particle size can be decreased by changing molar concentration of monomer in the reaction mixture. To reduce the particle size a lower concentration of 0.2M monomer was polymerised under the same reaction conditions and resulting polymer suspension was studied through SEM. The SEM pictures revealed smaller particles size which resulted in more surface area for the immobilisation of biomolecules. Figure 36 (a) shows SEM picture of the poly (4-amino methyl pyridine) particles with 1M 4AMP solution where as Figure 36 (b) shows much smaller particle size with 0.2M 4AMP. The precipitates of poly (4AMP) were washed and characterised through FTIR, midland imaging and SEM.

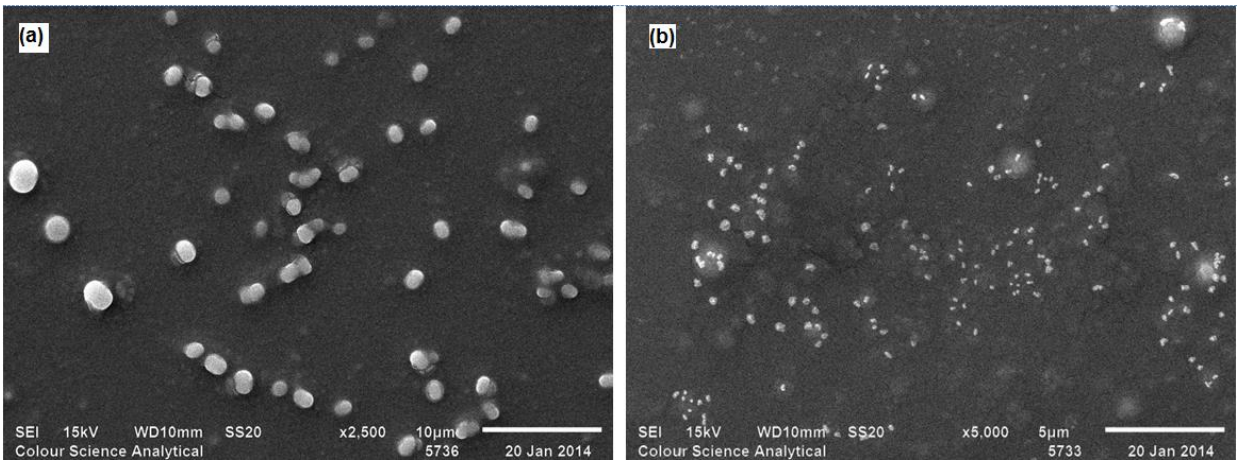

Figure 36 SEM pictures of poly (4-amp) particles at (a) 1M and (b) 0.2M monomer concentration

7.2.2 Electrochemical polymerisation

Polypyridines were also synthesised through electrochemical polymerisation. As it is new and novel polymer in the field of biosensors thereby initially electroploymeristaion was adapted as the preferred method of synthesis. 4AMP was deposited on gold electrode by cyclic voltammetry. The electroploymerisation was performed on µAUTOLABIII equipped with a three electrode system under constant potential conditions. An Ag/AgCl electrode was used as the reference electrode. The polymer film was electrodeposited onto gold electrode surface from 0.2M solution of 4-amino methyl

pyridine dissolved in 1M HCl. The potential range used for electrodeposition was 0.1 V to 1.0 V at a scan rate of 50mVs^{-1}.

Initially, CV was carried out for total 20 scans but after 12 scans a flat line was apparent and electrdeposited polymer also started to drip down from the electrode. Therefore, the numbers of scans were reduced to 8 scans and number of electrodes was prepared through 4-AMP electrodeposition. All experiments were carried out at room temperature. Once deposited with the polymer film, the poly (4-amp) modified electrode was thoroughly rinsed with distilled water for several times and later dried with a stream of argon gas.

Figure 37 shows the successive cyclic voltammograms recorded during the electrochemical oxidation of 4AMP on gold electrode.

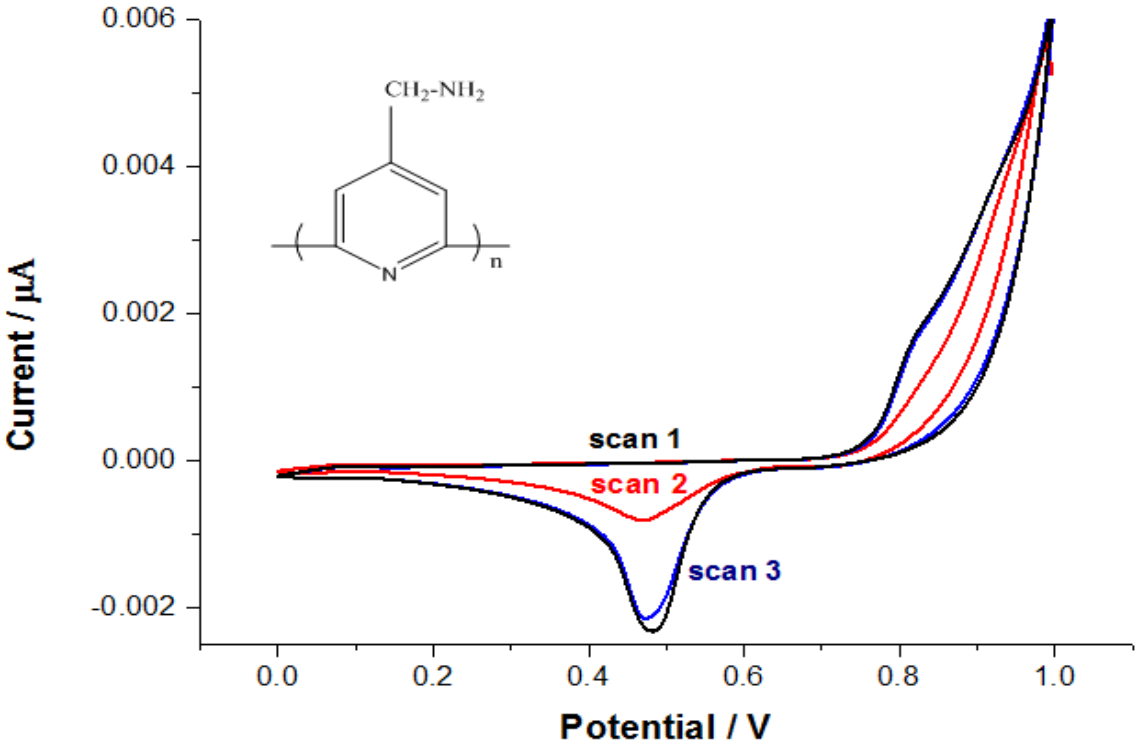

Figure 37 Cyclic voltammograms of poly(4-AMP)

The reduction peak of the product poly (4-AMP) was observed at about 0.48V during the first voltage scan for the monomer. Whereas the oxidation peak during the anodic scan was observed at 0.82V. As the scan continues, the oxidation peak decreased during

the second scan (Figure 33, scan 2) but increases again after the third scan (Figure 33, scan 3). This must be due to the increase in electroactivities of the surface film formed after the second scan. The increase in conductivity might have resulted from longer polymer chains as the scan number increases.

7.3 Characterisation of poly (4-aminomethyl) pyridine

7.3.1 FTIR analysis

An FTIR spectrum obtained from poly (4-amp) is shown in Figure 38.

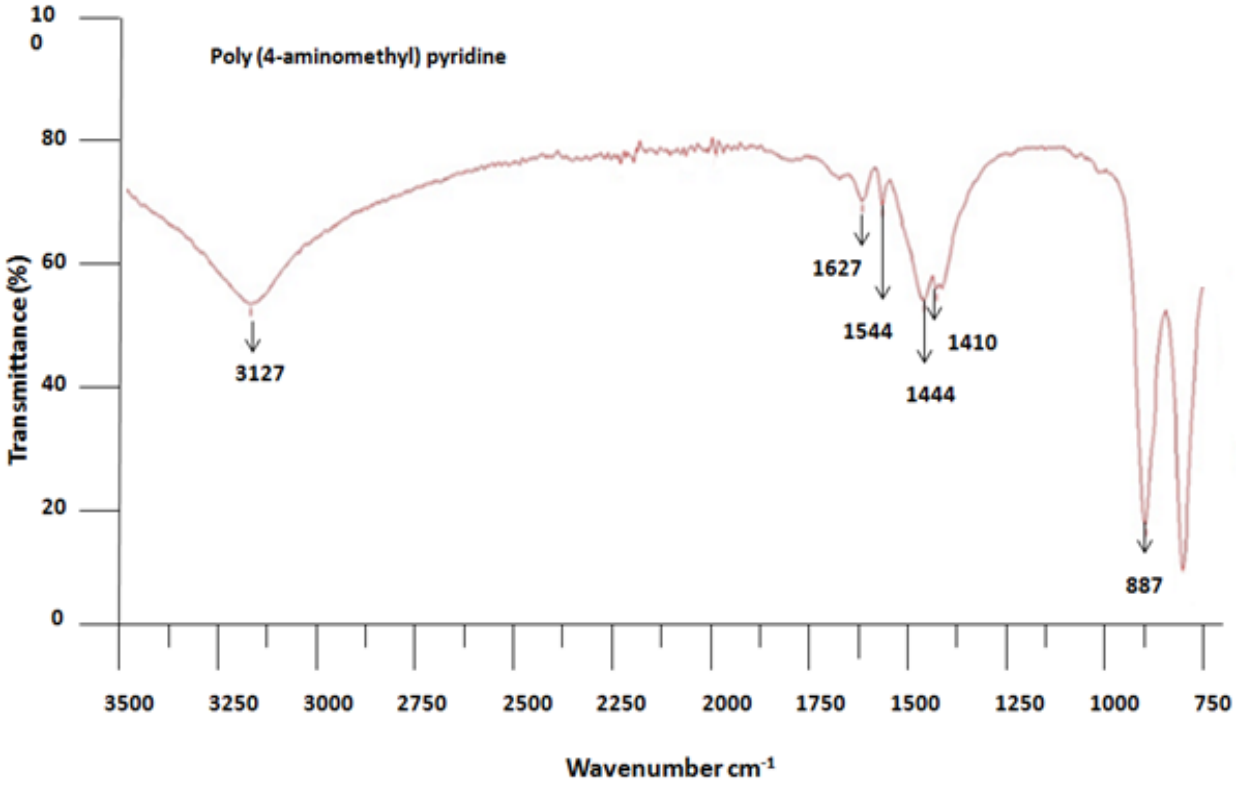

Figure 38 FTIR spectra of poly(4-amp)

In the spectrum, the N-H stretching band is clearly seen at 3127 cm^{-1} whereas N-H deformation bands of primary amines are at 1627 cm^{-1}. The band obtained at 1544 cm^{-1} can be associated with C=N stretching whereas absorption bands at 1444-1410 cm^{-1} evidenced to C-N stretching region for aromatic amines. The peak at 887 cm^{-1} is attributed to the out-of-plane bending of C-H. (Park *et al.*, 1996), (Abdolahi *et al.*, 2012).

7.3.2 SEM analysis of poly (4amp) modified surfaces

The morphologies of different electrode surfaces casted by poly (4-aminomethyl) pyridine were characterised by the scanning electron microscope. Figure 39a shows bare gold electrode surface which has uneven surface with obvious cracks on it. Once poly (4-amp) film was electrodeposited, it formed a thick film coating which covered the surface evenly and also filled all the cavities as shown in Figure 39b. Figure 39c shows SEM picture of drop casted electrodes, where a polymeric suspension was casted onto working electrodes. It shows a thin layer onto gold surface and size of cavities has also reduced which is apparent that the small particles of poly (4-amp) have been adsorbed onto the surface. The adsorption of particles between interstices filled the gaps and surface appeared even as compared to bare electrode.

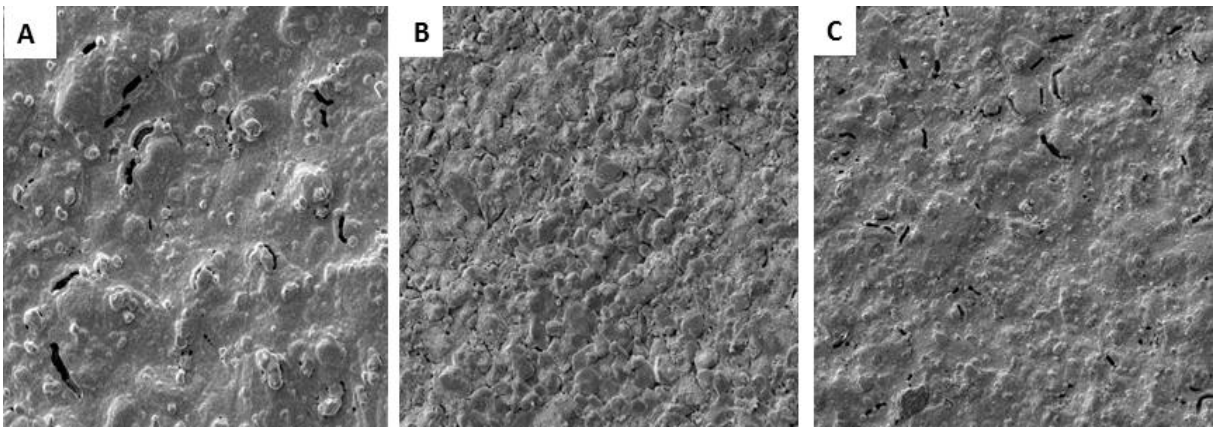

Figure 39 SEM analysis of a) bare electrode b) poly(4-amp) electrodeposited and c) poly(4-amp) drop casted

7.4 Impedance studies of 4-amp based immunosensors

Electrochemical impedance spectroscopy has been used as a sensitive and powerful technique to study sensor interfaces. The impedance of a surface can be analysed with the complex Nyquist plot, when real and imaginary impedance components are plotted as a function of a wide range of frequencies. Generally, an equivalent circuit model (Randles circuit) can be drawn out of the Nyquist plot to derive individual components of a sensor system for example solution resistance (R_s), double layer capacitance (C_{dl}), and charge transfer resistance (R_{ct}). During the layer-by-layer sensor construction or

analyte addition, the change in R_{ct} can be measured if the experiment is performed in the presence of a redox mediator. This process is known as faradic impedance measurement, where impedance to the redox mediator is detected due to increased deposition of material on the sensor surface. The change in R_{ct} can be normalised by calculating percentage change in R_{ct}. This can be done by calculating the percentage change of R_{ct} over immunosensors level R_{ct}. The normalisation is usually useful as the R_{ct} values among different electrodes vary because of sensor-to-sensor variability and multiple incubation steps.

The physiochemical properties of the sensor surface changes upon the chemical binding of both bio-receptor and analyte. Electrical impedance spectroscopy (EIS) system could be used to capture the impedance change on the sensor during the surface modification steps and analyte binding.

In this study, a poly (4-amp) layer was electrodeposited on the gold surface to immobilise half-antibody fragments. After the deposition of polymer, the electrode surface coated with poly (4-amp) was modified through sulpho-SMCC. Sulpho-SMCC comprises of a thiol directed maleimide group and an N-hydroxysuccinimide ester (NHS) which allows attachment to the amine group on poly (4-amp).

The NHS group of sulpho-SMCC covalently bound to the immobilised poly(4-amp), which allowed the opposing maleimide to bind to the reduced antibody. It was possible to bind the antigen by selectively cleaving the heavy chains at the hinge region with TCEP. This exposed at least one pair of thiol groups belonging to the cysteine residues that previously formed the disulphide bridges between the two heavy chains of the antibody. The half-antibody fragments therefore covalently bound to the maleimide group on the linker molecule, completing the functional immunosensor assembly.

Once immunosensors for *Neisseria gonorrhoea β-lactamase (+) ve*, *Neisseria gonorrhoea β-lactamase (-)ve* and *chlamydia* were constructed successfully they were interrogated and characterised through impedance spectroscopy. Electrochemical impedance spectroscopy (EIS) was conducted using FRA software on an AUTOLAB type III electrochemical workstation. Before testing with respective analyte either *Neisseria gonorrhoea* or *Chlamydia*, the fully fabricated biosensor was immersed into electron

mediator solution of 10mM $K_3[Fe(CN)_6]/K_4[Fe(CN)_6]$ for 30 minutes and then incubated with range of respective antigen concentrations. A set of heat killed bacterial concentrations were prepared ranging from 10^2 ml^{-1} to 10^8 ml^{-1} for each analyte. The difference in charge transfer resistance across the surface of the sensor was used to construct calibration curves for all the concentrations. The impedance features are discussed in terms of Nyquist plots to analyse the immunosensor response. All impedance experiments were performed in an electrolyte solution of 10 mM $K_3[Fe(CN)_6]/K_4[Fe(CN)_6]$ (1:1 ratio) in 10Mm PBS, pH 7.4. The study carried out on different types of sensors is discussed in details individually in the following section of this chapter.

7.4.1 Test of poly (4-amp) based sensors against Neisseria gonorrhoea

Two different sets of poly(4-amp) based sensors were constructed with both *Neisseria gonorrhoea β-lactamase (+)ve* and *Neisseria gonorrhoea β-lactamase (-)ve* respectively. Each set of sensors was incubated with particular antigen concentration starting form lowest and impedance spectra were recorded. A small amplitude perturbing sinusoidal voltage signal of 0.4 V was applied over the range 0.1 Hz -10,000 Hz to the electrochemical cell, containing the same redox mediator of $Fe(CN_6)^{3-/4-}$ in PBS at pH 7.2. The resulting current response was recorded using an EcoChemie μAutolab Type III frequency response analyser (FRA-2). This technique was applied for both NG *(+)ve* and NG *(-)ve* sensors and the results were analysed in the form of Nyquist plots.

The Randles equivalent circuit was applied to determine the electron transfer resistance (R_{ct}) between bulk solution and the working electrode interface. Nyquist plots showed data obtained from impedance spectroscopy plotted in the form of a complex plane diagram. This was comprised of the imaginary (-Z") *vs.* real impedance (Z') of a circuit, which are derived from the capacitance and resistance of the cell respectively.

The Nyquist plot shown in Figure 40 was plotted against NG *(+)ve* antibody concentration. It is evident that there is an gradual increase in electron transfer resistance following analyte recognition with the increase of *neisseria gonorrhoea* β-*lactamase (+)ve* antibody concentration.

In the Nyquist plot, the impedance spectra include a semicircle portion and a linear portion. The semicircle portion at higher frequencies corresponds to the electron-transfer limited process, and the linear portion at lower frequencies represents the diffusion-limited process. The semicircle diameter equals the charge-transfer resistance, R_{ct}.

The poly (4-amp) film modified gold electrode reveals a semicircle domain (Figure 40, curve 1), implying an electron-transfer resistance of the redox probe. After the electrode was conjugated with *NG (+) ve* concentration comprising 10^2 particles ml^{-1}, the R_{ct} (Figure 40, curve 2) was increased. Subsequently, 10^3 particles ml^{-1} were incubated on the modified electrode and the R_{ct} increased again and kept increasing until 10^6 particles ml^{-1} (Figure 40, curve 3-6) but decreases after 10^7 particles ml^{-1} (Figure 40, curve 7). The reason is that the protein layer on the electrode acted as the inert electron and mass-transfer blocking layer, and they hindered the diffusion of ferrocyanide toward the electrode surface significantly. The impedance data were fitted with modified Randle's equivalent circuit and it indicated good agreement with the circuit model (Chen *et al*., 2008) and the measurement system over the entire measurement frequency range.

In order to study specificity and selectivity of poly(4AMP) modified electrodes against Neisseria gonorrhoea it was necessary to get a negative control. Therefore ½ created *antidigoxin* was immobilised onto WE2 and tested against various concentrations and any change in impedance was recorded. The Nyquist plot shown in Figure 41 shows the change in impedance of the negative control, *antidigoxin*. The resulting Nyquist plot showed that nonspecific interactions are quite low as compared to specific interactions.

The experiment was repeated for multiple times and the data was analysed through calibatrion bar graph showing the standard mean of deviation as given in Figure 42. The trend shown in Figure 42 presents sabstantial deviation among repeated experiments. It suggests that the thickness and coverage of ploy(4AMP) layer onto the electrode varied considerably among various generated electrdes resulting variable results.

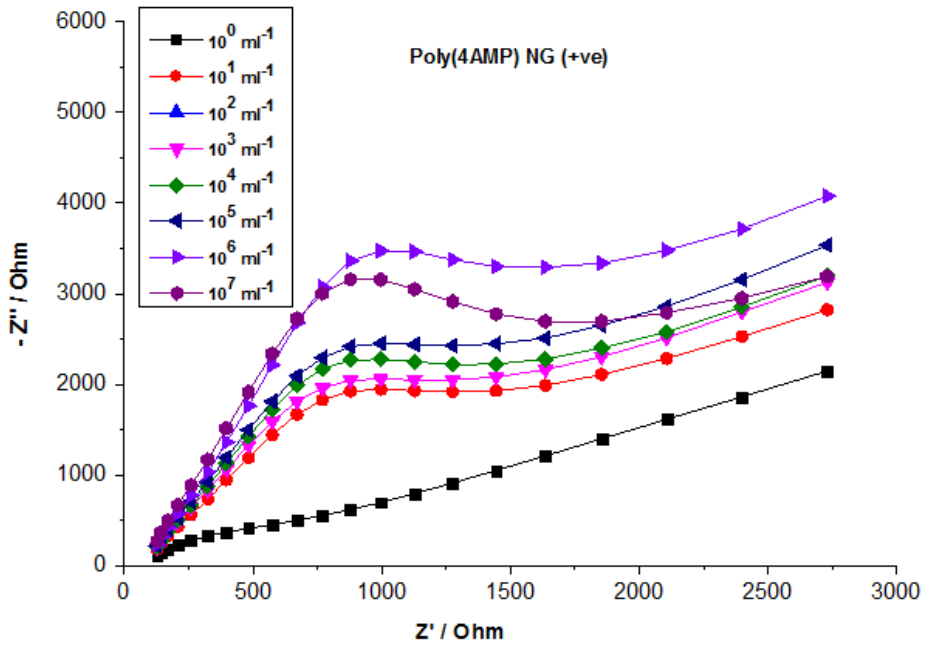

Figure 40 Nyquist plots of poly(4AMP)-NG (+)ve modified electrode exposed to various concentrations of *Neisseria gonorrhoea (+)ve*

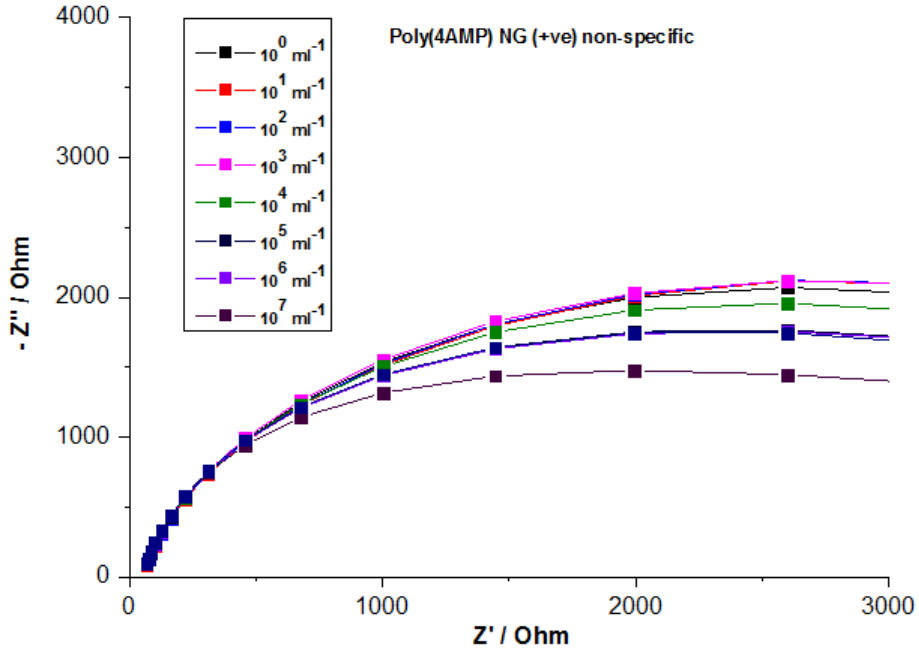

Figure 41 Nyquist plots of negative control of poly(4AMP) modified electrode exposed to various concentrations of NG (+)ve

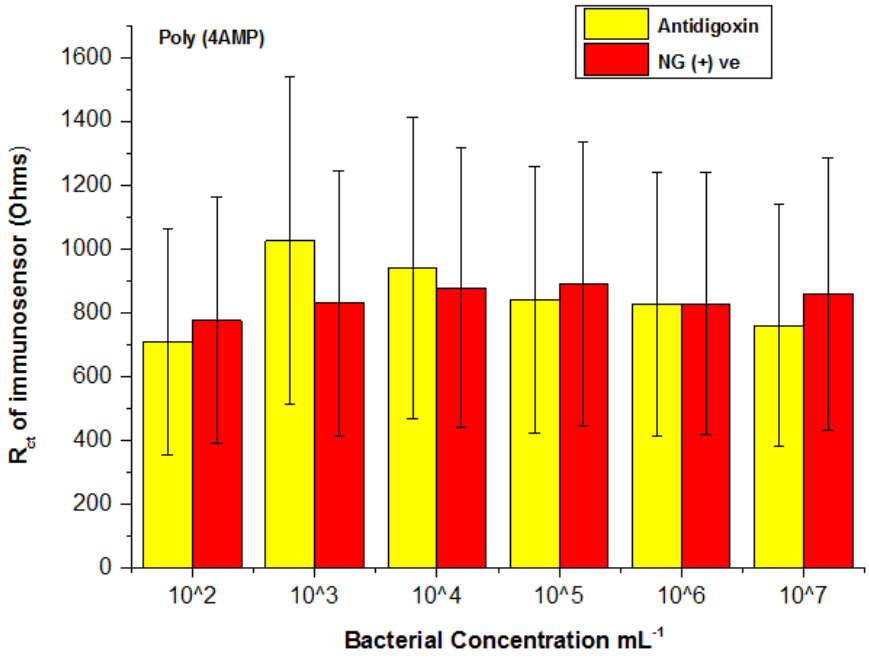

Figure 42 Standard deviation bar graph of poly(4AMP)-NG(+)ve modified immunosensor

The Nyquist plot shown in Figure 43 presents change in electron transfer resistance along with the increase of *Neisseria gonorrhoea β-lactamase (-)ve* antibody concentration. The resistance of poly(4AMP)-NG (-)ve based immunosensor gradually increased but the sensor crashed after introducing third concentration (10^3 ml^{-1}). The poly(4-amp) based surface recovered and showed increased resistance again for 10^6 ml^{-1} bacterial concentration but decreased after incubating with highier concentration of 10^7 ml^{-1}. This is evident that the polymer surface has been collapsed and pinholes may have been created onto the surface.

The apparent immunosensor surface collapse for poly (4-amp) surface could have been due to different orientation of binding. Once bacterial particles binds to antibodies loaded surface, any change in orientation might result in the disruption of the insulating layers of the analyte, allowing charge to flow across the electrode-solution interface. This trend was shown with a number of repeat experiments.

Similarly a negative control for NG(-) based sensor is shown in Figure 44 where *antidigoxin* was immobilised onto WE2 and tested against various concentrations of NG(-)ve. It is evident that the change is resistance is not appreciable and can be

neglected which proved that antidigoxin could be used as negative control of NG (-)ve immunosensor.

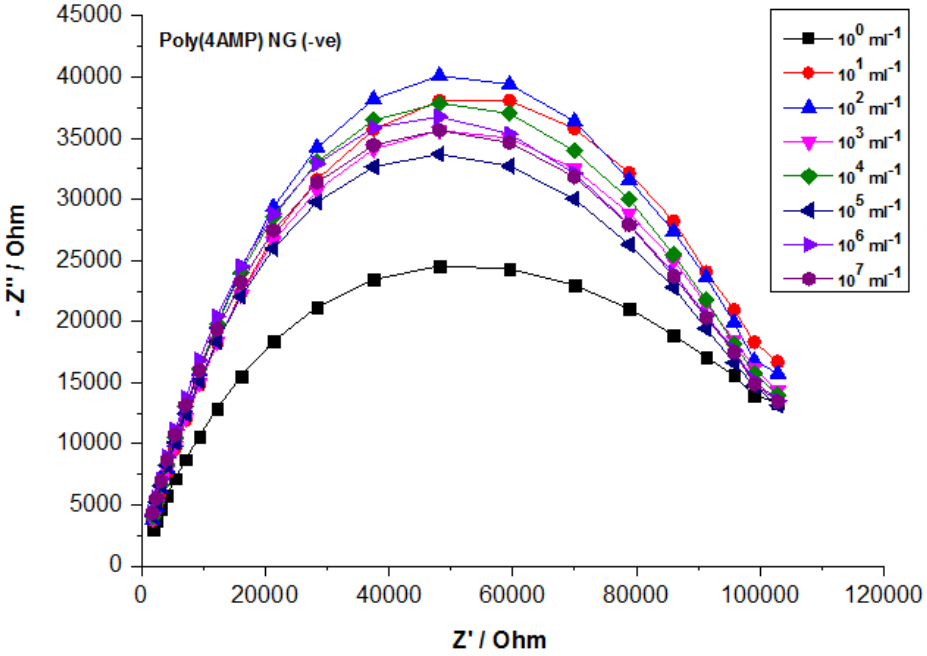

Figure 43 **Nyquist plots of poly(4AMP)-NG(+)ve modified electrode exposed to various concentrations of Neisseria gonorrhoea (-)ve**

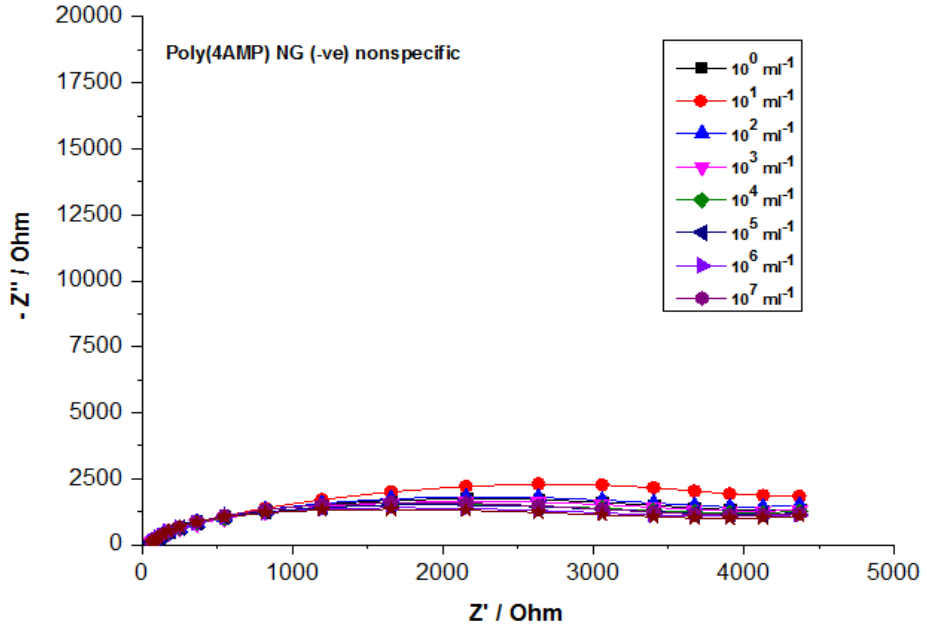

Figure 44 **Nyquist plots of negative control of poly(4AMP) modified electrode exposed to various concentrations of NG (-)ve**

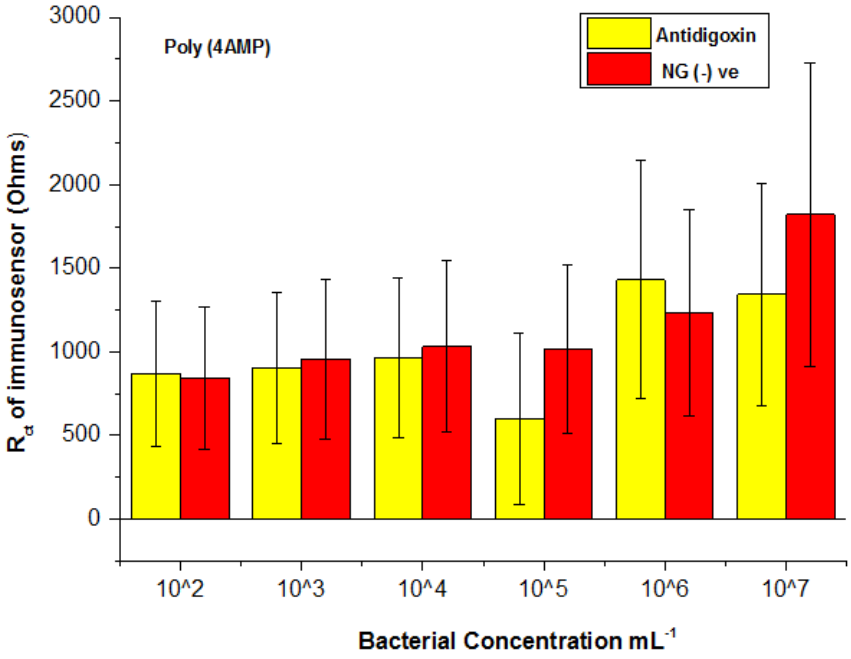

Figure 45 Standard deviation graph of poly(4AMP)-NG(-)ve modified immunosensor

As the experiment was repeated multiple times and various batches of sensors were constructed and tested against NG (-) ve, a standard deviation bar graph was constructed as shown in Figure 45.

It is apparent that the results varied to greater extent among different sensors which proves that poly (4AMP) does not appear to be excellent platform for the immobilisation of antibodies for further research work.

7.4.2 Test of poly (4-amp) based sensors against chlamydia

Following with the same protocol poly (4-amp) based sensors were constructed for *chlamydia* as well. The impedimetric data was collected by incubating with various concentrations of heat killed *chlamydia trachomatis*. Three sensors were used for each experiment and each sensor was interrogated in triplicate for reproducibility. Each sensor was then exposed to an increasing antigen concentration and impedance spectra were recorded. The process was repeated for the full range of antigen concentrations. Subsequent probing of the modified sensors with *chlamydia* antigen, demonstrated the principle of a labelless detection method for *chlamydia trachomatis*. Initial examination of the total impedance of each sensor at various concentrations allowed construction of

a calibration curve. Total impedances were recorded across concentration range of 10^2-10^7 ml^{-1} for the anti-chlamydia loaded poly (4-amp) -coated electrode at 1 Hz and Nyquist plot was built as shown in Figure 46.

The corresponding Nyquist plots of impedance spectra of poly(4AMP)-*Chlamydia* immunosensor shows the semicircle diameter which seems to decrease with the antigen concentration. It shows that R_{ct} decreased after incubation with bacterial particle and the trend kept following for all the bacterial concentraions. This implies that poly (4-amp) surface change its structure with different concentration adding of antigen as the antigen was not immobilised on the entire surface and thus do not act as a blocking layer. It was also noted that the concentration of antigen was increased at 10^4 ml^{-1}, the change of impedance spectroscopy becomes gradually weak, showing that immobilisation of the antibody on a gold electrode trends to saturation situation.

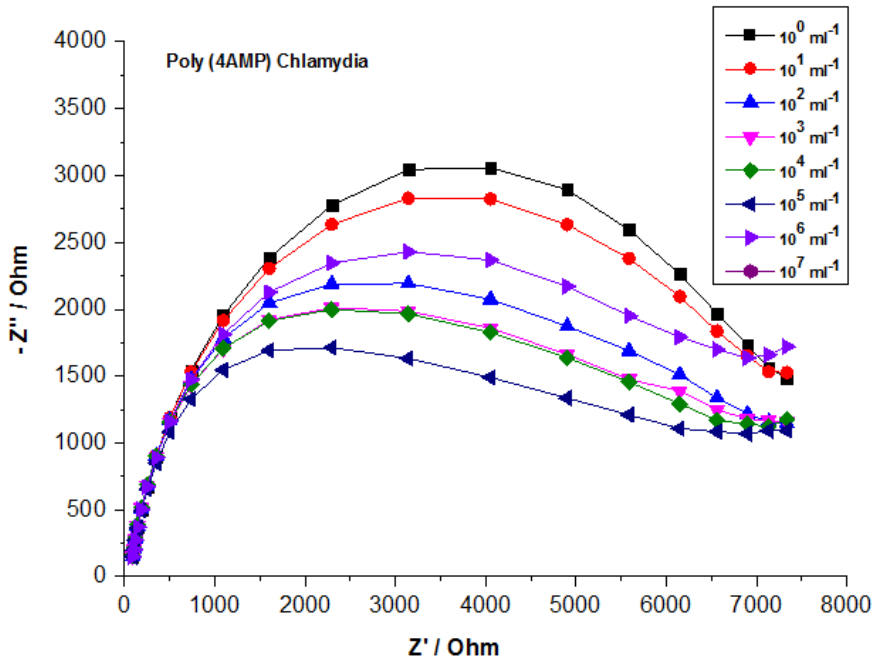

Figure 46 Nyquist plot of poly(4AMP)-Chlamydia modified electrode exposed to various concentrations of Neisseria

Similarly a negative control was tested against various Chlamydia concentrations and antidigoxin was used as nonspecific antibody. The Nyquist plot of nonspecific antibody (antidigoxin) at 1Hz is given in Figure 47. It is apparent that there was decrease in

resistance as various concentrations of Chlamydia concentrations were incubated onto the negative control.

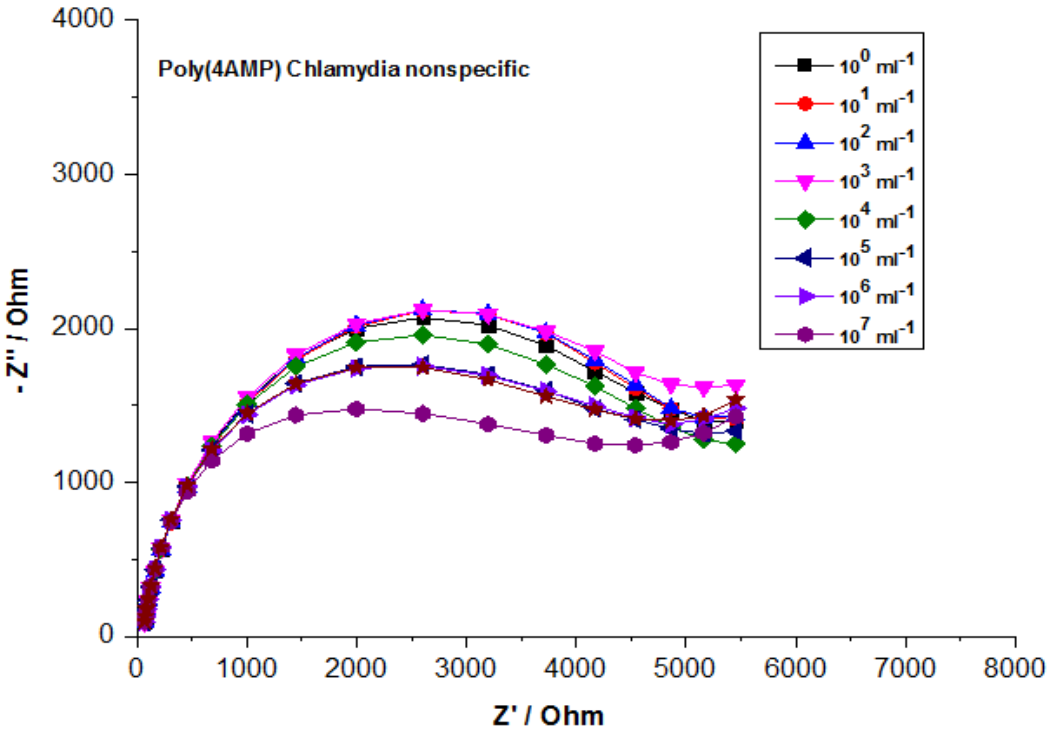

Figure 47 Nyquist plots of negative control of poly(4AMP) modified electrode exposed to various concentrations of *Chlamydia*

It is necessary to study the sensitivity and selectivity of an immunosensor thereby a number of sensors were developed and tested against various concentrations of analyte (*Chlamydia*) and results were plotted and interrogated in terms of standard mean of deviation. The bar graph presented in Figure 48 shows standard deviation of three different *Chlamydia* immunosensors.

The yellow bar represents nonspecific interactions where antidigoxin was used as negative control whereas red bar shows specific analyte where *Chlamydia* was tested against various concentrations of *Chlamydi*a heat killed pathogen. It is apparent that poly(4AMP) does not appear to be good platform for immunosensor construction and another polymer should be studied for further research work.

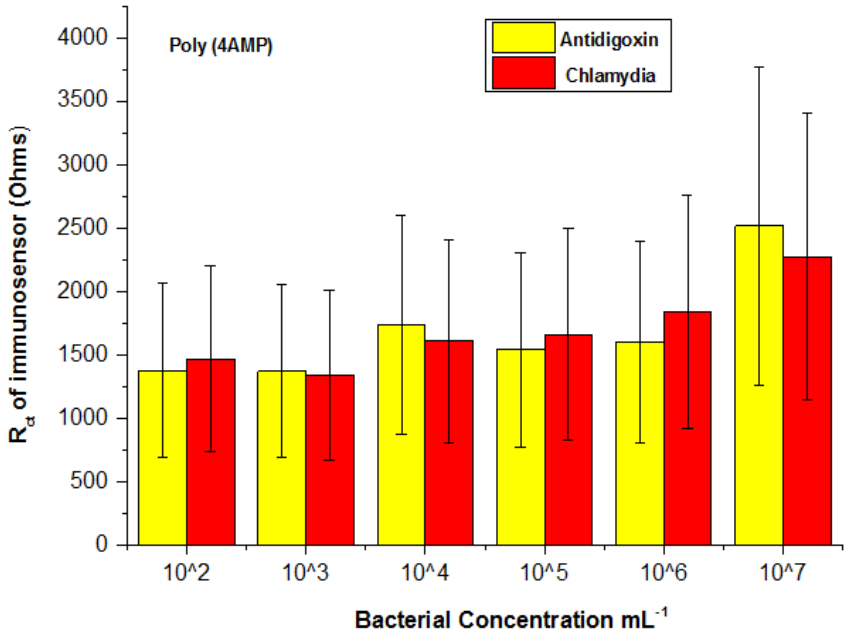

Figure 48 Standard deviation graph of poly(4AMP)-*Chlamydia* modified

7.4.3 Calibration curves against increasing antigen concentrations

Non-specific interactions have the potential to either exaggerate or mask specific interactions. Whereas specific binding of antigens will only occur when their antibodies is present, electrodes fabricated using a non-specific antibody should undergo the same non-specific binding events as those fabricated using specific antibodies. To study and eliminate non-specific interactions in poly(4-amp) based sensors, anti digoxin was immobilised on WE1 whereas specific antibody for example *chlamydia* was deposited onto WE2 and exposed to different concentration of antigen to record change in resistance.

Figure 49 shows calibration plots that correspond to the resistance change (ΔR_{ct}) at similar frequency with different concentrations of the specific and non specific antibodies. The curves generated as a result of exposure of particular anti-body and 4-amp film to increasing concentrations of respective antigen at 1 Hz. The curve displays the % impedance response against antigen concentration (bacterial particles/ml), normalised against the baseline response (zero antigen).

The changes of resistance are normalised following the equation 13:

$$\Delta R_{ct} = R_{ct\ (Specific\ Ab)} - R_{ct\ (nonspecific\ Ab)} / R_{ct\ (nonspecific\ Ab)} \times 100 \quad (13)$$

From previous study of immunosensors, it was hypothesised that when analyte was recognised, the double layer increased in thickness, causing capacitance to decrease. This blocked the flow of the redox species across the double layer, diminishing Warburg impedance (Billah *et al.*, 2008).

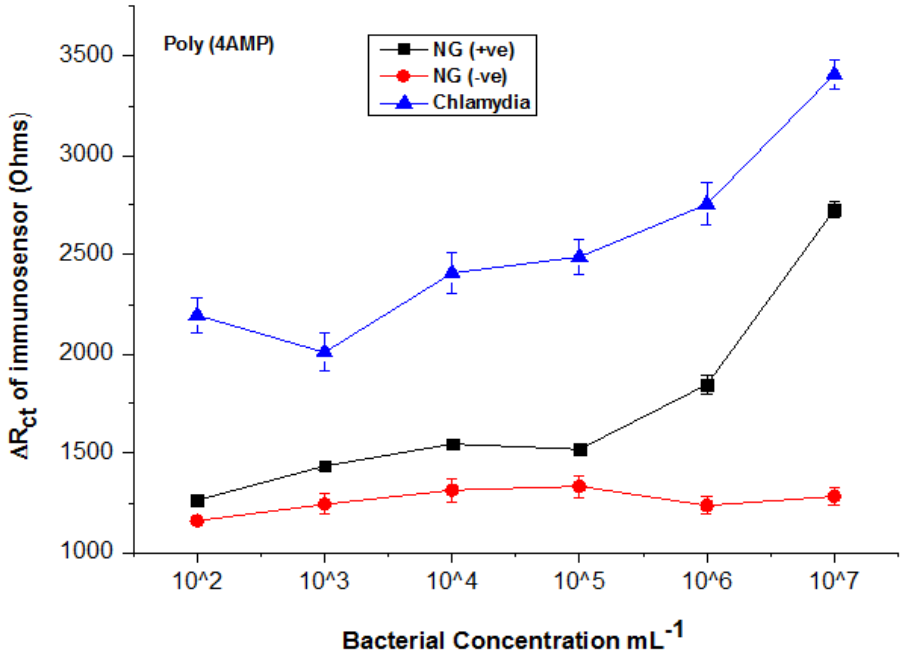

Figure 49 **R_{ct} calibration curve of poly(4AMP) immunosensor comprising normalised values**

From Figure 49, it is evident that the R_{ct} observed across the electrode–solution interface was higher generally for the *chlamydia* based immunosensor compared to the *NG (-) ve and NG (+) ve* based immunosensors. In case of *NG (+) ve* immunosensor there was gradual trend was recorded along with higher concentrations as shown in balck line. Whereas there was uneven trend shown in calibration of *NG (-)ve* shown in red where resistance increased gradually with the incubation of concentration ranging from 10^2 ml^{-1} to 10^4 ml^{-1} but decreased after introducing concentration of 10^5 ml^{-1}. The system recovers after incubating 10^6 ml^{-1} and resistance started to increase but again collapsed when higher concentration of 10^7 ml^{-1} was introduced. However in the calibration curve of *chlamydia* based immunosensor showed dramatic decrease in the

resistance of charge transfer across the surface after the addition of 10^2 *chlamydia* particles ml^{-1} and but kept increasing until 10^7 ml^{-1}. The trend of change in R_{ct} after additions of increased bacterial load with all three antibodies have clearly shown that poly(4-amp) is not an ideal polymer for the fabrication of immunosensor.

7.5 Discussion

The studies of poly (4-amp) based immunosensor presented in this chapter have shown that antibodies can be successfully immobilised onto the new conductive polymer surface. A set of poly (4-amp) based sensors were prepared to develop immunosensor against three types of antibodies. EIS was employed to characterise sensor construction and subsequent analyte detection. The response of the impedance biosensor system was interpreted by the Randles model equivalent circuit. The equivalent circuit consists of ohmic resistance (R_s) of the electrolyte, double layer capacitance (C_{dl}), charge-transfer resistance (R_{ct}) and Warburg impedance (Z_w) of the electrode. The parallel elements are introduced because the total current through the working electrode is the sum of distinct contributions from the Faradaic process (i_f) and double layer charging (i_c). Since all the current must pass through the uncompensated solution resistance, R_s is inserted as a series element in the equivalent circuit. Among these electrical elements in the equivalent circuit, R_s and Z_w represent bulk properties of the electrolyte solution and diffusion of the redox probe, whereas C_{dl} and R_{ct} depend on the dielectric and insulting features at the electrode/electrolyte interface. All these electrical elements are affected by the property change occurring at the electrode interface.

Initially, poly(4-amino methyl pyridine) based sensors were tested against various concentrations of *Neisseria gonorrhoea β–lactamase (+) ve, Neisseria gonorrhoea β–lactamase (-) ve* and *chlamydia trachomatis*. The response was interpreted in the form of Nyquist plot and the data was fitted into Randles model circuit.

Nyquist plot data of *NG (+)* and *(-) ve* showed the poly (4-amp) coated gold sensor impedance was reduced with the addition of analyte until certain concentration but increased afterwards. This is attributed to increase in thickness of double layer which resulted in increase of resistance and consequently capacitance decreased. The trend of

change in impedance has shown that the polymeric layer was disrupted with the addition of higher concentration of *NG (+) ve* and *(-) ve* pathogens. In the case of *NG (-) ve* there was gradual increase in resistance in agreement of increase of double layer thickness but the sensor collapsed and the charge transfer resistance decreased after 10^5 ml^{-1}. The sensor showed signs of recovery with the higher concentration of 10^6 ml^{-1} before collapsing again at 10^7 ml^{-1}. The disruption of the polymer layer by bacterial particles was consistent in repeat experiments of different sets of sensors interrogated by similar way through EIS.

However, this does not apply to data obtained from study of *chlamydia* as an analyte. It was evident from Nyquist plot of poly (4-amp) based *chlamydia* sensors that the immobilised antibodies did not insulate the electrode properly. Here, the sensing surface was perturbed after the introduction of analyte, causing a reduction in the charge transfer resistance at the electrode-solution interface. It appeared that the incubation of *chlamydia* particles onto the sensor surface disturbed the surface and might have caused "pinholes" into polymer layer. These "pinholes" permitted the current flow resulting in the increase of capacitance.

In light of the data obtained, it was suggested that the sensing platform of poly (4-amp) is not robust for analyte detection. Therefore it was decided that new surface chemistries and constructions would be investigated to immobilise the antibody against other conducting surfaces. Therefore, polyaniline, polypyrrole and polytyramine surfaces on the same screen printed gold electrodes were considered as possible surface layers for the immobilisation of antibodies.

CHAPTER 8 POLYANILINES BASED IMMUNOSENSORS

8.1 Introduction

Polyaniline (PANI), a conducting polymer of semi-flexible polymer family, was discovered over about 150 years ago. Among organic conducting polymers, polyaniline is regarded as one of the most promising conductive polymers due to its ease of synthesis, low cost, versatile processability and relatively stable electrical conductivity (Dhand *et al*., 2011).

Among the most promising applications of polyaniline is electrochemical biosensing, as it can act as a suitable matrix for the immobilisation of biomolecules. Polyaniline is compatible with biological molecules in neutral aqueous solutions. Moreover, based on its excellent conductivity and electroactivity, polyaniline can act as a mediator for enzyme electrodes, where polyaniline undergoes redox cycling and can couple electrons from the enzyme active centre to the electrode surface. Another advantage for the application of polyaniline in electrochemical biosensing is that polyaniline can be electrochemically synthesised directly on the electrode from aniline monomer, through galvanostatic, potentiostatic or potentiodynamic means. The preparation of polyaniline modified electrodes with the electropolymerisation method offers the potential to incorporate a wide range of dopants into the formed polyaniline film and gives good control over the film thickness (Luo *et al*., 2007).

After studying poly(4-amp) as a sensing layer for the immobilisation of antibodies it was necessary to generate another robust conductive layer for the successful immobilisation of targeted antibodies and get high impedance signals which could be reproduced easily. Bearing in mind all these facts, polyaniline was chosen as a conductive ink onto gold plated electrode surface. To achieve the desired results it is necessary to get a uniform layer onto the electrode surface which could be achieved through either electrodeposition or ink printing.

8.2 Polymerisation of aniline

8.2.1 Chemical polymerisation

Polyaniline can be prepared chemically or electrochemically by oxidative polymerisation. Chemical synthesis of aniline produces powdered polyaniline, while electrochemical synthesis can be used to generate thin films on a conductive substrate. Chemical oxidative polymerisation of aniline was carried out in a conventional aqueous solution and in micellar solutions of sodium dodecyl sulphate (SDS, anionic surfactant) (Kim *et al*., 2000) and dodecylbenzene sulphonic acid (DBSA, anionic surfactant) (Han *et al*., 2009) with APS as initiator as described in literature. Each synthesis will be discussed briefly along with conditions and resulting polymer suspension was characterised through FT-IR and SEM. The polymerisation reaction is given in Figure 50.

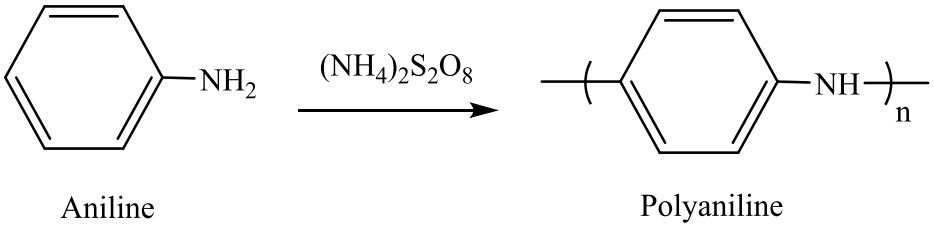

Figure 50 Polymerisation of aniline

8.2.1.1 Synthesis through micelle polymerisation

0.1M HCl solution was prepared by adding 4.098ml of 35% HCl in 500ml of distilled water and was used as an aqueous solution in micellar solution. 0.03M solution of aniline (ANI) was prepared by dissolving 0.68ml of aniline into 250 ml of distilled water. Aqueous micellar dispersion was prepared by introducing 50 ml of aniline solution in 50 ml of 0.2M SDS solution in distilled water. 1M ammonium peroxydisulphate ($(NH_4)_2S_2O_8$) in 0.1M HCl solution was used as an oxidant (initiator) and added into the mixture at a rate of 1.0 mL/min. The polymerisation was performed at 20 °C with the mechanical stirring at 500 rpm in a two-neck round bottomed flask mounted in a thermostat for 12 hours. The colour of the polymerisation solution changed as polymerisation proceeds. In the initial stage, aniline/SDS/APS solution was colourless

with high transparency. As the polymerisation proceeded, the colour of the solution changed to white through yellow, brown and finally to green, which indicates the formation of polyaniline emeraldine salt (ES). An excess amount of methanol was added into the HCl-doped polyaniline dispersion to precipitate polyaniline powder by breaking the hydrophilic-lyphophilic balance of the system and to stop the reaction. The precipitates were collected in a glass filter and washed two times each with methanol, acetone, and pure water to remove unreacted chemicals, aniline monomers and SDS. Then, the polyaniline particles were dried in the desiccator under the vacuum for 72 hours at room temperature.

The morphologies of polyaniline particles formed in micelles aqueous solution were studied with field emission scanning electron microscopy. The particles synthesised appear to be spherical but coagulation is apparent in Figure 51. The SEM images of polyaniline nanoparticles were captured after sputtering with gold for 10 s. The photographs were obtained at 20 kV and at a working distance 1 μm and 10 μm.

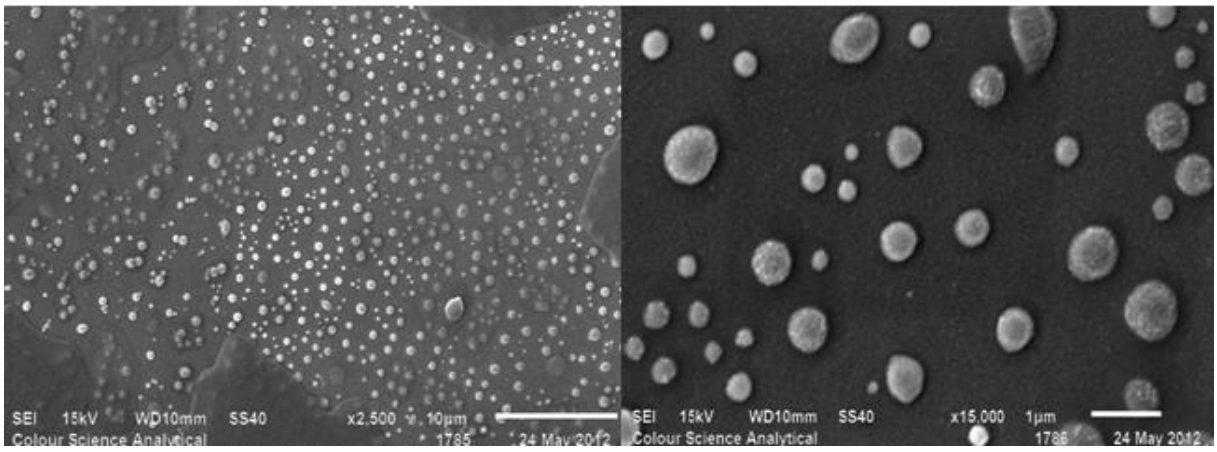

Figure 51 SEM images of polyaniline particles with micelle polymerisation

Polyaniline particles prepared through micelle polymerisation were found to be spherical and tend to coagulate very easily. The particles were suspended into 1% tween solution but they found to be very fine and coagulated to some extent. The smallest particles were found in the range of 35-40nm.

8.2.1.2 Synthesis through reverse micelle polymerisation

ANI (0.025 mol) was added into the micellar solution containing DBSA (0.0375 mol) dissolved in toluene (200 mL). The solution was mixed and sonicated at 50W for 10 min to make a homogeneous solution. As polymerisation of ANI is exothermic, the reaction mixture was kept in a cooling bath with magnetic stirring at 0 °C. APS (0.01mol) in distilled water (10 mL) was added dropwise into the micellar solution (200mL) for approximately 20 – 30 min. After an induction period of about 50 – 70 min (including time of APS addition), the whitish reaction mixture turned bluish and the colour became more pronounced as the polymerisation proceeded. The polymerisation was carried out for 2 hour at 0 °C under moderate stirring. Finally, a dark green PANI dispersion was obtained.

After polymerisation, methanol (50 mL) was poured into the solution. In a few minutes, the solution separated into a green upper solution and transparent reddish lower solution. In the upper solution, PANI – DBSA in the form of emeraldine salt was dispersed in toluene, and unreacted DBSA, APS, and by products ($(NH_4)_2SO_4$, etc.) were dissolved in the lower aqueous phase.

The SEM images shown in Figure 52 present that most of the particles size ranges under 100nm. These pictures have been captured at a working distance of 1 and 5μm and 20 kV through a SEM microscope. A small drop of the resulting dispersion was casted onto glass slide, dried in air and covered with slip.

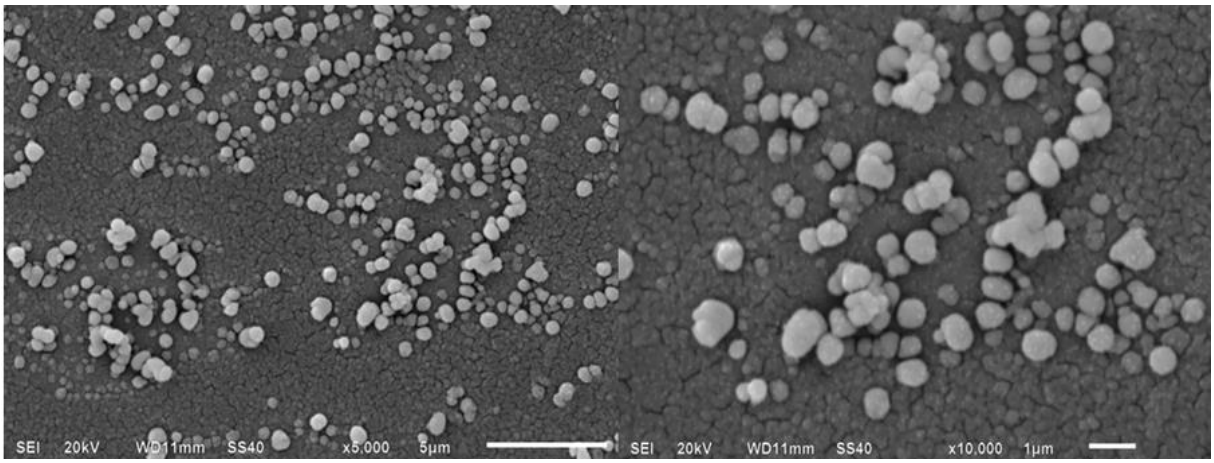

Figure 52 SEM pictures of polyaniline in reverse micelle polymerisation

The polyaniline particles prepared through reverse micelle polymerisation were found to be spherical of varying sizes due to adhesion of fine particles resulted into larger particles.

8.2.1.3 Synthesis of polyaniline fibres

Polyaniline nanofibres were prepared by interfacial polymerisation[5] or simply by rapidly mixing an aqueous solution of aniline and an oxidant, instead of slow addition of one reactant to the other. The stock solution of 0.3M solution of aniline was prepared in 1M HCl. 0.18 g of ammonium persulphate (APS) dissolved in 10 mL of 1 M HCl solution was used an oxidant.

Four different methods were employed for the synthesis of nanofibres based on reaction conditions applied to the polymerisation.

Method A*:* 10 mL of ammonium peroxydisulphate solution was added dropwise into 10 mL aniline solution at 5 mL/h while stirring at 1100 rpm. An ordinary magnetic stirrer bar was used to agitate the reaction mixture at 1100 rpm.

Method B*:* 10 mL ammonium peroxydisulphate solution was added dropwise into 10 mL aniline solution without stirring.

Method C*:* The two reactant solutions 10 mL each were mixed rapidly with vigorous shaking for 30 s and then left standing for 2 hours.

Method D: The two reactant solutions 10 mL each were mixed rapidly and stirred at 1100 rpm for 2 hours.

All the mixtures were left still or stirred with an ordinary magnetic stirrer at different speeds for 2 hours. Small drop of the resulting dispersion was casted on a silicon wafer, dried in air and coated with gold for SEM imaging.

Figure 53 shows scanning electron microscope (SEM) images of polyaniline nanofibres synthesised via the conventional method. Figure 53A shows that nanofibres were obtained in which the oxidant solution was added drop wise into the aniline solutions.

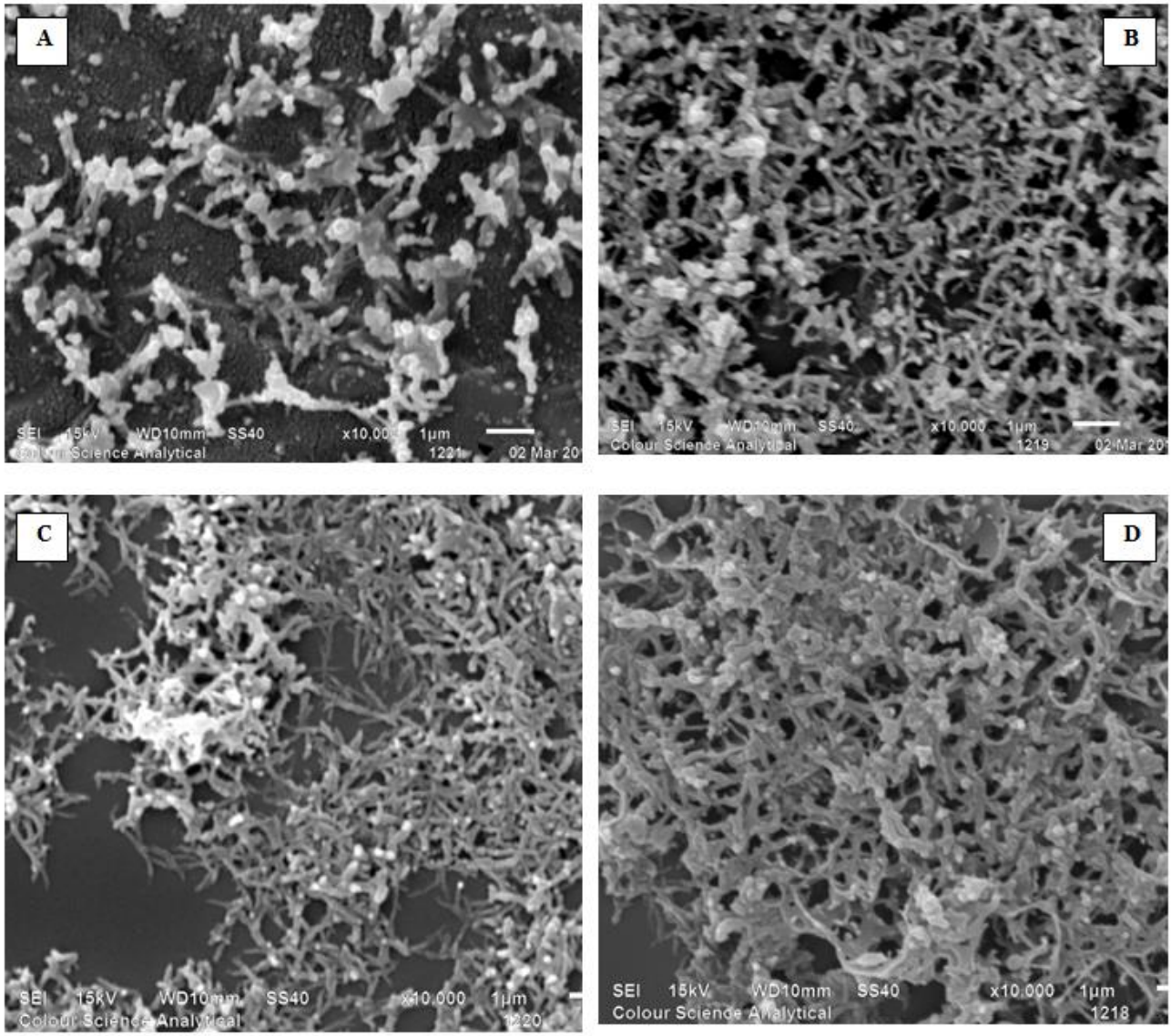

Figure 53 SEM pictures of polyaniline nanofibres

The product settled out quickly from the reaction solution, and film casted from its suspension was rough and discontinuous. It was found that the slow-addition polymerisation process with out stirring resulted into the product smooth nanofibres as shown in Figure 53B and 53C. However, when intense stirring was kept up during the entire polymerisation process, the fibres obtained found to be highly aggregated as shown in Figure 53D.

8.2.2 Electropolymerisation of polyaniline

Uniform deposition of the polymer on a suitable sensor surface has been another major challenge in biosensor fabrication. Electrochemical deposition of 1 M aniline in 0.5 M KCl and1 M HCl was performed sequentially cycling the working electrode potential

from 0 V to 1 V (vs. Ag/AgCl) and back to the starting potential at a scan rate of $50mVs^{-1}$. Electrochemical deposition of the polymer films was performed by cyclic voltammetry (CV).

The potential sweep was started from the lower potential limit (cathodic limit) towards anodic direction and back. The recorded voltammograms showed a single well-defined anodic peak and one corresponding cathodic peak. The polymer oxidation and reduction peaks showed an increase in current with successive cycles indicating the deposition of increasing amounts of electroactive polymer.

10mM solution of aniline was prepared in 0.5M KCl and 1 M HCl for electrodeposition of polyaniline. A starting potential of 1 V, cycling back to 0 V was applied to the gold working electrode using CV. The CV was carried out for 20 scans. The resulting cyclic voltammogram *vs.* Ag/AgCl reference electrode after each cycle is shown in Figure 54. The voltammogram showed two main oxidation peaks around 0.2 and 0.87V.

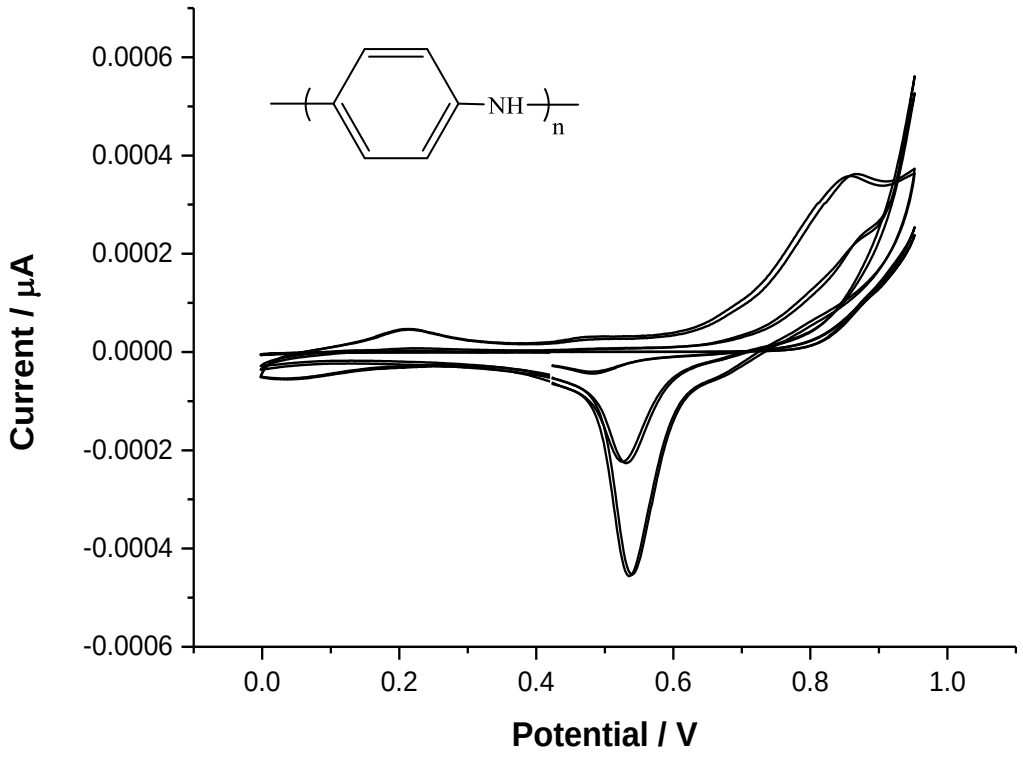

Figure 54 Cyclic voltammogram of polyaniline in 1M HCl

These peaks show the transformation of leucomeraldine base (LB) to emeraldine salt (ES) and ES to pernigraniline salt (PS), respectively. On the reverse scan, one reduction peak was observed at 0.52 V indicating the deposition of polyaniline film onto electrode surface. It was also found that the current responses increased on subsequent scans indicating that the nanoparticles aggregated/assembled on the gold electrode surface. The peak potentials also began to shift after a number of cycles. This may be as the result of film deposition which became thicker along with each scan. The increase in thickness of film increases the resistance of the electrode.

8.3 Characterisation of polyaniline

8.3.1 FTIR analysis

FT-IR spectra of PANI samples doped with HCl acid is shown in Figure 55. In the spectrum, a band observed at 3239cm^{-1} corrospond to then N-H stretching mode of secondary amine (Wasu and Raut 2014).

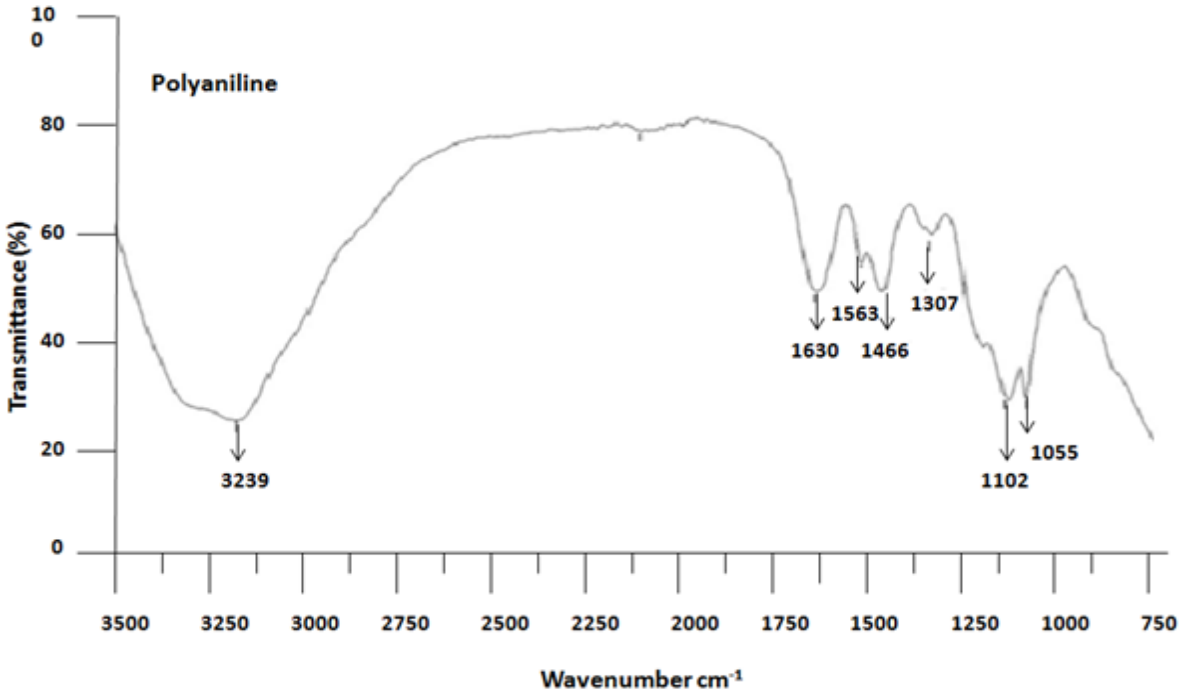

Figure 55 FT-IR spectrum of polyaniline

The absorption peak is also observed at 1630 cm^{-1} and it is attributed to C=C stretching in aromatic nuclei. A peak at 1563cm^{-1} is due to the quinonoid structure of PANI. Another one sharp peak at 1466cm^{-1} is corresponding to the benzenoid structure of PANI. The absorption band shown at 1307 cm^{-1} is due to aromatic amine (Arasia *et al*., 2009). The absorption bands appeared at 1102 and 1055 cm^{-1} reveals C-H bending vibrations. The same finding has been reported elsewhere (Vivekanandan *et al*., 2011).

8.3.2 SEM analysis of polyaniline modified sensor

The morphologies and microstructures of different electrode surfaces were characterised by the SEM observation. Figure 56A shows surface of bare gold electrode which has rough appearance and fissures at certain places.

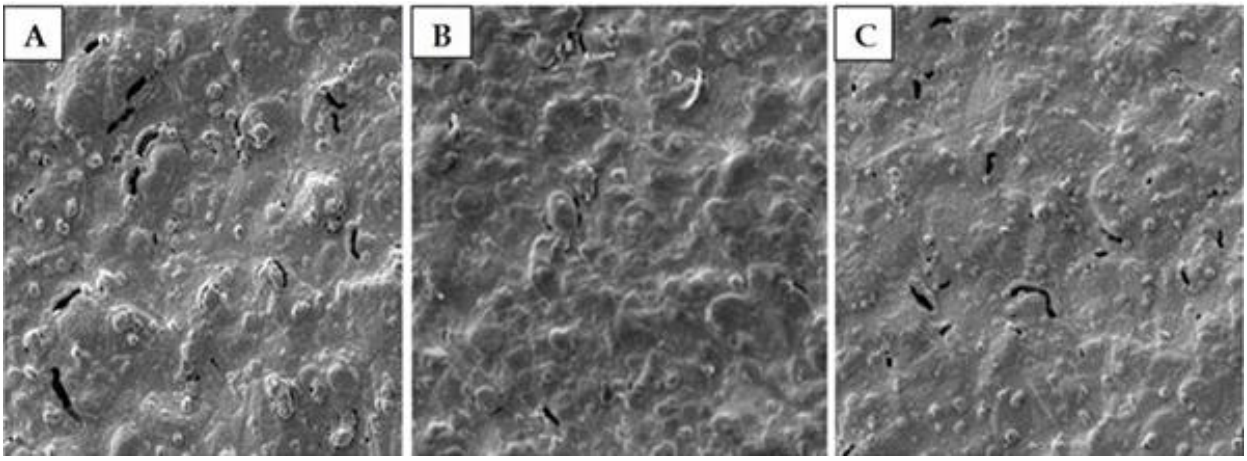

Figure 56 SEM analysis of polyaniline film film onto a) bare electrode b) polyaniline electrodeposited and c)polyaniline drop casted

Once polyaniline was electrodeposited a slightly thick film covered the bare gold electrode surface and smoothen it as shown in Figure 56B. The Figure 56C shows a thin polyaniline layer formation onto the electrode surface. Here polyaniline suspension was deposited onto the electrode through drop casting. It is apparent that polymer layer is thin and successfully adsorbed onto the surface as the size of cervices has reduced as compared to the bare electrode.

8.4 Impedance studies of polyaniline

Electrical impedance spectroscopy was used as an analyser to plot the electrode impedance over the applied frequency range. Generally, the impedance component is used to illustrate the equivalent resistance and the capacitance changes in the solid liquid interfacial phenomena. EIS measurement can be carried out in the solutions where the potential of the structure increases due to different concentration ratios. This approach can be recognised as a heterogeneous electron transfer reaction of the solution which can be evaluated using the electrical double layer structure. In order to obtain the faradic impedances of polyaniline based sensors, the Randels cell model of equivalent circuit was used to describe the process at the electrochemical interface.

8.4.1 Impedance studies of different forms of polyaniline modified electrode

Different forms of polyaniline chemically polymerised through oxidative polymerisation were casted on electrodes and were characterised by electrochemical impedance spectroscopy. Figure 57 depicts typical Nyquist plots (-Z' versus Z") of different types of polyaniline coated gold electron in an electrolyte solution of 10 mM $K_3[Fe(CN)_6]$/K4$[Fe(CN)_6]$.

The Nyquist curves obtained demonstrated that the Z' (real) component of the impedance increases steadily with decreasing frequency whereas the Z″ (imaginary) component increases to a maximum value (at frequencies in the range 5–10 Hz) but falls as the frequency approaches 1 Hz. This type of impedance spectrum is indicative of a surface-modified electrode system where the electron transfer is slow and the impedance is controlled by the interfacial electron transfer.

The Nyquist curves for all four forms of polyaniline comprises a depressed semicircle at high frequencies, which can be related to the combination of charge transfer resistance of polyaniline and the double-layer capacitance, followed by a straight line with a slope of nearly 45°. The straight line is due to the occurrence of mass transport process via

diffusion. Nyquist plot of all types of polyaniline particles suggested that polyaniline nanoparticles shown in black line are most conductive among all.

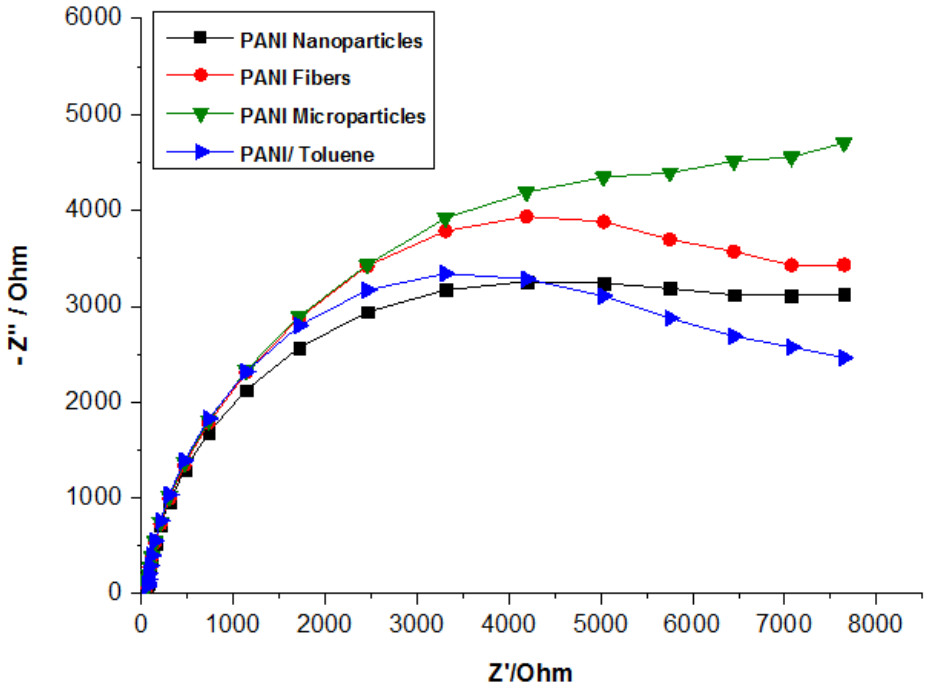

Figure 57 Nyquist plots (-Z' versus Z") of the various forms of polyaniline modified electrodes

Sensors were fabricated by electropolymerisation of polyaniline on the screen-printed gold electrodes, to produce a smooth conductive substrate. Polyclonal antibodies of *Neisseria gonorrhoea β-lactamase (+) ve* and *Neisseria gonorrhoea β-lactamase (-) ve* and *chlamydia* were subsequently incorporated onto the polyaniline layer using a SMCC system for site-specific immobilisation. The sensors were then probed with varying concentrations of respective antigens (*Neisseria gonorrhoea* and *Chlamydia trachomatis*) and the impedimetric response at each concentration was recorded. Each sensor results will be discussed individually in the following section.

8.4.2 Test of polyaniline based sensors against Neisseria gonorrhoea

Initially, polyaniline based sensors based experiments were conducted on *Neisseria gonorrhoea β-lactamase (+) ve* and *Neisseria gonorrhoea β-lactamase (-) ve* individually. The modified electrodes were prepared by electrodepositing polyaniline in 0.5M KCl and 1M HCl for 20 scans. Once prepared, the conductive surface of these electrodes was

activated by incubating them with 4mg.ml^{-1} SMCC for 1 hour. After incubation is completed, relevant half generated antibodies were added and incubated for another 2 hours. The fully formed immunosensors were then exposed to increasing concentrations of bacteria, for 10 min duration for each dilution. The electrode was rinsed, dried in argon and the impedance studies were carried out after each bacterial addition. The impedance data across the interface was obtained by immersing the electrode in the mediator $Fe(CN)_6^{3-/4-}$, at an applied potential of 0.4 V and frequency range 0.1 Hz to 10,000 Hz.

Data shown in Figure 58 are derived from *Neisseria gonorrhoea β-lactamase (+) ve* in the form of Nyquist plots modelled to a modified Randles equivalent circuit. Direct measurements of the total impedance involve the resistance of the solution, R_s and the double-layer capacitance $C_{dl.}$ Furthermore, the interpretation of the impedance spectra due to the chemical reaction is symbolised by charge transfer resistance R_{ct} and Warburg impedance Z_w. The Nyquist plot for NG(+)ve suggested that charge transfer resistance decreased along with the increasing concentrations.

As antigen-antibody immobilisation occurs on the sensor surface, the electrical double-layer capacitance changes while altering the measure impedance. The charges passing through the solution experience the resistance of the solution and the double layer capacitance due to the immobilisation. The charge transfer resistance of NG(+)ve immunosensor implies that the charged particles leaked through the double layer due to the electrochemical reactions on the sensor surface.

The negative control of PANI-NG(+)ve was studied through immobilisation of *antidigoxin* as a nonspecific analyte. The negative control was tested against various concentrations of NG(+)ve and the resulting Nyquist plot is shown in Figure 59. The change in resistance after incubating various bacterial concentrations of NG (+)ve was recorded and the data was plotted in the form of Nyquist plot. The negative control showed a slight increase in R_{ct} across the electrical interface upon increasing concentration of bacterial binding, but not to the same extent as specific analyte binding. The experiment was repeated number of times to study the potential of reproduacability of PANI based immunsensors and the resulting data was used to form a calibration graph with error bars presenting standard mean of deviation.

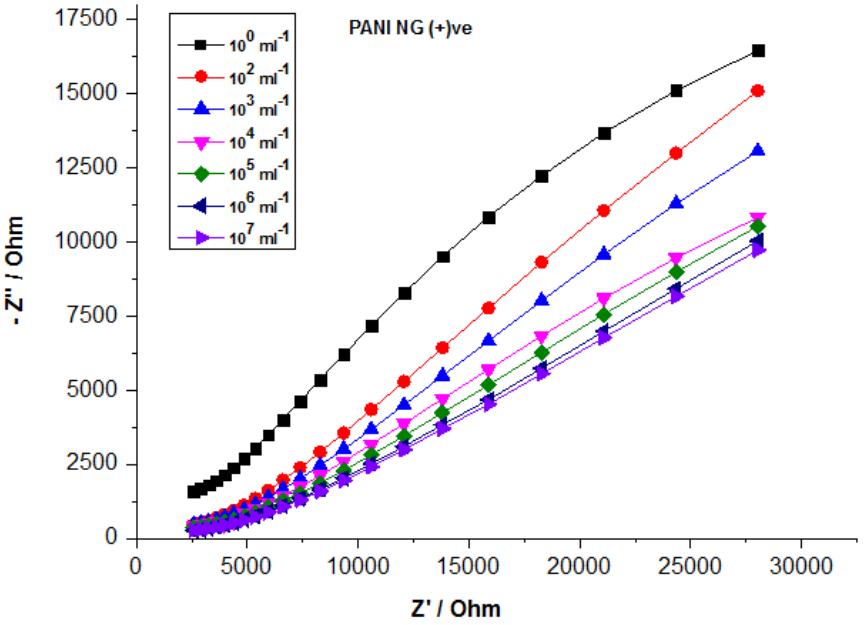

Figure 58 **Nyquist plots of a polyaniline-NG(+)ve modified electrode exposed to various concentrations of Neisseria gonorrhoea (+)ve**

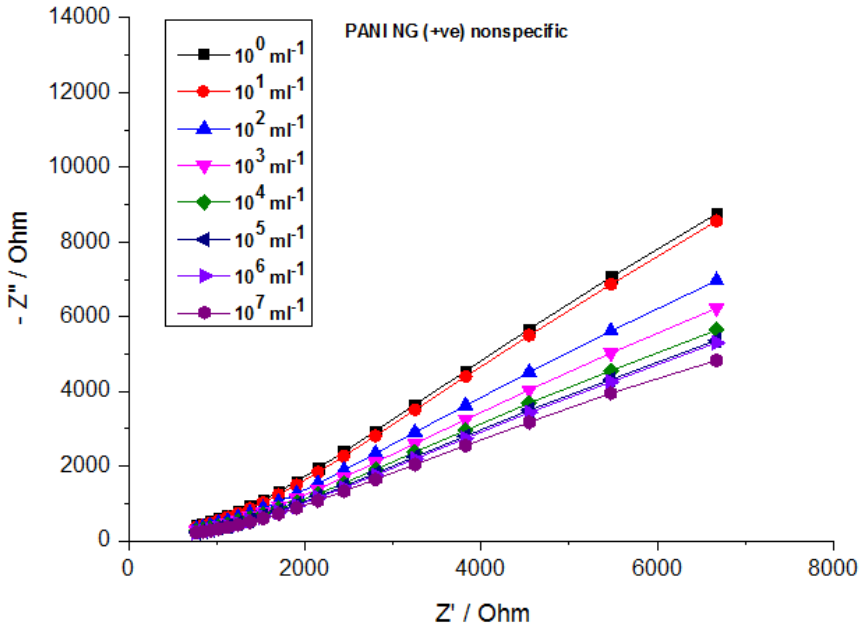

Figure 59 **Nyquist plots of negative control of PANI modified electrode exposed to various concentrations of NG(+)ve**

The bar graph presented in Figure 60 shows standard deviation for number of sensors. The reproducability of PANI based sensor seems high as compared to poly(4AMP) based sensors.

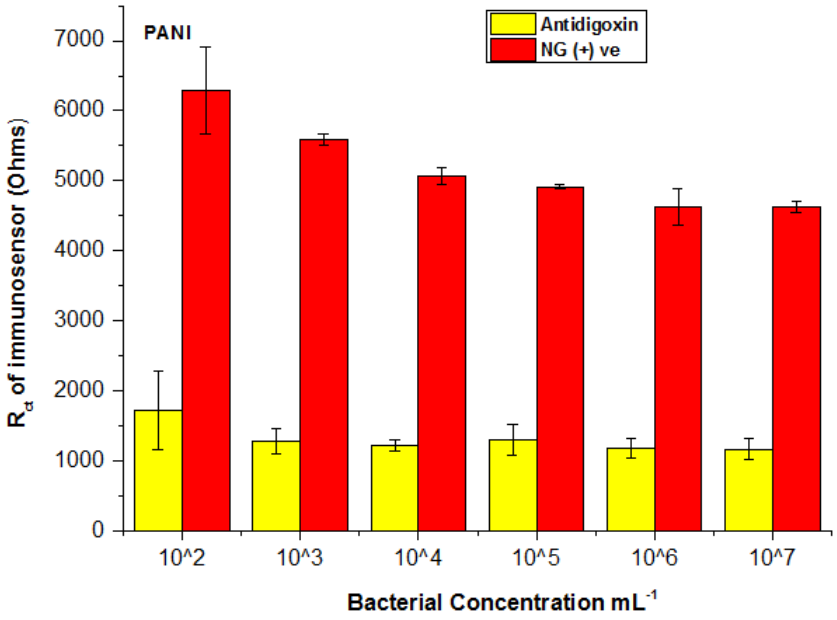

Figure 60 Standard deviation graph of PANI-NG(+)ve modified immunosensor

Once NG (+)ve immunosensors were interrogated *Neisseria gonorrhoea β-lactamase (-) ve* were tested against NG (-)ve bacterial concentrations and the resulting Nyquist plot is shown in Figure 61. Similarly the Nyquist plot of the negative control of PANI-NG(-)ve immunosensor is presented in Figure 62.

The semicircle diameter in Nyquist plots shown in graph in Figure 61 seems to decrease with the increase of the antigen concentration implying that there might be very low number of antibodies immobilised onto polyaniline modified surface. It is apparent that as there might be low number of immobilised antibodies therefore antibodies did not coverthe entire surface hence they do not act as a blocking layer and passivated the surface completey. The impedance pattern is evident that there might be pinholes

through out the surface and the current was passed through them and increased the conductance of the sensor.

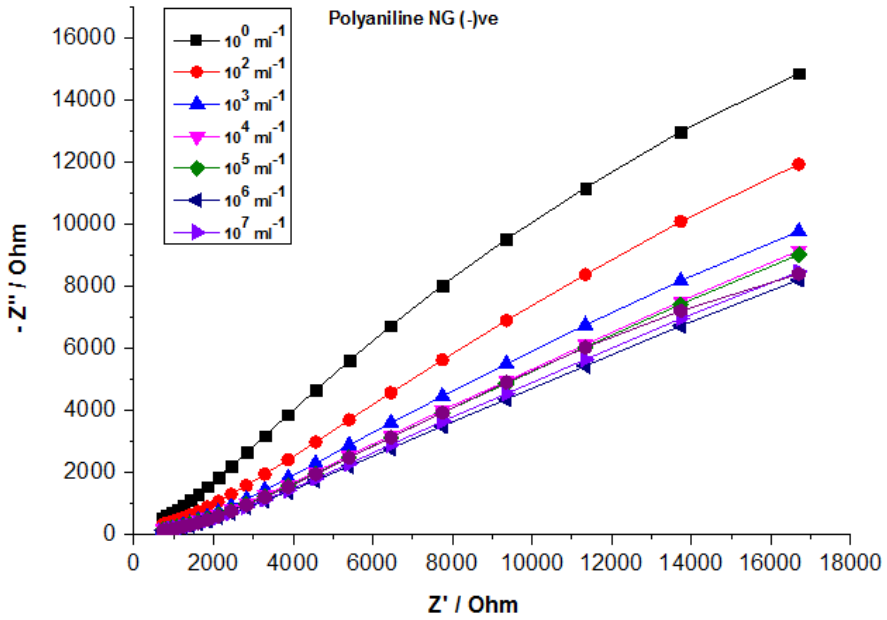

Figure 61 **Nyquist plots of a polyaniline-NG(-)ve modified electrode exposed to various concentrations of *Neisseria gonorrhoea (-)ve***

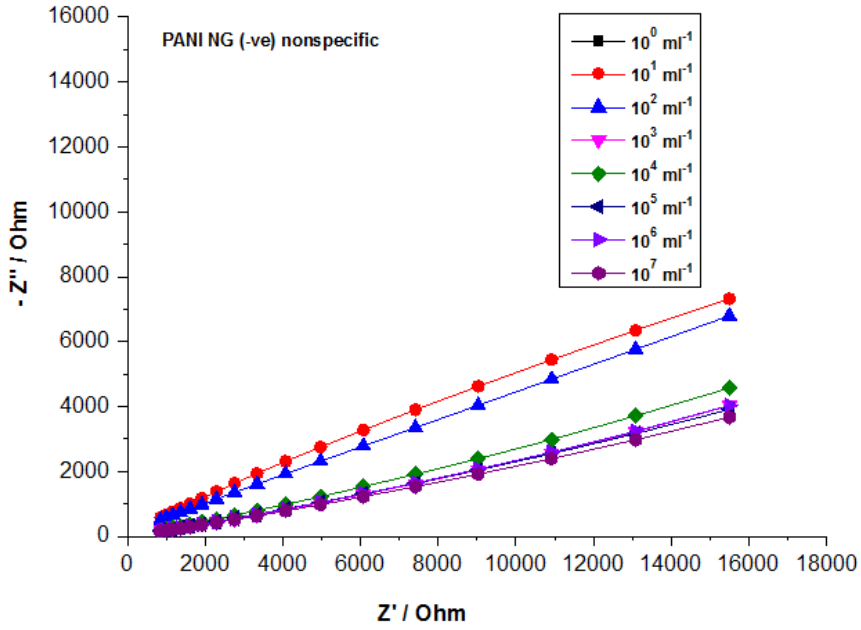

Figure 62 **Nyquist plots of negative control of PANI modified electrodes exposed to various concentrations of NG (-)ve**

When the concentration of antigen was increased over 10^5 ml^{-1} the change in impedance became gradually weak as apparent, showing that the gold electrode surface

trends to saturation situation. The trend followed the same pattern as *Neisseria gonorrhoea β-lactamase (+) ve* and in both cases the saturation was attained at 10^4 ml^{-1}.

A number of sensors were fabricated and tested against various concentrations and repeated experimental data was used to construct bar graph to study the standard mean of deviation as given in Figure 63. The yellow bar represents nonspecific whereas the red bar represents specific interaction of NG (-)ve pathogen.

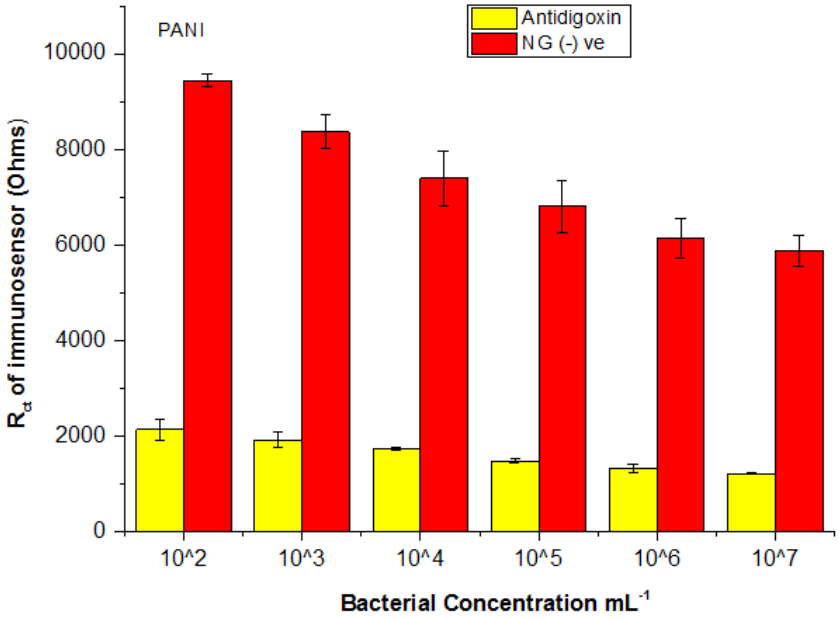

Figure 63 Standard deviation graph of PANI-NG(+)ve modified immunosensor

It was found that nonspecific interactions were low whereas there was appreciable change in case of specific binding. The reproduability of PANI based immunosensors was found to be very high.

8.4.3 Test of polyaniline based sensors against chlamydia

After construction of functional immunosensors for *Neisseria gonorrhoea*, another set of polyaniline modified electrodes were tested against *Chlamydia trachomatis*. The *chlamydia* based polyaniline sensors were tested against increasing concentrations of *chlamydia* in PBS. Each concentration was incubated on the electrode surface for 10 min, rinsed in dH_2O and dried under argon prior to interrogation by EIS. The concentration of *chlamydia* applied ranged from 10^2 to 10^8 particles ml^{-1} and data was collected using

the redox mediator $Fe(CN_6)^{3-/4-}$ at a voltage of 0.4 V. Figure 64 shows data from analyte capture using the polyaniline based immunosensing surface in the form of Nyquist plot. The negative control of PANI based *Chlamydia* immunosensors is given in Figure 65.

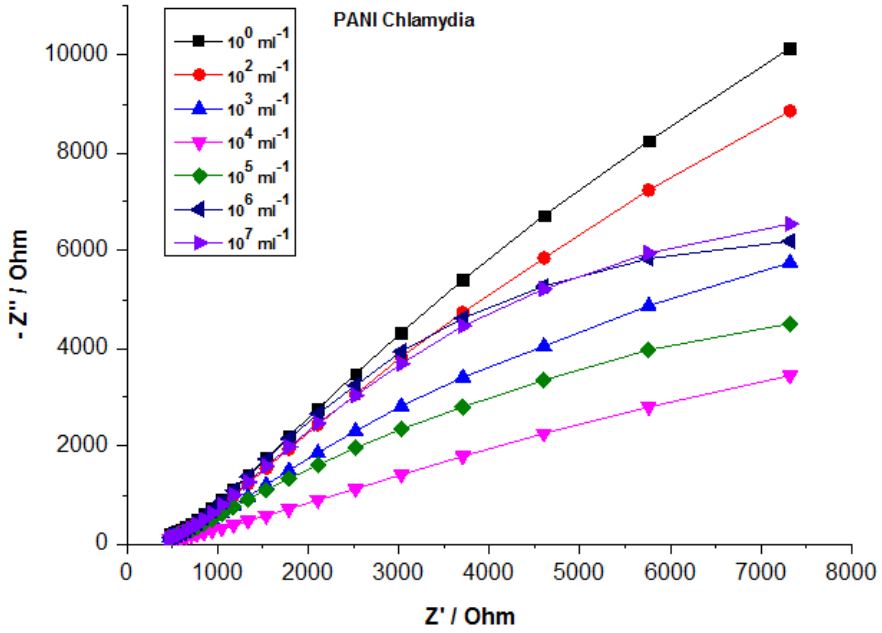

Figure 64 **Nyquist plots of a polyaniline-NG(-)ve modified electrode exposed to various concentrations of Chlamydia**

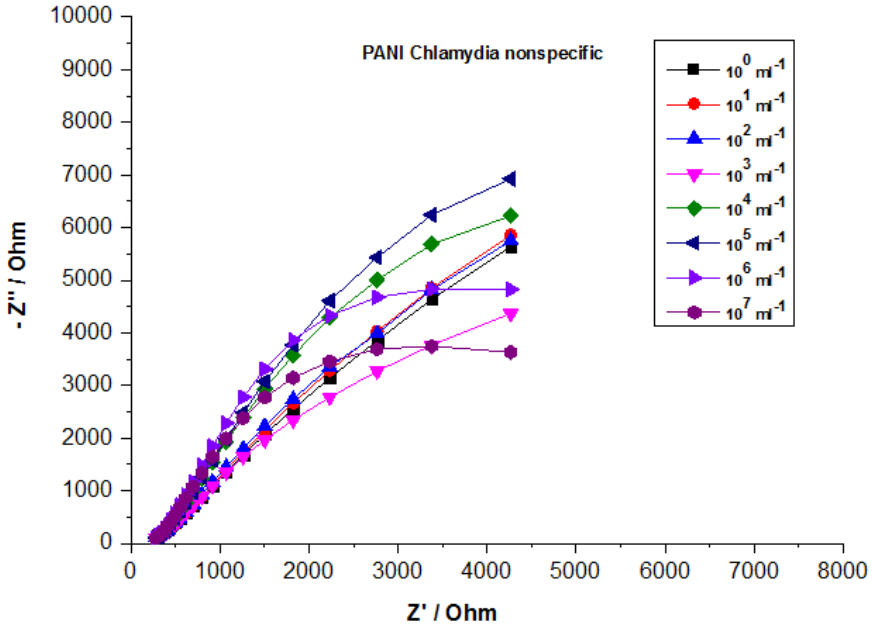

Figure 65 **Nyquist plots of negative control of PANI modified electrodes exposed to various concentrations of Chlamydia**

There was appreciable change in resistance for nonspecific binding although it is low in intensity as compared to specific binding.

It was observed that resistance decreased steadily after binding of 10^2 chlamydia particles ml^{-1} and kept decreasing until concentration of 10^4 ml^{-1}. After the addition of concentration 10^5 ml^{-1} resistance increased10^6 ml^{-1} but again decreased on addition of the higher concentration of 10^8 ml^{-1}.

The apparent immunosensor surface collapse for polyaniline surface could have been due to the random distribution of the bacteria and antibody. It again supported the concept that antibodies and bacterial particles were unable to cover the sensor surface completely therefore the current could flow through the spaces and resistance decreased. This would also result in the antigen disrupting the polymeric layers once again allowing charge to flow across the electrode-solution interface.

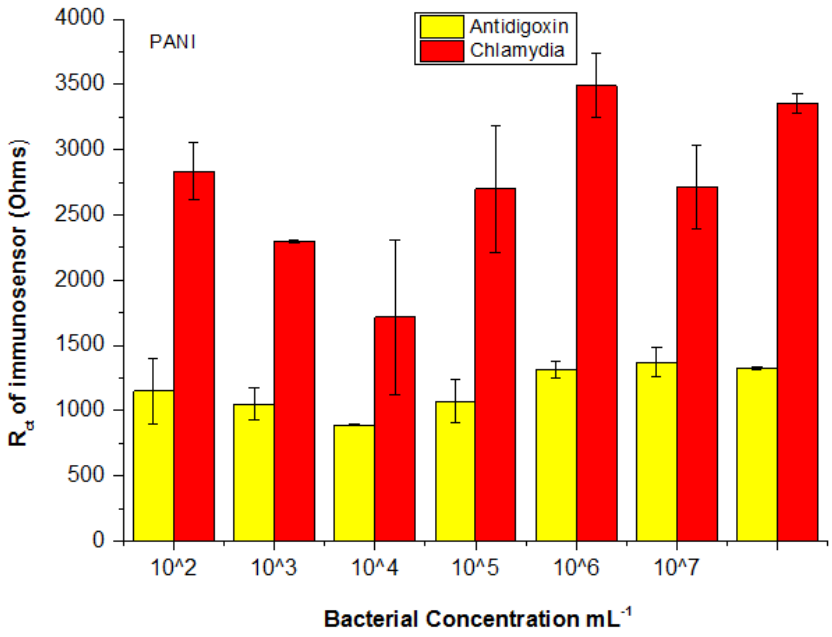

Figure 66 Standard deviation graph of PANI-Chlamydia modified immunosensor

This trend was shown with a number of repeat experiments. The standard deviation for both specific and nonspecific binding of number of sensors is given in the form of bar graph presented in the Figure 66.

8.4.4 Calibration curves against increasing antigen concentration

Upon exposure to a range of concentrations of antigen, complex plane impedance analyses were used to the possible charge transfer at the surface, with respect to the related mechanisms between the antibody and the polymer. These effects were subsequently monitored to assess the impedance of the polymer thereby determining the amount of bound antigen at the sensor surface.

The total impedance of the system increased along with the increasing antigen concentration from the 10^2 up to 10^7 ml^{-1}. The percentage impedance changed from the baseline at 1Hz used to form the basis of a calibration profile for differentiation of various concentrations of bacterial concentration applied to antibody-polyaniline films on screen printed gold electrodes. Calibration profiles for all three sample antibodies with control (anti-digoxin) sensors were constructed. Figure 67 shows the Faradaic calibration profile obtained at 1 Hz.

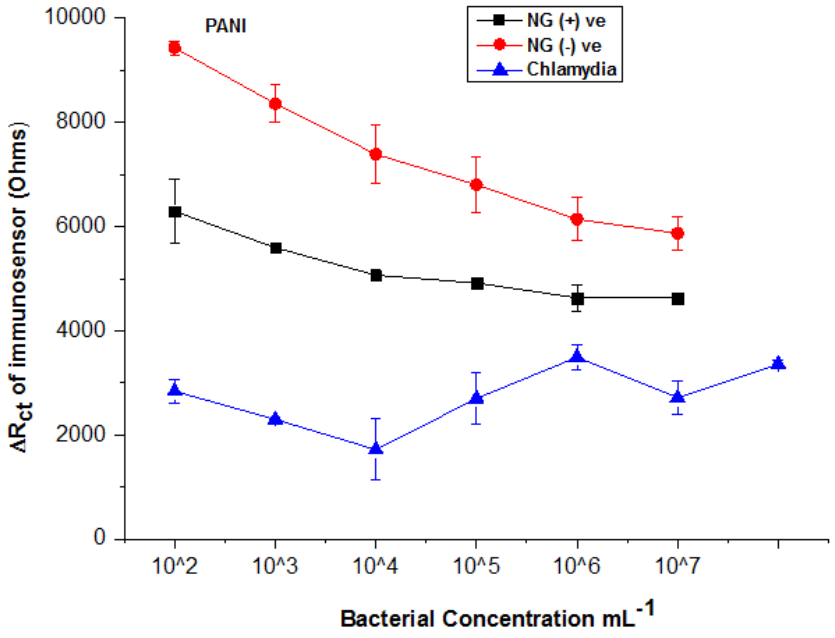

Figure 67 R_{ct} calibration curve of poly(4AMP) immunosensor comprising normalised values

The curves generated as a result of exposure of antibodies immobilised onto PANI modified electrodes to increasing concentrations of relevant antigens, *Neisseria gonorrhoea β-lactamase (+) ve. Neisseria gonorrhoea β-lactamase (-) ve* and *Chlamydia*

trachomatis at selected frequency. The curve displays the % impedance response against antigen concentration (bacterial particles/ml), normalised against the baseline response (zero antigen). The frequency (1 Hz) was chosen because of the greatest impedance response which increased along with each concentration. The mean impedance value at each concentration (*Z*") was normalised against the mean impedance value at zero antigen concentration, i.e. Z/Z^0 and expressed as the percentage impedance response with respect to the baseline trace. The calibration curve indicated that there was linear increase in impedance for *Neisseria gonorrhoea* β-*lactamase (+) ve* shown in black line and *Neisseria gonorrhoea* β-*lactamase (-) ve* shown in red line and *chlamydia trachomatis* shown in blue line, at the concentration range (10^2–10^7 ml^{-1}).

The gradual increase in response along with concentration for all three types of antibodies depicts that there non-specific interaction is minimal. As *anti-digoxin* has shown limited interaction with tested analytes therefore *anti-digoxin* was kept as nonspecific control for further experiments.

8.5 Summary

Biosensors based on polyaniline were prepared and tested against various concentrations of *Neisseria gonorrhoea* and *chlamydia* antibodies. The aim of this research work was to study the potential of polyaniline as conductive layer for the immobilisation of antibodies. EIS was employed to characterise sensor construction and subsequent analyte detection.

In the biosensor, the conductive layer with excess amino groups provides robust platform for immobilisation of antibodies. In the present study polyaniline was considered as possible immobisation conductive layer to form biosensors against *Neisseria gonorrhoea* and *Chlamydia trachomatis*. Polyaniline modified electrodes were incubated with sulpho-SMCC for the surface modification followed by *Neisseria gonorrhoea β-lactamase (+) ve*, *Neisseria gonorrhoea β-lactamase (-)ve* and *Chlamydia trachomatis* antibodies. All prepared electrodes were interrogetd with EIS and Nyquist plots were used for the comparison and interpretation of data.

The Nyquist plot for *Neisseria gonorrhoea β-lactamase (+) ve*, *Neisseria gonorrhoea β-lactamase (-)ve* and *Chlamydia trachomatis* showed that charge transfer resistance (R_{ct}) across polyaniline modified electrode reduced after addition of concentration and kept decreasing with subsequent addition of concentrations for all three analytes. The decrease in R_{ct} can be justified by the formation of 'pinholes' through which current flowed, consistent with data observed for all analytes. The formation of polyaniline layer onto the gold electrode surface passivated the surface, but R_{ct} was again reduced after bacterial capture. It was thought that it was because of bacterial incubation which disrupted the polymer layer and increased the capacitance of a biosensor because of current flow. This disruption of the polymer surface by bacterial analyte was consistent with the data seen with other bacterial sensors and therefore it is suggested that this sensing platform is not suitable for targeted analyte detection.

The studies carried out on polyaniline based electrodes showed that polyaniline was not suitable as immobilising platform for antibodeis. Therefore new conductive polymers would be investigated to successfully immobilise theses antibodies.

Keeping in view the surface chemistry of conductive layer poly (3-aminopropyl) pyrrole was considered as a new potentially suitable polymer. Poly (3-aminopropyl) pyrrole has free amino groups which are available that could bind with antibodies. There is an alkyl chain in the polymer structure which can also provide better orientation of antibodies.

CHAPTER 9 POLY (3-AMINO PROPYL PYRROLE) BASED IMMUNOSENSORS

9.1 Introduction

Conducting polymers have been previously utilised as electrode materials in biosensing applications. Electrons can readily transfer between the conducting polymers and biomolecules, such as hydrogen peroxide (H_2O_2) and glucose, during a redox process, producing a detectable electrocatalytic response which can be monitored by simple electrochemical methods such as cyclic voltammetry (CV) and amperometry (Weng *et al*., 2014).

Polypyrrole (PPy) was amongst the first reported conducting polymers to be utilised in biosensing. Conducting polymers including polypyrrole and its derivatives have been the major sources of electrochemically generated enzymatic electrodes. Wollenberger electrodeposited PPy with horseradish peroxidase (HRP) onto pyrographite or platinum electrodes for mediatorless hydrogen peroxide detection (Wollenberger *et al*., 1990). Since then, a series of conducting polymer biosensors have been studied for the detection of various biomolecules, including glucose, lactate and cholesterol (Retama *et al*., 2004; Chaubey *et al*., 2002).

Although electrochemically fabricated conducting polymer/enzyme biosensors have been extensively studied, these fabrication methods are still limited to a laboratory scale and are not suitable for mass production. For biomedical applications modification with biological moieties is desired to enhance the specific covalent attachment of proteins, peptides, and enzymes (Hegewald *et al*., 2009). Successful immobilisation of antibodies onto a conductive polymer modified electrode is the main target. Another goal from future perspective is to chemically synthesise these polymers so that the polymeric suspension could be utilised for ink formulation and printing diagnostic sensors. In previous studies (Rajesh *et al*., 2004) efforts are being made to stop the desorption of enzyme to a maximum extent from immobilisation materials to obtain an increased stability of the enzyme electrode. It has been shown that this could only be

achieved if there would be a strong and an efficient bonding between the enzyme and the immobilising material.

Although pyrrole and its substituted compounds produces conductive polymers and do not require acid during polymerisation however commercial pyrroles with free amino groups are not generally available or they usually are very expensive. Therefore amine-based conducting N-(3-Amino propyl) pyrrole was synthesised in the laboratory. Efforts were made to polymerise N-(3-Amino propyl) pyrrole through electrochemical and chemical polymerisation. The polymer produced through electrodeposition and oxidative polymerisation was characterised through SEM, western blotting imaging and FTIR. The blotting images and FTIR showed that there were plenty of amino groups which could be utilised to immobilise particular antibodies. Therefore poly-(3-aminopropyl pyrrole) was considered as prospective polymer for immobilisation of *Neisseria gonorrhoea* and *Chlamydia trachomatis* antibodies.

9.2 Polymerisation of 3-aminopropyl pyrrole

9.2.1 Synthesis of N-(3-amino propyl) pyrrole

As chemical oxidation is more amendable to larger scale production as the polymer can be dissolved/dispersed in suitable solvents and processed by multiple techniques (wet-spinning, spin coating, printing etc.). Also the physical properties of chemically prepared PPy, such as particle size and morphology (Lo, 2006) can be controlled by optimising the synthesis conditions (Weng *et al*., 2011).

It has been shown in previous studies that chemically synthesised polypyrroles are not as highly conductive as the electrochemically prepared material (Weng *et al*., 2014). Therefore efforts have been made to synthesise substituted pyrrole which could be chemically polymerise and could generate a conductive layer for biosensing experiments. N-(3-Amino propyl) pyrrole (3-APPy) was synthesised by the reduction of N-(2-cyanoethyl) pyrrole according to procedure described in literature (Massoumi *et al*., 2012; Hegewald *et al*., 2009).

A solution of 1-cyanoethyl pyrrole (0.041 mol) in anhydrous ether was added into a suspension of $LiAlH_4$ (0.1 mol) in anhydrous ether (300 ml) and the mixture was refluxed for 20 hours. After cooling, the excess hydride was destroyed by the successive addition of water (3.4 ml), a solution of 15% NaOH (3.4 ml) and water (10.2 ml). The solution was heated to 40 °C for 2 hours and was filtered before evaporating to dryness. Yellow oil was obtained as a final product with a yield of about 80%. A schematic presentation is given in Figure 68.

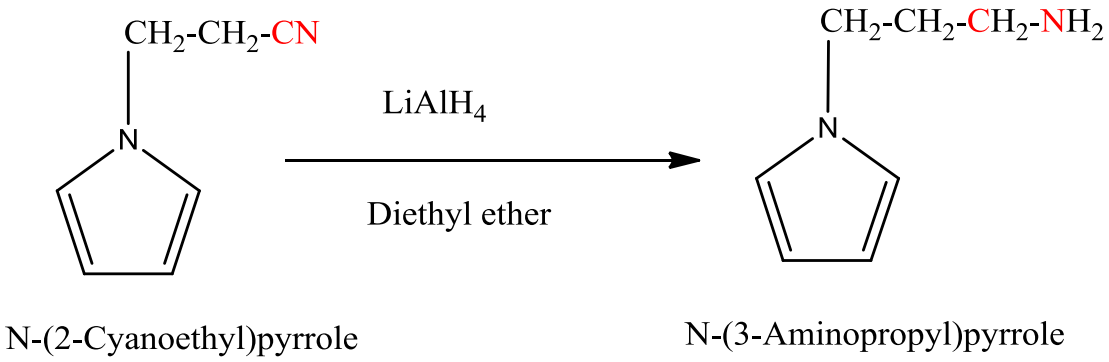

Figure 68 Synthesis of N-(3-Amino propyl) pyrrole

NMR of N-(3-aminopropyl) pyrrole was recorded H NMR δ ($CDCl_3$): 1.94 (m, 2H, CH_2-2); 2.71 (t, 2H, CH_2-3); 3.97 (t, 2H, CH_2-1); 6.18 (d, 2H, CH-β); 6.70 (2H, CH-α) which is in accordance to values given in the literature (Rajesh *et al.*, 2005).

9.2.2 Chemical polymerisation of N-(3-Amino propyl) pyrrole

N-(3-Amino propyl) pyrrole was polymerised through chemical oxidation where ammonium per sulphate (APS) was used as an oxidant. Two different type of polymers were syntthesised through oxidative chemical polymerisation. The first polymer synthesised was a copolymer of 3APPy and pyrrole whereas the second polymer synthesised was homopolymer of 3APPY. The co-polymerisation of N-(3-Amino propyl) pyrrole with pyrrole has already been reported in the literature (Massoumi *et al.*, 2012) but the homopolymerisation of N-(3-Amino propyl) pyrrole has never been reported before.

9.2.2.1 Copoylmerisation of N-(3-Amino propyl) pyrrole

A copolymer of pyrrole and N-(3-Amino propyl) pyrrole was synthesised through chemical polymerisation. Equimolar solutions (0.5 M each) of N-(3-Amino propyl) pyrrole and pyrrole were prepared in 1M p-toluene sulphonic acid sodium salt (Na-pTSA). 1M APS was added into the reaction mixture with continuous stirring. As the polymerisation started a light brown colouration appreared which turned into dark brown precipitates as the polymerisation continued. The precipitates were filtered and characterised through SEM and midland blotting. The polymerisation reaction is given in Figure 69.

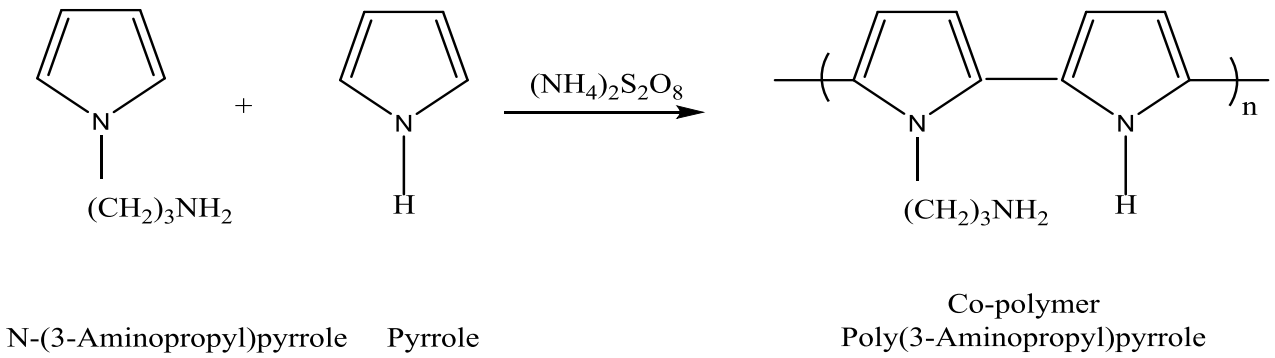

Figure 69 Schematic presentation of copolymerisation of pyrrole and N-(3-Amino propyl) pyrrole

The 3APPy copolymer suspension was diluted further with 1% triton solution to prevent coagulation and characterised through SEM shown in Figure 70.

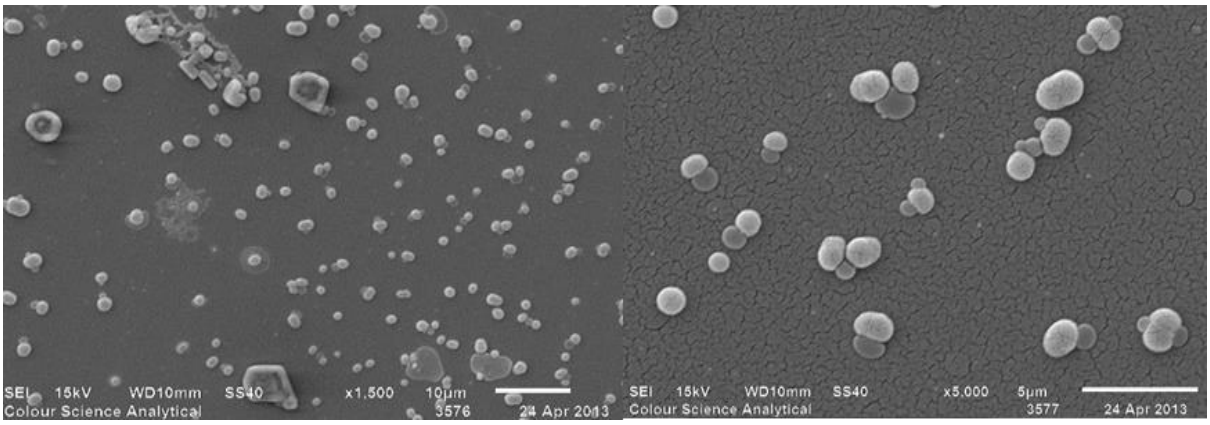

Figure 70 SEM picture of 3-Amino propyl pyrrole co-polymer at 1500 and 5000 magnifications

The copolymer particles appeared to be very small in size which coagulated very easily. The higher magnification of 5000 revealed small spherical particles clearly visible among larger particles which is evident that the copolymer consists of tiny particles which coagulated to form larger particle.

9.2.2.2 Homopolymerisation of N-(3-Amino propyl) pyrrole

The polymerisation of N-(3-Amino propyl) pyrrole was carried out at room temperature by mixing 20 mL of 1M solution of N-(3-aminopropyl) pyrrole into 10mL of 1 M p-toluene sulphonic acid sodium salt (Na-pTSA) solution. After thorough mixing, 2mL of 1 M APS solution was added into the solution dropwise. Soon after adding oxidant solution, dark green precipitates (ppt) were formed which were washed with water many times, filtered and dried. The schematic presentation of oxidative polymerisation is given in Figure 71.

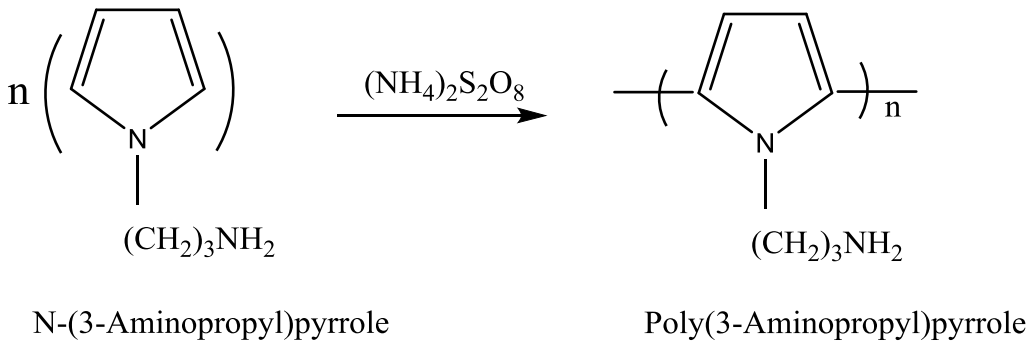

Figure 71 Schematic presentation of polymerisation of 3-APPy

In-situ polymerisation was carried out to study the deposition and adhesion of poly (3-APPy) onto gold surface. The in-situ polymerisation was performed by placing 50µL of 1M 3APPY in Na-pTSA onto the working electrode and equal volume of oxidant i.e. 50µL of 1M APS was added into the monomer solution. Soon after the addition of oxidant very dark brown precipitates were formed instantly. After allowing the polymerisation to proceed for one minute, the sensors were washed and observed under the optical microscope.

Poly (3-APPy) showed very good adherence to gold surface and a thin film was observed over the gold surface. On the higher resolution poly (3-APPy) seemed to penetrate deeply into the pores as apparent from Figure 72.

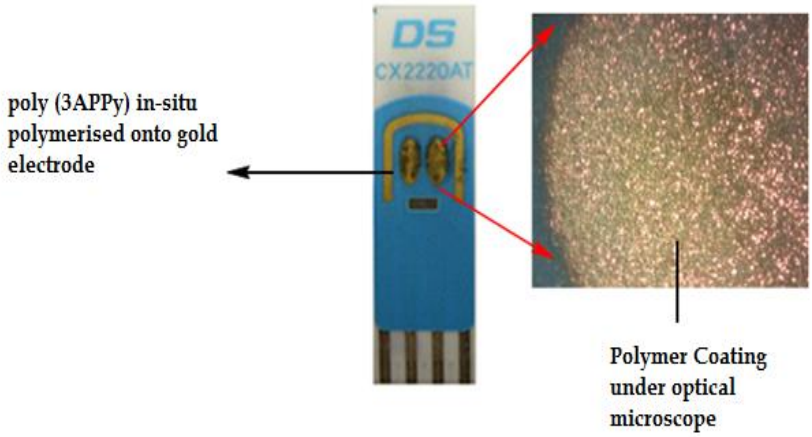

Figure 72 In-situ polymerisation of 3APPy onto drop sensor

The polymeric suspension of 3APPy were characterised through SEM as shown in Figure 73. Poly (3APPy) in Figure 73 (A) appeared as round particles and tends to coagulate very easily. If the particles are studied more closely at higher resolution of 10,000 at a working distance of 1µm as shown in 73 (B), small nano particles are clearly visible and they appear to coagulate to form larger particles of varying sizes.

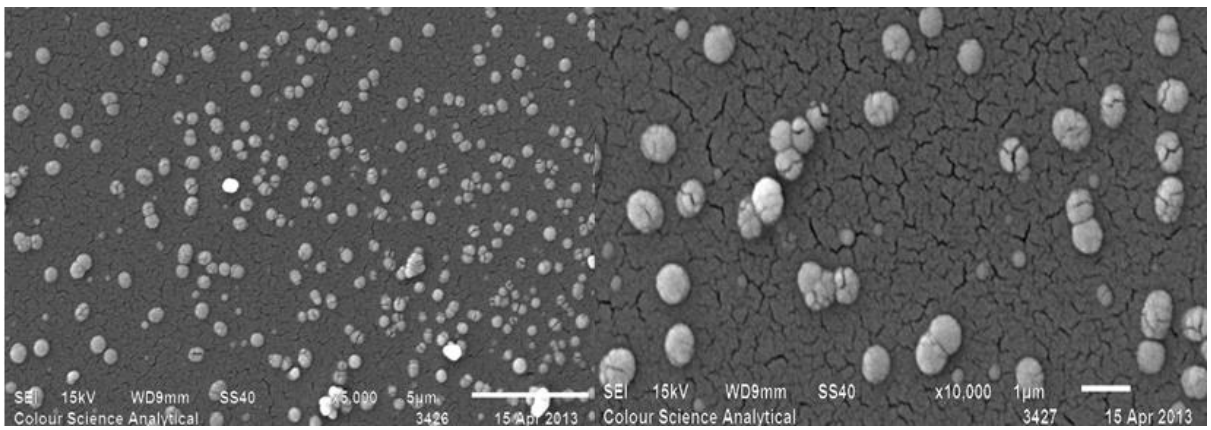

Figure 73 SEM pictures of poly (3-amino propyl) pyrrole at (A) 5,000 and (B) 10,000 magnifications

A chemiluminescence based technique, Midland blotting was carried out on both types of polymers to interrogate the number of free available $-NH_2$ groups. Both

homopolymer and copolymer based sensors were prepared through electrodeposition and imaged through G:BOX Gel imaging system as shown in Figure 74.

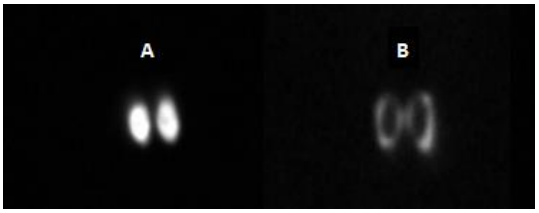

Figure 74 Chemiluminescence analysis of (A) Homopolymer of 3APPy and (B) Copolymer of 3APPy

3APPy homopolymer labelled as (A) showed very high intensity of light which depicts that 3APPy homopolmer has high number of amino groups which are distributed evenly onto the surface. Whereas the copolymer of 3APPy labelled as (B) showed very weak signal wth low intensity of light. There was uneven distribution of light intensity onto electrode surface which shows that very few $-NH_2$ groups are available and are mostly located at the edges of electrode.

9.2.3 Electropolymersation of N-(3-Amino propyl) pyrrole

Once 3-APPy was successfully polymerised through oxidative chemical polymerisation it was also electropolymerised through cyclic voltammetry. The electrodeposition of poly (3-APPy) onto gold sensors was carried out in 1M solution of 3-APPY in 1M sodium salt of p-toluene sulphonic acid (Na^+-TSA). The potential range for the electroploymerisation was kept -0.2V to +0.8V at a scan rate of $50mVs^{-1}$. The resulting voltammogram is shown in Figure 75. The electrodeposition of 3APPy was carried out for 10 scans. Once 10 scans were finished, a thin and smooth film of polymer was apparent which covered evenly the electrode surface.

The voltammogram showed that during first scan, as the electropolymerisation preceded an oxidation peak appeared at 0.48V whereas a reductive peak appeared at 0.45V. On next three scans the oxidation peak decreased but oxidation peak was increased again after 5^{th} sacn. This must be due to the increase in electroactivities of the surface film formed after the few scans. The increase in conductivity might have resulted from longer polymer chains as the scan number increases.

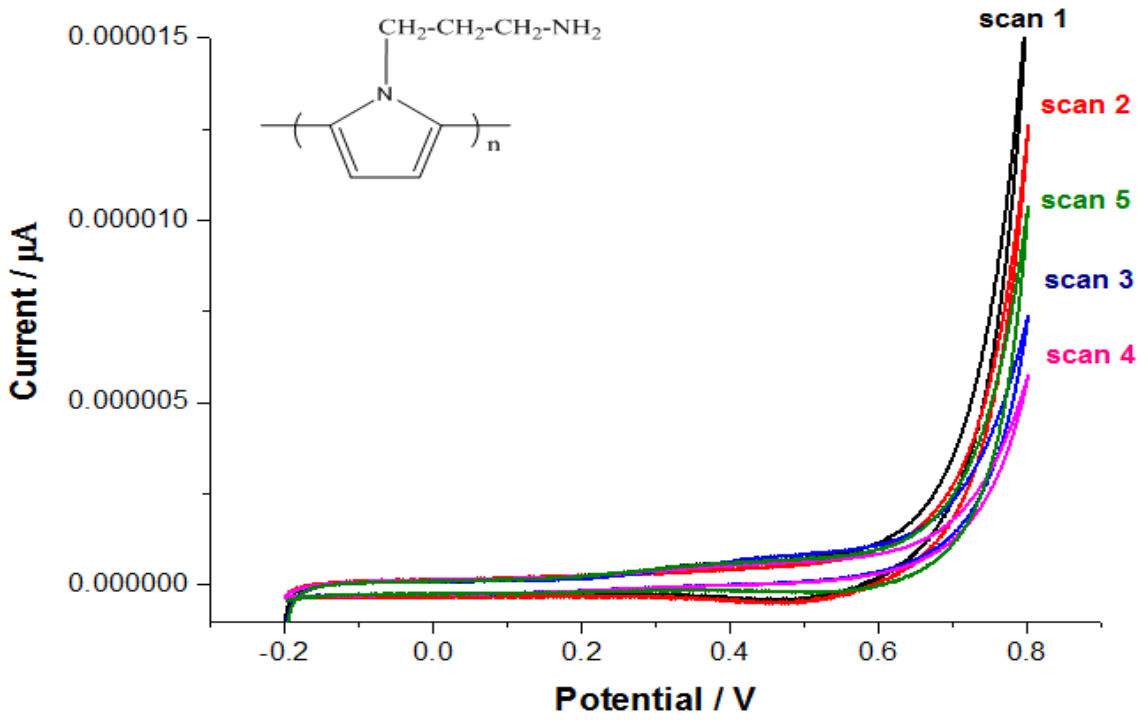

Figure 75 Cyclic voltammograms of 3APPy in 1M-Na+-TSA

9.3 Characterisation of poly (3-amino propyl pyrrole)

9.3.1 FTIR analysis

FT-IR spectra of poly(3-aminopropyl pyrrole) was recorded and is shown in Figure 76. In a spectrum, the polymer showed the absorption band at 3195 cm^{-1} which is due to C-H stretching vibrations. The absorption peak observed at 1657 $cm^{-1}$and is attributed to C=N stretching in aromatic ring.

The band obtained at 1478 cm^{-1} corresponds to C-C stretching in aromatic compounds. The weak band at 1239 cm^{-1} is related to the stretching vibration of the pyrrole ring. The sharp band at 1089 cm^{-1} corresponds to the N-H in-plane deformation (Lallemand *et al.*, 2007).

The polymer showed an absorption band at 857 cm^{-1} which confirms the primary aromatic amines (Massoumi *et al.*, 2012).

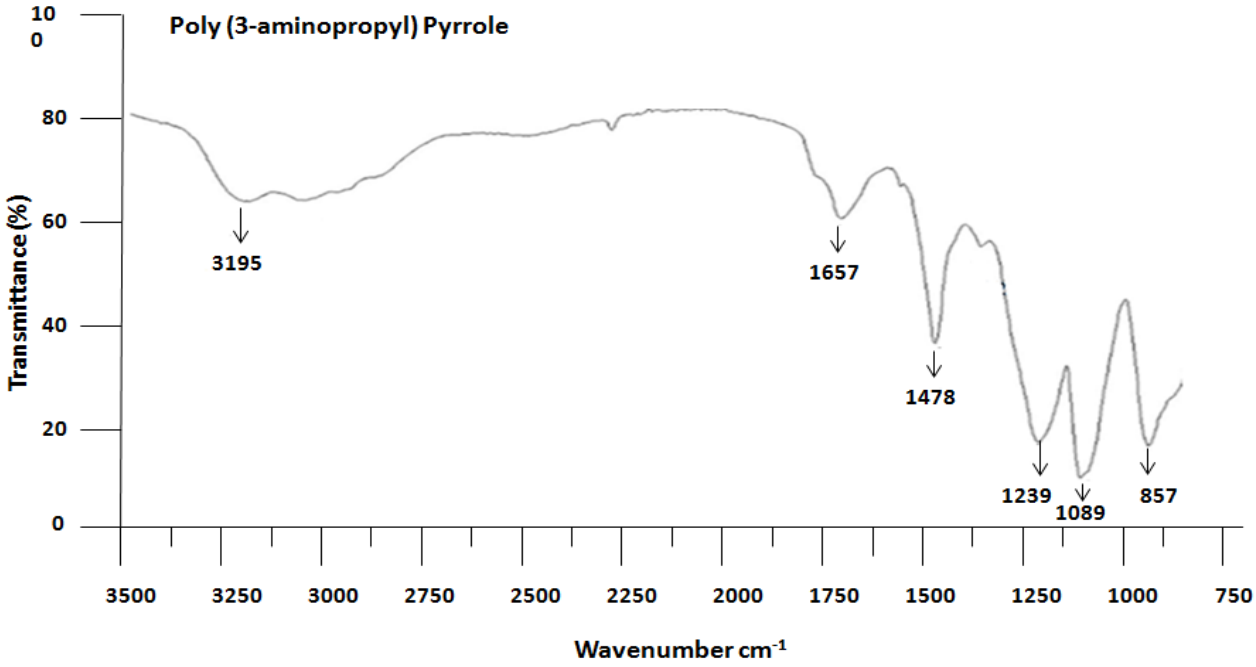

Figure 76 FTIR spectra of poly (3-amino propyl) pyrrole

9.3.2 SEM analysis of poly (3APPy) modified surfaces

Two different types of sensors were prepared through coating 3APPy polymer film on the gold electrode. The methods employed to prepare sensors were electrodeposition and drop casting. The surfaces of electrodes prepared through different means of poly (3-APPy) deposition were characterised through SEM. The morphologies and microstructures of both electrode surfaces were compared with a bare gold electrode.

It is apparent in the Figure 77 (A) the bare gold surface has fissures and cavities but once poly (3-APPy) was electrodeposited onto the bare electrode it has smoothen the surface by filling the voids as shown in Figure 77 (B). The electrodeposition has casted a thin layer of poly (3-APPy) onto gold surface as there are small cracks scattered through out the film. In case of dropcasted poly (3APPy) electrode shown in Figure 77 (C), the polymer appears to be adsorbed into the surface and the cavities appears smaller as compared to the bare electrode.

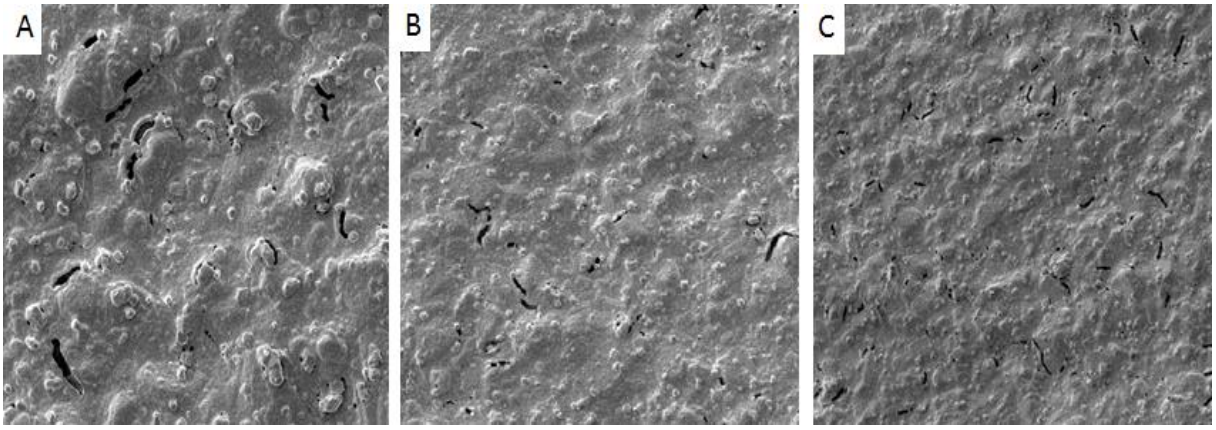

Figure 77 SEM analysis of poly (3APPy) film onto a) bare electrode b) poly (3-APPy) electrodeposited and c) poly (3-APPy) drop casted

9.4 Impedance studies of poly (3-APPy) based immunosensors

9.4.1 Test of poly (3-APPy) based sensors against Neisseria gonorrhoea

Formation of antigen-antibody complexes onto conductive supports yields a chemically modified film on the surface that alters the impedance features of the interface. The formation of the antigen-antibody complex perturbs the double-charged layer (C_{dl}) existing at the electrode/electrolyte interface resulting in the increase of its thickness. This results in the change in capacitance along with change in electron transfer resistance at the interface (Katz and Willner, 2003).

Poly (3-amino propyl pyrrole) showed enough amino groups to immobilise antibodies. A set of electrodes were prepared by electrodeposited poly (3APPy) onto gold electrodes. Once surface activation of electrodes was carried out after incubation with sulpho-SMCC, ½ generated antbodies of *Neisseria gonorrhoea β-lactamase (+) ve* and *Neisseria gonorrhoea β-lactamase* were immobilised onto the activated electrode surface. The fully prepared biosensors were interrogated through EIS against various concentrations of analytes. Any change in resistance was recorded and respective Nyquist plot for was plotted for the interpretation of data. Nyquist plot of *Neisseria*

gonorrhoea sensor based on poly (3APPy) plotted against various concentrations of heat killed *Neisseria gonorrhoea β-lactamase (+) ve* pathogen is shown in Figure 78. The Nyquist plot depicts that the diameter of semicircle increased along with increasing bacterial concentration. The negative control against NG (+)ve is given in Figure 79.

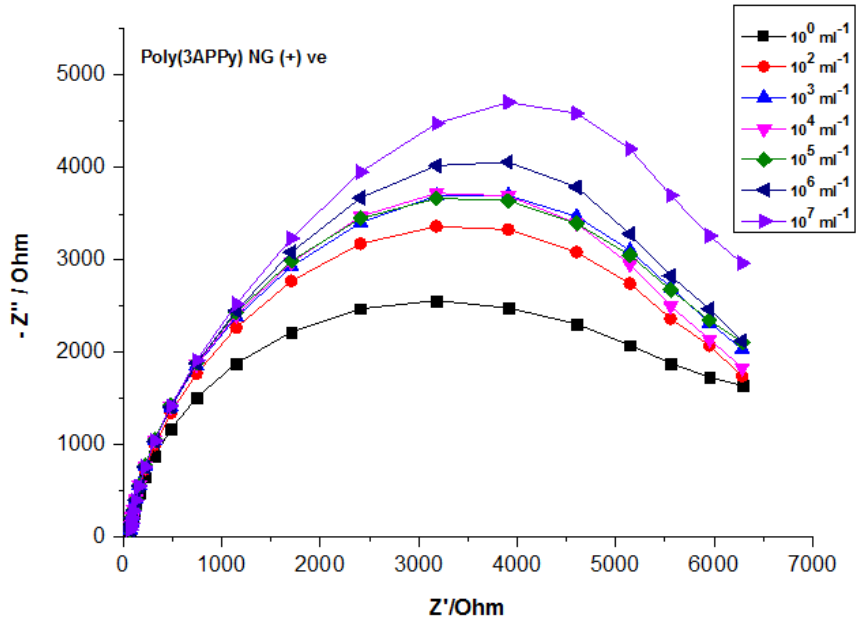

Figure 78 **Nyquist plots of a poly(3APPy)-NG(+)ve modified electrode exposed to various concentrations of Neisseria gonorrhoea (+)ve**

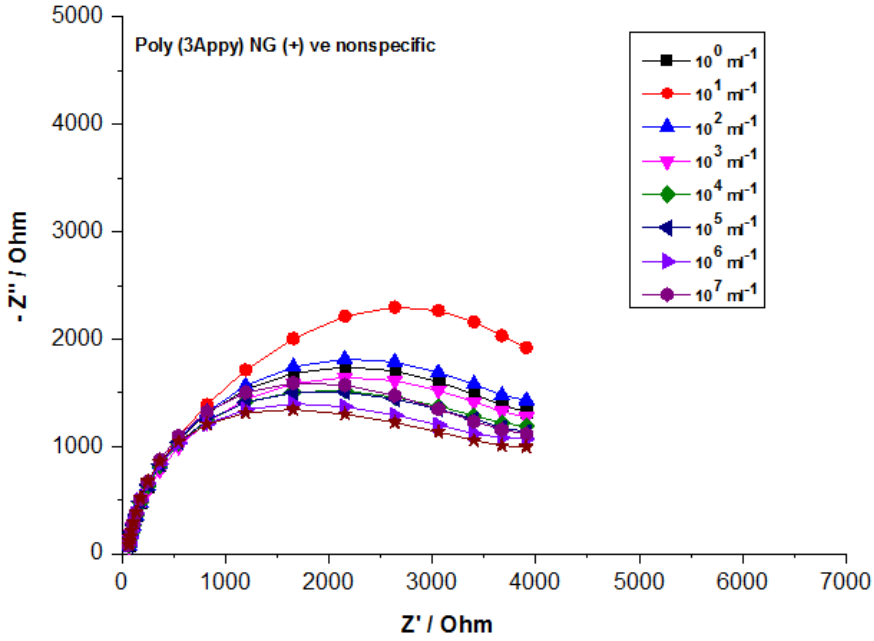

Figure 79 **Nyquist plots of negative control of poly(3APPy) modified electrodes exposed to various concentrations of NG (+)ve**

The standard mean of deviation bar graph for poly(3APPy)-NG(+)ve is shown in Figure 80 which shows good selectivity and specificity of poly(3APPy). The yellow bar represents *antidigoxin* as nonspecific and the red bar represents NG(+)ve as specific binding analyte. At 1Hz the deviation was higher for 10^4 ml^{-1} whereas 10^5 ml^{-1} showed lower deviation. In case of *antidigoxin* the results seemed to be consistant for number of tested immunosensors.

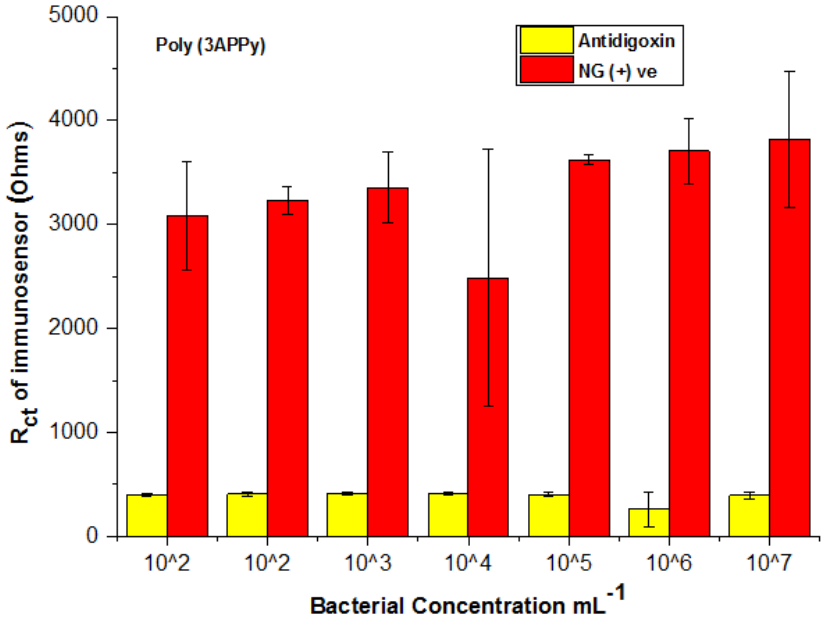

Figure 80 Standard deviation graph of poly(3APPy)-NG(+)ve modified immunosensor

Similarly poly (3APPy) based *Neisseria gonorrhoea β-lactamase (-) ve* sensors were interrogated against various concentrations of respective heat killed bacterial concentrations. The data obtained after impedance studies was again plotted in the form of Nyquist plot as shown in Figure 81. All concentrations were prepared in the range of 10^2–10^6 mL^{-1}. In Nyquist plots shown in Figure 81 along with negative control presented in Figure 82 is almost similar to Nyquist plots for NG (+) ve, where the charge transfer resistance (R_{ct}) increases gradually as the bacterial concentration increases after consecutive incubations. It is apparent that the Z' component and the –Z" component of impedance both increased with decreasing frequency from the baseline trace. The impedance spectras for analytes, *Neisseria gonorrhoea β-lactamase (+) ve* and *Neisseria gonorrhoea β-lactamase (-) ve* follow the theoretical shape typically seen for a Randle's equivalent circuit.

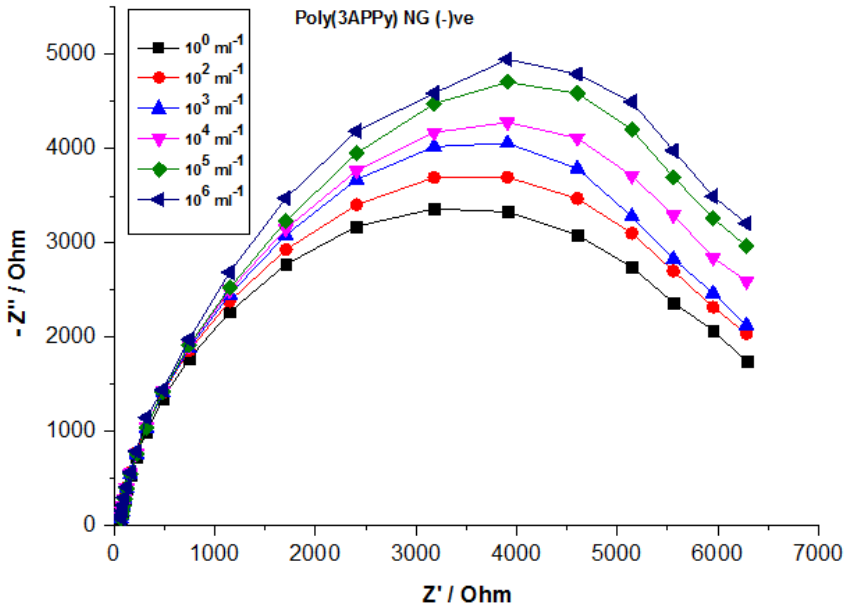

Figure 81 **Nyquist plots of a poly(3APPy)-NG(-)ve modified electrode exposed to various concentrations of Neisseria gonorrhoea (-)ve**

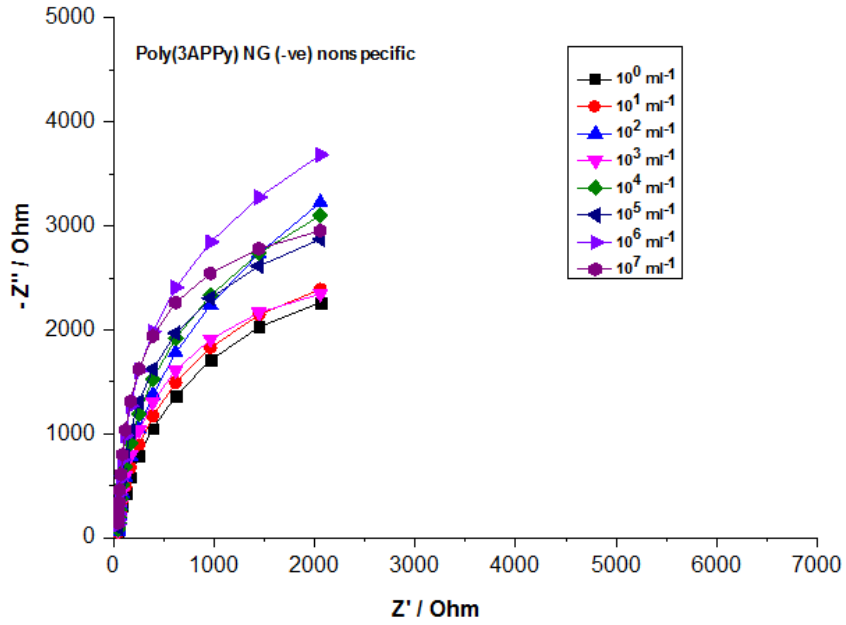

Figure 82 **Nyquist plots of negative control of poly(3APPy) modified electrodes exposed to various concentrations of NG (-)ve**

The Nyquist plot for NG (-)ve include a compressed semicircle portion at higher frequencies, which corresponds to the electron transfer limited process, followed by a linear part characteristic of lower frequency attributable to a diffusion limited electron transfer. It is also evident from Nyquist plot there was a proportional increase of R_{ct}

with antigen concentration which may be attributed to more bacterial particles binding to the immobilised antibodies, providing a kinetic barrier for the electron transfer. The calibration bar graph for various immunosensors is presented in Figure 83.

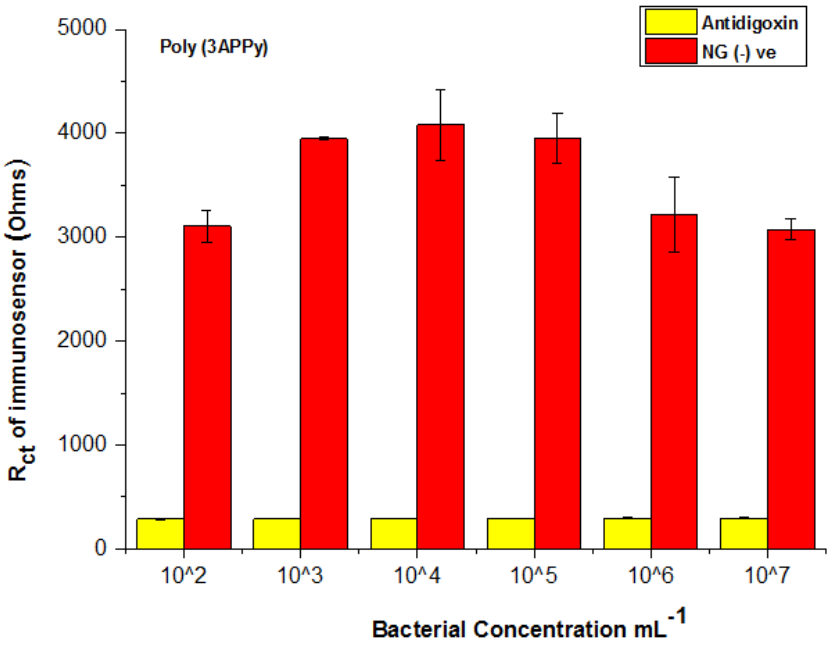

Figure 83 Standard deviation graph of poly(3APPy)-NG(+)ve modified immunosensor

The yellow bar in the graph represents nonspecific binding which is apparently very low as compared to specific binding presented in the form of red bar. The error bars showed very good stability and reproducibility of poly(3APPy) based immunosensors.

9.4.2 Test of poly (3-APPy) based sensors against chlamydia

Poly (3-amino propyl) pyrrole based sensors showed promising results against *Neisseria gonorrhoea* therefore a set of poly (3-APPy) sensors were fabricated to test against various concentrations of *Chlamydia trachomatis*. The poly (3-APPy) based sensors were prepared by following the same protocol as decribed in section 9.4.1. The fully constructed immunosensor were immersed into ferricyanide solution for 30 minutes prior to exposure against various concentrations of *chlamydia trachomatis*. Mean while a number of concentrations were prepared ranging from 10^2-10^7 particles ml^{-1} through serial dilution in PBS-EDTA buffer solution of pH 7.2. Each concentration

was incubated for 10 minutes starting from lowest towards highest. After incubation each sensor was interrogated through EIS and any change in impedance was recorded and a Nyquist plot was plotted as shown in Figure 84.

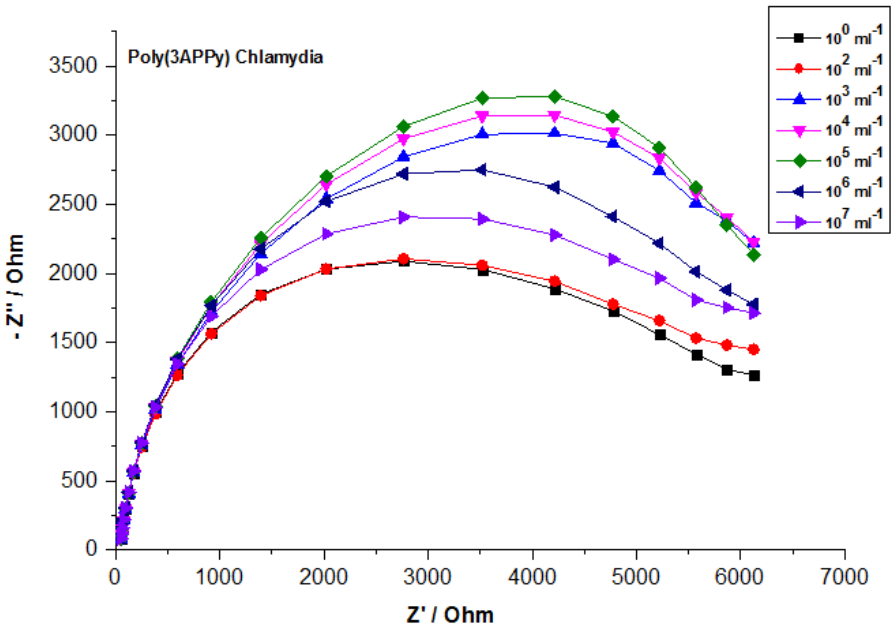

Figure 84 Nyquist plots of a poly(3APPy)-Chlamydia modified electrode exposed to various concentrations of Chlamydia

It was observed that after incubation with the first *Chlamydia trachomatis* concentration of 10^2 ml^{-1}, there was no substantial change in impedance but when poly (3APPy) sensors were incubated with next concentration of 10^3 ml^{-1} the impedance rises suddenly.

This increase in R_{ct} is attributed to the binding of antigen, *Chlamydia trachomatis* to immobilised antibody producing a barrier layer that inhibits the charge transfer for a redox probe. Also, it has been observed that the high concentration of analyte may create hindrance to itself to gain access to the antibody binding sites (Chornokur, 2011).

At the highest concentration 10^6 ml^{-1}, a drop in impedance was observed, which might be due to some electron channelling to the electrodes from a surface saturated with bound bacteria and started to disrupt the surface layer. The Nyquist plots of antidigoxin showing nonspecific binding against poly(3APPy)-*chlamydia* based immunosensor is presented in Figure 85.

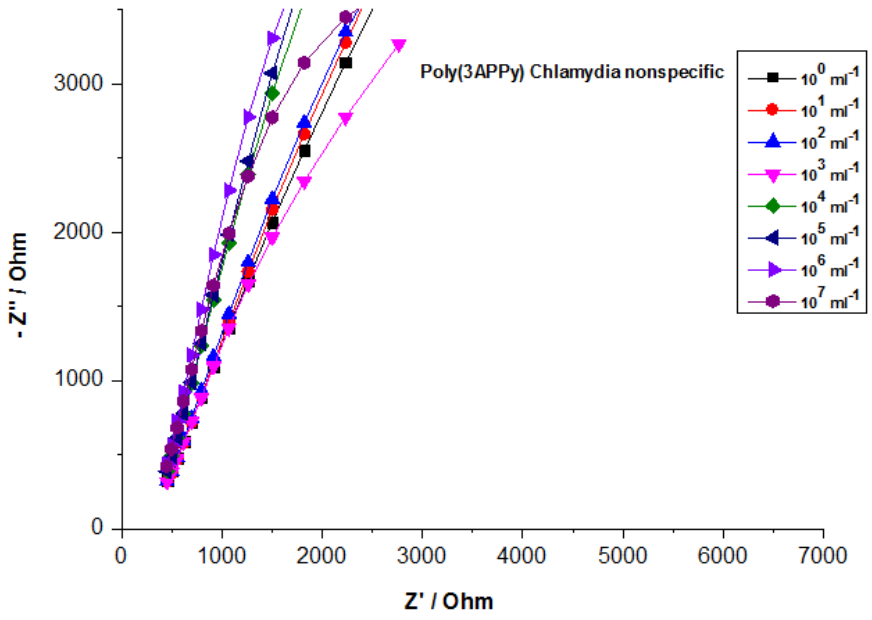

Figure 85 Nyquist plots of negative control of poly(3APPy) modified electrodes exposed to various concentrations of Chlamydia

Once *Chlamydia* concentration was incubated onto *antidigoxin* sensor the resistance increased and kept increasing along with higher concentrations but the change in R_{ct} is less then specific analyte (*Chlamydia*). The bar graph presented in Figure 86 shows standard of deviation of *Chlamydia* based immunosensors. The specific and non specific bacterial binding is found to be consistant among various batches of immunosensors and the change in resistance is showed in the form of red and yellow bars for analyte and control. The error bars presented in the graph depicts that there was very less varation among number of sensors which showed good feasibility of poly (3APPy) as potential conductive layer for the immobilisation of antibodies.

The yellow bar representing nonspecific binding depicts that there was very low bacterial binding showing that *antidigoxin* could be used a nonspecific or control for further experiments.

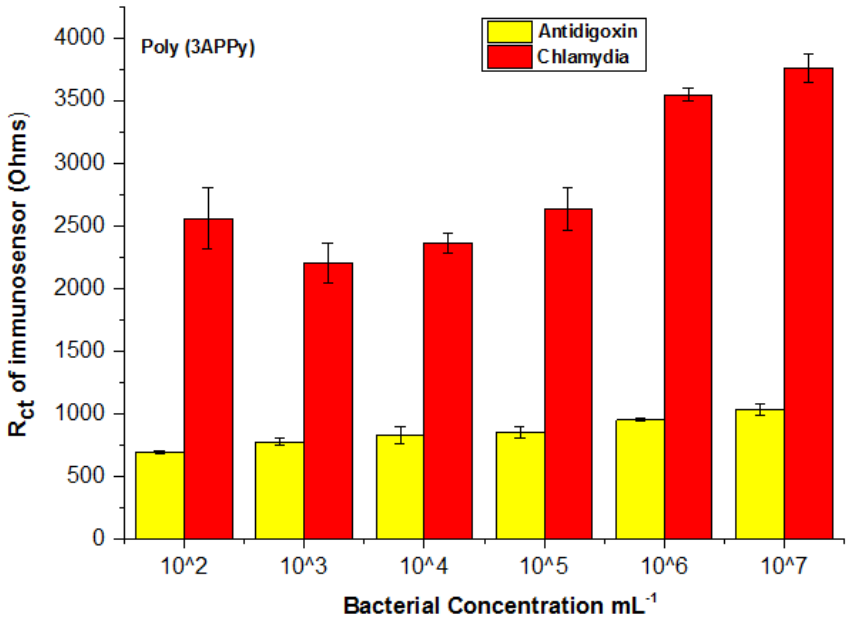

Figure 86 Standard deviation graph of poly(3APPy)-Chlamydia modified immunosensor

9.4.3 Calibration curves against increasing antigen concentrations

Usually, nonspecific adsorption is a major problem in label-free immunosensing, since it cannot be distinguished from specific adsorption in unlabelled electrochemical sensing antigens. To confirm that the above-observed impedance changes arise from specific interaction between respective antigen and the Ab, at the same time to reveal the selectivity of the binding, contrast experiments were performed. On the same sensor, specific and nonspecific antibody were immobilised onto WE1 and WE2 respectively. After the immobilisation the electrode was exposed to various concentrations of a bacterial concentrations and response was recorded.

The curves shown in Figure 87 are generated as a result of exposure of 3APPy based *Neisseria gonorrhoea β-lactamase (+) ve, Neisseria gonorrhoea β-lactamase (-) ve* and *Chlamydia trachomatis* to increasing concentrations of respective antigen at 1 Hz. The curve displays the % impedance response against antigen concentration (bacterial particles/ml) which were normalised against the baseline response (zero antigen). In the calibration curve, % change in impedance was plotted against bacterial concentration, the R_{ct} increased gradually with the increase of the *Neisseria gonorrhoea β-lactamase (+) ve, Neisseria gonorrhoea β-lactamase (-) ve* concentrations which

showed that protein structures bound to the surface of an electrode performed as barriers to electrical transfer. On the other hand in case of *chlamydia trachomatis* there was slight change in the gradual trend. The % response of change in impedance decreased after the incubation of first concentration of 10^2 ml^{-1} but started to increase after incubating higher concentration.

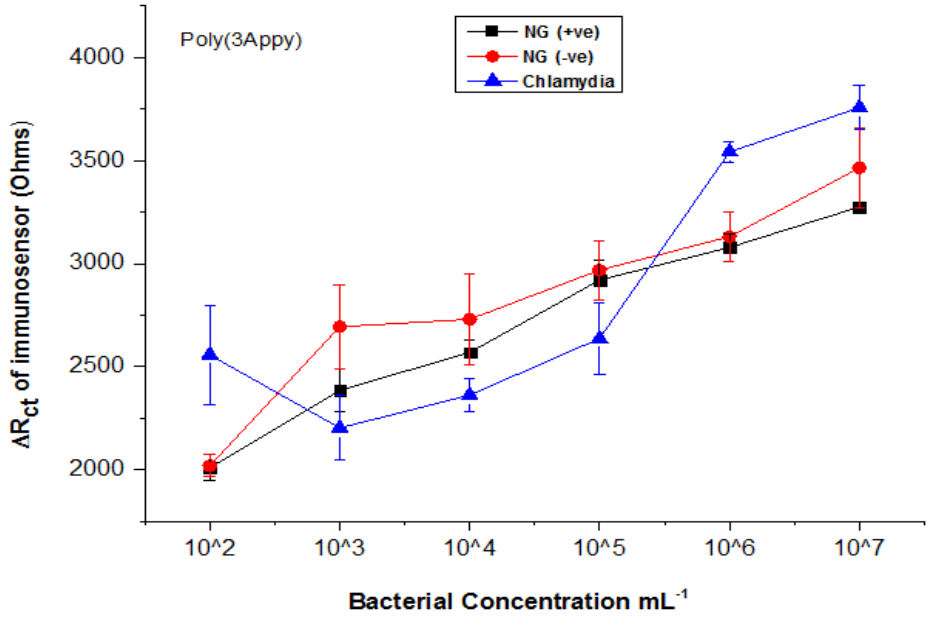

Figure 87 **R_{ct} calibration curve of poly(4AMP) immunosensor comprising normalised values**

Overall the impedance studies of poly(3-APPy) based sensors for all three analytes looked very promising for *Neisseria gonorrhoea* and *chlamydia trachomatis* and showed the detection limit of 10^2 ml^{-1}.

9.5 Summary

In this study, a chemical oxidative polymeristaion of 3-amino propyl pyrrole was carried out which has never been reported before in literature. A copolymer of pyrrole and 3-amino propyl pyrrole was synthesised through chemical polymerisation by using APS as an oxidant. The polymerisation was carried out at room temperature and dark brown thick precipitates were filtered soon after addition of 1M APS into the reaction mixture. Once poly (3APPy) suspension was deposited onto the electrode surface, it was

characterised through Midland imaging and it was found that electrode surface has very few numbers of $-NH_2$ groups available for the immobilisation of antibodies. Therefore a homopolymer of 3APPy was synthesised through oxidative polymerisation and deposited onto the gold electrode through both drop casting and electrochemical deposition. The prepared electrode surfaces were studied through Midland imaging and it showed remarkable number of free-NH_2 groups. The high number of available amino groups could provide a good surface layer for the immobilisation of antibodies. Therefore few sets of electrodes were prepared through electrodeposition of poly (3APPy) and antibodies were immobilised onto them following sulfo-SMCC protocol. Electrodeposited poly (3-aminopropyl) pyrrole was used as a base layer to conjugate ½ generated antibodies via a sulpho-SMCC bridge. Impedance studies were carried out after incubating sensors with bacterial concentrations. The data obtained for *Neisseria gonorrhoea* and *chlamydia trachomatis* was plotted in the form of Nyquist plot. An equivalent electrical circuit model was proposed to fit the experimental results. It was observed that with increasing bacteria concentration, the value of R_{ct} continuously increased which indicated that antigen was captured at the site of antibody and the electron transfer process was hindered.

The modification of electrode with poly (3-APPy) provided highly effective surface for antigen immobilisation. The Nyquist plot for all three analytes *Neisseria gonorrhoea β-lactamase (+) ve, Neisseria gonorrhoea β-lactamase (-) ve* and *chlamydia trachomatis* showed gradual increase in R_{ct} along with increase in bacterial concentration. This indicated that there was gradual increase in thickness of surface layer along with concentration as a result of effective binding of bacterial particles with respective immobilised antibodies. This may have been because reduced antibodies were immobilised with greater control and in the correct orientation for bacterial binding. This is in contrast to the random orientation of antibodies, which may have led to steric hindrance of bacterial particle interaction with the sensing surface.

The immunosensors based on poly (3-Appy) have showed good detection limit of 10^2 ml^{-1} for *Neisseria gonorrhoea* and *chlamydia trachomatis.* Overall, it can be concluded that the fabricated poly (3-APPy) based biosensor are efficient for *Neisseria gonorrhoea* and *chlamydia trachomatis* bacteria in the specified concentration range.

CHAPTER 10 POLYTYRAMINE BASED IMMUNOSENSOR

10.1 Introduction

The polymer film coated on the transducer surface for the immobilisation of biomaterial must be able to efficiently spread the electrical potential produced by the biochemical reaction to the transducer, to ensure reproducibility and to amplify the signal. The use of nanoscale polymer films permits better selectivity and faster measurements and has stimulated the development of new polymer films of varied chemical natures. Electropolymerisation of conducting polymers, such as polypyrrole (PPy), polyaniline, polyacetylene, polyindole, polythionine and polythiophene, has been studied extensively for the development of biosensors. This is because these polymers have a high conductivity and stability in both air and aqueous solution. Also, the thickness of the electropolymerised film and the amount of immobilised enzyme can be controlled easily during electropolymerisation.

After conducting polymers, non-conducting polymers are emerging as a novel support matrix for the immobilisation of biomolecules because they offer impressive advantages, including excellent perm selectivity and high reproducibility, in addition to most of the reported merits of conducting polymers. The biosensors based on immobilising enzymes in nonconducting films have some advantages over conducting films: First, the film thickness of the nonconducting polymer is self-controlled during electropolymerisation, and a very thin and uniform film can be obtained. Biosensors prepared in this way generally have the advantages of fast response and high sensitivity because of relatively high enzyme loading. Second, the nonconducting polymer films are generally found to be more effective in both preventing the biosensor from fouling and eliminating the interference from electroactive species, such as ascorbic acid and uric acid (Zhang and Deng, 1996). Furthermore, nonconducting films are well suited for capacitance measurements where the electrode surface needs to be properly insulated (Loyprasertb *et al*., 2010). An example of a non-conducting polymer is the thin electropolymerised film of poly[1,3-diaminobenzene (DAB)], which can be used to eliminate electrochemical interference from ascorbate, urea, acetaminophen and other

oxidisable species (Miao *et al*., 2004). Previous studies indicated that monomers containing aromatic groups that are directly bonded to oxygen are easier to polymerise. The synthesis of such polymers is reproducible, producing films with good mechanical resistance, which allows higher stability to the modified electrode. The use of non-conducting polymers of phenol and its derivatives for the development of biosensors has been reported (Situmorang *et al*., 2001; Tran *et al*., 2003). The routes of polymerisation of tyramine [4-(2-aminoethyl) phenol] have been extensively studied for application as support for biosensors (Suprun *et al*., 2004).

Tyramine (Tyr) was chosen as monomer in this study due to its pendant amine group. This polymer presents one primary aliphatic amine per tyramine moiety which can be used to attach to organic molecules or to biomolecules of interest. For instance, the amino group can covalently bond through a carboxamide or a phosphoramidate bond and anchor to the transducer. Thus, poly-Tyr has been employed for enzyme (Tran *et al*., 2003), antibody immobilisation, oligonucleotide (ODN) (Situmorang *et al*., 2001) and antigen detection at vey low concentrations (Loyprasertb *et al*., 2010). The electrochemical polymerisation of phenol derivatives such as tyramine (Ty) has received a considerable attention for its applications in bio- and immuno-sensors due to the presence of a free amine group which facilitates immobilisation of bio-recognition molecular species. Moreover, the phenol moiety is known to be preferably oxidised to initiate the polymerisation reaction (Khudaish *et al*.,2012). Conductive properties can also be improved depending on the experimental conditions under which the electrodes are modified. The use of acidic aqueous medium to produce poly-[4-(2-aminoethyl) phenol], poly-Tyr, enables the formation of thicker films with improved conductive properties than those obtained in neutral or alkaline solutions.

10.2 Polymerisation of tyramine

10.2.1 Chemical polymerisation

A significant amount of studies have been done on polyaniline and this constitutes a large family of polymers which are formed by oxidative either electrochemically or chemically of aniline or its derivatives. Aminophenols are interesting electrochemical

materials since, unlike aniline and other substituted anilines, they have two groups (–NH_2 and–OH) which can be oxidised. Therefore, they can show electrochemical behaviour resembling anilines and phenols (Thenmozhi *et al.*, 2011). The extensive literature survey shows that some work has been carried out in aminophenol and their application in different fields specially polytyramine in biosensors. Previuosly no attempt was made to synthesise polytyramine through chemical oxidation method. As the aim of this study is to develop printed medical device therefore an attempt has been made to chemically polymerise tyramine through oxidative polymerisation. During this research work for the first time tyramine was chemically polymerised successfully in the laboratory. Initially 200mM tyramine solution was prepared in 1M HCl whereas 1M APS solution was added into the reaction mixture with continuous stirring but there was no polymerisation. In a second experiment tyramine was successfully polymerised in NaOH solution. The schematic presenatation of polymerisation of tyramine is given in Figure 88.

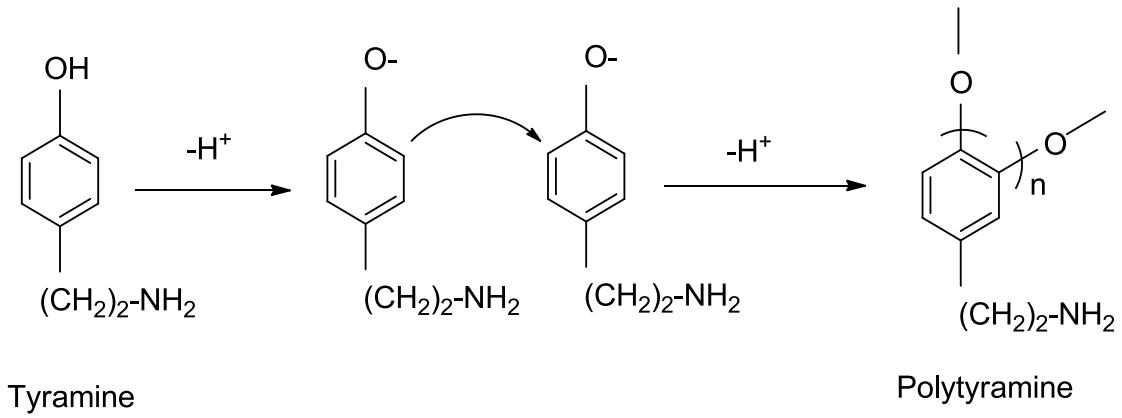

Figure 88 Schematic presentation of the tyramine polymerisation

The oxidative polymerisation of tyramine was carried out with 0.2 M solution of tyramine in 1M NaOH. 0.5M $FeCl_3$ used as an oxidant. The polymerisation was performed at room temperature. Once polymerisation was completed, thick brown precipitates were collected filtered and washed several times with dH_2O to remove any impurities.

The resulting polytyramine particles were characterised through SEM. SEM pictures of polytyramine are given in Figure 89. It showed that most of polytyramine particles were

cubical shaped and dispersed evenly in the solution. There was also some coagulation apparently visible on higher resolution.

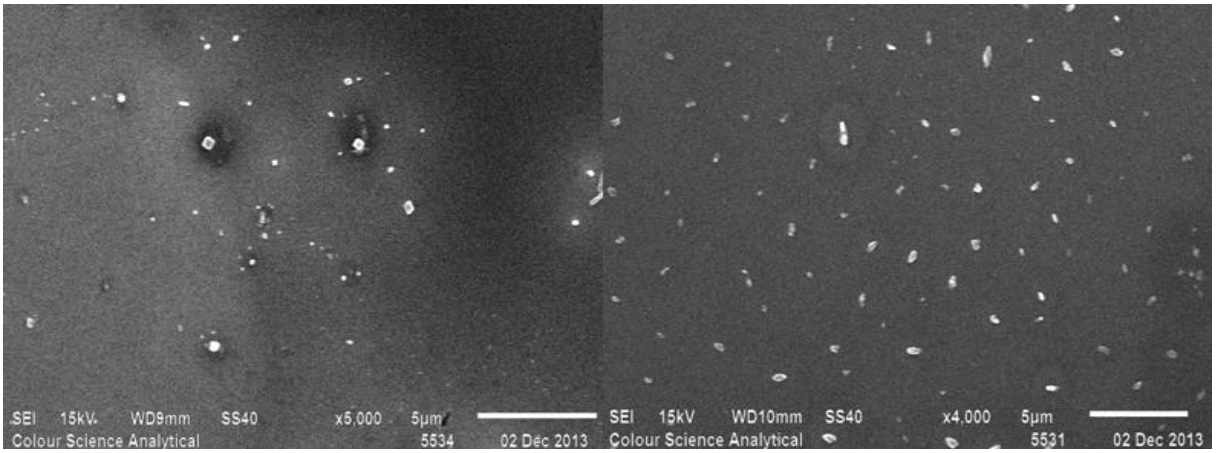

Figure 89 SEM pictures of polytyramine at (A) 4,000 and (B) 10,000 magnifications

10.2.2 Electropolymerisation

Electropolymerisation of tyramine was carried out in 0.025M tyramine solution in 0.3 M NaOH in methanol by using GPES software on an AUTOLAB type III electrochemical. The solution was allowed to stand for couple of minutes to allow undissolved NaOH to settle down. Once settled, a small amount of the solution was taken into the beaker and polymerised at the voltage ranging from 0V to 1.6 V at the scan rate of 100 mVs^{-1}. Total two scans were carried out and a uniform polytyramine film was electrodeposited on the gold electrode.

Following electroploymerisation, polytyramine electrodes were rinsed with dH_2O and blow-dried gently in a stream of argon. Figure 90 shows typical cyclic voltammogram obtained form electropolymerisation of polytyramine. The first cycle showed that oxidation of tyramine was irreversible for all pH values. During continuous potential cycling a gradual decrease in the peak current was observed, but oxidation of the monomer continued after second scan. It was obvious that as the number of cycles was increased the poor conductivity of the polytyramine films resulted in passivation of the electrode and hence electrodeposition current was decreased (Miscoria *et al*., 2006). After several cycles, the electrode was sufficiently blocked such that only very small

oxidation currents were observed. As with the electroploymerisation of other phenols, linking occurs through the ortho position of the phenol group leaving the amine available for covalent attachment of enzyme (Situmorang *et al.*, 1999).

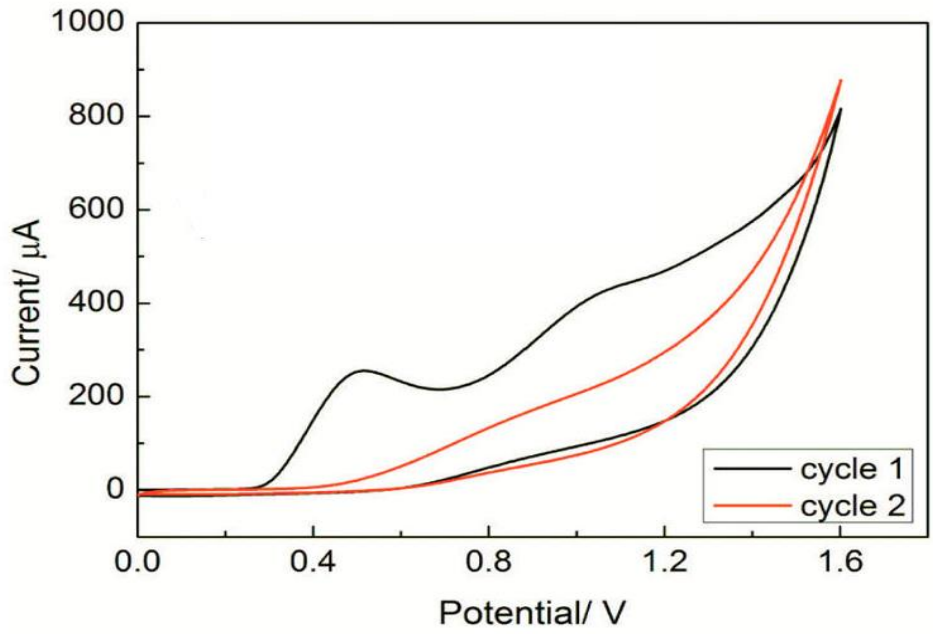

Figure 90 Cyclic voltammogram of polytyramine

The electrochemical trend demonstrated the reversible reaction (protonation/deprotonation) associated with the transfer of one electron and one proton between the monomer and its cationic phenoxy radical (Miao *et al.*, 2005). This initiation step was followed by dimerisation reaction (one electron + one proton) of the phenoxy radical with Tyr molecule (linkage via ortho position) to form a dimmer (oligomerisation) followed by nucleation of oligomers and subsequent deposition of the polymer on the electrode surface as depicted in literature (Khudaish *et al.*, 2012).

10.3 Characterisation of polytyramine

10.3.1 FTIR analysis

The FT-IR spectrum of a polytyramine formed through oxidative polymerisation with $FeCl_3$ was recorded along with peaks selection as shown in Figure 91.

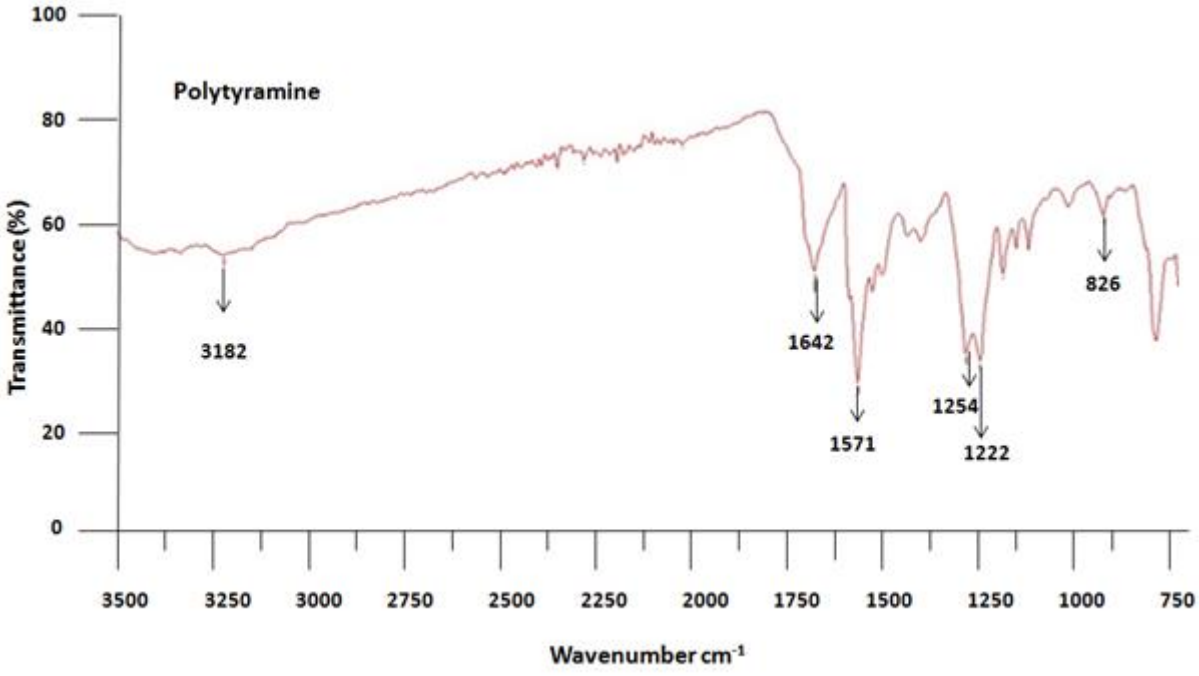

Figure 91 FTIR spectra of polytyramine

In the FTIR spectra, peak found at 3182 cm^{-1} is evident of C-H strectching in an aromatic compound. The two peaks at 1642 and 1571 cm^{-1} are attributed to the C=C stretching of benzene and quinone rings respectively. The peaks at 1254 cm^{-1} and 1222 cm^{-1} are assigned to the C-N stretching vibrations, because the C-N stretching vibrations in aromatic amines are in the range of 1280-1180 cm^{-1}. The peak observed at 826 cm^{-1}, corresponds to the C_b–H out of plane vibration (Thenmozhi *et al.*, 2011).

10.3.2 SEM analysis of polytyramine modified surfaces

SEM images shown in Figure 92 were obtained before and after polytyraime deposition on gold electrodes. Two different types of electrodes were prepared. Keeping in mind of feasibility of printing sensors, drop casting was adapted as alternative method to electrodeposition. The resulting polymer surfaces onto gold electrode were analysed under SEM and compared with bare gold electrode. It was revealed that drop sensors had rough surface with crevices as shown in Figure 92 (A). Polytyramine has smothened the surface after electrodeposition by covering the surface crevices which appeared quite small after layer formation as given in Figure 92 (B).

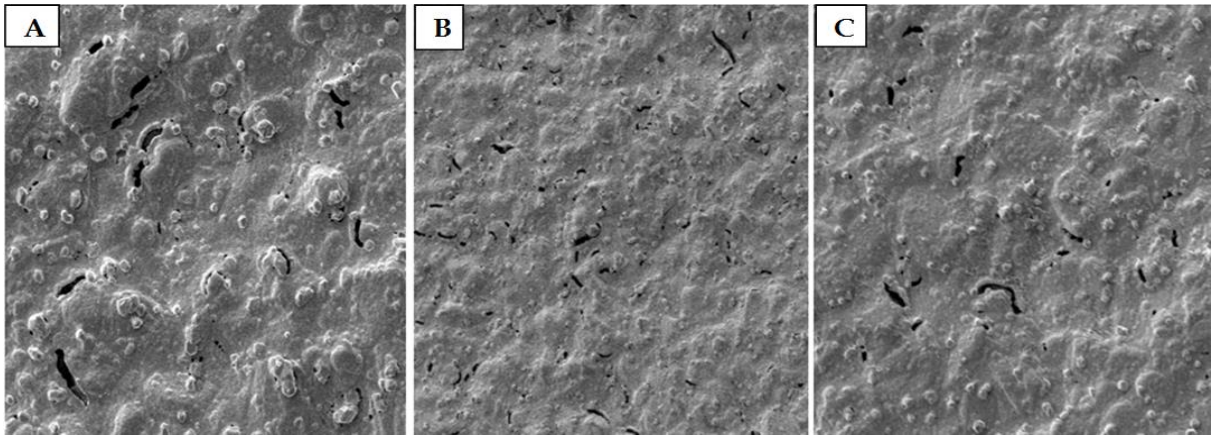

Figure 92 SEM analysis of polytyramine film a) bare electrode b) PTyr electrodeposited and c) PTyr drop casted

When polytyramine was casted onto the gold surface through drop, it apparently gave a thin and uniform film covering the electrode surface as shown in Figure 92 (C).

10.4 Impedance studies of polytyramine based immunosensors

Proper insulation of the electrode surface is an essential feature in capacitive biosensors. The degree of electrode insulation can be probed with cyclic voltammetry using an electro-active species in the contacting aqueous solution. The proper covering of transducer is necessary to facilitate the electron transfer between electroactive species and the electrode which occur either by tunnelling through the layer covering the electrode surface or by approaching the electrode at a defect "pinhole" in the polymer layer. The successful formation of a polytyramine film on the electrode surface seems to effectively prevent the penetration of the conducting ions.

The immunosensors based on polytyramine were constructed through electrodepsotion through cyclic voltammetry. The polymer deposited surface was activated through sulpho-SMCC before immobilising reduced antibodies. Once constructed, these fully generated sensors were incubated with *Neisseria gonorrhoea β-lactamase (+) ve*, *Neisseria gonorrhoea β-lactamase (-) ve* and *chlamydia trachomatis* concentrations ranging from 10^2 ml^{-1} to 10^7 ml^{-1}. Impedance studies were carried out on polytyramine

biosensors after incubating with various concentrations of *Neisseria gonorrhoea* and *Chlamydia* and changes in impedance were recorded.

10.4.1 Test of polytyramine based sensors against Neisseria gonorrhoea

EIS had been successfully applied to characterise immunosensor formation in previous studies (Geng *et al*., 2008; Zhang *et al.*, 2006). Polytyramine based immunosensors were tested against both strains of *Neisseria gonorrhoea β-lactamase (+) ve* and *Neisseria gonorrhoea β-lactamase (-) ve*. A small amplitude perturbing sinusoidal voltage signal of 0.4 V was applied over the range 0.1 Hz - 10,000 Hz to the electrochemical cell, containing the same redox mediator of $Fe(CN_6)^{3-/4-}$ in PBS at pH 7.2. The resulting current response was recorded using μAutolab Type III frequency response analyser (FRA-2). This technique was applied for all bacterial sensors and results were presented in the form of Nyquist plot, over repeats of number of electrodes. EIS was chosen as a suitable technique because it measures the total resistance encountered when a current flows through the cell. Once prepared, functional immunosensors based on polytyramine were immersed in $Fe(CN)_6^{3-/4-}$ solution for 30 minutes before testing against increasing concentrations of *Neisseria gonorrhoea β-lactamase (+) ve* in PBS. Each electrode was incubated with concentration on the electrode surface for 10 min, rinsed in dH_2O and interrogated by EIS. The concentration of *Neisseria gonorrhoea β-lactamase (+) ve* applied ranged from 10^2 to 10^7 particles ml^{-1} and data was collected. Nyquist plot shown in Figure 93 shows that change in charge transfer resistance in *Neisseria gonorrhoea β-lactamase (+) ve* immunosensor.

It is clearly shown that the R_{ct} increases gradually as the bacteria concentration increases after consecutive incubations from 10^2 ml^{-1} up to 10^8 ml^{-1}. The increase in R_{ct} is attributed to the binding of bacteria to immobilised *Neisseria gonorrhoea β-lactamase (+) ve* antibody producing a barrier layer that inhibits the charge transfer for a redox probe. It is necessary to study nonspecific bacterial binding along with specific. Therfore again *antidigoxin* was used as control and immobilised onto polytyramine coated gold electrode following the protocol. Once immobilisation is completed a

number of sensors were incubated with NG(+)ve bacterial concentrations and interrogated through EIS. The resulting Nyquist plot is given in Figure 94.

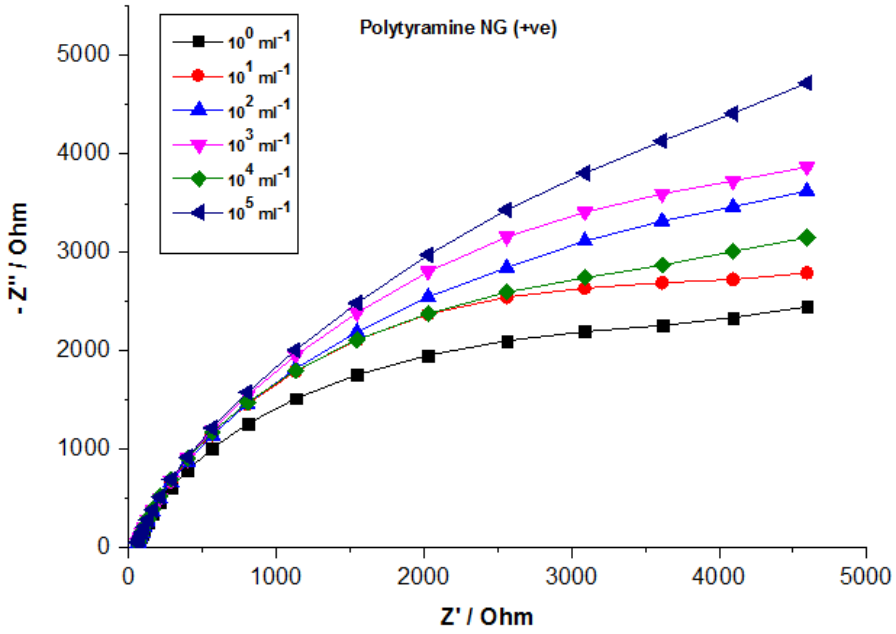

Figure 93 **Nyquist plots of a polytyramine-NG(+)ve modified electrode exposed to various concentrations of Neisseria gonorrhoea (+)ve**

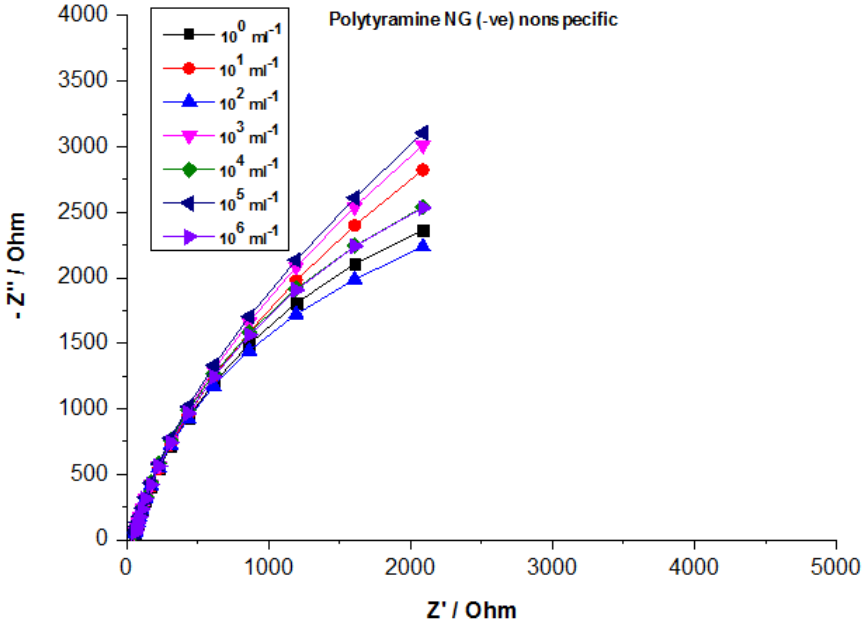

Figure 94 **Nyquist plots of negative control of polytyramine modified electrodes exposed to various concentrations of NG (+)ve**

The experiment was repeated several times to study the selectivity of polytyramine based NG(+)ve immunosensor and a bar graph was created along with error bars as presented in Figure 95. The bar graph showed almost consistant results with number of electrodes.

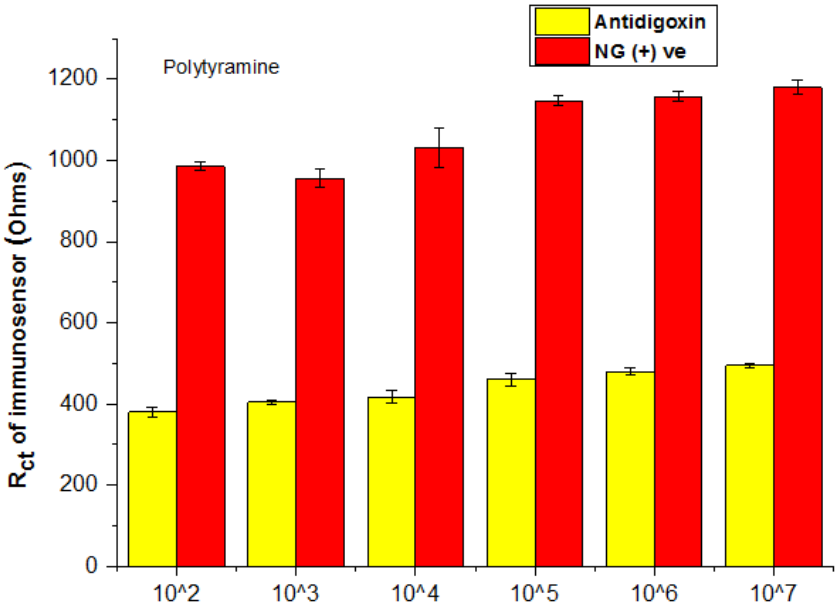

Figure 95 Standard deviation graph of polytyramine-NG(+)ve modified immunosensor

Similarly various concentrations of *Neisseria gonorrhoea β-lactamase (-) ve* were tested against polytyramine sensors. The impedance plot against various concentrations of NG (-)ve is shown in Figure 96 along with control in Figure 97. The increases in the semicircle diameters in Nyquist plot shown in impedance spectra in Figure 67 and Figure 68 follow the theoretical shape typically seen for a Randle's equivalent circuit. As the first concentration of 10^2 ml^{-1} was incubated on polytyramine sensor the resistance increased. There was again appreciable change in charge transfer resistance for 10^3 ml^{-1} concentration but the signal strength reduced after the addition of higher concentration of 10^4 ml^{-1}. This might be because of saturation of the surface which gradually increased after the attachment of bacterial particles and started to cause stearic hindrance. The resistance of polytyramine sensors increased along with the concentration which is because of increase of thickness of layer on the surface of electrode. The increase in resisatnce was quite apparent for initial two concentrations of 10^2 ml^{-1} and 10^3 ml^{-1} but

there was small increase in resistance was noted after incubating with 10^4 ml^{-1} to 10^6 ml^{-1}.

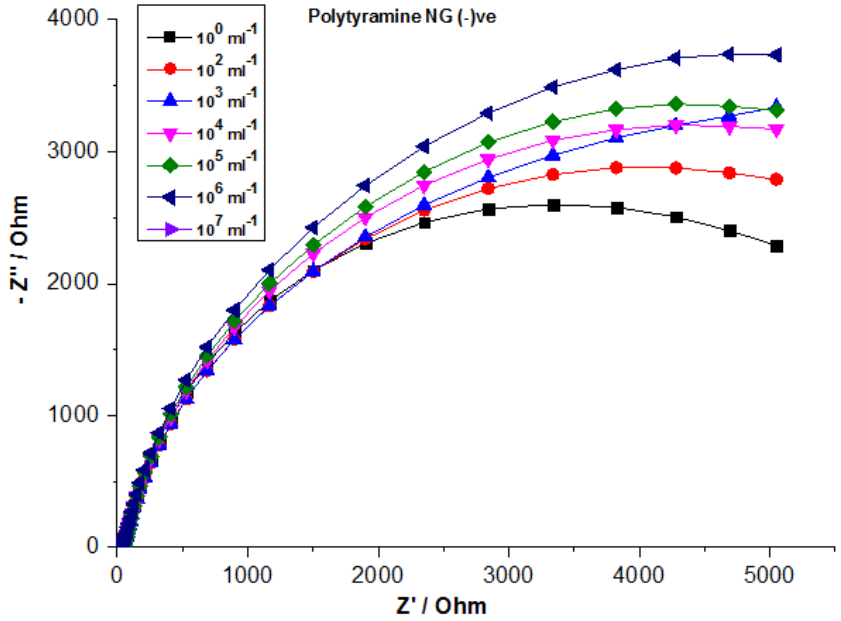

Figure 96 **Nyquist plots of a polytyramine-NG(-)ve modified electrode exposed to various concentrations of Neisseria gonorrhoea (-)ve**

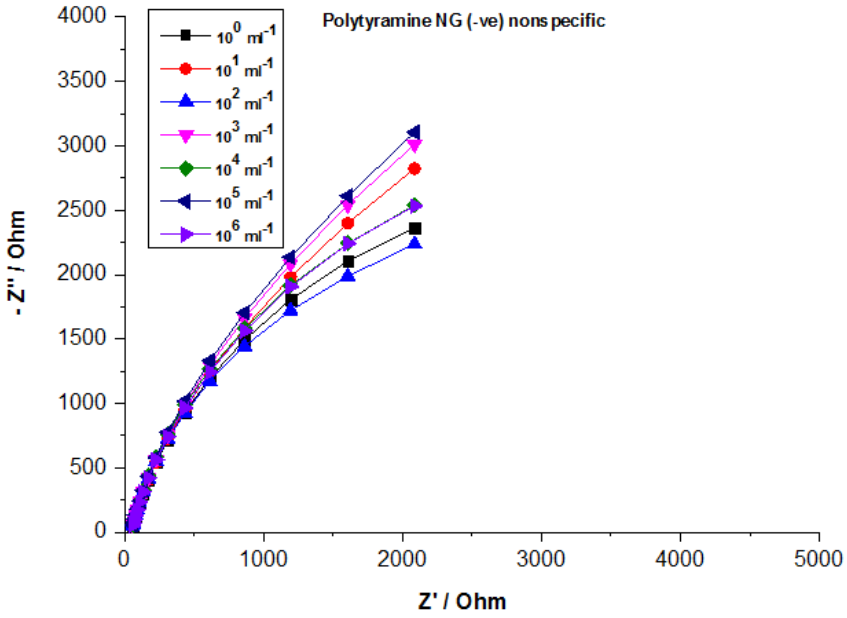

Figure 97 **Nyquist plots of negative control of polytyramine modified electrodes exposed to various concentrations of NG (-)ve**

The bar graph presented in Figure 98 showed standard mean of deviation of sets of polytyramine-NG(-)ve immunosensors.

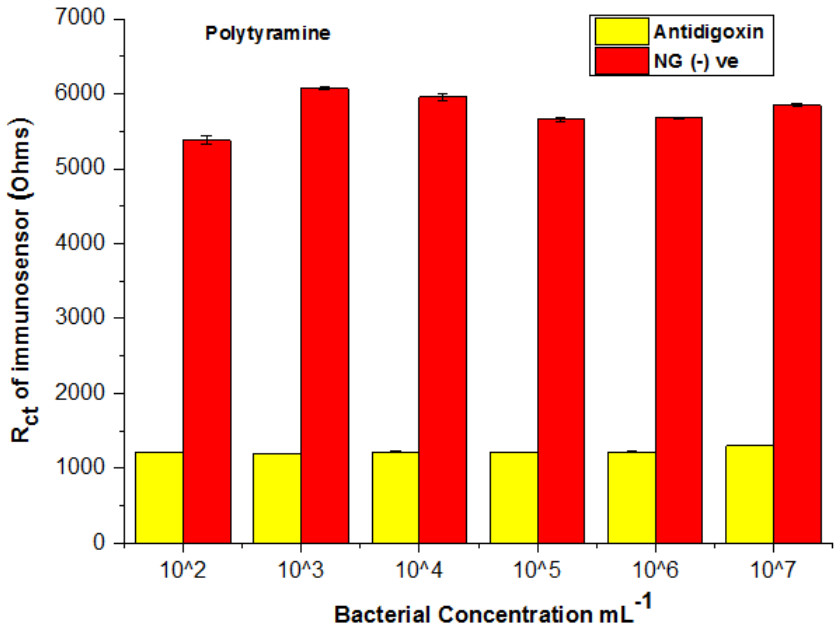

Figure 98 Standard deviation graph of polytyramine-NG(-)ve modified immunosensor

It is evident that there is very low standard mean of deviation among number of polytyramine-NG(-)ve immunosensors and the reproduceability of the sensor is quite high.

10.4.2 Test of polytyramine based sensors against chlamydia

A set of polytyramine modified sensor based on *Chlamydia* were constructed and tested against heat killed *Chlamydia trachomatis* to study the potential of polytyramine as a robust platform for the immunosensor. Three sensors were used for each experiment and each sensor was interrogated in triplicate for reproducibility. The sensor was incubated with PBS, pH 7.2 to record the impedance spectra of blank polytyramine based immunosensor. The polytyramine based sensor was then exposed to 10^2 ml^{-1} *Chlamydia trachomatis* concentration. The process was repeated for higher antigen concentrations ranging from 10^3 ml^{-1} to 10^6 ml^{-1}. The change in impedance was interpreted in the form of Nuquist plot. Figure 99 shows the impedimetric data collected, presented in the form of a Nyquist plot depicting the faradic (Z') and

capacitive (-Z'') components of the ac impedance analysis of the polytyramine immunosensor following exposure to *chlamydia trachomatis* antigen.

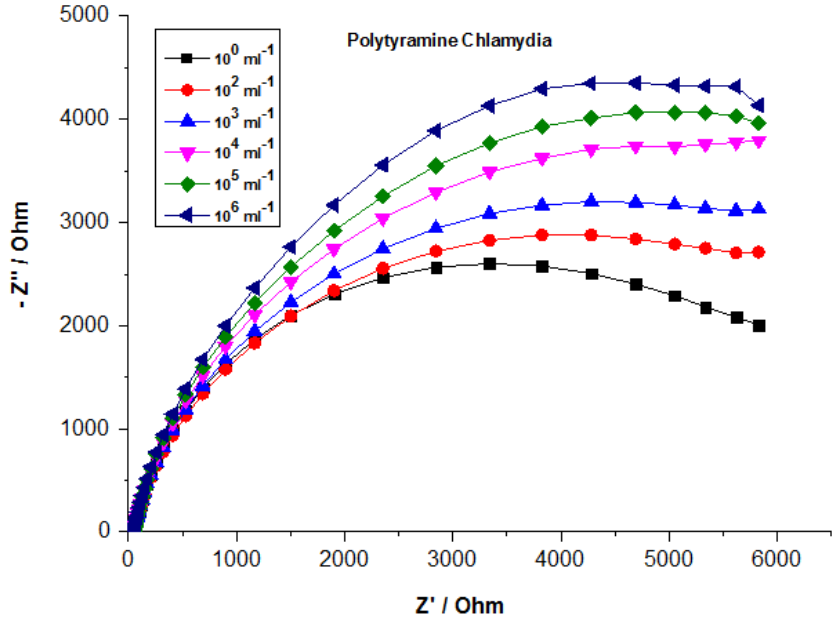

Figure 99 **Nyquist plots of a polytyramine-Chlamydia modified electrode exposed to various concentrations of Chlamydia**

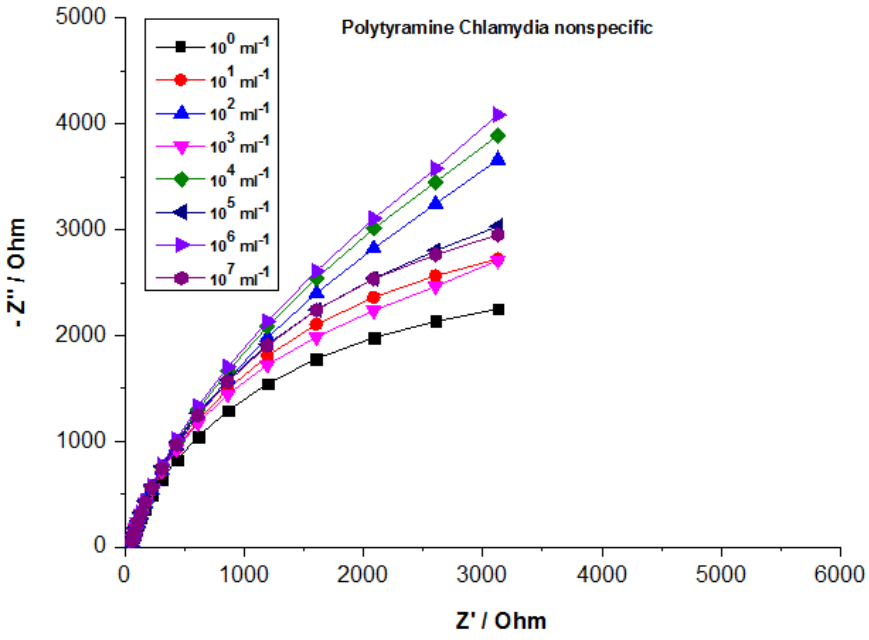

Figure 100 **Nyquist plots of negative control of polytyramine modified electrodes exposed to various concentrations of Chlamydia**

It can be seen from that there was a measurable signal response for the faradic component (Z') and the capacitive component (Z'') of the Nyquist Plot for increasing concentrations of *chlamydia* exposed to polytyramine sensors. The charge-transfer mechanism between the antibody/antigen has occurred which is evident with the increase in the resistive (Z') component of the total impedance. The capacitive resistance (Z'') increases to a larger extent at greater antigen concentrations (towards 10^6 ml^{-1}). The negative control of polytyramine-*Chlamydia* immunosensor was constructed through immobilisation of ½ generated antidigoxin onto WE2 following standard protocol. The negative control was tested against various concentrations of *Chlamydia* and the resulting Nyquist plot is presented in Figure 100. The Nyquist plot of negative control showed appreciable nonspecific binding with *Chlamydia* bacterial particles. Although the bacterial binding is low as compared to specific binding yet there was a continuous increase in resistance along with the concentrations. The impedance studies of negative control shows that bacterial particles get attached to the polytyramine-*antidigoxin* layer and blocked the surface resulting in the decrease of Rct across the electrical interface. The experiment was repeated number of times and calibration curve was constructed using standard mean of deviation through bar graph presented in Figure 101.

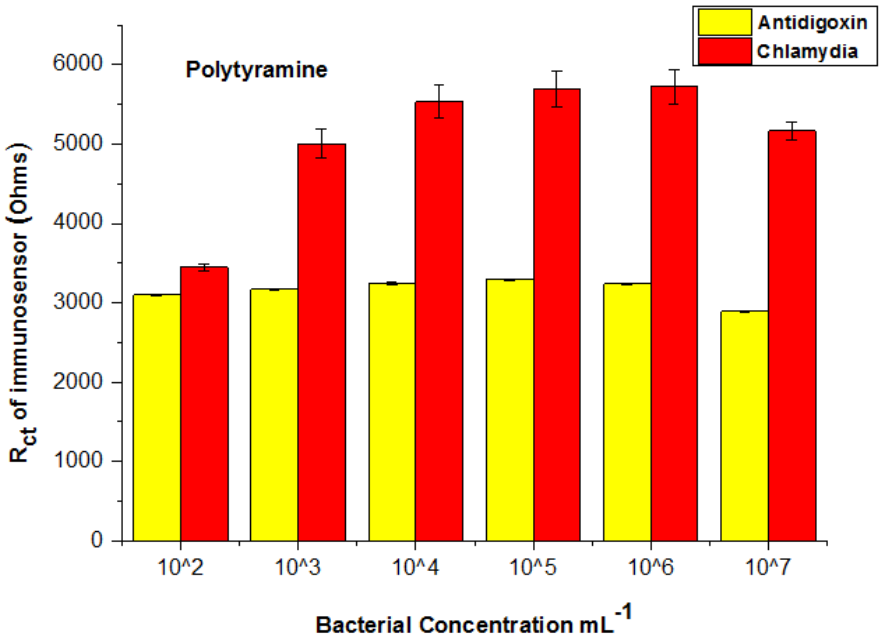

Figure 101 Standard deviation graph of polytyramine- *Chlamydia* modified immunosensor

The eror bars given in Figure 101 shows that the results are almost same for the nonspecific binding whereas there is slight variation of results in case of specific analyte. In the bar graph yellow bar representing *antidigoxin* and red bar representing *Chlamydia* showed that there was gradual increment of Rct across the electrode surface but the decreased after the saturation point achived at 10^7 ml^{-1}.

10.4.3 Calibration curves against increasing antigen concentrations

Usually, nonspecific adsorption is a major problem in label-free immunosensing, since it cannot be distinguished from specific adsorption in labelless electrochemical sensing antigens. The impedance changes of immunosensor against specific analyte can be calculated by minimising non-specific interactions. To calculate impedance changes arise from specific interaction between specific analyte (*Neisseria gonorrhoea* and *Chlamydia*) a calibration curve was constructe for each analyte as shown in Figure 102.

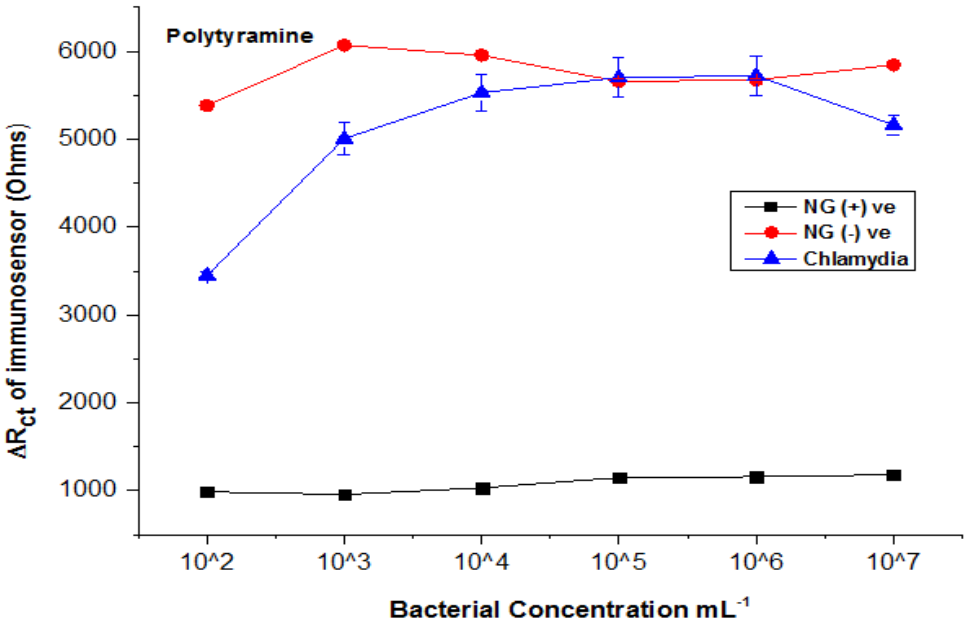

Figure 102 R_{ct} calibration curve of polytyramine immunosensor comprising normalised values

The change of resistance of all concentration on single frequency of 1Hz was calculated and normalised by substartcting non-specific interactions as decribed in section 7.4.3. The curve was generated by plotting normalised values against bacterial

concentrations.The calibration plots of normalised values of resistance change (ΔR_{ct}) at similar frequency with different concentrations of the analytes against specific and non specific antibodies.

It was observed that there was only a slight variation on the impedance of nonspecific antibody (i.e. *antidigoxin*) with the increase of bacterial concentration. Such small changes of the electron-transfer resistance of the nonspecific adsorption are acceptable. This indicated that the observed changes of the electron-transfer resistance with targeted antigen were due to specific antibody-antigen interaction. Without much interference from nonspecific adsorption, the studied immunosensor has good selectivity.

10.5 Summary

The electropolymerised polytyramine has been reported as a new nonconducting-polymer-based immobilisation matrix for the development of biosensors. The research work presented in this chapter is based on polytyramine immunoosensors, constructed to produce highly reproducible, sensitive, and stable sensors to detect *Neisseria gonorrhoea β-lactamase (+) ve*, *Neisseria gonorrhoea β-lactamase (-) ve* and *Chlamydia trachomatis*.

Polytyramine was electrodeposited onto gold electrode and characterised through SEM, cyclic voltammetry and western blotting imaging. The blotting images showed excess amino groups enough to immobilise antibodies. Once polytyramine showed potential to immobilise antibodies, three different types of sensors were constructed based on *Neisseria gonorrhoea β-lactamase (+) ve*, *Neisseria gonorrhoea β-lactamase (-) ve* and *Chlamydia trachomatis*. Each set of sensor was tested against various concentrations of respective heat killed bacteria and Nyquist plot was plotted. The data was fitted into Randles circuit model. It was evident that the semicircle diameters in the Nyquist plots of *Neisseria gonorrhoea β-lactamase (+) ve*, *Neisseria gonorrhoea β-lactamase (-) ve* and *Chlamydia trachomatis* increased along with the particular bacterial concentration. It shows that increasing antigen bound to the sensor interface elicited increased electron

transfer resistance which results into stronger blocking of electron transfer to the redox probe.

Nyquist plot of all three antibodies showed almost similar results but the response was quite evident for *chlamydia trachomatis*. There was gradual increase in charge transfer resistance along with concentration showing that bacterial particles have adhered on the surface upon subsequent incubation. The successive adhesion had increased the thickness of film and as a result R_{ct} increased. Polytyramine based immunosensors showed good response and reliability as possible immobilisation matrix for antibodies.

Overall the study proved to be useful for the application of nonconducting polymers on the development of biosensitive materials. Polytyramine based sensors can be employed in successful construction of biosensors in the health care field.

CHAPTER 11 CONCLUSIONS AND FUTURE WORK

11.1 General conclusions

The overall aim of this project was to develop a biosensor for rapid detection of diseases as conventional detection methods are time consuming and expensive.

The initial work was performed to develop vapour sensor as a point-of-care device for diabetes mellitus and pulmonary tuberculosis. It is known that variation in the composition of volatile components in breath can indicate certain diseases, such as diabetes, at a relatively early stage of development of the illness. After the analysis of exhaled endogenous VOCs, it is possible to separate patients with diabetes mellitus type 2 from healthy controls. This is a first step towards the development of a non-invasive test using breath gas of at-risk persons and making it an attractive option for large-scale testing of at-risk populations. Electronic nose have received considerable attention in the field of health care devices. It was proposed that QTC material could be utilised for the sensor fabrication and could be employed as a gas sensor for electronic nose. The initial testing of QTC based sensors showed large, fast response to selected vapours and has proved as that it has potential as sensor in an electronic nose.

The positive response of QTC sensor against selected vapours acetone and ammonia showed its potential in a wide variety of sensing applications. This could lead to the development of an array of vapour sensors made by using different binding polymers that could distinguish between different solvent vapours. This method may also lead to the identification of mixed chemical vapour composition. Unfortunately, the research work couldn't go due to certain limitations and confidentiality issues.

Later, the research work was focused onto development of sensor for rapid detection of certain STIs. Current detection methods for most of the STIs are time consuming and require expertise from sampling to identifying the disease. The most popular emerging technique for bacterial detection is voltammetry through capture of bacterial RNA or DNA. Although a popular and sensitive technique, the application of voltammetry still requires sample preparation, similar to that of PCR, to extract genetic material from

samples prior to analysis. As such, it is thought that EIS of whole bacterial particles is better as no sample preparation is required and the time needed for data analysis from each method is comparable.

Other methods used to detect bacteria include, Optical methods (i.e. spectroscopy and fibre optics), QCM, SAW, SPR, MEMs and AFM. The speed of many of these technologies depends upon the age of the specialist machinery and sophistication of the accompanying software used for data analysis and whether this can be performed in real-time. Without exception, all the technologies currently being developed for bacterial detection require highly skilled scientists for operation of the machinery and interpretation of data. The same limitations in terms of accessibility, ease of use, time and cost apply to each technique mentioned to varying degrees. Therefore no particular method currently stands out as a leader in the field, most likely to be commercialised first.

Among STIs, *Neisseria gonorrhoea* and *Chlamydia trachomatis* are recognised as two of most prevalent sexually transmitted bacterial infections. In an effort to prevent the spread of these diseases, increased attention is being focused on early diagnosis and treatment of symptomatic or asymptomatic infected individuals. The research work was conducted to prepare and characterise an impedimetric immunosensor for the detection and quantitation of *Neisseria gonorrhoea* and *Chlamydia trachomatis.*

Due to the highly sensitive and selective nature of the recognition between antigen (Ag) and antibody (Ab), immunoassays are very useful in widespread applications such as medical detection, processing quality control, and environmental monitoring.

The aim was to prepare and characterise electrochemical impedance spectroscopic biosensor for bacterial detection. Conductive polymers are excellent platforms for the immobilisation of biomolecules at electrodes. Electrochemical immunosensors are concerned with the formation of a recognition complex between the sensing biomaterial and the analyte under investigation in a monolayer or thin-film configuration, on an electronic transducer. Four different types of polymers were employed to form a conducting layer onto the transducer element which includes poly (4-amino methyl)

pyridine, polyaniline, poly (3-amino propyl) and polytyramine. Whereas, screen printed gold electrodes were used for the construction of immunosensor.

The formation of a complex on a conductive or semi-conductive surface (antibody–antigen binding) may alter the capacitance and the resistance at the surface–electrolyte interface and this phenomenon was employed to determine the concentration of the required analytes *Neisseria gonorrhoea* and *chlamydia*.

Kinetics and mechanisms of electron-transfer processes that correspond to the biocatalytic reaction occurring at modified electrodes were derived from Faradaic impedance spectroscopy (FIS).

In this study, novel impedimetric immunosensors based on conductive polymers were successfully developed to specifically detect *Neisseria gonorrhoea β-lactamase (+) ve, Neisseria gonorrhoea β-lactamase (-) ve* and *chlamydia trachomatis*. The method of immobilisation was to cross-link antibodies by a highly targeted molecule. Therefore, the development of appropriate conductive surface with excessive amino groups was required. Initially, PANI and poly (4AMP) were used as conductive surfaces for immobilisation of antibodies. Once fabricated, the reduced antibodies were immobilised onto the gold electrode coated with polymer by using the linker molecule sulpho-SMCC which reacted with the primary amine to immobilise the half-antibodies. The impedance studies of fully constructed sensors were carried out in the presence of a redox probe, $[Fe(CN)_6]^{3-/4-}$. All types of sensors were incubated against various concentrations of heat killed pathogens which were diluted through serial dilutions ranging from 10^2 ml^{-1} to 10^8 ml^{-1}. All imunosensors were interrogated through EIS and change in impedance was recorded after incubating them with various concentrations.

Initially, poly(4-amino methyl pyridine) based sensors were prepared through electrodeposition of 4AMP onto gold electrode followed by immobilisation of antibodies through sulfo-SMCC activation and then tested against various concentrations of *Neisseria gonorrhoea β–lactamase (+) ve, Neisseria gonorrhoea β–lactamase (-) ve* and *chlamydia trachomatis*. The response was interpreted in the form of Nyquist plot and the data was fitted into Randles model circuit.

The electron transfer resistance R_{ct}, was measured in the poly (4-AMP) biosensor. The attachment of bacterial cells retarded the interfacial electron-transfer kinetics and increased the electron-transfer resistance. The total electron transfer resistance after cell attachment was expressed as

$$R_{ct} = R_c + R_{cell} \quad (14)$$

Where R_c and R_{cell} are the charge-transfer resistance of the antibody-immobilised electrode and the variable charge transfer resistance introduced by the attached bacterial cells.

A typical Nyquist plots were obtained, comprising of a semicircle lying on the Z' axis continued with a straight line. The semicircle portion observed at the higher frequencies corresponds to the charge-transfer-limited process, while the linear part is characteristic of the lower frequencies and represents the diffusion-limited processes. The intercept of the semicircle with the Z' axis at high frequency is equal to R_s. The diameter of the semicircle is equal to the charge-transfer resistance, R_{ct}.

The charge transfer (R_{ct}) of poly (4-amino methyl) pyridine based sensors increased with the increasing cell concentration. The poly (4AMP) immunosensors showed a gradual response from 10^2 to 10^3 particles mL^{-1} for *Neisseria gonorrhoea β–lactamase (+) ve* and *Neisseria gonorrhoea β–lactamase (-) ve*. The detection limit of poly (4AMP) immunosensors against *Neisseria gonorrhoea* and *chlamydia* was found to be 10^2 particles mL^{-1}.

In a similar way the polyaniline based sensors were studies and interrogated against various concentrations of selected analytes. The response of polyaniline modified sensors was plotted in the form of a Nyquist plot. A decrease of the diameters of the semicircles was observed along with the increase in bacterial concentrations of *Neisseria gonorrhoea β–lactamase (+) ve, Neisseria gonorrhoea β–lactamase (-) ve* and *chlamydia trachomatis*. It showed that the binding between antibody and antigen led to more severe distortion in the polyaniline film, which increased the charge transfer on the gold surface therefore charge transfer resistance decreased along with the concentration. In the case of *Neisseria gonorrhoea β-lactamase (+) ve* at a bacterial

concentration of 10^6 ml^{-1}, the change in R_{ct} comparatively showed insensitivity to the changes in the bacterial concentration, probably due to surface saturation. The saturation limit for *Neisseria gonorrhoea β-lactamase (-) ve* based immunosensor was found to be 10^4 mL^{-1} and for *Chlamydia trachomatis* the saturation limit was 10^3 mL^{-1}. Once the saturation limit was achieved the conductive polymeric layer started to distort and resistance started to decrease.

Similarly the dense polymer layers of polyaniline and poly (4-aminomethyl pyridine) immunosensor were disrupted after the addition of higher concentration of analyte. Poly (4-aminomethyl pyridine) collapsed after the addition of high concentration of *Neisseria gonorrhoea* which resulted into decrease in charge transfer resistance but sensor showed signs of recovery after additions of higher concentrations of antigen. Similarly polyaniline based immunosensors showed gradual decrease in resistance along with increasing concentrations of analyte which showed that the electrode surface does not have enough antibodies attached to the surface to passivate the transducer completey. This disruption of the surface layer by bacterial analyte and decrease in resistance suggested that both polyaniline and poly (4-aminomethyl pyridine) were not suitable as sensing platforms for biosensing experiments. Therefore, it was decided that a more robust sensing platform needed to be constructed and new possible immobilisation matrixes should be investigated.

Poly (3-aminopropyl pyrrole) copolymer and polytyramine had previously been used as a conducting surface layer for use in amperometric based sensors. Therefore, they were considered as possible conducting layers for the immobilisation of *Neisseria gonorrhoea β–lactamase (+) ve, Neisseria gonorrhoea β–lactamase (-) ve* and *chlamydia trachomatis*. However, it was essential to confirm that the selected polymers had functional groups which could be utilised for immobilisation chemistry. To conserve and ensure correct orientation of amino groups for the immobilisation of antibodies both chosen polymer were imaged through western blotting system. The results demonstrated that the immunosensor constructed by poly (3APPy) and polytyramine had sufficient amino groups which showed high affinity to antibodies.

The impedimetric interrogation of poly (3-APPy) and polytyramine sensors yielded positive results with more rigorous, reproducible data collected at the lower end of the

frequency range (1–10 Hz). The specific interactions and resultant complexes formed gave rise to an overall increase in terms of impedance change from the baseline response at the electrode/solution interface. Plots of the real (Z') and imaginary (-Z") components of the impedance at a specific frequency provided information for construction of calibration curves, recorded by multiple interrogations of both sample and control sensors, with respective antigen. In case of poly (3-APPy) based sensors the charge transfer resistance increases along with increase in bacteria concentrations of *Neisseria gonorrhoea β–lactamase (+) ve* and *Neisseria gonorrhoea β–lactamase (-) ve*. The detection limit of *Neisseria gonorrhoea β–lactamase (+) ve , Neisseria gonorrhoea β–lactamase (-) ve* and *Chlamydia trachomatis* was found to be$10^2 ml^{-1}$ and saturation limit was found to be $10^6 ml^{-1}$ whereas saturation limit of *Chlamydia trachomatis* was $10^5 ml^{-1}$ before the polymeric layer collapsed and pinholes were created onto the electroactive surface.

The polytyramine based immunosensors showed promising results against *Neisseria gonorrhoea β–lactamase (+) ve, Neisseria gonorrhoea β–lactamase (-) ve* and *Chlamydia trachomatis*. The saturation limit shown by polytyramine sensors was also found in the range of $10^6 ml^{-1}$.

As expected, negative controls of the reduced *anti-digoxin* immunosensor tested with both antigens showed some non-specific binding. However, specific binding resulted in a much greater response in the charge transfer resistance of the sensor, as observed on the calibration curve. The immunosensors responses for both specific and non-specific binding were also reproducible.

Due to time limitations for securing ethical approval and clinical samples, the immunosensor constructed in this study has not been interrogated in relevant samples, which is something that should definitely be explored with future experiments.

Although there is potential for many of these biosensors to become commercialised, many issues potentially block the successful transition from laboratory to GPs surgeries. Development and commercialisation may be limited by widespread adoption as well as the large steps required to bring the sensors to market with a feasible per unit cost.

11.2 Future Work

The research work presented in the thesis has showed very promising results. However there were number of technical issues observed during the development immunosensors. Such issues are important enough to be discussed for future studies to improve the results.

Due to time constraints, the stability of the immunosensor over time was not investigated. This is clearly one aspect of the immunosensor construction that would need to be investigated. It is important because medical sensors must have a shelf-life of months for their production and proven to be economically viable. However, antibodies are very stable and could be stored for quite long.

This study used one immunosensor for the detection of increasing concentrations of pathogen, repeated in triplicate using three different electrodes. Therefore, the insulating effect caused by bacterial binding may be cumulative. As all concentrations were incubated on one immunosensor therefore it is not comparable to one electrode interrogated using EIS only once with an unknown bacterial concentration. If there was no financial restrain, the experiment should be run with one immunosensor for each concentration of bacterial sample. This was not done for this study as DropSens electrodes cost between 2.95 – 4.95 Euros each. If experiments were to be repeated in triplicate, over 100 electrodes would be required for each calibration curve. It would be interesting to see how this curve would compare to the final calibration achieved from this study.

In addition, the immunosensor would need to be rigorously tested in urine samples containing pathogens. However, the limit of detection for this immunosensor is as low as 10^3 bacterial particles mL^{-1} and thus the sensor would be useful in diagnosing infection at very early stages.

Finally, nonspecific binding of unintended targets could be tremendous practical challenge, and further work should be done towards optimising probe surfaces and processing sensor data to eliminate false signals. The performance of impedance

biosensor heavily depends on the availability of recognition molecules on electrode surface. The surface organisation of capture molecules plays an important role in determining the availability of recognition molecules which influences the affinity of a target for a receptor. Non-specific adsorption is another important factor that should be considered when engineering electrode surface since it increases background signal.

A number of aspects of production would need to be addressed to reduce the time need to collect and analyse data before this sensor could be commercialised. Although there is a long way to go before this assay could feasible be commercialised, it is hoped that the work described in this thesis will assist others in their future work in developing immunosensors for the detection and quantitation of pathogens. Building on this work, immunosensors may improve the speed and accuracy of future healthcare diagnostics, thus improving patient care and outcome.

APPENDIX

NMR OF n-(3-aminopropyl) pyrrole)

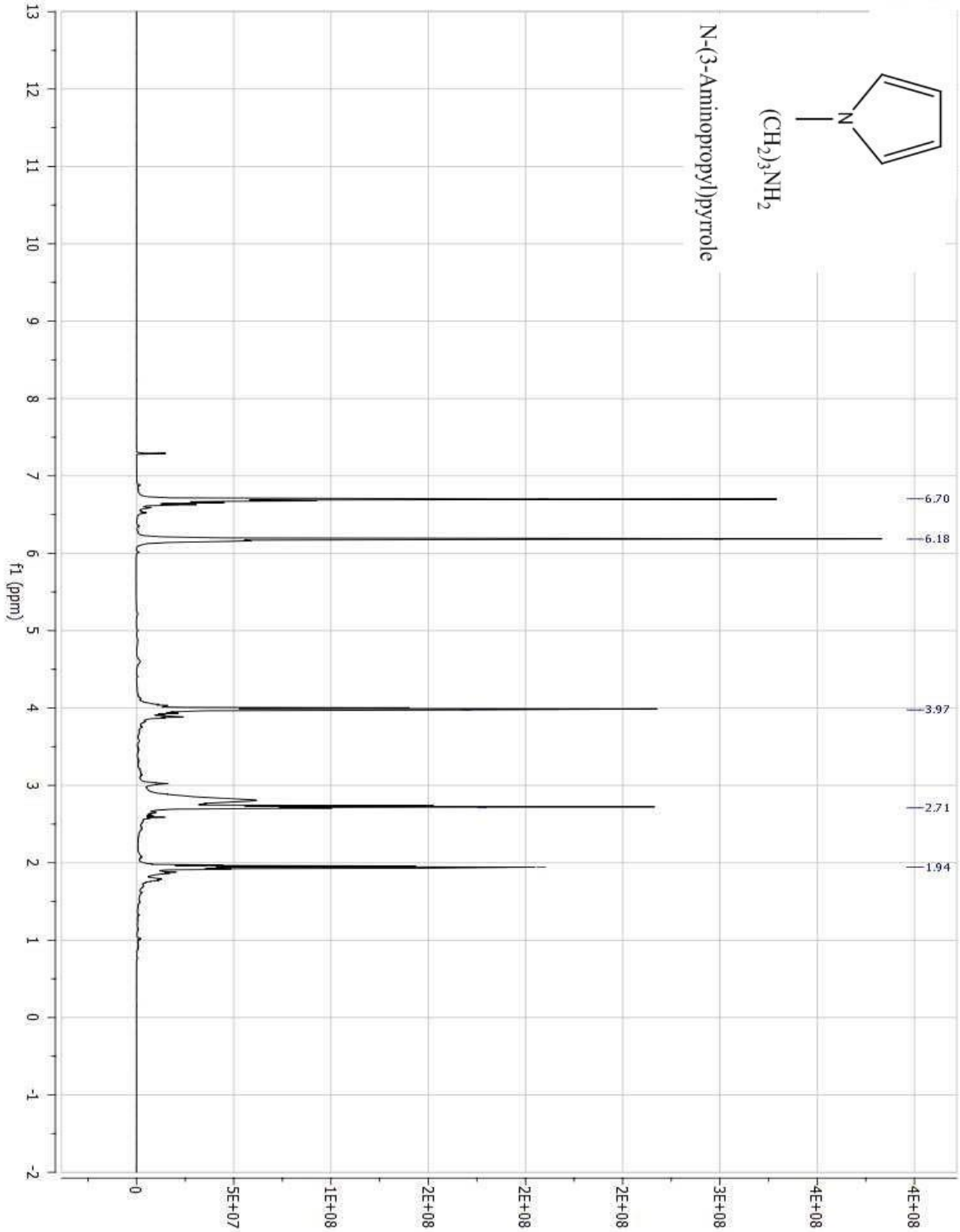

REFERENCES

Abrahao. O., Machado. A., Silva. S., Madurro. M., Castro. M., Sonoda. T., Tyramine electropolymerisation revisited by DFT and experimental study. *Journal of Molecular Structure.* 2013, **1037**, p.200-209.

Abdolahi. A., Hamzah. E., Ibrahim. Z., Hashim. S., Synthesis of uniform polyaniline nanofibers through interfacial polymerisation. *Materials.* 2012, **5**, p. 1487-1494.

Ahuja. T., Mir. A., Kumar. D., Rajesh. K., Biomolecular immobilisation on conducting polymers for biosensing applications. *Biomaterials.* 2007, **28**, p.791-806

Albers. J., Grunwald. T., Nebling. E., Piechotta. G., Hintsche. R., Electrical biochip technology - a tool for microarrays and continuous monitoring. *Anal. Bioanal. Chem.* 2003, **377**(3), p.521-527.

Alema . C., Casanovas. J., Torras. J., Oscar. B., Armelin. E., Oliver. R., Estrany. F., Cross-linking in polypyrrole and poly(N-methylpyrrole): Comparative experimental and theoretical studies. *Polymer.* 2008, **49**, p. 66-1077.

Amine. A., Mohammadi. H., Bourais. I., Palleschi. G.,Enzyme inhibition-based biosensors for food safety and environmental monitoring. *Biosensors and Bioelectronics.* 2006, **21**, p.1405-1424.

Pournaras. A., Koraki. T., Prodromidis. M., Development of an impedimetric immunosensor based on electropolymerised polytyramine films for the direct detection of salmonella typhimurium in pure cultures of type strains and inoculated real samples. *Analytica Chimica Acta.* 2008, **624**, p.301-308.

Aradilla. D., Armelin. E., Oliver. R., Iribarren. J., Characterisation and properties of poly[N-(2-cyanoethyl)pyrrole]. *Macromol. Chem. Phys.* 2010, **211**, p.1663-1673.

Arasia. Y., Jeyakumarib. J., Sundaresanb. B., Dhanalakshmic. V., Anbarasand. R., Thestructural properties of Poly(aniline)—Analysis via FTIR spectroscopy. *Spectrochimica Acta Part A*. 2009, **74**, p.1229–1234.

Arenkov. P., Kukhtin. A., Gemmell. A., Voloshchuk. S., Chupeeva. V., Mirzabekov. A., Protein microchips: use for immunoassay and enzymatic reactions. *Anal Biochemistry.* 2000, **278**, p.123-131.

Arora. P., Sindhu. A., Dilbaghi. N., Chaudhury. A., Biosensors as Innovative tools for the detection of food borne pathogens. *Biosensors and Bioelectronics.* 2011, **28**, p.1-12.

Bagiyan. G .A., Koroleva. I .K., Soroka. N. V., Ufimtsev. A. V., Oxidation of thiol compounds by molecular oxygen in aqueous solutions. *Russ Chem Bull.* 2003, **52**, p.1135-1141.

Bard. A. J., Faulkner. L. R., *Electrochemical Methods: Fundamentals and Applications.* Wiley, 2000.

Barsoukov. E and Macdonald. T. R; *Impedance Spectroscopy Theory, Experiment, and Applications.* 2nd ed. Hoboken,. New Jersey: John Wiley & Sons, Inc., 2005.

Barton. A., Collyer. S. D., Davis. F., Gornall. D., LawK. A., Lawrence. D., Mills. W., Myler. S., Pritchard. A., Thompson. M., Higson. S. J., Sonochemically fabricated microelectrode arrays for biosensors offering widespread applicability: Part I. *Biosensors and Bioelectronics.* 2004, **20**, p.10.

Barton. A. C., Collyer. S. D., Davis. F., Garifallou. G. Z., Tsekenis. G., Tully. E., O'Kennedy. R., Gibson. T., Milner. P.A., Higson. S. P. J., Labeless AC impedimetric antibody-based sensors with pg ml^{-1} sensitivities for point-of-care biomedical applications. . *Biosensors and Bioelectronics.* 2009, **24**(5), p.328-338.

Balint. R., Cassidy. N., Cartmell. S. H., Conductive polymers: Towards a smart biomaterial for tissue engineering. *Acta Biomaterialia.* 2014, **10**, p.2341-2354.

Bedzyk. M. J., Bommarito. G. M., Caffrey. M., Penner. L., Diffuse-double layer at a membrane-aqueous interface measured with x-ray standing waves. *Science.* 1990, **248**, p.52-56.

Berggren. C., Bjarnason. B., Johansson. G., Capacitive biosensors *Electroanalysis.* 2001, **13**(3), p.173-181.

Bhadra. S., Nikhil K. S., Joong. H.L., Progress in preparation, processing and applications of polyaniline. *Progress in Polymer Science.* 2009, **34**, p.784-812

Bidan. G., Electro conducting conjugated polymers: new sensitive matrices to build up chemical or electrochemical sensors. A review. *Sensors and Actuators B.* 1992, **6**, p.45-56.

Billah. M., Hays. H., Milner. P.A., Development of a myoglobin impedimetric immunosensor based on mixed self-assembled monolayer onto gold. *Microchim. Acta.* 2008, **160**(4), p.447-454.

Bloor. D., Williams. E. J., Laughlin. P. J., and Lussey. D., Metal–Polymer Composite with Nanostructured Filler Particles and Amplified Physical Properties. *Applied Physics Letters.* 2006, **88**, p.102-104.

Briand. E., Salmain. M., Herry. J. M., Perrot. H., Compere. C., Pradier. C. M., Building of an immunosensor: How can the composition and structure of the thiol attachment layer affect the immunosensor efficiency? *Biosensors and Bioelectronics.* 2006, **22**, p.440-449.

Brogan. K. L., Wolfe. K. N., Jones. P. A., Schoenfisch. M. H., Direct oriented immobilisation of F (ab') antibody fragments on gold. *Anal Chim Acta 496.* 2003, **496**, p.73-80.

Bruins. M., Rahim. Z., Bos. A., Sande. W., Endtz. H., Belkum. A., Diagnosis of active tuberculosis by e-nose analysis of exhaled air. *Tuberculosis.* 2013, **93**, p.232-239.

Chassignol. M., Thuong. T., Phosphodisulphide bond: a new linker for the oligonucleotide conjugation. *Tetrahedron Lett.* 1998, **39**, p.8271–8274.

Chaubey. A., Malhotra. B. D., Mediated biosensors. *Biosensors & Bioelectronics.* 2002, **17**, p.441-456

Chen. S., Wang. Y., Choi. S., Applications and technology of electronic nose for clinical diagnosis. *Open Journal of Applied Biosensor.* 2013, (2), p.39-50.

Chen. X., Wang. Y., Zhou. J., Yan. W., Li. X and Zhu. J., Electrochemical impedance immunosensor based on three-dimensionally ordered macroporous gold film. *Anal. Chem.* 2008, **80**, p.2133-2140.

Chitte. H. K., Walunj. V. E., Shinde. G. N., Synthesis of polypyrrole using ferric chloride ($fecl_3$) as oxidant together with some dopants for use in gas sensors. *Journal of Sensor Technology.* 2011, **1**, p. 47-56.

Chornokur. G., Phelan. C., Tanner. R., and Bhansali. S., Impedance-based miniaturised biosensor for ultrasensitive and fast prostate-specific antigen detection. *Journal of Sensors.* 2011, **2011**, p.1-7

Cosnier. S., Biosensors based on electropolymerised films: new trends. *Anal Bioanal Chem.* 2003, **377**, p.507-521

Cassagneau T, Caruso F. Conjugated polymer inverse opals for potentiometric biosensing. *Advanced Material*. 2002, 14, p.1837–41.

Daniels. J. S; Label-Free Impedance Biosensors: Opportunities and challenges. *Electroanalysis.* 2007, **19**(12), p.1239-1258.

D'Amicoa. A., Natale C. D., Paolesse R., Macagnanoc. A., Martinelli. E., Pennazza. G., Santonico. M., Bernabei. M., Roscioni. C., Galluccio. G., Bonof. R., Finazzi. E., Rullo. S., Olfactory systems for medical applications. *Sensors and Actuators B.* 2008, **130**, p.458-466

Dempsey. S., Graham. A., Bloor. D., Atkinson. D and Szablewski. M., Vapor sensing properties of a conductive polymer composite containing nickel particles with nano-scale surface features. In: *13th IEEE International Conference on Nanotechnology*, *Beijing, China*. 2013, p.665-670

Dhand. C., Datta. M., Malhotra. B.D., Recent advances in polyaniline based biosensors. *Biosensors and Bioelectronics.* 2011, **26**, p.2811-2823

Ding. C. F., Zhao. F., Zhang. M. L., Zhang. S. S., Hybridisation biosensor using 2,9-dimethyl-1,10-phenantroline cobalt as electrochemical indicator for detection of hepatitis B virus DNA *Bioelectrochemistry.* 2008, **72**(1), p.28-33.

Dong. Y., Shannon. C., Heterogeneous immunosensing using antigen and antibody monolayers on gold surfaces with electrochemical and scanning probe detection. *Anal. Chem.* 2000, **72**, p.2371-2376.

D'Orazio. P., Biosensors in clinical chemistry. *Clinica Chimica Acta.* 2003, **334**, p.41-69.

Ehrhart. J. C., Renaud. L., Madrange. J. P., Thomas. L., Morisot. J., Brosseau. A., Tauc. P., Tran. P. L., A new immunosensor for breast cancer cell detection using antibody-coated long alkylsilane self-assembled monolayers in a parallel plate flow chamber. *Biosensors & Bioelectronics.* 2008, **24**(3), p.467-474.

Fan. X., White. I. M., Shopova. S. I., Hongying. Z., Suter. J., Sun. Y., Sensitive optical biosensors for unlabeled targets: A review. *Analytica Chimica Acta.* 2009, **620**, p.8-26.

Fend. R., Geddes. R., Lesellier. S., Vordermeier. H. M., Corner. L. L., Gormley. E., Costello. E., Hewinson. R. G., Marlin. D. J., Woodman. A. C., Chambers. M. A., Use of an electronic nose to diagnose mycobacterium bovis infection in badgers and cattle. *Journal of Clinical Microbiology.* 2005, p.1745-1753

Fend. R., *Development of Medical Point-of-Care Applications for Renal Medicine and Tuberculosis based on Electronic Nose Technology*. PhD thesis, Cranfield University, 2004.

Fend. R., Kolk. A., Bessant. C., Klatser. P., Woodman. A. C., Prospects for clinical application of electronic-nose technology to early detection of mycobacterium tuberculosis in culture and sputum. *Journal of Clinical Microbiology.* 2006, **44**(6), p.2039-2047.

Gebbert. A., Alvarez. M., Stoecklein. W., Schmid. R.D., Real-time monitoring of immunochemical interactions with a tantalum capacitance flow-through cell. *Analytical Chemistry.* 1992, **64**(9), p.997-1003.

Geng. P., Zhang. X. N., Meng. W., Wang. Q.J., Zhang. W., Jin. T., Feng. Z., Wu. Z. R., Self-assembled monolayers-based immunosensor for detection of Escherichia coli using electrochemical impedance spectroscopy. *Electrochimica.* 2008, **53**(14), p. 4663-4668.

Gerard. M., Chaubey. A., Malhotra. B. D., Immobilisation of lactate dehydrogenase on electrochemically prepared polypyrrole–polyvinylsulphonate composite films for application to lactate biosensors. *Electrochimica Acta.* 2000, **46**, p.723-730.

Gerard. M., Chaubey. A., Malhotra. B. D., Application of conducting polymers to biosensors. *Biosensors & Bioelectronics.* 2002, **17**, p.345-360.

Gibson. T., Prosser. O., Hulbert. J., Electronic noses: an inspired idea? *Chemistry and Industry.* 2000, **17**, p.287-290.

Gooding. J. J; Yang. W; Liu. J; Self-Assembled Monolayers into the 21st Century: Recent Advances and Applications. *Electroanalysis.* 2003, **15**(2), p.81-97.

Graham. A., *Electrical Properties and Vapour Sensing Characteristics of a Novel-Metal Polymer Composite*. PhD thesis, Durham University, 2008.

Grant. S., Davis. F., Pritchard. J. A., Law. K. A., Higson. S. P. J., Gibson. T., Labeless and reversible immunosensor assay based upon an electrochemical current-transient protocol. *Analytica Chimica Acta.* 2003, **495**, p.21-33.

Grant. S., Davis. F., Pritchard. J. A., Law. K. A., Higson. S. P. J., Gibson. T., Label-free and reversible immunosensor based upon an ac impedance interrogation protocol. *Analytica Chimica Acta.* 2005, **537**, p.163-169.

Grieshaber. D., MacKenzie. R., Voros. J., Reimhult. E., Electrochemical biosensors - sensor principles and architectures. *Sensors.* 2008, **8**(3),p.1400-1458.

Grubo. N. M., Jankowiak. R., Porter. M. D., Small. G. J., Novel biosensor chip for simultaneous detection of DNA-carcinogen adducts with low-temperature fluorescence. *Biosensors & Bioelectronics.* 2004, **9**,p.547–556.

Guan. J. G., Zhang. Q. J., Impedimetric biosensors. *Journal Of Bioscience And Bioengineering.* 2004, **97**(4), p.219-227.

Guo. S., Wang. E., Synthesis and electrochemical applications of gold nanoparticles. *Analytica Chimica Acta.* 2007, **598**(2), p.181-192.

Guo. Z., Thiel. A. J., Wang. R., Smith. L. M;., (Direct fluorescence analysis of genetic polymorphisms by hybridisation with oligonucleotide arrays on glass supports. *Nucleic Acids Res.* 1994, **22**, p.5456–5465.

Guo. D., Li. N., Zhang. L., and Yang. J., A Novel breath analysis system based on electronic olfaction. *IEEE Transactions on Biomedical Engineering.* 2010, **57**, p.2753-2764.

Habermüller. K., Ramanavicius. A., Laurinavicius. V., Schuhmann. W., An oxygen-insensitive reagentless glucose biosensor based on osmium-complex modified polypyrrole. *Electroanalysis.* 2000, **12**(17), p.1383-1389.

Hahn. S., Mergenthaler. S., Zimmermann. B., Holzgreve. W., Nucleic acid based biosensors: The desires of the user. *Bioelectrochemistry.* 2005, **67**(2), p.151-154.

Hands. P. J. W., Laughlin. P. J., Bloor. D., Metal–polymer composite sensors for volatile organic compounds: part 1. flow-through chemi-resistors. *Sensors and Actuators B.* 2012, **162**, p.400-409.

Han. M. G., Cho. S. K., Geun. S., Soon. S., Preparation and characterisation of ployaniline nanoparticles synthesized from dbsa micellar solution. *Synthetic Metals.* 2002, **126**, p.53-61.

Han. Y. G., Kusunose. T., Sekino. T., One-step reverse micelle polymerization of organic dispersible polyaniline nanoparticles. *Synthetic Metals.* 2009, **159**, p.123-132.

Hands. P. J. W; *Vapour Sensing Applications and Electrical Conduction Mechanisms of a Novel Metal-Polymer Composite*. PhD thesis, Durham University, 2003.

Hays. C. W., Milner. P.A., Prodromidis. M. I., Development of capacitance based immunosensors on mixed self-assembled monolayers. *Sensors and Actuators B.* 2006, **114**(2), p.1064-1070

Hayat. U., Bartlett. P. N., Dodd. G. H., Electrochemical synthesis and study of polydiphenylamine. *J. Electroanalytical. Chemistry.* 1987, **220**, p.281-289.

Hearty. S., Leonard. P., Quinn. J., Kennedy. R. O., Production, characterisation and potential application of a novel monoclonal antibody for rapid identification of virulent Listeria monocytogenes. *Journal of Microbiological Methods.* 2006, **66**, p.294-313.

Hedstrom. M., Galaev. I., Mattiasson. B., Continuous measurements of a binding reaction using a capacitive biosensor. *Biosensors and Bioelectronics.* 2005, **21**, p.41-49.

Hegewald. J., Pionteck. J., Synthesis and characterisation of oxazinone and oxazoline substituted pyrroles: Towards electrically conducting bi-functional copolymers. *Synthetic Metals.* 2009, **159**, p.103-113.

Helali. S., Impedimetric Immunosensor for Pesticide Detection. In: Rinken, T. ed. *State of the Art in Biosensors - Environmental and Medical Applications.* [Online]. InTech, 2013.

Hilmiye and Uygun. Impedimetric Biosensors for Label-Free and Enzymeless Detection. In: Rinken, T. ed. *State of the Art in Biosensors - General Aspects*. InTech, 2013.

Hui. C. Y., Ronald. K., Lasky. C., Kramer. E., Case-II diffusion in polymers. II. Steady state front motion. *Journal of Applied Physics,1987,* 61**,** 14

Hodneland. C. D., Min. D. H., Mrksich. M., Supramolecular chemistry and self-assembly special feature: Selective immobilisation of proteins to self-assembled monolayers presenting active site-directed capture ligands. *Proc Natl Acad Sci USA* 2002, **99**, p.5048–5052.

Horsburgh. L. E., Synthesis and characterisation of polypyridines. *Synthetic Metals.* 1999, **101**, p.113-114.

lvarez. N., Ordieres. M., Blanco. P., Aptamers as recognition elements for label-free analytical devices. *Trends in Analytical Chemistry.* 2008, **27**(5), p.437-447.

Johnson. R., Newhall. W., Papp. J. R., Knapp. J. S., Black. C. M., Gift. T.L., Steece. R., Markowitz. L. E., Devine. O. J., Walsh. C. M., Wang. S., Gunter. D. C., Irwin. K. L., Berman. S. M., *Screening Tests To Detect Chlamydia trachomatis and Neisseria gonorrhoea Infections — 2002*.

Julian. W., Gardner. P. N. B., A brief history of electronic noses. *Sensors and Actuators B,.* 1994, **18-19**, p.211-221.

Juliet. P.S., Biosensor for tuberculosis detection using MEMS device. In: *3rd International Conference on Electronics, Biomedical Engineering and its Applications*, *Hong Kong (China)*. 2013.

Kaneto. R., A new tyrosinase biosensor based on covalent immobilisation of enzyme on N-(3-aminopropyl) pyrrole polymer film. *Current Applied Physics.* 2005, **5**, p.178-183.

Kar. P., Pradhan. N. C., Adhikari. B., A novel route for the synthesis of processable conducting poly(m-aminophenol). *Materials Chemistry and Physics.* 2008, **111**, p.59-65.

Katz. E., Willner. I., Probing biomolecular interactions at conductive and semiconductive surfaces by impedance spectroscopy: routes to impedimetric immunosensors, DNA sensors, and enzyme biosensors. *Electroanalysis.* 2003, **15**(11), p.913-948.

Katz. E., Alfonta. L., Willner. I., Chronopotentiometry and faradaic impedance spectroscopy as methods for signal transduction in immunosensors. *Sensors and Acutators B.* 2001, **76**, p.134-142.

Kharitonov. A., Alfonta. L., Katz. E., Willner. I., Probing of bioaffinity interactions at interfaces using impedance spectroscopy and chronopotentiometry. *Journal of Electroanalytical Chemistry.* 2000, **487**, p.133-142.

Kharitonov. A. S and Barnes. P. J., Biomarkers of some pulmonary diseases in exhaled breath. *Biomarkers.* 2002, **7**(1), p.1-32.

Khudaish. A., Al-Harthi. S., Al-Hinai. A. T., A solid state sensor based polytyramine film modified electrode for the determination of dopamine and ascorbic acid in a moderately acidic solution. *Journal of Electroanalytical Chemistry.* 2012, **676**, p.27-34.

Kim. K. H., Kabir. E., A Review of breath analysis for diagnosis of human health. *Trends in Analytical Chemistry.* 2012, **33**, p.1-8.

Kim. B. J., Han. M. G., and Soon. S., Preparation of polyaniline nanoparticles in micellar solutions as polymerization medium. *Langmuir.* 2000, **16**, p. 5841-5845

Kolk. A., Hoelscher. M., Maboko .L., Jung. J., Kuijper. S., Cauchi. M., Bessant. C., Stella. S., Dutta. R., Gibson. T., Reither. K., Electronic-nose technology using sputum samples in diagnosis of patients with tuberculosis *Journal of Clinical Microbiology.* 2010, **48**(11), p.4235-4238.

Krasteva. N., Fogel. Y., Bauer. R. E., Müllen. K., Joseph. Y., Matsuzawa. N. Vapor sorption and electrical response of Au-nanoparticle-dendrimer composites. *Advanced Functional Materials,* 2007. **17(6)**, p.881-888.

Kuila. T., Khanra. P., Mishra. A. K., Kim. N. H., Lee. J. H., Recent advances in graphene-based biosensors. *Biosensors and Bioelectronics 26.* 2011, **26**, p.4637-4648.

Kulkarni. M., Apte. S., Naik. S. D., Ambekar. J. D., Kale. B. B., Ink-jet printed conducting polyaniline based flexible humidity sensor. *Sensors and Actuators B.* 2013, **178**, p.140-144.

Kumar. A., Goyal. R. N., Mechanism of the electrochemical oxidation of 2-amnopyridine at a pyrolytic graphite electrode. *J. Electroanalytical. Chemistry.* 1988, **242**, p.209-220.

Lallemand.F., Auguste. D., Amato. C., Hevesi. L., Delhalle. J., Mekhalif. Z., Electrochemical synthesis and characterisation of N-substituted polypyrrole derivatives on nickel. *Electrochimica Acta*. 2007, **52**, p. 4334–4341.

Lee. J. W., Walsh. D. P., Chang. Y., Nitrophenol resins for facile amide and sulfonamide library synthesis. *J Comb Chem.* 2003, **5**, p.330–335.

Leonard . P., Hearty. S., Quinn. J., Kennedy. R. O., A generic approach for the detection of whole Listeria monocytogenes cells in contaminated samples using surface plasmon resonance. *Biosensors and Bioelectronics.* 2004, **19**, p.1331-1335.

Li. L. D., Chen. Z. B., Zhao. H. T., Guo. L., Mu. X., An aptamer-based biosensor for the detection of lysozyme with gold nanoparticles amplification. *Sensors and Actuators B: Chemical.* 2010, **149**(1), pp.110-115.

Li. D., Huang. J., Kaner. R. B., Polyaniline nanofibers: a unique polymer nanostructure for versatile applications. *Accounts Of Chemical Research.* 2009, **42**, p.135-146.

Lin. C., Chen. C., Huang. C. H., Ding. S. J., Chang. C., Development of the multi-functionalised gold nanoparticles with electrochemical-based immunoassay for protein A detection. . *Journal of Electroanalytical Chemistry.* 2008, **619**, p.39-45.

Lillie. G., Vadgama. P., Electrochemical impedance spectroscopy as a platform for reagentless bioaffinity sensing. *Sensors and Acutators B.* 2001, **78**, p.249-257.

Liu. X., Cheng. S., Liu. H., Hu. S., Zhang. D., and Ning. H., A survey on gas sensing technology. *Sensors.* 2012, **12**, p.9635-9666.

Liu. G., Nanomaterial labels in electrochemical immunosensors and immunoassays. *Talanta.* 2007, **74**, p.308-318

Liu. Z., Ma. Z., Fabrication of an ultra sensitive electrochemical immunosensor for CEA based on conducting long-chain polythiols. *Biosensors and Bioelectronics.* 2013, **46**, p.1-7.

Lo. Y., Berdichevsky. Y., Polypyrrole nanowire actuators. *Advanced Materials.* 2006, **18**, p.122-126.

Losic. D., Shapter. J. G., Gooding. J. J., Integrating polymers with alkanethiol self-assembled monolayers (SAMs): blocking SAM defects with electrochemical polymerisation of tyramine. *Electrochemistry Communications.* 2002, **4**, p.953-959.

Loyprasert. S., Hedström. M., Thavarungkul. P., Kanatharana. P., Mattiasson. B., Sub-attomolar detection of cholera toxin using a label-free capacitive immunosensor. *Biosensors and Bioelectronics.* 2010, **25**, p.1977-1983.

Lu. B., Smyth. M. R., Kennedy. R., Oriented immobilisation of antibodies and its applications in immunoassays and immunosensors. *Analyst.* 1996, **121**, p.29-32.

Luo. X., Morrin. A., Killard. A. J., Smyth. M. R., Application of nanoparticles in electrochemical sensors and biosensors. *Electroanalysis.* 2006, **18**(4),p. 319-326.

Luo. X., Vidal. G. D., Killard. A. J., Morrin. A., Smyth. M. R., Nanocauliflowers: a nanostructured polyaniline-modified screen-printed electrode with a self-assembled polystyrene template and its application in an amperometric enzyme biosensor. *Electroanalysis.* 2007, **19**, p.876-883.

Massoumi. B., Fathalipour. S., Mohammadi. R., Entezami. A. A., Novel conducting poly-schiff base of N-(3-aminopropyl) pyrrole salicylaldehyde and its copolymers with pyrrole: synthesis and characterisation. *Designed Monomers and Polymers.* 2012, **6**(3), p.1-12.

MacBeath. G., Schreiber S. L., Printing proteins as microarrays for high-through put function determination. *Science.* 2000, **289**, p.1760-1763.

McGrath. L., Mallon. P., Dowey. L., Silke. B., Norwood. W., Elborn. S., Breath isoprene during acute respiratory exacerbation in cystic fibrosis. *European Respiratory Journal.* 2000, **16**(6), p.1065-1070.

Miao. Y., Chen. J., Wu. X., Using electropolymerised non-conducting polymers to develop enzyme amperometric biosensors. *Trends in biotechnology.* 2004, **22**(5), p.227-231.

Miao. Y., Jianrong. C., Yong. H., Electrodeposited nonconducting polytyramine for the development of glucose biosensors. *Analytical Biochemistry.* 2005, **339**, p.41-45.

Miekisch. W., Schubert. J. K., Schomburg. J. E., Schomburg. N., Diagnostic potential of breath analysis—focus on volatile organic compounds. *Clinica Chimica Acta.* 2004, **347**, p.25-40.

Minh. T. D., Blake. D. R., Galassetti. P. R., The clinical potential of exhaled breath analysis for diabetes mellitus. *Diabetes Research and Clinical Practice I.* 2012, **97**, p.195-205.

Miscoria. S. A., Barrera. G. D., Rivas. G. A., Glucose biosensors based on the immobilisation of glucose oxidase and polytyramine on rodhinized glassy carbon and screen printed electrodes. *Sensors and Actuators B.* 2006, **115**, p.205-212.

NHS. *Chlamydia.* [Online]. 2013. [Accessed]. Available from: http://www.nhs.uk/conditions/Chlamydia/Pages/Introduction.aspx.

Nambiar. S., John. T., Yeow. W., Conductive polymer-based sensors for biomedical applications. *Biosensors and Bioelectronics.* 2011, **26**, p.1825-1833.

Niemeyer. C. M., Nanoparticles, proteins, and nucleic acids: biotechnology meets materials science. *Angew. Chem. Int. Ed.* 2001, **40**, p.4128-4159.

Nirmalya. K., Vijayamohanan. C., Self-assembled monolayers as a tunable platform for biosensor applications. *Biosensors & Bioelectronics.* 2002, **17**, p.1-12.

Paredi. P. P., Kharitonov. S. A., Leak. D., Ward. S., Cramer. D., Barnes. P. J., Exhaled ethane, a marker of lipid peroxidation, is elevated in chronic obstructive pulmonary disease. *American Journal of Respiratory and Critical Care Medicine.* 2000, **162**, p.369-374.

Park. D. S., Shim. Y. B., Park. S. M., Characterisation of electrochemically prepared polyaminopyridines. *Electroanalysis.* 1996, **8**(1), p.44-49.

Peng. H., Soeller. C., Sejdic. J. T., Conducting polymers for electrochemical DNA sensing. *Biomaterials.* 2009, **30**, p.2132-2149.

Phillips. M., Austin. J., Cameron. R., Cataneo. R., Greenberg. J., Kloss. R., Maxfield. R., Munawar. M., Pass. H., Prediction of lung cancer using volatile biomarkers in breath. *Cancer Biomarkers.* 2007, **3**(2), p.95-109.

Phillips. M., Cataneoa. R. N., Cheema. T., Greenberg. J., Increased breath biomarkers of oxidative stress in diabetes mellitus. *Clinica Chimica Acta.* 2004, **344**, p.189-194.

Phillips. M., Dalay. V. B., Bothamley. G., Cataneo. R. N., Lam. P. K., Natividad. M. P., Schmitt. P., Wai. J., Breath biomarkers of active pulmonary tuberculosis. *Tuberculosis.* 2010, **90**, p.145-152.

Phillips. M., Cataneo. R. N., Ditkoff. B., Fisher. P., Greenberg. J., Gunawardena. R., Kwon. C. S., Oskoui. F. R. and Wong. C., Volatile markers of breast cancer in the breath. *The Breast Journal.* 2003, **9**(3), p.184-191.

Phillips. M., Gleeson. K., Hughes. J. M., Greenberg. J., Cataneo. R. N., Baker. L., McVay. W. P., Volatile organic compounds in breath as markers of lung cancer: a cross-sectional study. *The Lancet.* 1999, **353**, p.1930-1933.

Pichetsurnthorn. P., Vattipalli. K., Prasad. S., Nanoporous impedemetric biosensor for detection of trace atrazine from water samples. *Biosensors and Bioelectronics.* 2012, **32**, p.155-162.

Pingarro. A., Gold nanoparticle-based electrochemical biosensors. *Electrochimica Acta.* 2008, **53**, p.5848-5867.

Prasad. S., Quijano. J., Development of nanostructured biomedical micro-drug testing device based on in situ cellular activity monitoring. *Biosensors and Bioelectronics.* 2006, **21**, p.1219-1230..

Phillips. M., Greenberg. J; Increased pentane and carbon disulfide in the breath of patients with schizophrenia. *Journal of clinical pathology.* 1993, **46**(9), p.861-864.

Rabeah. K. A., Ionescu. R. E., Cosnier. S., Marks. R.S., Synthesis and characterisation of a pyrrole-alginate conjugate and its application in a biosensor construction. *Biomacromolecules.* 2005, **6**, p.3313-3319.

Rajesh, V.B., Takashima. W., Kaneto. K., An amperometric urea biosensor based on covalent immobilisation of urease onto an electrochemically prepared copolymer poly (N-3-amino propyl pyrrole-co-pyrrole) film. *Biomaterials.* 2005, **26**, pp.3683–3690.

Rahman. M. A., Kumar. P., Park. D. S., Shim. Y. B., Electrochemical sensors based on organic conjugated polymers. *Sensors.* 2008, **8**, p.118-142.

Randles., J. B., kinetics of rapid electrode reactions. *Discussions Of The Faraday Society.* 1947, **1**, p.11-19.

Retama. J. R., Mecerreyes. D., Ruiz. B., Design of an amperometric biosensor using polypyrrole-microgel composites containing glucose oxidase. *Biosensors and Bioelectronics.* 2004, **20**, p.1111-1117.

Ricci. F., Micheli. L., Palleschi. G., A review on novel developments and applications of immunosensors in food analysis. *Analytica Chimica Acta.* 2007, **605**, p.111-139.

Righettoni. M., and Tricoli. A., Toward portable breath acetone analysis for diabetes detection. *Journal of Breath Research.* 2011, **5**, p.1-16.

Righettoni. M., Amann. A., Pratsinis. S. E., Gas sensors by flame aerosol deposition: correlations between blood glucose and breath components from portable gas sensors and mass spectroscopy. *Journal of Breath Research.* 2011, **5**(3), p.1.

Righettonia. M., Tricoli. A., Gassa. S., Schmid. A., Amannb. A., Pratsinis. S. E., Breath acetone monitoring by portable Si:WO_3 gas sensors. *Analytica Chimica Acta.* 2012, **738**, p.69-75.

Rushworth. J., Ahmed. A., Milner. P. A., midland blotting: a rapid, semi-quantitative method for biosensor surface characterisation. *Biosensors & Bioelectronics.* 2013, **4**(5), p.1-7.

Salmain. B. E., Herry. M., Perrot. H., Compere. C., Pradier. C. M., Side-chain selective and covalent labelling of proteins with transition organometallic complexes. perspectives in biology. *Comptes Rendus Chimie.* 2003, **6**, p.249-258.

Sarac. S., Sezgin. A., Ates. S., Turhan. M., Monomer concentration effect on electrochemically modified carbon fiber with poly[1-(4-methoxyphenyl)-1H-pyrrole] as microcapacitor electrode. *Advances in Polymer Technology.* 2009, **28**(2), p.120-130

Shen. G., Anand. M. F., Levicky. R., X-ray photoelectron spectroscopy and infrared spectroscopy study of maleimide-activated supports for immobilisation of oligodeoxyribonucleotides. *Nucleic Acids Res.* 2004, **32**, p.5973-5980.

Situmorang. M., Gooding. J. J., Hibbert. B. D., A sulphite biosensor fabricated using electrodeposited polytyramine: application to wine analysis. *The Analyst.* 1999, **124**, p.1775-1780.

Situmorang. M., Gooding. J. J., Hibbert. D. B., Barnett. D., Electrodeposited polytyramine as an immobilisation matrix for enzyme biosensors. *Biosensors & Bioelectronics.* 1998, **13**, p.953-963.

Situmorang. M., Gooding. J. J., Hibbert. D. B., Barnett. D., Immobilisation of enzyme throughout a polytyramine matrix: a versatile procedure for fabricating biosensors. *Analytica Chimica Acta.* 1999, **394**, p.211-222.

Situmorang. M., Gooding. J. J., Hibbert. D. B., Barnett. D., Development of potentiometric biosensors using electrodeposited polytyramine as the enzyme immobilization matrix. *Electroanalysis.* 2001, **13**(18), p.1469-1475.

Stamm. W. E., Guinan. M. E., Johnson. C., Starcher. T., Holmes. K. K., McCormack. W. M., Effect of treatment regimens for Neisseria gonorrhoea on simultaneous infection with Chlamydia trachomatis. *New England Journal of Medicine.* 1984, **310**, p.545-549.

Steffens. C., Leite. F., Bueno. C., Manzoli. A., Herrmann. P. S., Atomic Force Microscopy as a Tool Applied to Nano/Biosensors. *Sensors*. 2012, **12**, p. 8278-8300.

Strother. T., Cai. W., Zhao. X., Hamers . R. J., Smith. L. M., Synthesis and characterisation of DNA-modified silicon surfaces. *Journal American Chemical Society.* 2000, **122**, p.1205-1209.

Suprun. E.V., Budnikov. H.C., Evtugyn. G. A., Brainina. K. Z., Bi-enzyme sensor based on thick-film carbon electrode modified with electropolymerised tyramine. *Bioelectrochemistry.* 2004, **63**, p.281-284.

Tenreiro. A., Cordas. C. M., Abrantes. L. M., Oligonucleotide immobilisation on polytyramine-modified electrodes suitable for electrochemical DNA biosensors. *Portugaliae Electrochimica Acta.* 2003, **21**, p.361-371.

Thenmozhi. G., Kumar. D., Gopalswamy. M., Santhi. J., Synthesis, characterisation and biological applications of conducting poly (p- amino phenol) and its nano compound. *Der Pharma Chemica.* 2011, **3**(4), p.116-126.

Tenreiro. A., Cordas. C., Abrantes. N. M., Progress in the understanding of tyramine electropolymerisation mechanism. *J Solid State Electrochem.* 2007, **11**, p.1059-1070.

Thevenot. D. R., Durst. R. A., Wilson. S. G., Electrochemical biosensors: recommended definitions and classification. *Biosensors & Bioelectronics.* 2001, **16**, p.121-132.

Thermo Fisher Scientific. 2014. *Chemistry of Crosslinking* [Online]. 3747 Meridian Rd, Rockford, IL USA 61101.

Tran. L. D., Phama. M. C., Ledoan. T., Angiari. C., Daoc. L. H., Teston. F., A polytyramine film for covalent immobilization of oligonucleotides and hybridisation. *Synthetic Metals.* 2003, **139**, p.251-263.

Tully. E., Kennedy. R., Higson. P., The development of a 'labeless' immunosensor for the detection of Listeria monocytogenes cell surface protein, Internalin B. *Biosensors and Bioelectronics.* 2008, **23**, p.906-912.

Uma. H. J., Lee. S. H., Min. J; Kim. H., Choi. Y. W., Electrochemically oriented immobilisation of antibody on poly-(2-cyano-ethylpyrrole)-coated gold electrode using a cyclic voltammetry. *Talanta.* 2011, **84**, p.330-305.

Valério. E., Tenreiro. A., Abrantes. L. M., Preliminary studies towards the development of DNA biosensors for detection of cylindrospermopsin a cyanobacterial toxin. *Portugaliae Electrochimica Acta.* 2008, **26**, p.77-89.

Vijayendran. R. A., Leckband. D. E., A quantitative assessment of heterogeneity for surfaceimmobilised proteins. *Anal Chem.* 2001, **73**, p.471-480.

Vivekanandan. J., Mahudeswaran. A., Vijayanand. P. S., Synthesis, characterisation and conductivity study of polyaniline prepared by chemical oxidative and electrochemical methods. *Archives of Applied Science Research.* 2011, **3**(6), p.147-153.

Vidal. J. C., Castillo. J. R., Recent advances in electro polymerised conducting polymers in amperometric biosensors. *Microchim Acta.* 2003, **143**, p.93-111.

Wang. J., Musameh. M., Carbon nanotube/teflon composite electrochemical sensors and biosensors. *Analytical Chemistry.* 2003, **75**, p.2075-2080.

Was. M. B., Raut. A. R., Synthesis and characterisation of polyaniline based conducting polymers. *Journal of Chemistry and Chemical Sciences.* 2014, **4**(2), p.90-97.

Wu. J., Tango. J., Dai. Z., Yan. F., Murr. N., A disposable electrochemical immunosensor for flow injection immunoassay of carcinoembryonic antigen. *Biosensors and Bioelectronics.* 2006, **22**, p.102-108.

Wang. R. M., Chen. X., Ma. J., Ma. Z. F., Ultrasensitive detection of carcinoembryonic antigen by a simple label-free immunosensor. *Sensors and Actuators B.* 2013, **176**, p.1044-1051.

Wang. J., Electrochemical biosensors: Towards point-of-care cancer diagnostics. *Biosensors and Bioelectronics.* 2006, **21**, p.1887-1892.

Wang. C., Sahay. P., Breath analysis using laser spectroscopic techniques: breath biomarkers, spectral fingerprints, and detection limits. *Sensors.* 2009, **9**, p.8230-8263.

Warrington. R., Higson. S. P., Polymer modified electrodes for the reversible oxidation-reduction of NAD^+/NADH for use within amperometric biosensors. *Biomed. Sci. Instrum.* 2001, **37**, p.75-80.

Weng. B., Morrin. A., Shepherd. R., Crowley. K., Killard. A. J., Innisb. P. C., Wallace. G., Wholly printed polypyrrole nanoparticle-based biosensors on flexible substrate. *Journal of Materials Chemistry. B.* 2014, **2**, p.793-800.

Weng. B., Shepherd. R., Chen. J., Wallace. G., Gemini surfactant doped polypyrrole nanodispersions: an inkjet printable formulation. *Journal of Material. Chemistry.* 2011, **21**, p.1918-1925.

Wahl., A short history of electrochemistry. *Galvanotechtnik.* 2005, **96** (8), p.1820–1828

Wijayawardhana., *Biomedical diagnostic science and technology. .* New York.: Marcel Dekker, 2002.

Wilson. A. D., Lester D. G., Oberle C. S, Development of conductive polymer analysis for the rapid detection and identification of phytopathogenic microbes. *The American Phytopathological Society.* 2004, **94**(5), p.419-423.

Wilson. A. D., Baietto. M., Applications and advances in electronic-nose technologies. *Sensors.* 2009, **9**, p.5099-5149.

Wollenberger. U., Bogdanovskaya. V., Bobrin. S., Scheller. F., Tarasevich. M., Enzyme electrodes using bioelectrocatalytic reduction of hydrogen peroxide. *Anal. Lett.* 1990, **23**, p.1795-1809.

Wua. J., Sensitive enzymatic glucose biosensor fabricated by electrospinning composite nanofibers and electrodepositing Prussian blue film. *Journal of Electroanalytical Chemistry.* 2013, **694**, p.1-5.

Wu. H., Cui. C., Yang. W., Ma. H., Wang. X., Rapid quantitative detection of brucella melitensis by a label-free impedance immunosensor based on a gold nanoparticle-modified screen-printed carbon electrode. *Sensors.* 2013, **13**, p.8551-8564..

Wu. Z. S., Li. J. S., Deng. T., Luo. M. H., Shen. G. L., Yu. R., A sensitive immunoassay based on electropolymerised films by capacitance measurements for direct detection of immunospecies. *Analytical Biochemistry.* 2005, **337**, p.308-316.

Xiang. L., Lu. Y., Using personal glucose meters and functional DNA sensors to quantify a variety of analytical targets. *Nature chemistry.* 2011, **3**, p.697-704.

Yamamoto. T., Nishiyama. T.,Harada. G., Takeuchi. M., Electrochemical activity of polypyridine in aqueous acidic media. *Journal of Power Sources.* 1999, **79**, p.281-283.

Yao. C., Zhu. T., Qi. Y., Zhao.Y., Xia. H., Fu. W., Development of a quartz crystal microbalance biosensor with aptamers as bio-recognition element. *Sensor.* 2010, (10), p.5859-5871.

You. C., Gider. B., Ghosh. P. S., Kim. I. B., Erdogan. B., Krovi. S. A., Bunz. U., Rotello. V. M., Detection and identification of proteins using nanoparticle–fluorescent polymer 'chemical nose' sensors. nature nanotechnology. 2007, 2, p.318-326.

Yu. D. H., Blankert. B., Vire. J. C., Kauffmann. J. M., Biosensors in drug discovery and drug analysis. . *Analytical Letters.* 2005, **38**(11), p.1687-1701.

Yusof. Y., Yanagimoto. Y., Uno. S., Nakazato. K., Electrical characteristics of biomodified electrodes using nonfaradaic electrochemical impedance spectroscopy. *World Academy of Science, Engineering and Technology.* 2011, **5**, p.246-250.

Zhang. Z., Liu. H., Deng. J., A Glucose biosensor based on immobilisation of glucose oxidase in electropolymerised o-aminophenol film on platinized glassy carbon electrode. *Anal. Chem.* 1996, **68**, p.1632-1638.

Zhu. H., Bilgin. M., Bangham. R., Hall. D., Casamayor. A., Bertone. P., Lan. N., Janse. R., Bidlingmaier. S., Houfek. T., Mitchell. T., Miller. P., Dean. R. A., Gerstein. M., Snyder. M.,

Global analysis of protein activities using proteome chips. *Science.* 2001, **293**, p.2101-2105.

Zimmermann,J., Nicolaus,T., Neuert. G., Blank. K., Thiol-based, site-specific and covalent immobilization of biomolecules for single-molecule experiments. *Nature Protocols.* 2010, **5**, p. 975 – 985.